UNIVERSITY OF CALIFORNIA

Los Angeles

Stimulus-specificity of NFkappaB signaling in macrophages

A dissertation submitted in partial satisfaction of

the requirement for the degree Doctor of Philosophy

in Molecular Biology

by

Adewunmi Olumuyiwa Adelaja

2020

`

ABSTRACT OF THE DISSERTATION

Stimulus-specificity of NFkappaB signaling in macrophages.

by

Adewunmi Olumuyiwa Adelaja

Doctor of Philosophy in Molecular Biology

University of California, Los Angeles, 2020

Professor Alexander Hoffmann, Chair

Macrophages are ubiquitous tissue-resident cells that are essential for tissue homeostasis and function. Macrophages initiate, coordinate, and resolve the inflammatory response to pathogens, as well as coordinate tissue repair programs. The inflammatory program of macrophages is largely controlled by the inducible transcription factor NFκB. The temporal pattern of NFκB activity (signaling dynamics) regulates the immune response of macrophages to a diverse set of ligands. The extent to which NFκB signaling dynamics are stimulus-specific is not known. Furthermore, the functions of macrophages are regulated by the cytokine milieu. The effect that cytokine milieu may have on the stimulus specificity of NFκB signaling dynamics in primary macrophages has not been reported.

In Chapter 2, I examined the specificity of the temporal pattern of NFκB nuclear translocation in response to diverse ligands associated with host, bacteria and viruses. Using macrophages isolated from knockin mice that express a fluorescent NFκB fusion

protein at endogenous levels, I measured and tracked nuclear NFκB in individual cells over many hours using an automated image acquisition and analysis workflow. Using supervised machine learning, I quantified the stimulus specificity of NFκB signaling dynamics by measuring the performance of ligand classification using NFκB activity alone. Then, I tested the hypothesis that NFκB signaling dynamics are less stimulus-specific in macrophages from a mouse model of a systemic autoimmune disease (Sjögren's syndrome (S.S.)). My results indicated that oscillatory characteristics that define host-associated and virus-associated ligands are greatly diminished. Close examination of results showed that the sensitivity of classifying host-associated ligands is nearly abolished in SS macrophages. Furthermore, dose response studies of NFκB signaling dynamics revealed that the dose specificity of bacterium-associated ligands, but not host- and virus-associated ligands, are diminished in S.S. macrophages.

In Chapter 3, I explored the effect of the cytokine milieu on the stimulus specificity of NFκB signaling dynamics. Using time-lapse, live cell microscopy, I examined the effect of IFNγ, IL-4, and TNF conditioning on stimulus specificity of host-, virus-, and bacterium associated ligands. Supervised machine learning revealed that NFκB response to virus-associated ligands and bacterium-associated ligands are less distinguishable in the context of IFNγ conditioning. In contrast, NFκB responses to host-associated and pathogen-associated ligands is more distinguishable in the context of IFNγ conditioning. Examination of NFκB dynamics in IFNγ conditioned macrophages revealed a loss of oscillatory character in response to virus-associated ligands but not to host-associated ligands. Since host-associated and virus-associated ligands induce predominantly oscillatory dynamics in naïve macrophages, abrogation of oscillatory character in response to virus-associated but not to host-associated ligands in IFNγ conditioning makes the NFκB oscillations a distinguishing

hallmark of host-associated ligands, at the expense of distinguishing virus-associated ligands from bacterium-associated ligands.

The results showed that NFκB dynamics are more stimulus-specific in the context of IL-4 conditioning. Close examination of the NFκB dynamics showed IL-4 conditioning diminishes responsiveness of NFκB translocation to virus-associated ligands, while it preserves the responsiveness to bacterium-associated and host-associated ligands and differentially enhances peak prominence of NFκB to bacterium-associated ligands but not to host-associated ligands.

Finally, interrogating the effects of TNF conditioning on stimulus specificity of NFκB dynamics revealed that bacterium-associated ligands are nearly indistinguishable in the absence of constitutive tonic TNF. Further, NFκB response to host-associated and bacterium-associated ligands are less distinguishable. In the absence of constitutive, tonic TNF, oscillatory characteristics of NFκB signaling are abolished, which means that host- and bacterium-associated ligands both induce non-oscillatory NFκB signaling, whereas NFκB responsiveness to virus-associated ligands is nearly abolished. Furthermore, the absence of constitutive, tonic TNF and feedforward, paracrine TNF abrogate the dose specificity of NFκB signaling in response to bacteria-associated and host-associated ligands, respectively. In conclusion, the work presented in this dissertation shows that the stimulus-specificity of NFκB signaling in macrophages is greatly diminished in a murine model of Sjögren's Syndrome, an autoimmune disorder and that cytokine milieu control the specificity of NFκB signaling in macrophages. These findings suggest that modulation of NFκB signaling in macrophages by IFNγ, IL-4, and TNF signaling pathways may yield fruitful pharmaceutical targets for treating autoimmune and infectious diseases.

The dissertation of Adewunmi Olumuyiwa Adelaja is approved.

Jonathan Braun

Manish Butte

Stephen Smale

Roy Wollman

Alexander Hoffmann, Committee Chair

University of California, Los Angeles

2020

DEDICATION

To my family, thank you for your unconditional love, support, and encouragement. Thank you for always being there for me and for being good role models. Thank you for nurturing a culture of integrity, intellectual curiosity, and unyielding drive to succeed.

To Dr. Stuart Mangel, who advised me and trained as an undergraduate student and kickstarted my academic journey. Thank you for setting me on this path of scientific inquiry.

To my thesis advisor, Dr. Alexander Hoffmann, whose enthusiasm for science is infectious. Thank you for your unwavering dedication to scientific rigor and mentorship.

TABLE OF CONTENTS

LIST OF FIGURES

LIST OF SUPPLEMENTARY TABLES

ACKNOWLEDGEMENTS

None of the work presented in this dissertation would have been possible without the support, encouragement, and advice from my mentors and colleagues.

I want to thank my thesis committee (Prof. Jonathan Braun, Prof. Manish Butte, Prof. Alexander Hoffmann, Prof. Stephen Smale, Prof. Roy Wollman) for their mentorship and guidance and being excellent scientific role models.

I want to acknowledge my thesis advisor, Prof. Alexander Hoffmann, for his unwavering commitment to scientific excellence. I am grateful for the collegial, collaborative work environment that he has built. He continually recruits and retains amazing people with whom I have been privileged and honored to work. His leadership has fostered a culture of scientific curiosity and camaraderie.

I am grateful to members of the Hoffmann Lab who have made the past five years intellectually engaging. I am thankful for all their support and collegiality. I am grateful to Dr. Quen Cheng and Dr. Marie Oliver Metzig for being model physician-scientists, for their collegiality, kindness, insightful comments and feedback; Dr. Kim Ngo, Dr. Yi Liu, Dr. Eason Lin, Dr. Koushik Roy, Dr. Anup Mazumber, and Dr. Supriya Sen for their friendship, kindness, generosity and scientific acumen and for teaching me biochemical assays, EMSAs, flow cytometry, and immunoblots; Dr. Brooks Taylor and Dr. Jesse Vargas for teaching time-lapse imaging and image analysis; Dr. Simon Mitchell, Dr. Frank Cheng, Diane Lefaudeux, Dr. Ying Tang, Dr. Haripriya Mukunkarajan, Ning Wang, Fay Lin, and Katherine Sheu for their quantitative insights and friendship; Dr. Catera Wilder and Dr.

Stefanie Luecke for friendship, kindness, gregariousness, scientific insights, and sharing their expertise in immunology.

I am grateful to the scientific mentors that I have had at UCLA: Prof. Kelsey Martin, Prof. Siavash Kurdistani, Prof. Leanne Jones, Prof. Carlos Portera-Cailliau, Prof. Luisa Iruela-Arispe, Prof. Baljit Khakh, Prof. Peter Bradley.

I want to thank the administrators at UCLA-Caltech MSTP (Susie Esquivel, Josie Alviar), MBI (Jen Miller, Ashley Terhost), MIMG (Jennifer Chung, Vicki Yeung), and VBTG (Liz Duarte) for making my graduate school experience as smooth as possible.

I want to thank my funding sources for supporting me over the past few years: UCLA-Caltech MSTP (T32GM008042), Vascular Biology Training Grant (T32HL69766) and F31 NRSA (1F31AI138450-01A1).

VITA

Education

Year	Degree	School	Location
2013 – Present	M.D. (in progress)	David Geffen School of Medicine at UCLA	Los Angeles, California
2008 – 2012	Bachelor of Science	The Ohio State University (OSU)	Columbus, Ohio

Fellowships and Awards

Fellowships & scholarships

2013 - Present	Medical Scientist Training Program
2019 - 2020	NRSA F31 Fellowship
2015 – 2019	Vascular Biology Training Grant
2008 – 2012	Morrill Scholars Excellence Scholarship
2008 - 2010	Health Sciences Scholars Program
2008	William H. Hockman Memorial Scholarship

Awards

2020	Keystone Symposia Future of Science Fund scholarship
2020	American Physician-Scientist Association Travel Award
2019	Runner-up Merck KGaA InnovationCup International Competition
2019	American Physician-Scientist Association Travel Award
2019	Travel Award to Cold Spring Harbor Systems Immunology Conference
2018	Travel Award to Cold Spring Harbor Biological Data Science Conference
2018	American Physician-Scientist Association Travel Award
2018	Eastland-Fairfield Career & Technical Schools Hall of Fame Inductee
2017	American Physician-Scientist Association Poster Award
2017	MD/PhD National Student Conference Travel Award
2012	Honors Research Distinction in Biology
2009	College of Arts and Sciences Rising Star Award
2008	Fairfield Career Center American Citizenship Award

Publications

Adelaja, A., Hoffmann, A. (2019). Signaling crosstalk mechanisms that may fine-tune pathogen-responsive NFκB*. Front. Immunol.* 10:433. DOI: 10.3389/fimmu.2019.00433

Mitchell, S. *, Mercado, E.*, **Adelaja, A.,** Ho, J., Fortmann, K., Cheng, Q., Ghosh, G., Hoffmann, A. (2019). An NFκB activity calculator to delineate signaling crosstalk: Type I and II interferons enhance NFκB via distinct mechanisms*. Front. Immunol.* 10:1425. DOI: 10.3389/fimmu.2019.01425

Cheng, Q.J., Ohta. S., Sheu K.., Spreafico R., **Adelaja, A.**, Taylor, B., Hoffmann, A. (2020). NFκB dynamics determine the stimulus-specificity of epigenomic reprogramming in macrophages. bioRxiv DOI: 10.1101/2020.02.18.954602.

Taylor, B.*, **Adelaja, A*.,** Liu, Y., Luecke, S., Hoffmann, A. (2020). Identification and physiological significance of temporal NFκB signaling codewords deployed by macrophages to classify immune threats. bioRxiv. DOI: 10.1101/2020.05.23.112862.

Tang, Y, **Adelaja. A.,** Ye, X., Deeds, E., Wollman, R., Hoffmann A. Information transmission from dynamical patterns of biochemical signaling. *in preparation.*

Adelaja, A., Sen, S., Hoffmann, A. Stimulus-specificity of NFκB dynamics in conditioned macrophages. *In preparation.*

Oral Presentations

Adelaja, A. Machine learning reveals loss of specific innate immune responses in autoimmunity. NIAID Fellowship Workshop. Webinar. April 2020.

Adelaja, A. Decoding the specificity of the innate immune response to pathogen-associated stimuli. UCLA CFAR/AIDS Institute. Los Angeles, CA, June 2019.

Adelaja, A., Taylor, B., Hoffmann, A. Characterizing Inflammatory Stimulus Encoding via NFκB Dynamics. Biological Data Sciences Meeting. Cold Spring Harbor, NY, November 2018.

Adelaja, A., Taylor, B., Hoffmann, A. Context-specific regulation of NFκB signaling in macrophages. MBI Annual Retreat. Los Angeles, CA, March 2018.

Adelaja, A., Taylor, B., Hoffmann, A. Single-cell analysis of NFκB signaling in activated macrophages. ImmunologyLA. Los Angeles, CA, June 2017

Professional experience

2019 – 2021 Board member, Associated Students UCLA Board of Directors

2019 – 2020 MD/PhD representative, MSC at David Geffen School of Medicine, UCLA

2014 – 2020 Career Mentor, Re-applicant Program at DGSOM, UCLA

2014 – 2016 Director of Communication, UCLA Graduate Student Association

2014 – 2015 Vice-Chair for Technology, American Physician Scientist Association

2014 – 2015 Chapter Vice-President, Student National Medical Association

2010 – 2012 Research Assistant, Department of Neuroscience, Ohio State University

2010 – 2012 Chapter Associate Director, Phi Delta Epsilon Medical Fraternity

2009 – 2010 Director of Government Relationships, Undergraduate Student Government

Chapter 1 : General Introduction

Macrophages are immune sentinel cells that respond to pathogen invasion and tissue injury by initiating and coordinating both local and system-wide immunity (Wynn et al., 2013). These cells are ubiquitously distributed in tissues (Bauer et al., 2001) and can sensitively detect inflammatory cytokines and pathogen-associated molecular patterns (PAMPs), which indicate viral, bacterial, or fungal invasion (Medzhitov and Horng, 2009). Immune activation must be appropriate to each stimulus: the functional response to the cytokine TNF must be distinct from the response to a pathogen; further, the needs of a macrophage responding to bacterial or viral invasion are distinct. Furthermore, the functional response must be appropriate in scale to the quantity of the stimulus.

The temporal coding hypothesis posits that information about the extracellular stimulus is represented in the time-domain, i.e. the temporal pattern of a signaling activity (Behar and Hoffmann, 2010; Hoffmann and Baltimore, 2006; Purvis and Lahav, 2013). Biochemical studies in primary fibroblasts showed that the temporal pattern of the inducible, inflammatory transcription factor NFκB RelA activity is stimulus-specific at the cell population level (Covert et al., 2005; Werner et al., 2005) and that it controls the expression of immune response genes (Hoffmann et al., 2002). Although pioneering single-cell microscopy studies confirmed complex temporal patterns (Ashall et al., 2009; Nelson et al., 2004; Tay et al., 2010), they relied upon fluorescent-protein-NFκB RelA fusion proteins ectopically expressed in immortalized cell lines. Potential artefacts arising from ectopic expression of a reporter-effector protein have been reported (Barken et al., 2005; Mothes et al., 2015), and prolonged cell culture adaptation of immortalized cell lines was found to diminish their responsiveness to immune threats (Cheng et al., 2015). These limitations have not allowed the literature to explore the biological significance of temporal coding in primary immune cells and whether it is a useful concept for understanding immune

pathology. Reasons for why no studies of single-cell NFκB trajectories in primary macrophages have been reported thus far include challenges associated with generating knockin fluorescent protein reporters that are not overexpressed and reliable high-throughput image analysis of morphologically heterogeneous cells.

While the temporal pattern of NFκB activity (signaling dynamics) has been shown to be qualitatively stimulus specific, the extent of stimulus specificity is not known and has not been quantified or examined in depth. The information that NFκB may reliably convey about stimuli is not established. Furthermore, the effect that tissue microenvironments may have on the stimulus specificity of NFκB activity has not been reported. The overall aim of this dissertation is to examine the extent of the stimulus specificity of NFκB signaling dynamics in macrophages, examine whether stimulus specificity of NFκB signaling is perturbed in a model of autoimmunity and characterize how the cytokine milieu regulates stimulus specificity of NFκB dynamics in macrophages.

In Chapter 2, I examined how well different categories of inflammatory stimuli may be classified by the temporal pattern of NFκB activity in macrophages. Then, I examined whether classification of stimulus information is affected in a murine model of Sjögren's syndrome (SS), a systemic autoimmune disorder. Using a new mVenus-RelA knockin mouse strain and a high-throughput imaging workflow to investigate the NFκB temporal code in single, primary macrophages, I quantitated the classification performance of ligand identity (TNF, P3CK4, CpG, LPS, and p(I:C), ligand source (host, bacterium, virus) and ligand type (cytokine and pathogen-associated molecular patterns (PAMP)) in murine macrophages from healthy mice and the murine model of Sjögren's syndrome. Using supervised machine learning, I showed that NFκB signaling dynamics are sufficient to distinguish ligand identity and that misclassification of ligand identities is a result of the confusion that exists

within ligands associated with bacterial infection (CpG, Pam3CSK4, and LPS). This analysis suggests that NFκB signaling dynamics alone classify ligand sources more accurately than ligand identity. Comparison of stimulus classification using NFκB signaling in BMDMs from healthy mice and from a murine model of Sjögren's syndrome revealed that precision and sensitivity of ligand classification is abrogated in the disease model. In particular, the sensitivity and precision of TNF classification are greatly diminished. Furthermore, I characterized the dose response of NFκB signaling activity for five different ligands (TNF, P3C4, CpG, LPS, and p(I:C)) in Sjögren's syndrome macrophages and healthy controls. I showed that dose classification shows a greater dependence on linear dose response relationship in Sjögren's macrophages. Furthermore, I showed that the proportion of oscillatory trajectories is more dose-responsive in the SS condition compared to healthy controls. Finally, assessment of the dose classification for all ligands revealed that the sensitivity and precision of high doses of bacterium-associated ligands (CpG, Pam3CSK4, and LPS) are greatly diminished in SS macrophages compared to healthy controls.

In Chapter 3, I characterized the effects of prototypical cytokine milieu on the classification of ligand source and ligand type. I examined the effects of T-cell cytokines — interferon (IFN)-γ and interleukin (IL)-4) — and the inflammatory cytokine, TNF, on stimulus-specificity of NFκB signaling in macrophages. Using supervised machine learning, I showed that classification of ligand source (bacteria, virus, host) is greatly diminished in classically activated macrophages (M_1), polarized by the Th1 cytokine, IFNγ. Specifically, I showed that in the context of M_1 polarization, NFκB signaling dynamics poorly distinguish virus-associated ligands from bacterium-associated ligands; however, ligand type (host, pathogen) are more distinguishable in M_1 macrophages compared naïve macrophages.

Then, I showed that the classification of ligand source and ligand type by NFκB signaling dynamics is improved in alternatively activated macrophages (M_{2a}), polarized by the Th2 cytokine IL-4. Notably, the classification of TNF using NFκB dynamics is greatly improved in M_{2a} conditioned macrophages. Furthermore, I showed that paracrine, feedforward TNF potentiates the dose classification of TLR ligands such as CpG and that loss of tonic TNF diminishes accurate ligand and dose classification. In summary, I showed that cytokine conditioning of macrophages by IFNγ, IL-4, and TNF regulates the trade-offs in the stimulus-specificity of NFκB signaling.

Bibliography

Barken, D., Wang, C.J., Kearns, J., Cheong, R., Hoffmann, A., Levchenko, A., 2005. Comment on "Oscillations in NF-κB Signaling Control the Dynamics of Gene Expression." Science 308, 52; author reply 52. https://doi.org/10.1126/science.1107904

Bauer, J., Bahmer, F.A., Wörl, J., Neuhuber, W., Schuler, G., Fartasch, M., 2001. A strikingly constant ratio exists between Langerhans cells and other epidermal cells in human skin. A stereologic study using the optical disector method and the confocal laser scanning microscope. J. Invest. Dermatol. 116, 313–8. https://doi.org/10.1046/j.1523-1747.2001.01247.x

Behar, M., Hoffmann, A., 2010. Understanding the temporal codes of intra-cellular signals. Curr. Opin. Genet. Dev. 20, 684–693. https://doi.org/10.1016/j.gde.2010.09.007

Cheng, Z., Taylor, B., Ourthiague, D.R., Hoffmann, A., 2015. Distinct single-cell signaling characteristics are conferred by the MyD88 and TRIF pathways during TLR4 activation. Sci. Signal. 8, ra69. https://doi.org/10.1126/scisignal.aaa5208

Covert, M.W., Leung, T.H., Gaston, J.E., Baltimore, D., 2005. Achieving stability of lipopolysaccharide-induced NF-kappaB activation. Science 309, 1854–7. https://doi.org/10.1126/science.1112304

Hoffmann, A., Baltimore, D., 2006. Circuitry of nuclear factor kappaB signaling. Immunol. Rev. 210, 171–186. https://doi.org/10.1111/j.0105-2896.2006.00375.x

Hoffmann, A., Levchenko, A., Scott, M.L., Baltimore, D., 2002. The IκB-NF-κB Signaling Module: Temporal Control and Selective Gene Activation. Science 298, 1241–5. https://doi.org/10.1126/science.1071914

Medzhitov, R., Horng, T., 2009. Transcriptional control of the inflammatory response. Nat. Rev. Immunol. https://doi.org/10.1038/nri2634

Mothes, J., Busse, D., Kofahl, B., Wolf, J., 2015. Sources of dynamic variability in NF-κB signal transduction: a mechanistic model. Bioessays 37, 452–62. https://doi.org/10.1002/bies.201400113

Purvis, J.E., Lahav, G., 2013. Encoding and decoding cellular information through signaling dynamics. Cell 152, 945–56. https://doi.org/10.1016/j.cell.2013.02.005

Werner, S.L., Barken, D., Hoffmann, A., 2005. Stimulus Specificity of Gene Expression Programs Determined by Temporal Control of IKK Activity. Science 309, 1857–61. https://doi.org/10.1126/science.1113319

Wynn, T. a., Chawla, A., Pollard, J.W., 2013. Macrophage biology in development, homeostasis and disease. Nature 496, 445–455. https://doi.org/10.1038/nature12034

Chapter 2 : Supervised machine learning reveals specificity of NFκB temporal code in health and disease.

Abstract

Acute and chronic inflammatory pathologies involve misregulation of macrophage functions. Physiologically, macrophages are immune sentinels that initiate inflammatory responses via the transcription factor NFκB. The temporal pattern of NFκB activity determines which genes are expressed, suggesting that a temporal signaling code specifies a stimulus-appropriate immune response. To examine the temporal pattern of NFκB activity in individual macrophages with high resolution, I developed tools to enable high-throughput analysis of live, primary macrophages responding to host- and pathogen-derived stimuli. Our results indicate that the temporal pattern of NFκB activity is ligand-specific and dose-specific. In particular, "oscillatory" trajectories are a hallmark of the responses to the host cytokine TNF. Remarkably, examining macrophages derived from a systemic autoimmune disease model suggests that the miscoding of TNF as a pathogen-derived stimulus, may underlie sporadic inflammatory pathology. Furthermore, NFκB dynamics in response to bacteria-associated ligands are less dose-specific and distinguishable in the disease-associated macrophages. Overall, this study demonstrates that the temporal NFκB signaling code is sufficient for classifying immune threats and demonstrates the biological significance of the stimulus specificity of NFκB signaling.

Introduction

Autoimmune pathologies are characterized by the presence of auto-antibodies and immune attack of specific tissues, but the etiology is not uniform (Marshak-Rothstein, 2006). One cause may be found in errors in the negative selection of auto-reactive B-cell or T-cell clones in secondary lymphoid organs (Marshak-Rothstein, 2006); another contributor may be inappropriate immune activation by immune sentinel cells (Marshak-Rothstein, 2006).

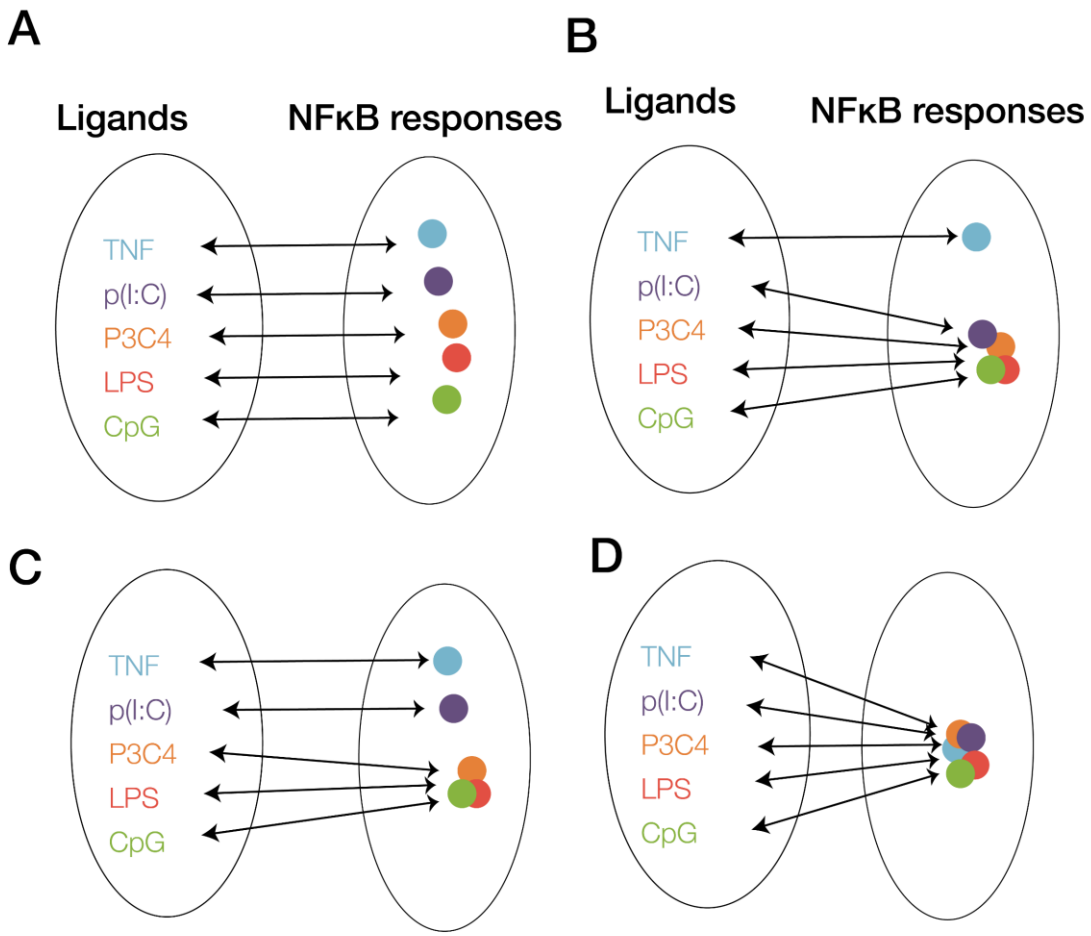

Figure 2.1. Varying degrees of NFκB ligand specificity

Schematic showing mapping of NFκB responses to ligand identity (A), to ligand sources (host, viruses, and bacteria) (B), to ligand types (cytokines and PAMPs) (C), and to ligand presence (D).

Sjögren's syndrome (SS) is a systemic autoimmune disorder, which is characterized by progressive destruction of tissues exposed to the environment, such as eyes, mouth and throat, and skin rashes (Marshak-Rothstein, 2006). Interestingly, several genetic variants in regulators of the inflammatory transcription factor NFκB are associated with SS patients (Lisi et al., 2012; Nordmark et al., 2013; Ou et al., 2008; Sisto et al., 2013) and a mouse strain containing similar variants recapitulates some of the SS pathognomonic characteristics (Bailu Peng et al., 2010). However, it remains unknown how these alleles affect control of NFκB dynamics.

Although the temporal pattern of NFκB activity has been shown to be stimulus-specific in qualitative and bulk assays, the extent to which NFκB signaling is ligand-specific and dose-specific is not known. Prior studies have examined NFκB activity in response to few ligands—classically TNF and LPS—in fibroblast cell lines using bulk assays or with over-expressed NFκB reporters in single-cell assays. The extent of the stimulus specificity of NFκB signaling in primary macrophages has not been explored. It remains unknown whether NFκB communicates the identities of ligands (TNF, CpG, Pam3CSK4, LPS, poly(I:C), etc.), the sources of ligands (host, virus, bacteria), or the types of ligands (host cytokines or pathogen-associated molecular patterns (PAMPs) (Fig. 2.1).

Here, I employed a novel mVenus-RelA knockin mouse strain and a high-throughput imaging and analysis workflow to investigate the temporal pattern of NFκB activity in single, primary macrophages. Supervised machine learning was used to examine stimulus specificity of NFκB signaling dynamics in primary macrophages from healthy mice and disease models of a systemic autoimmune disease, Sjögren's syndrome.

Results

Primary macrophages show distinct stimulus responsive NFκB dynamics

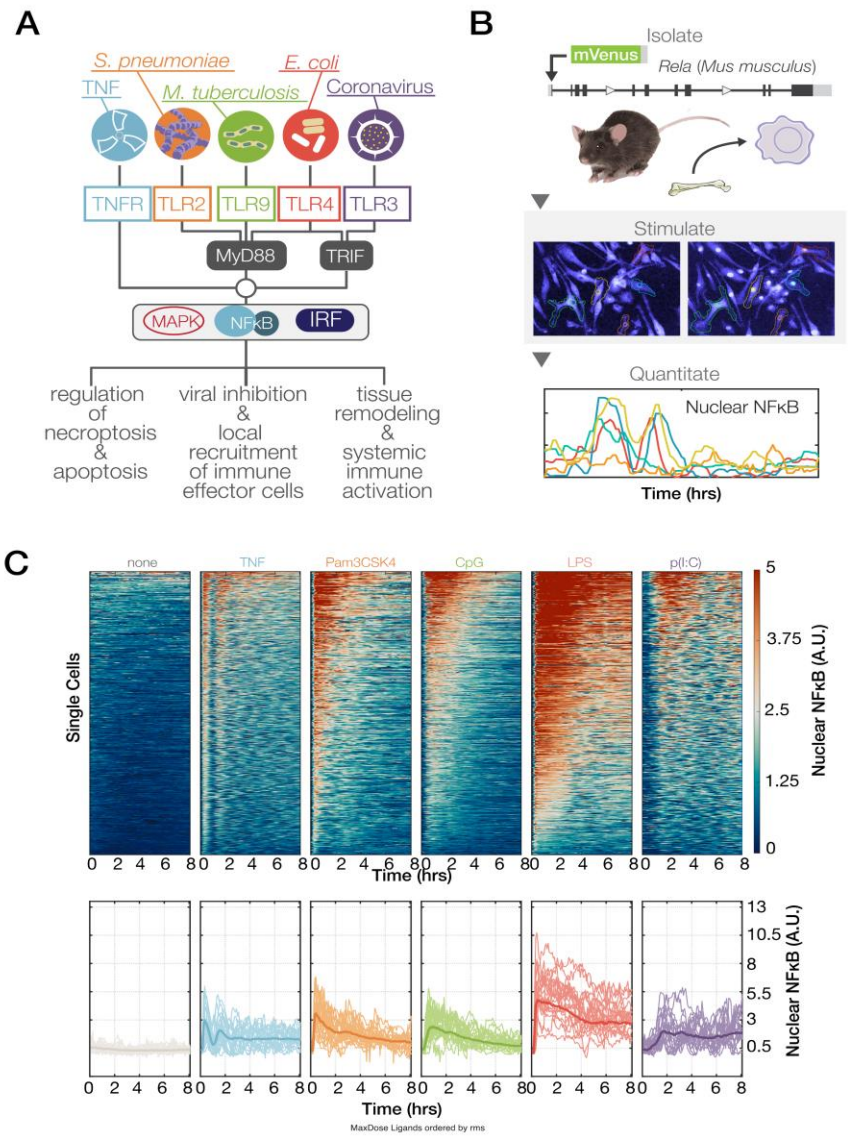

Figure 2.2. Examining stimulus responsive NFκB dynamics

(A) Schematic of the innate immune signaling network activating NFκB. Environmental information is transmitted via ligand-specific signaling pathways that converge on a few key transcription factors, including NFκB, but produce stimulus-specific physiological responses. (B) Workflow diagram: A knockin mouse line expressing mVenus-RelA was generated. Bone marrow-derived macrophages (BMDMs) were differentiated, imaged, tracked, and quantified in multiple stimulus conditions. (C) Single cell heatmaps of NFκB nuclear localization trajectories in response to 10 ng/mL TNF, 1 μg/mL Pam3CSK4, 1 μM CpG, 100 ng/mL LPS, and 100 μg/mL p(I:C). Each row of a heatmap corresponds to a single cell's trajectory. Heatmaps are ordered by the average value of a trajectory.

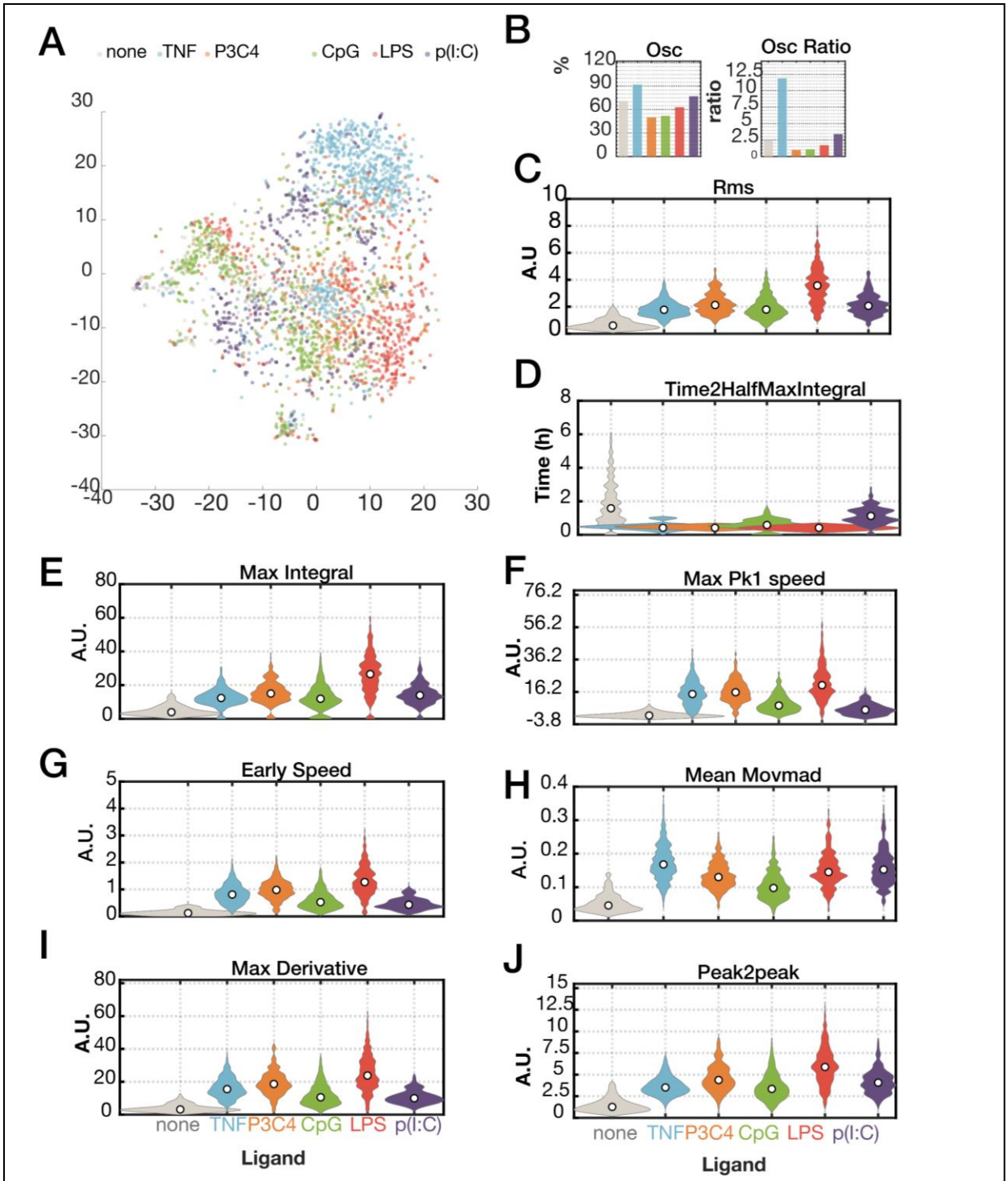

Figure 2.3. NFκB features distinguish ligands.

(A) t-SNE plot of NFκB dynamical features. (B) Proportion of trajectories with oscillatory character. (C) Average NFκB activity. (D) Time to half-maximum activity. (E) Total activity. (F) Maximum peak 1 speed. (G) Early speed. (H) Average moving variability. (I) Maximum speed. (J) Maximum amplitude difference.

To study temporal patterns of nuclear NFκB in primary macrophages in response to prototypical immune threats (Fig. 2.2A) at single-cell resolution, a mouse strain expressing a mVenus-RelA fusion protein was generated, similar to a previous GFP-RelA design (De Lorenzi et al., 2009) whose low fluorescence limited experimental studies (Sung et al., 2009). Macrophages, differentiated from primary bone-marrow cells derived from homozygous mVenus-RelA mice (Fig. 2.2B), showed normal levels of nuclear NFκB binding activity (data not shown). Upon stimulation with a variety of different ligands and doses, and time-lapse imaging for several hours, the amount of nuclear NFκB fluorescence was quantitated in single cells using a fully automated image processing pipeline that enabled tracking of live cells using minimal levels of a nuclear marker (Selimkhanov et al., 2014; Zambrano et al., 2016) and label-free identification and segmentation of cell cytoplasm.

Striking differences in the NFκB dynamics induced by prototypical PAMP (LPS) and cytokine (TNF) stimuli, are apparent at the single-cell level (Fig. 2.2C). TNF induced oscillatory translocations between cytoplasm and nucleus that rapidly became desynchronized, matching biochemical data (Hoffmann et al., 2002). By contrast, LPS induced more than 4 hours of sustained nuclear localization that also matched biochemical data from primary fibroblasts (Covert et al., 2005; Werner et al., 2005).

With an experimental workflow established, NFκB translocation dynamics in response to a large number of stimulation conditions, encompassing TNF and four different PAMPs, associated with diverse bacterial and viral pathogen classes (the TLR ligands CpG (TLR9), Pam3CSK4 (TLR1/2, referred to as P3C4), LPS (TLR4), and Poly(I:C) (TLR3, referred to as p(I:C))) were recorded. The responses to CpG and P3C4 closely resemble the

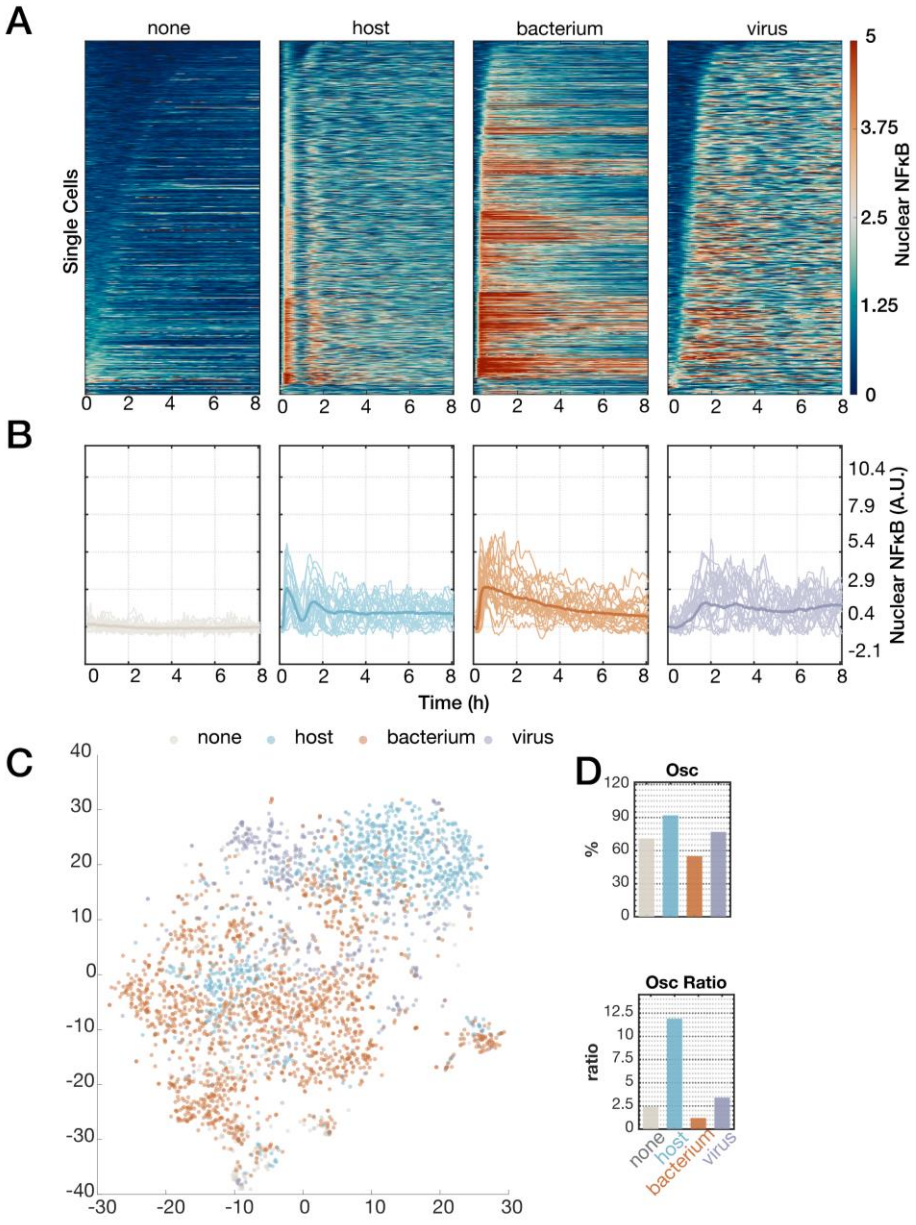

Figure 2.4. NFκB dynamics distinguish ligand sources.

(A) Heatmaps of NFκB nuclear translocation in response to ligands derived from host (10 ng/mL TNF), bacteria (1 μM CpG, 1 μg/mL Pam3CSK4, 100 ng/ml LPS) and viruses (100 μg/mL p(I:C)). Heatmaps ordered by Time to half-maximum integral. (B) Median nuclear NFκB activity (bold line) and sample trajectories (light lines) of trajectories in A. (C) t-SNE of NFκB dynamics features. (D) Percentage of trajectories with oscillatory character (top) and ratio of oscillatory trajectories to non-oscillatory

largely non-oscillatory trajectories seen with LPS stimulation, albeit with much shorter duration (Fig.2.2C) and total activity (Fig.2.3E). Poly(I:C) induces both oscillatory and non-oscillatory NFκB activity (Fig. 2.3B) but with a very significant delay (> 30 mins) in the

onset of signaling compared to the other ligands (Fig.2.2C, Fig.2.3). Interestingly, the ligands that signal in the endosomal compartment, p(I:C) and CpG, tend to induce NFκB activity with slower kinetics (Fig. 2.3F, J, G, I).

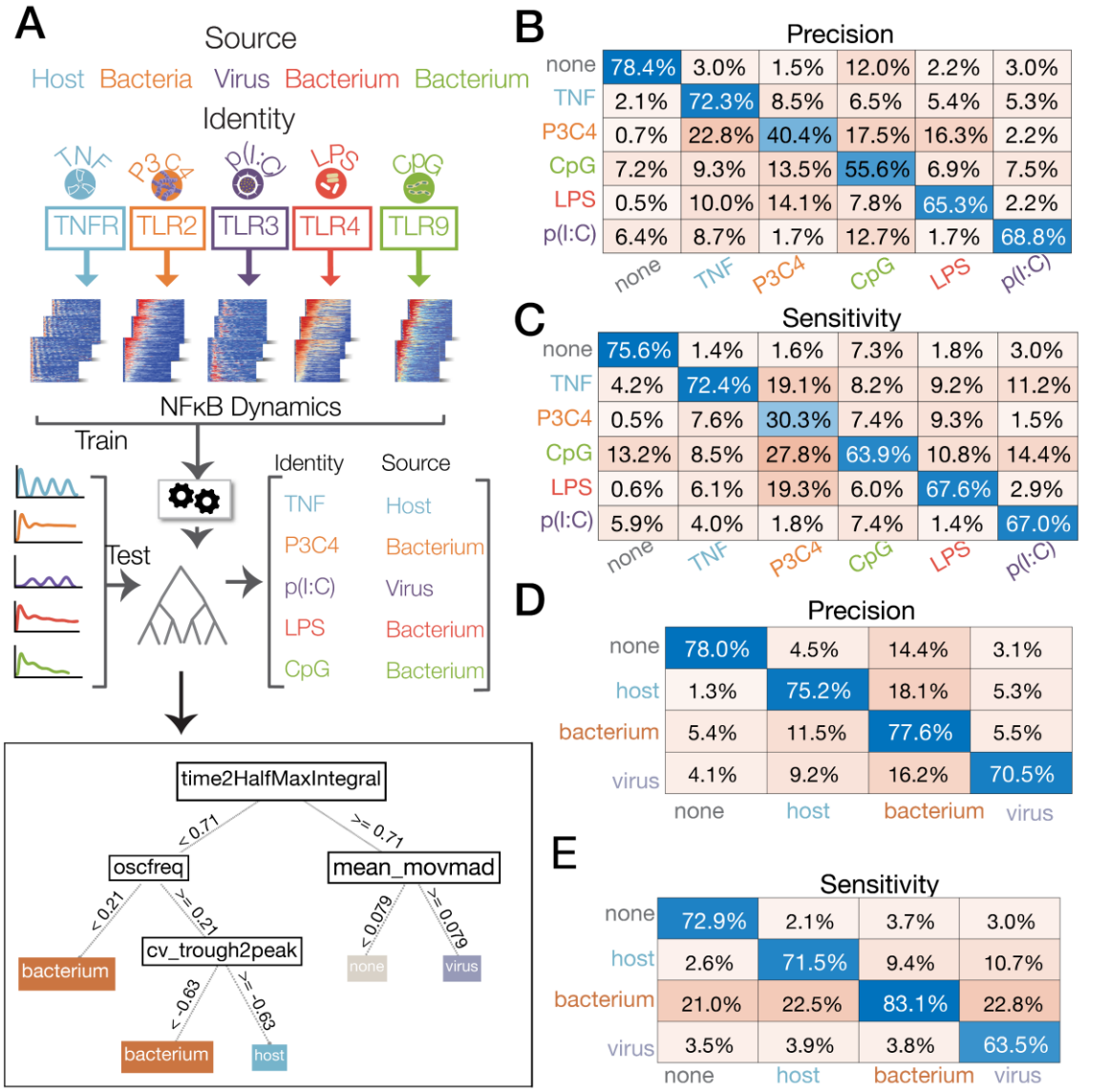

Figure 2.5. Classification of NFκB features reveals points of confusion.

(A) Schematic of stimulus classification by NFκB signaling. (B) Confusion matrix showing classification precision of ligand identity. (C) Confusion matrix showing classification sensitivity of ligand identity. (D) Confusion matrix showing classification precision of ligand source (host, bacteria, virus). (E) Confusion matrix showing classification sensitivity of ligand source. True labels on the X-axis; Predicted labels on the Y-axis.

When NFκB trajectories are organized by ligand source, stereotypic patterns are easier to visualize and observe (Fig. 2.4A-C). The oscillatory character in NFκB responses induced present in host and virus-associated ligands is apparent (Fig.2.4A). The proportion of cells with oscillatory trajectories exceeds 90% for host, 75 % for virus, but less than 60% for bacterium (Fig. 2.4D).

Machine learning of NFκB signaling dynamics distinguishes stimuli

To determine whether NFκB signaling dynamics (temporal pattern of NFκB activity) suffice to distinguish these ligands, we used supervised machine learning and trained decision-trees models to classify the identity and source of ligands using features of NFκB signaling (Fig. 2.5A).

I chose this classification algorithm because of its performance and interpretability (Alpaydin, 2014; Caruana and Niculescu-Mizil, 2006). With this algorithm, interrogation of classification decisions becomes trivial (Fig. 2.5A). Correct classification of ligand identities occurred in the majority, but misclassifications (off-diagonal values) were not uniformly distributed (Fig. 2.5B-E). With supervised machine learning, classifier performance can be readily visualized, summarized, and examined with confusion matrices. The precision confusion matrix shows the proportion of class predictions that is correct, whereas the sensitivity/recall confusion matrix the shows proportions of a class that is correctly identified as such. The diagonal of the confusion matrix shows the correct classifications. The off-diagonal cells show the incorrect classifications. Classification of TNF shows the highest precision at 72.3%, followed by p(I:C) at 68.8%, LPS at 65%, CpG at 55.6% and P3C4 at 40.4%. Inspection of the P3C4 precision reveals that NFκB responses misclassified as P3C4 are usually TNF (22.8%), CpG (17.5%), and LPS (16.3%), but not p(I:C) at 2.2%

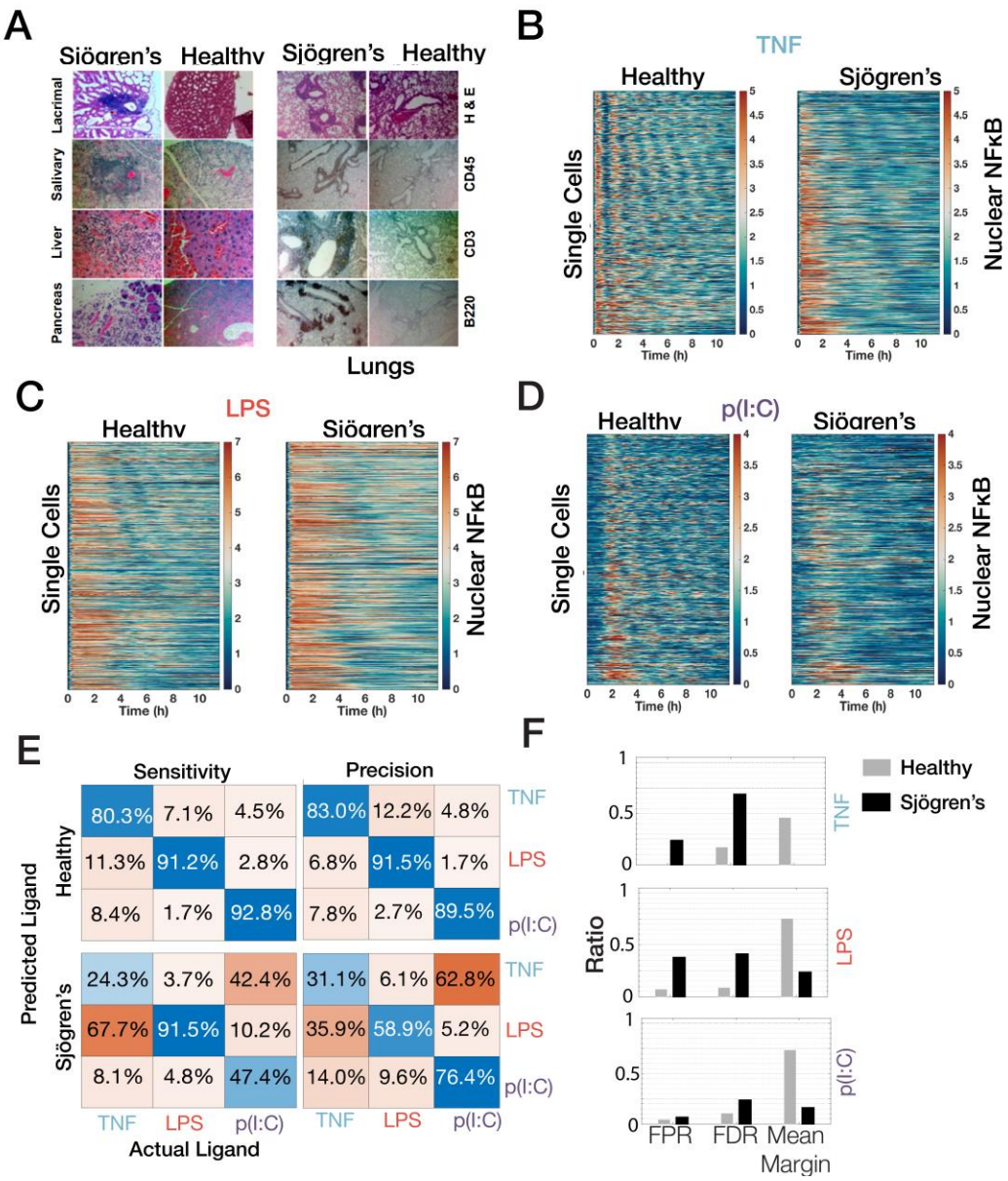

Figure 2.6. A Sjögren's syndrome mouse model shows more confusion in classifying stimuli based on NFκB dynamics.

(A) Histology from Sjögren's disease mouse model showing immune cell infiltrates into lacrimal and salivary glands, liver, pancreas and lungs (Peng et al., 2010). Heatmaps comparing 10 ng/mL TNF (B), 100 ng/mL LPS(C), 50 μg/mL p(I:C) (D) stimulation in BMDMs from healthy and Sjögren's disease mouse model. (E) Classification of ligand identity in healthy and Sjögren's mouse model macrophages by a machine learning classifier trained on healthy macrophage data. (F) False positive rate (FPR), false discovery rate (FDR), and mean margin of classification in E.

(Fig. 2.5B). The sensitivity confusion matrix provides information as to which ligands are most frequently selected when P3C4-induced NFκB responses are misclassified: CpG is

most common wrong prediction at 27.8% followed by LPS at 19.3% and TNF at 19.1% (Fig. 2.5C). This finding suggests bacterium-associated ligands induce less distinguishable NFκB dynamics. Unsurprisingly, classification of ligand source, rather than ligand identity, shows improved performance (Fig. 2.5D,E). Interestingly, the precision confusion matrix shows NFκB responses induced by BAMPs (bacterium-associated molecular patterns) are most frequently misclassified as host at 18.1% and vice versa at 11.5% (Fig. 2.5D). Furthermore, the sensitivity confusion matrix shows that NFκB responses induced by host-associated and VAMPs (virus-associated molecular patterns) are most frequently misidentified as BAMPs (Fig. 2.5E).

Diminished ligand specificity of NFκB signaling dynamics in autoimmune disease

I assessed whether a mouse model of Sjögren's syndrome (SS) (Bailu Peng et al., 2010) (Fig. 2.6A), which harbors genetic variants in the regulatory region of the NFκB regulator IκBα, may be associated with signaling confusion, such that cells exposed to one stimulus might miscommunicate the presence of a different stimulus to nuclear target genes. We bred the mVenus-RelA reporter into this mouse model and then derived bone marrow-derived macrophages for stimulation with the cytokine TNF, the bacterial PAMP LPS, and the viral PAMP poly(I:C). Unlike macrophages from healthy mice, these SS macrophages showed non-oscillatory NFκB trajectories in response to all stimuli (Fig. 2.6B – D).

I examined the accuracy of stimulus classification using an ensemble-of-decision trees algorithm, specifically, a bootstrap-aggregated ensemble which trains a decision tree on independently sampled subsets of the data. The mean margin scores of ligand classification were greatly diminished in SS macrophages, concomitant with an elevation in the false positive and false discovery rates for TNF and LPS (Fig. 2.6F). Furthermore, the sensitivity of TNF and poly(I:C) classification in SS macrophages was greatly diminished

(24.3%/47.4%, respectively, versus 80.3%/92.8% in healthy controls, Fig. 2.6E), as there was increased confusion between Poly(I:C) versus LPS, and TNF versus LPS. These analyses indicate that SS macrophages have diminished ability to generate ligand-specific NFκB signaling dynamics and suggest that signaling codeword confusion and mistranslation may play a role in the etiology of sporadic inflammatory diseases.

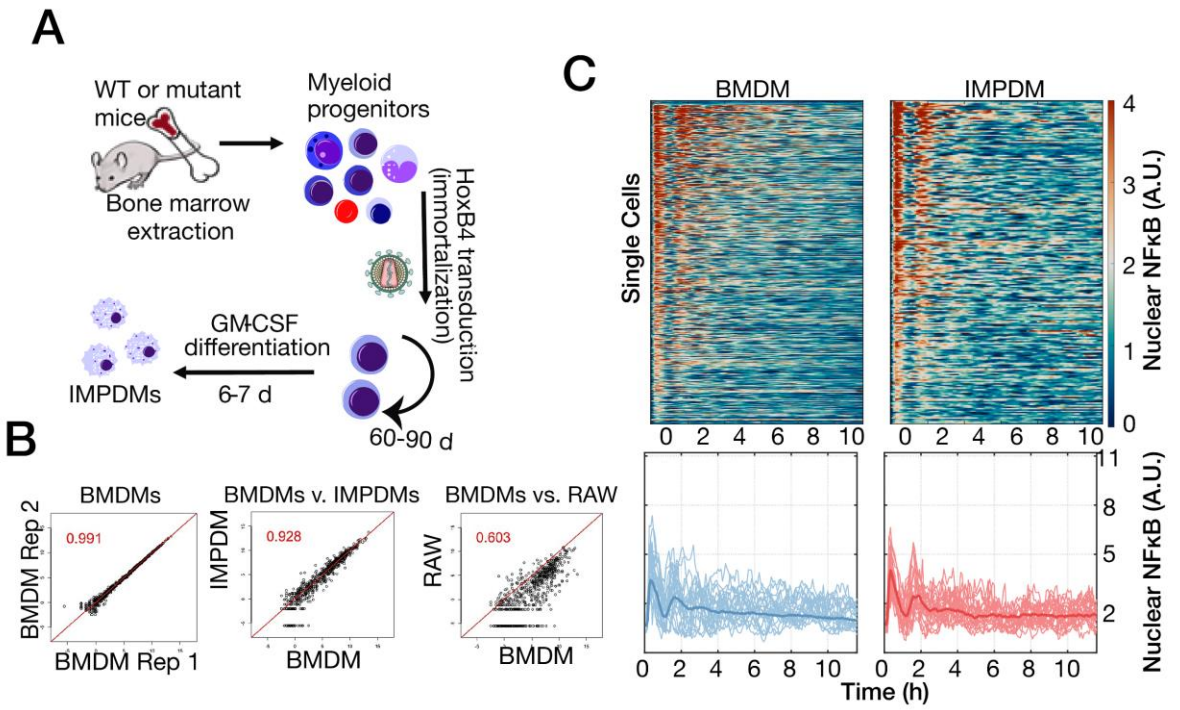

Figure 2.7. IMPDMs produce similar NFκB dynamics as BMDMs.

(A) Experimental procedure for generating immortalized myeloid progenitor derived macrophages (IMPDMs). (B) Transcriptomic analysis shows highly concordant gene expression profiles between IMPDMs and BMDMs in response to LPS stimulation. (C) Heatmaps comparing single-cell NFκB trajectories between BMDMs and IMPDMs in response to 10 ng/mL TNF stimulation. Transcriptomic data from Supriya Sen and Roberto Spreafico.

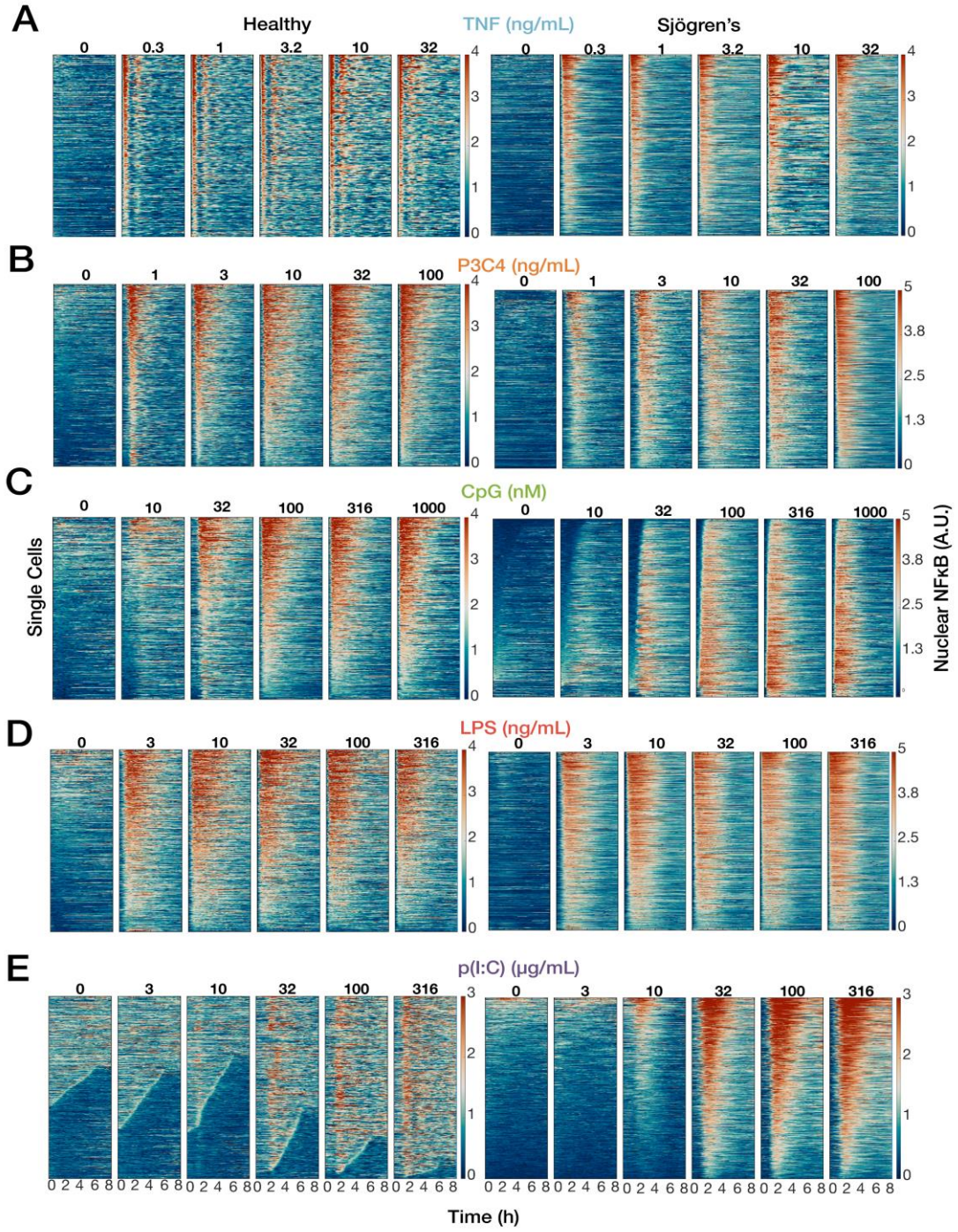

Figure 2.8. Dose response of NFκB dynamics is perturbed in Sjögren's syndrome mouse model.

Dose response of NFκB dynamics to TNF (A), P3C4 (B), CpG (C), LPS (D), and p(I:C) (E) in IMPDMs from healthy mice (left) and Sjögren's syndrome mice (right). Heatmaps (A) are sorted by maximum first peak speed. Heatmaps in (B) are sorted by 1st peak amplitude (left) and early speed (right). Heatmaps in (C) are sorted by 1st peak amplitude (left) and Time to Half-maximum Integral (right). Heatmaps in (D) are sorted by 1st peak amplitude (left) and 1st peak speed (right). Heatmaps in (E) are sorted by Total duration (left) and average activity (right).

Diminished dose specificity of BAMPs in autoimmune disease

To examine the dose specificity of NFκB signaling dynamics to a broad range of doses for each of the aforementioned ligands in healthy macrophages and SS macrophages, a total of 60 experimental conditions were required: 5 ligands x 6 doses x 2 genotypes. To perform such an extensive set of experiments, I used macrophages derived from immortalized myeloid progenitors (IMPs) (Fig. 2.7A). These IMP-derived macrophages (IMPDMs) have a similar transcriptomic profile as BMDMs (Fig. 2.7B) and similar response to NFκB stimuli (Fig. 2.7C). As in SS BMDMs, oscillatory NFκB dynamics are abolished in SS IMPDMs (Fig. 2.8). For TNF, maximum 1st peak speed is the most important feature that distinguishes different doses in healthy and SS IMPDMs (Fig 2.8A, 2.9A, 2.14, 2.15). For P3C4 ,1st peak height and the early speed are the most important features for dose discrimination in healthy and SS IMPDMs, respectively (Fig 2.8B, 2.9B, 2.16, 2.17). For CpG, 1st peak height and time to half-maximum activity are the most important features for dose discrimination in healthy and SS IMPDMs, respectively (Fig .2.8C, 2.9C, 2.18, 2.19). For LPS, 1st peak height and maximum 1st peak speed activity are the most important features for dose discrimination in healthy and SS IMPDMs, respectively (Fig 2.8D, 2.9D, 2.20, 2.21). For p(I:C), 1st peak height and maximum 1st peak speed activity are the most important features for dose discrimination in healthy and SS IMPDMs, respectively (Fig. 2.8E, Fig. 2.9E, 2.22, 2.23). Interestingly, the most important feature for dose classification in response to bacterium-associated ligands is 1st peak height in healthy IMPDMs, but in SS IMPDMs the most important features represent the kinetics of early activity (maximum 1st peak speed, early speed, and time to half-maximum activity). These

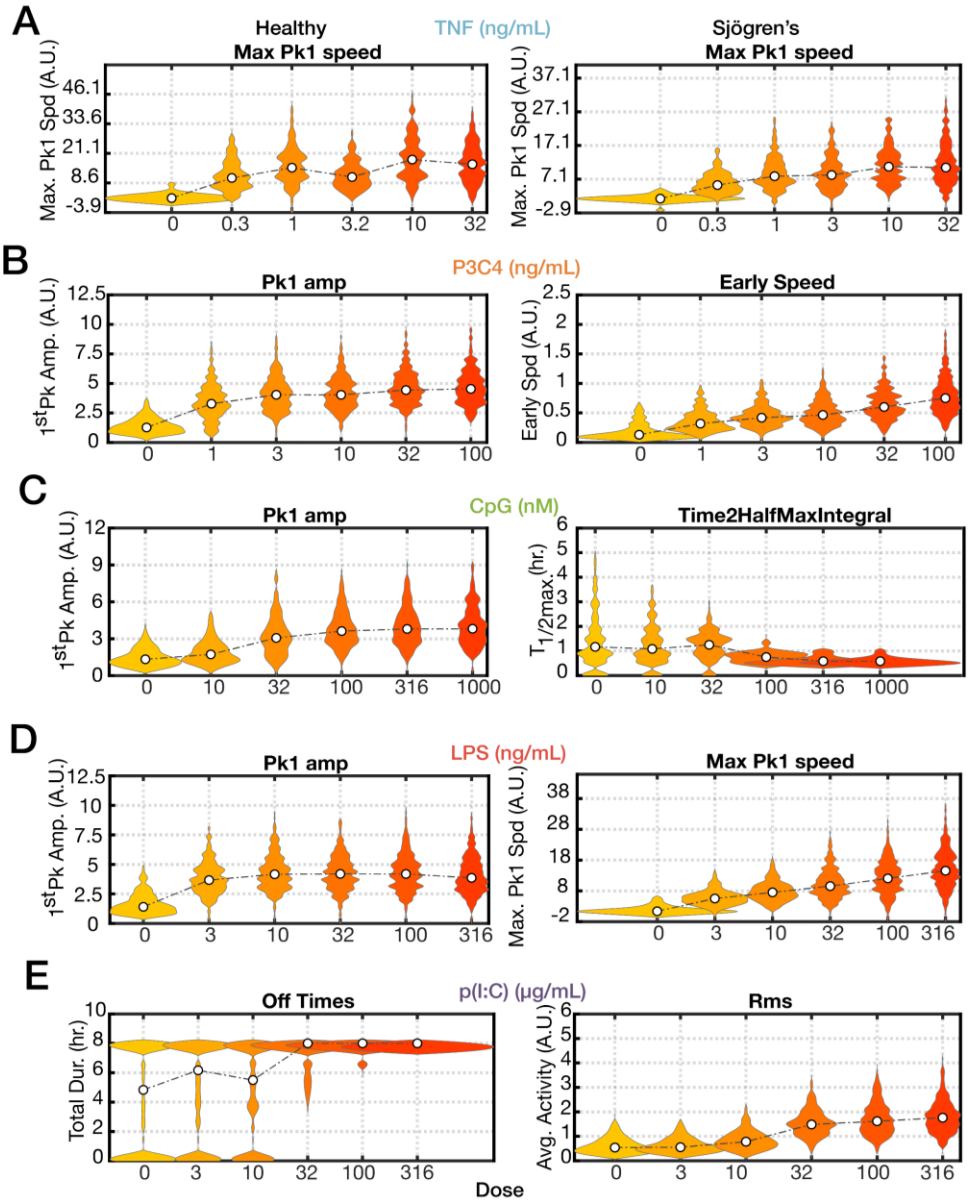

Figure 2.9. Distinct dose-discriminative NFκB features in response to BAMPs in macrophages from Sjögren's syndrome mouse model.

(A) Violin plots of maximum first peak speed in response to TNF. (B) Violin plots of 1st peak amplitude (left) and early speed (right) in response to P3C4. (C) Violin plots of 1st peak amplitude (left) and Time to Half-maximum Integral (right) in response to CpG. (D) Violin plots of 1st peak amplitude (left) and 1st peak speed (right) in response to LPS. (E) Violin plots of Total duration (left) and average activity (right).

important features in SS IMPDMs follow a more linear dose response compared to the top features in healthy IMPDMs (Fig. 2.9). Finally, the proportion of oscillatory trajectories is more dose responsive in SS IMPDMs compared to healthy controls: the proportion of

oscillatory trajectories as a function of dose declines more steeply in SS IMPDMs (Fig. 2.10).

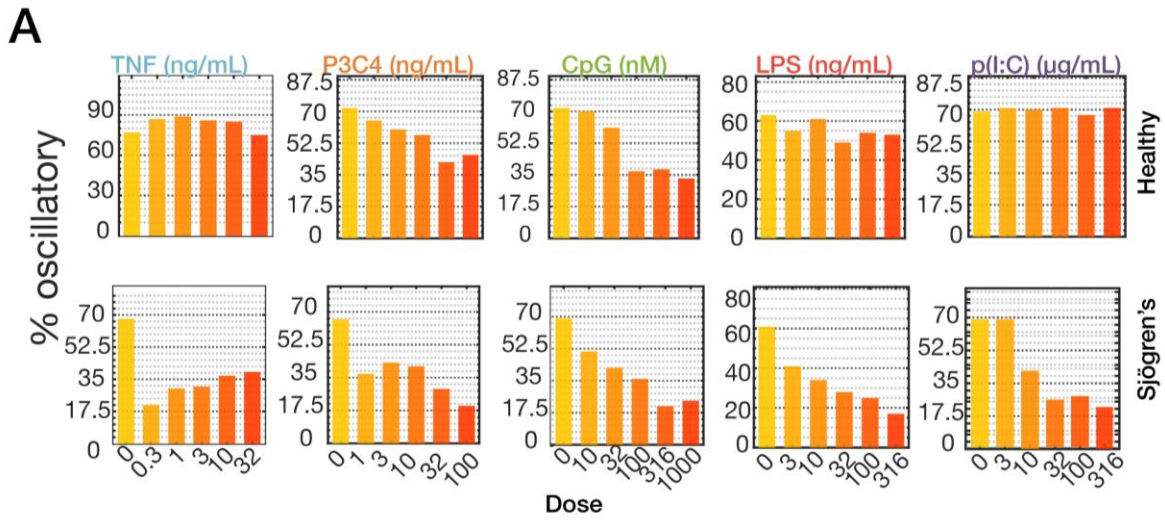

Figure 2.10. Proportion of oscillatory NFκB dynamics is more dose responsive in macrophages from Sjögren's syndrome mouse model.

(A) Proportion of oscillatory trajectories (frequency > 0.42 hr^{-1}) in macrophages derived from healthy mice (top) and Sjögren's syndrome mouse model (bottom).

To quantify how dose classification compares between healthy IMPDMs and SS IMPDMs, I trained an ensemble of decision trees (using an error correcting output codes (ECOC)) algorithm, which splits a multi-class problem into a series of binary classification problem. The features used for classification were a transformation of the time series trajectories into smaller dimensional space using an autoencoder. Dose classification of responses to bacterium-associated molecular patterns (BAMPs: CpG, P3C4, LPS) show reduced precision and sensitivity at medium to high doses (Fig. 2.11). Unsurprisingly, the most frequent misclassified and misidentified doses are directly adjacent to the actual dose.

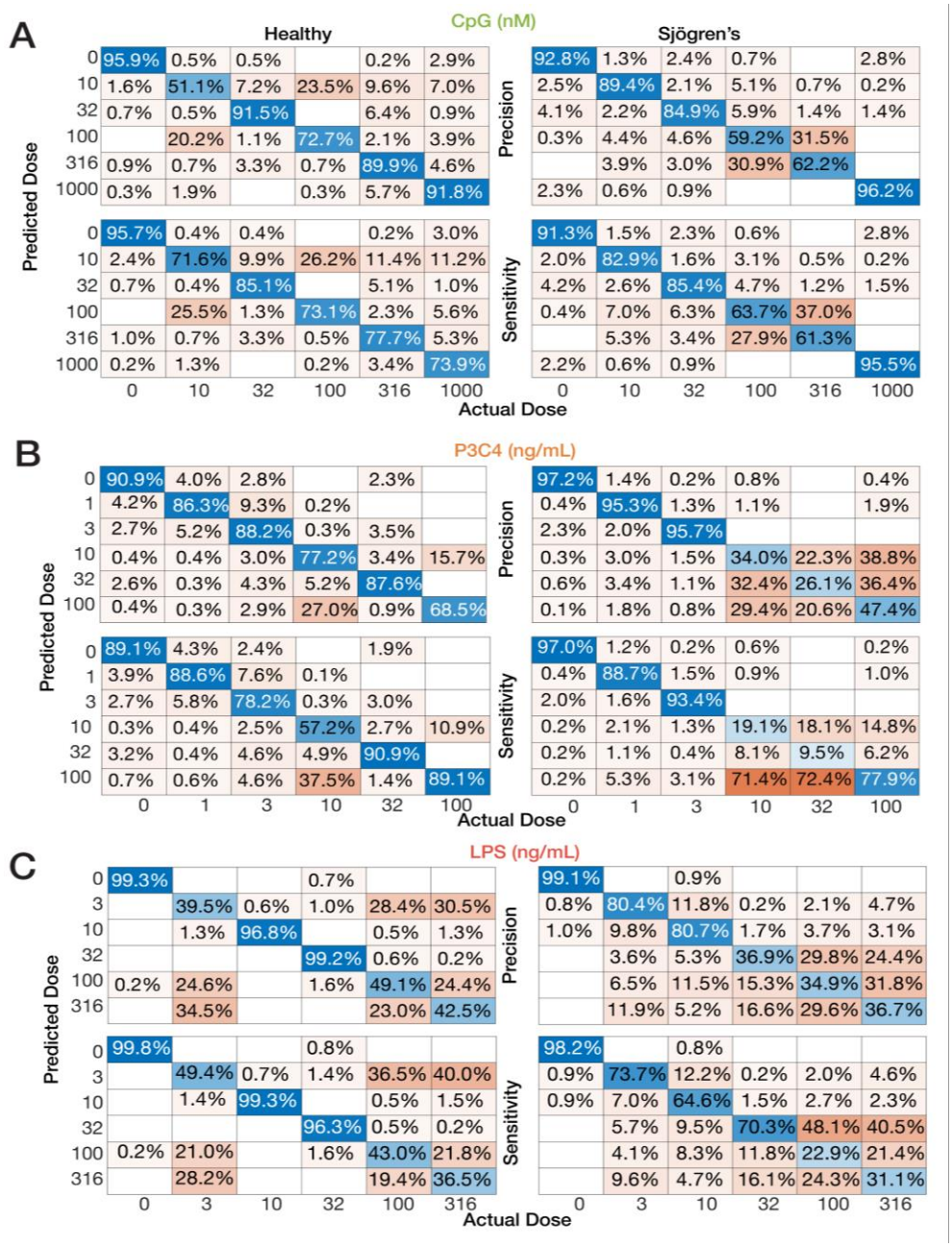

Figure 2.11. Dose discrimination in response to bacterial PAMPs is diminished in macrophages from Sjögren's syndrome mouse model.

Confusion matrices showing precision (top) and sensitivity (bottom) of dose classification based on NFκB dynamics in response to CpG (A), P3C4 (B), and LPS (C) in macrophages from healthy (left) and Sjögren's syndrome mouse model (right).

Discussion

In this work, I show that NFκB signaling dynamics (temporal pattern of NFκB activity) suffice to classify NFκB-activating ligands and that classification accuracy is greatly diminished in the context of the systemic autoimmune disorder, Sjögren's syndrome. These findings were made possible by the development of new experimental and computational tools that provided an unprecedented quantity and quality of experimental data in primary cells responding to diverse immune threats. As cell lines show reduced responsiveness (Cheng et al., 2015) and ectopic expression of reporters can lead to artefactual oscillatory dynamics (Barken et al., 2005), a new NFκB mVenus-RelA knock-in mouse strain was generated to allow imaging of primary macrophages, the cell type that functions as the sentinels of the immune system. I was able to study not only the dose-response relationships but also characterize NFκB responses to pathogen-derived and host-derived ligands to which these primary macrophages respond vigorously. A robust automated image analysis pipeline and machine learning classification workflow enabled rigorous and quantitative analysis.

It is well established that the temporal trajectories of NFkB activity are correlated with gene expression (Hoffmann et al., 2002; Lane et al., 2017; Martin et al., 2020; Werner et al., 2005). The results suggest that the features identified here may specify the stimulus-specific expression of those genes that are able to differentiate between their relative presence or absence. Some prior work has described molecular mechanisms that particular target genes employ to "decode" specific NFκB signaling features. "Peak amplitude/fold change", for example, was described to be sensed effectively by an incoherent feedforward loop involving the NFκB-responsive generation of p50 homodimers (Lee et al., 2014). Stimulus-specific duration of NFκB was found to be differentiated by two mechanisms:

whereas stimulus-specific expression of core regulators of the inflammatory response was mediated by an mRNA half-life of a few hours, pro-inflammatory initiators tend to employ a chromatin-based mechanism that involves the movement of a nucleosome (Sen et al., 2020). Interestingly, the oscillatory dynamics do not necessarily control the stimulus-specific expression of primary response target genes (Barken et al., 2005), but appears to determine the capacity of NFκB to generate *de novo* enhancers in macrophages and thus affects the potential for gene expression induced by subsequent stimuli (Cheng et al., 2020).

A hallmark of all single-cell datasets is the heterogeneity within an isogenic, identically stimulated population. Confusion here means for example that some (but not all) cells stimulated with CpG produce NFκB responses that are indistinguishable from some (but not all) cells stimulated with Pam3CSK4. I suggest that the capacity (or lack thereof, i.e. confusion) for mounting specific responses is a fundamental functional characteristic of macrophages as immune sentinel cells. Furthermore, given macrophages' functional plasticity, I expect that this characteristic of capacity for stimulus-discrimination be similarly tuned—determined by the context of microenvironmental cytokines and exposure histories. In this study, macrophages derived from a mouse model of the systemic inflammatory disease, Sjögren's syndrome, showed dramatically increased levels of ligand confusion and dose confusion for bacterium-associated ligands. This particular model involves genetic variants in the IκBα promoter but the impact on NFκB signaling dynamics at the single cell level was unknown. While cells are capable of responding to diverse immune threats, the reduction in specificity adds to the understanding of this systemic autoimmune disease and may contribute to its etiology. Future studies will address whether these concepts apply to other autoimmune or inflammatory diseases.

Within the context of the innate immune signaling network, NFκB is only one of four prominent PAMP-responsive pathways, and therefore functions in conjunction with the JNK-AP1, MAPKp38/ERK-TTP/CREB, TBK-IRF3-ISGF3 axes to control gene expression responses (Cheng et al., 2017). While bacterial ligands LPS, CpG, and Pam3CSK4 are poorly distinguished at the level of NFκB dynamics (Fig. 2.3), only LPS activates TBK-IRF3-ISGF3 and thus produces highly distinct gene expression program. Furthermore, MAPKp38 activation is specific to the high dose of LPS (Gottschalk et al., 2016) allowing for much better dose distinction than that based on NFκB dynamics alone. Elucidating how coordinated combinatorial and temporal codes specify macrophage responses to diverse stimuli will be a major undertaking of future research.

Supplemental Figures

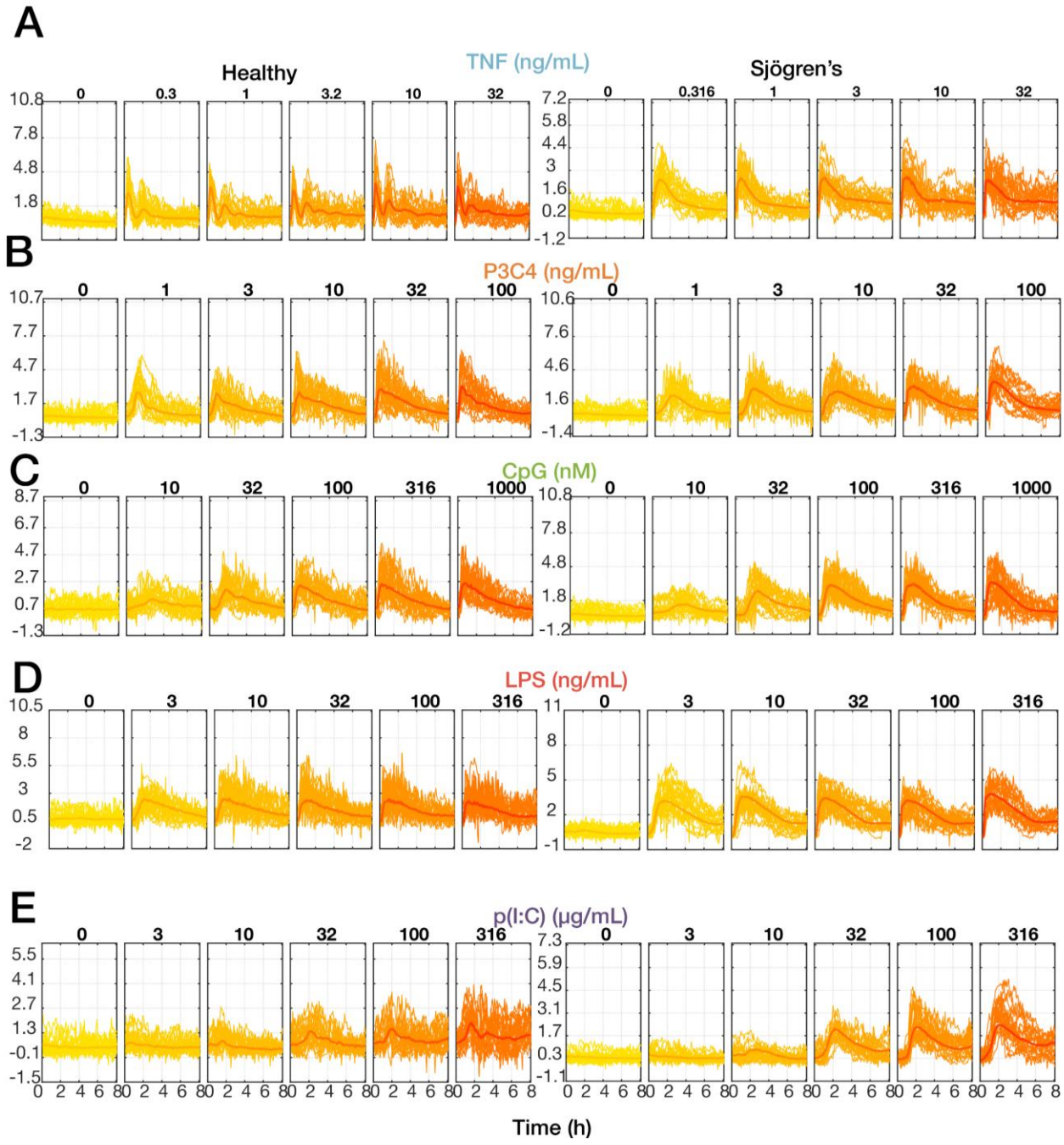

Figure 2.12. Representative NFκB trajectories.

Line plots of median NFκB trajectories and sample trajectories in response to TNF (A), P3C4 (B), CpG (C), LPS (D), p(I:C) (E) in macrophages from healthy mice (left) and Sjögren's syndrome mouse model (right).

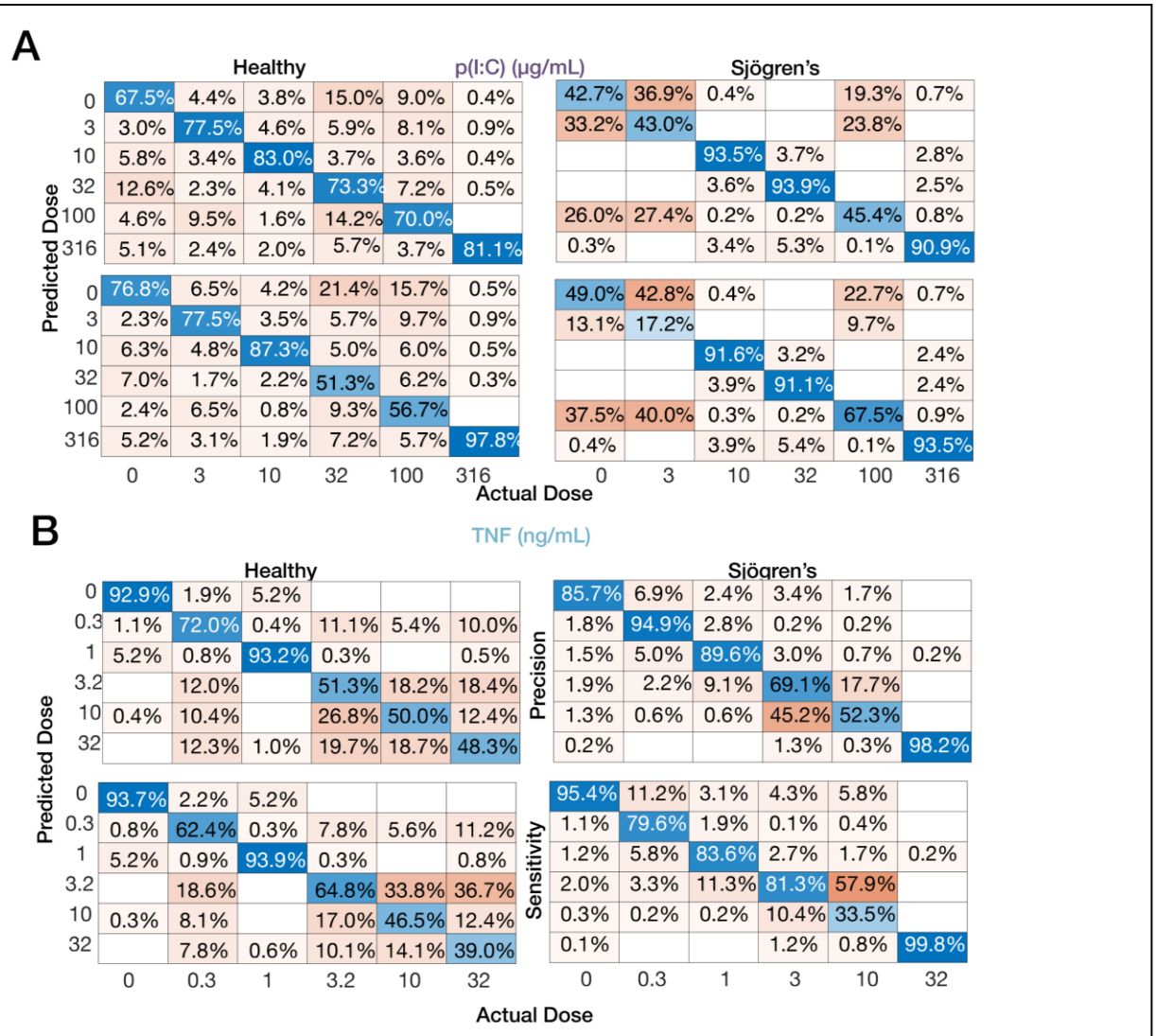

Figure 2.13. Dose discrimination in response CpG and TNF stimulation.

Confusion matrices showing precision (top) and sensitivity (bottom) of dose classification based on NFκB dynamics in response to p(I:C) (A) and TNF (B) in macrophages from healthy mice (left) and Sjögren's syndrome mouse model (right).

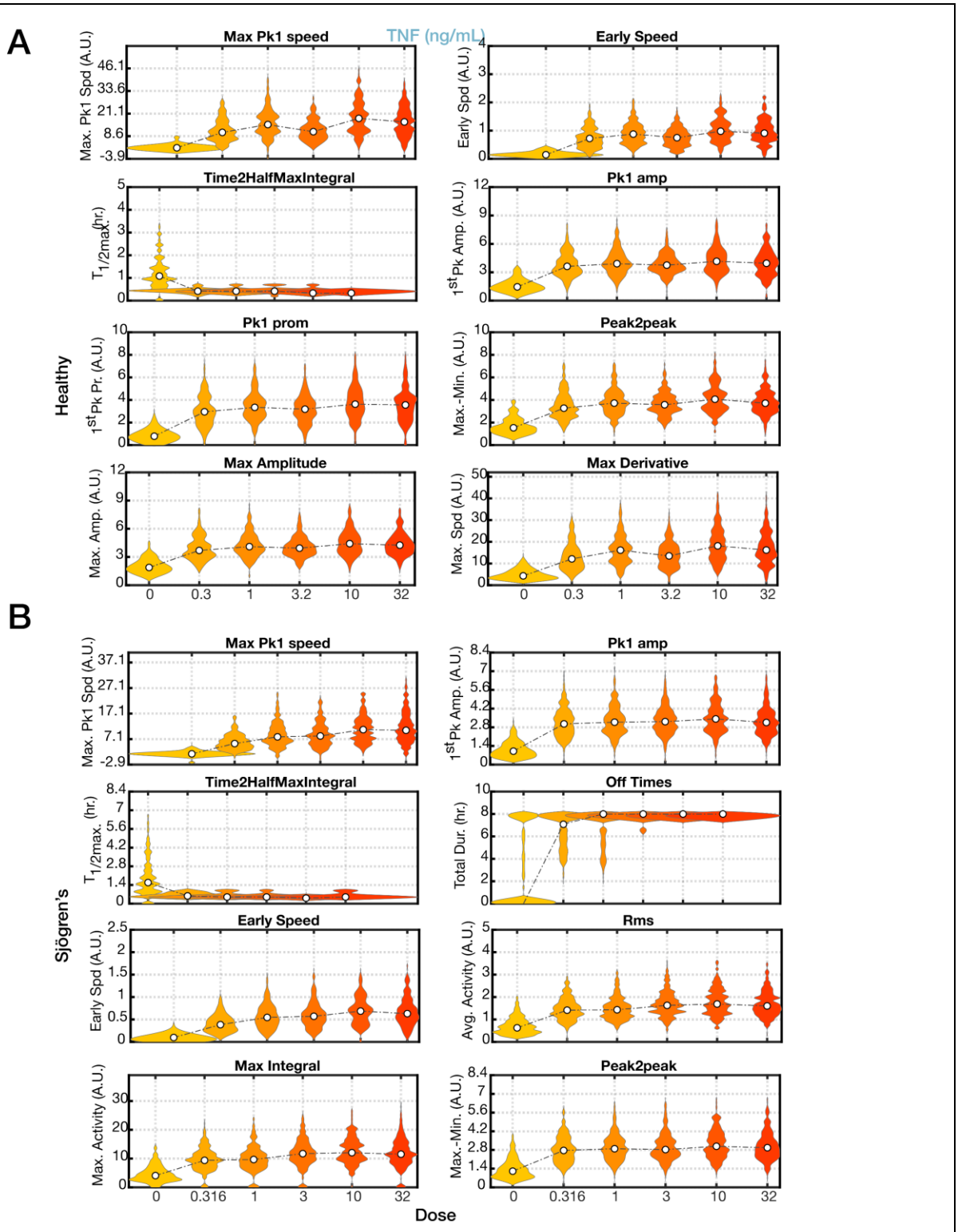

Figure 2.14. Important features for dose classification in response to TNF.

Most important features for dose discrimination in TNF-stimulated macrophages from healthy mice (A) and from Sjögren's syndrome mouse model (B).

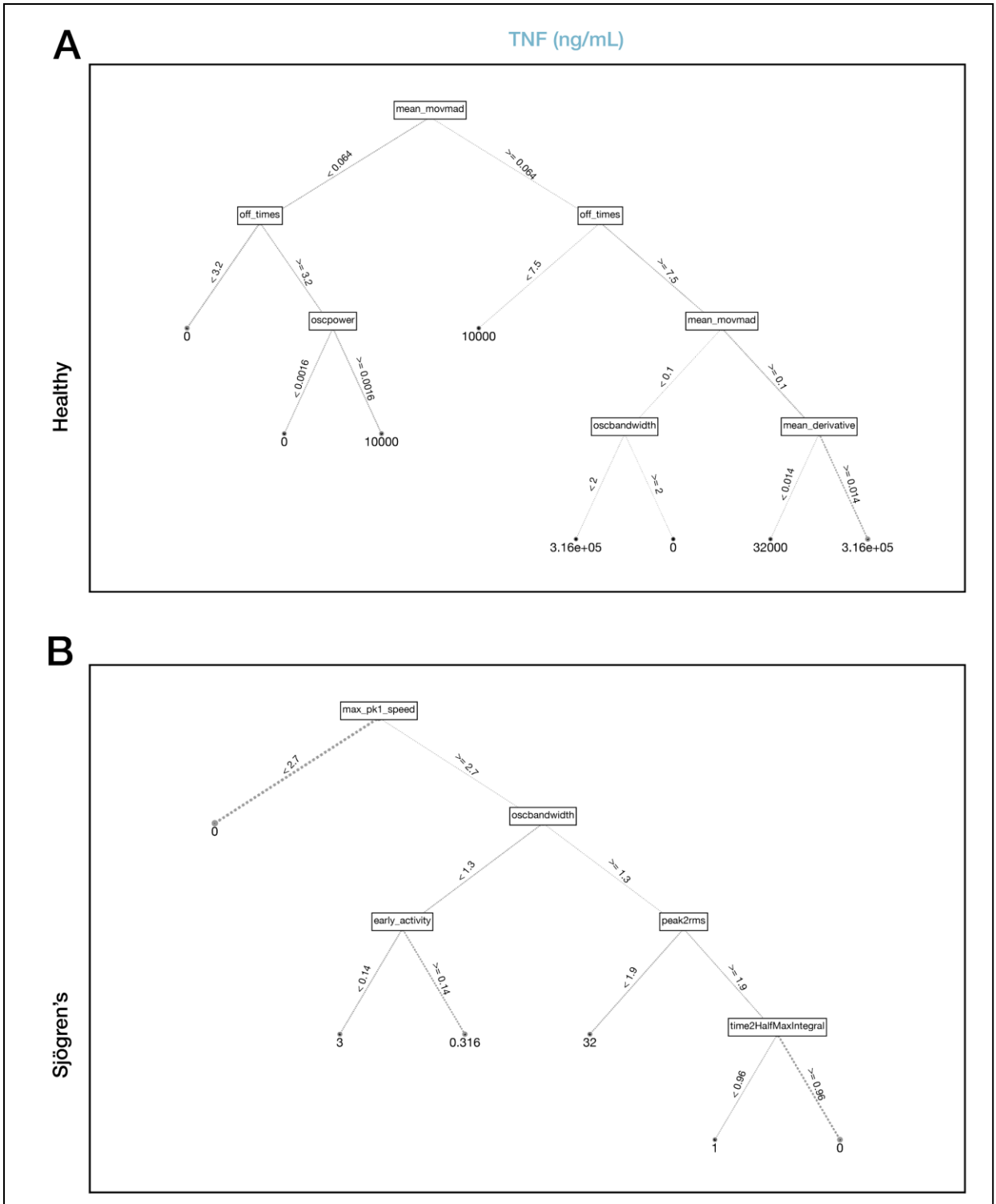

Figure 2.15 Sample decision tree for classifying TNF doses in macrophages from healthy (A) and Sjögren's syndrome mouse model (B).

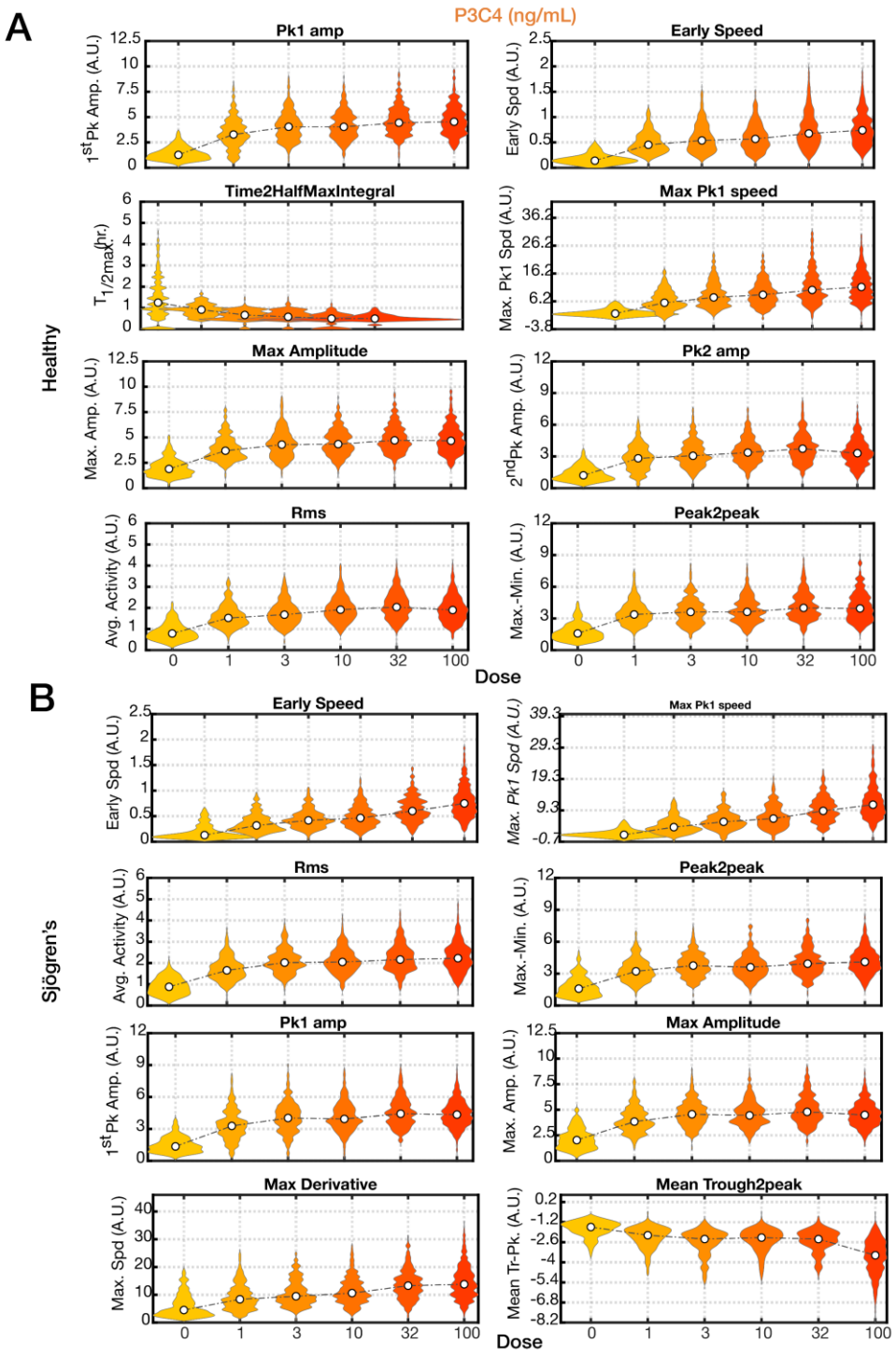

Figure 2.16. Important features for dose classification in response to P3C4.

Most important features for dose discrimination in P3C4-stimulated macrophages from healthy mice (A) and from Sjögren's syndrome mouse model (B).

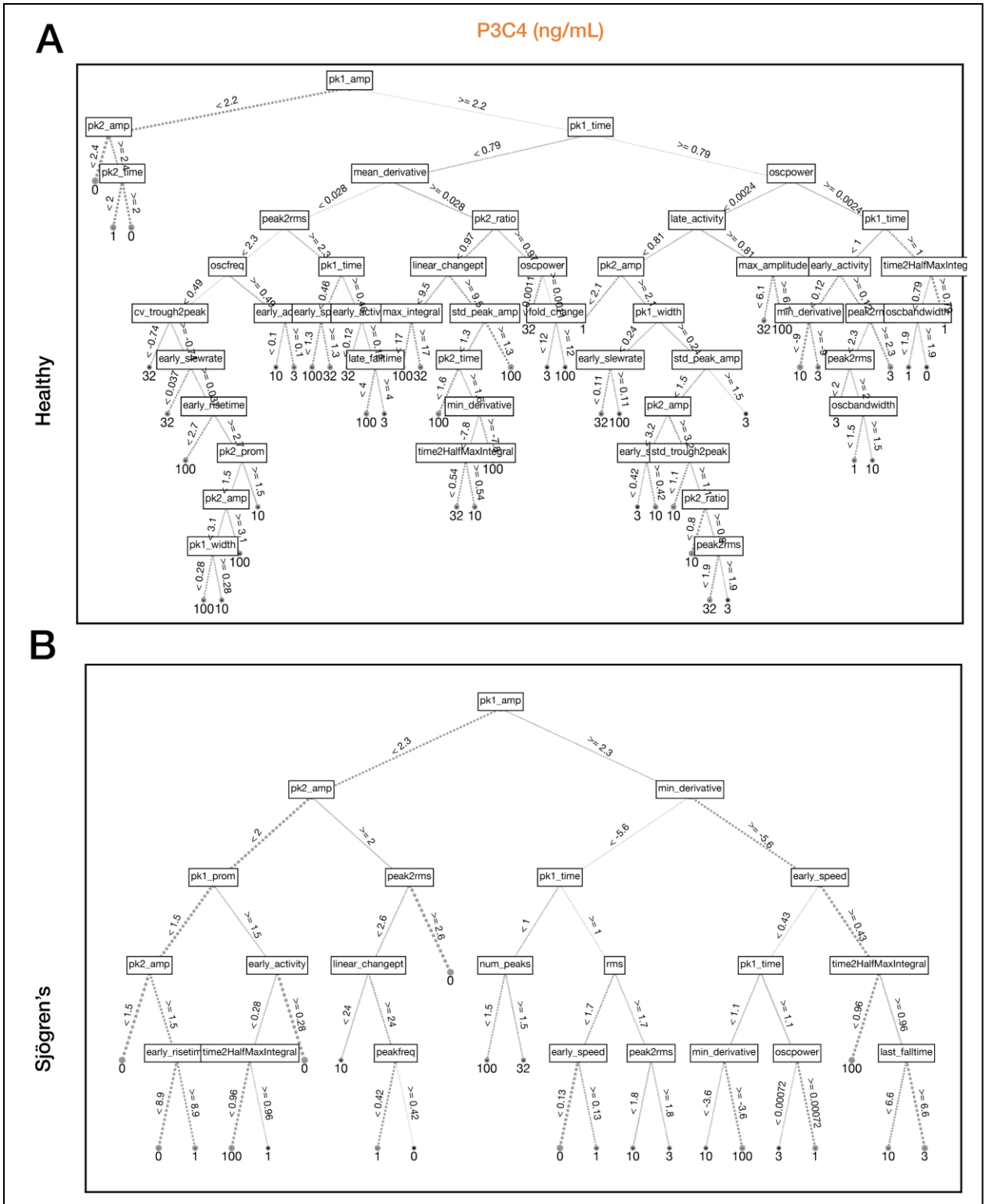

Figure 2.17. Sample decision tree for classifying P3C4 doses in macrophages from healthy (A) and Sjögren's syndrome mouse model (B).

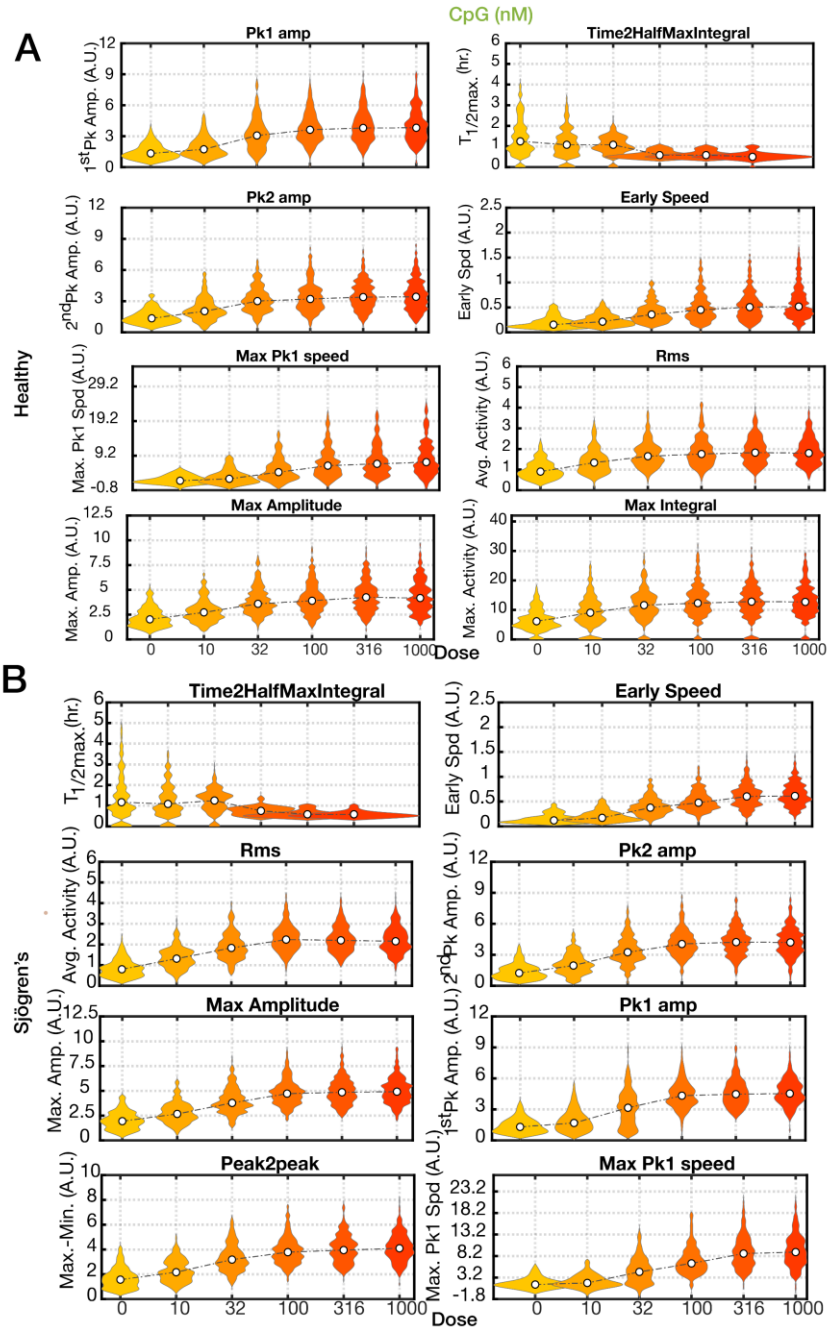

Figure 2.18. Important features for dose classification in response to CpG.

Most important features for dose discrimination in CpG-stimulated macrophages from healthy mice (A) and from Sjögren's syndrome mouse model (B).

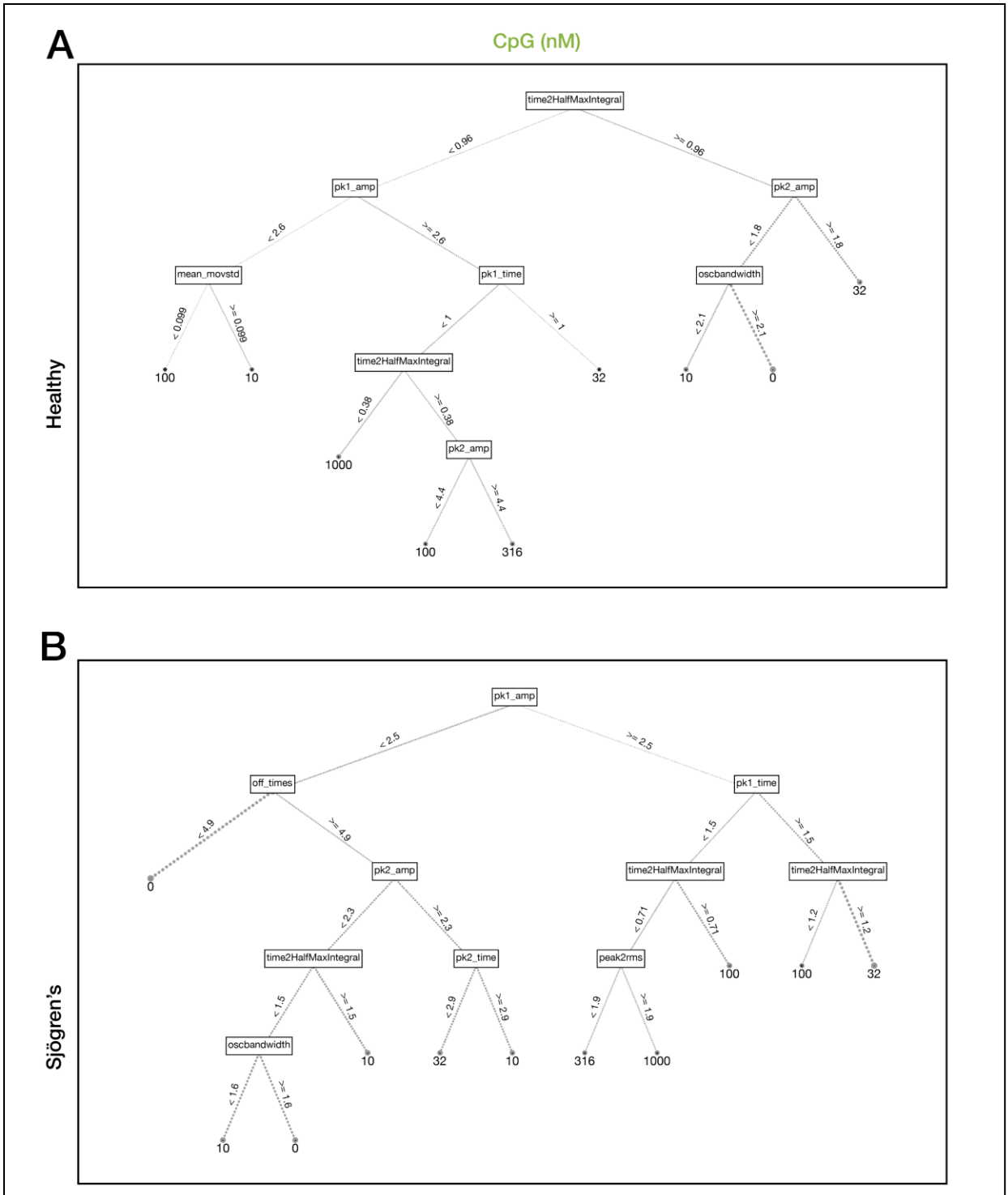

Figure 2.19. Sample decision tree for classifying CpG doses in macrophages from healthy (A) and Sjögren's syndrome mouse model (B).

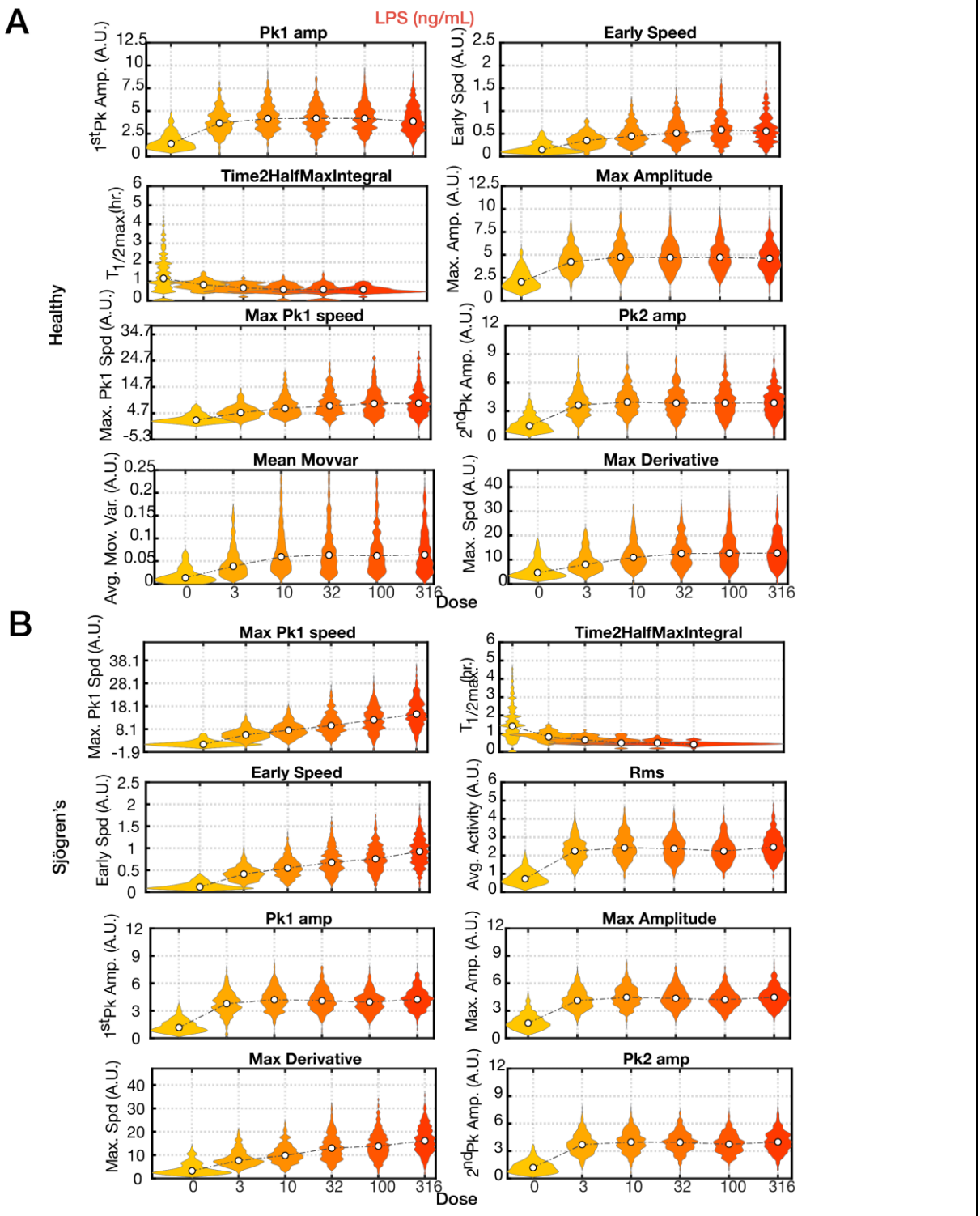

Figure 2.20. Important features for dose classification in response to LPS.

Most important features for dose discrimination in LPS-stimulated macrophages from healthy mice (A) and from Sjögren's syndrome mouse model (B).

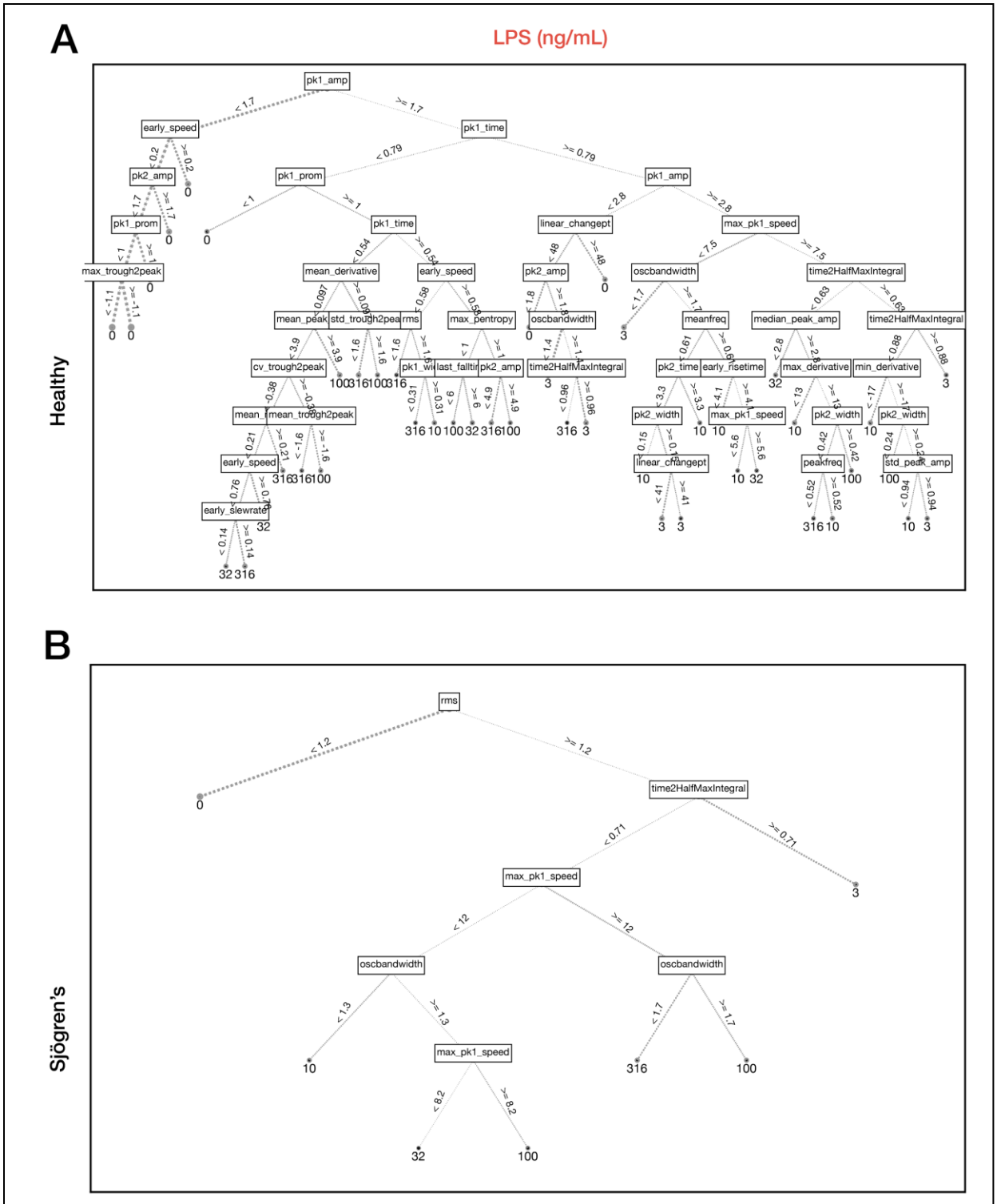

Figure 2.21. Sample decision tree for classifying LPS doses in macrophages from healthy (A) and Sjögren's syndrome mouse model (B).

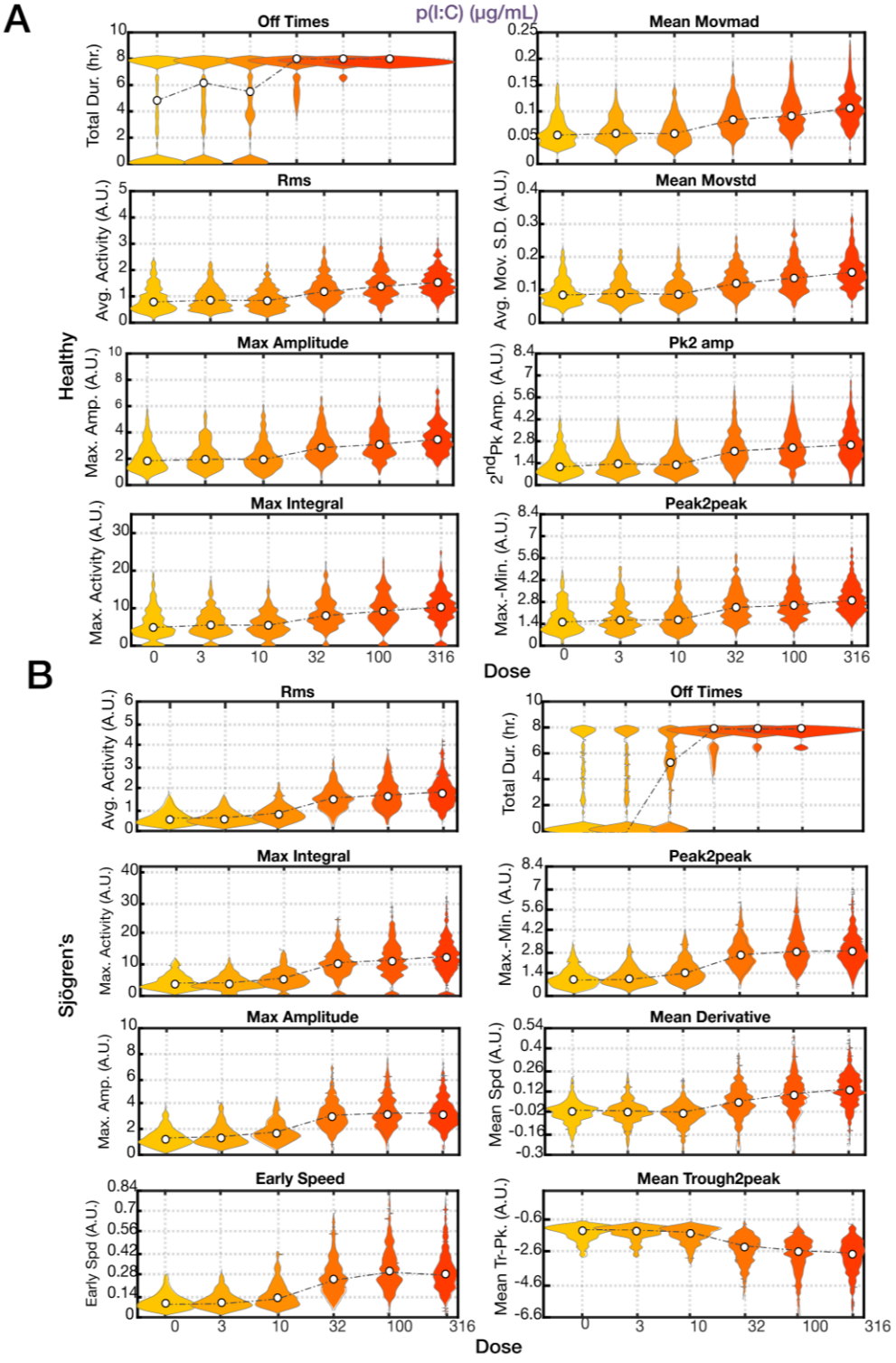

Figure 2.22. Important features for dose classification in response to p(I:C).

Most important features for dose discrimination in p(I:C)-stimulated macrophages from healthy mice (A) and from Sjögren's syndrome mouse model (B).

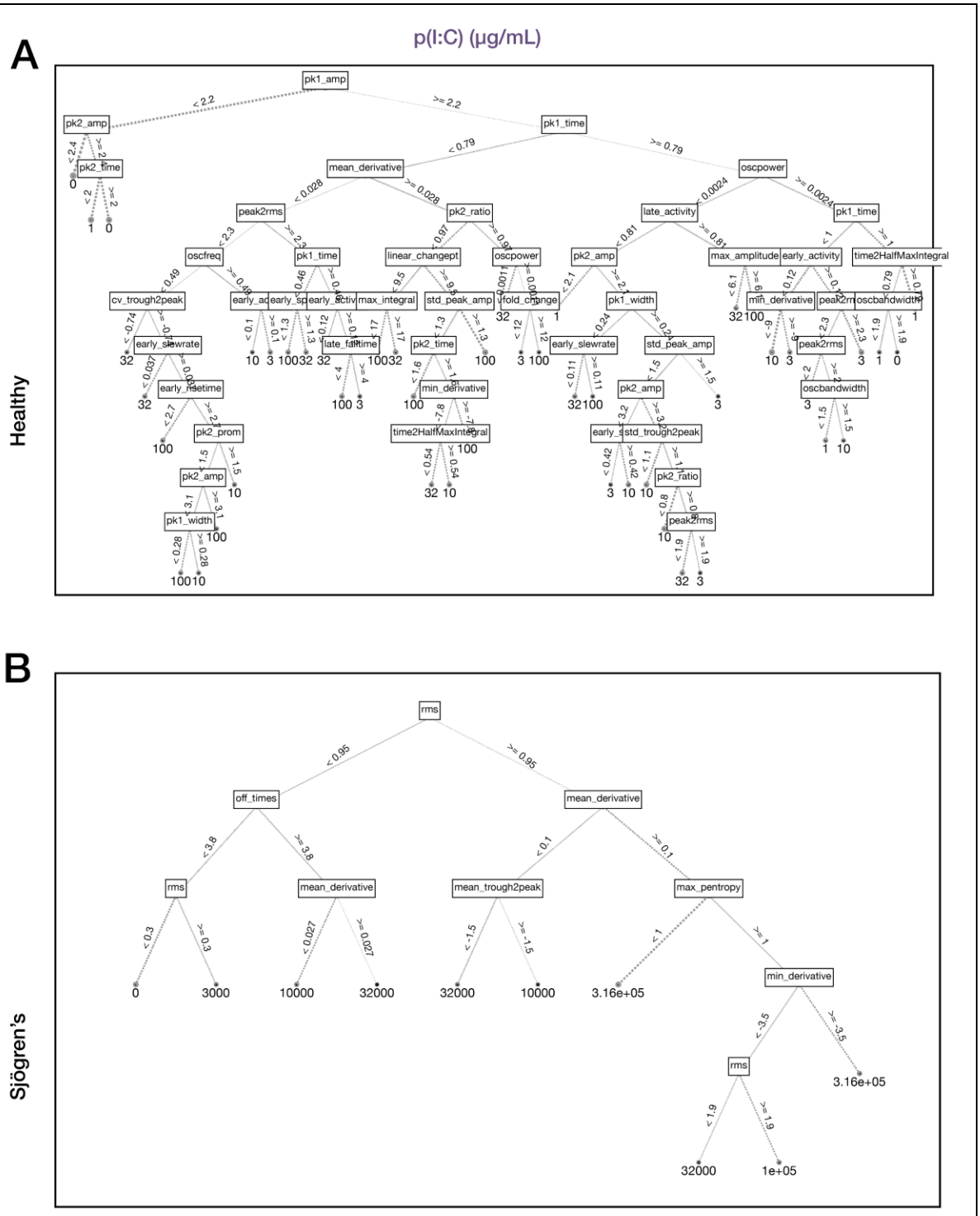

Figure 2.23. Sample decision tree for classifying p(I:C) doses in macrophages from healthy (A) and Sjögren's syndrome mouse model (B).

Material and methods

Mouse Models. The mVenus-RelA endogenously-tagged mouse line was generated by Ingenious Targeting Laboratory. A donor sequence encoding the monomeric variant of the Venus fluorescent protein (Koushik et al., 2006) joined by a short flexible linker sequence directly upstream of the start codon of the murine *Rela* locus was used to generate, via homologous recombination, a tagged embryonic stem cell line, that was implanted to yield heterozygous mice. These mice were then bred with a mouse line constitutively expressing the *Flp* recombinase to remove the *Neo* resistance marker included in the homologous donor sequence. We then back-crossed the resultant mice with wild-type C57BL/6J mice to remove the *Flp* background and generate homozygously tagged mice. For the Sjögren's syndrome mouse model, we crossed mVenus-RelA mice into a IκBα$^{M/M}$ line. This strain harbors mutated κB sites in the IκBα promoter (B. Peng et al., 2010).

Macrophage Cell Culture. BMDMs were prepared by culturing bone marrow monocytes from femurs of 8-12 week old mice in CMG 14-12-conditioned medium or L929 -conditioned medium using standard methods (Cheng et al., 2015; Takeshita et al., 2000). BMDMs were re-plated in imaging dishes on day 4, then were stimulated on day 7.

IMPDMs were differentiated from myeloid progenitor cells immortalized using HoxB4 transduction (Ruedl et al., 2008). IMPDMs were re-plated in imaging dishes on day 6, then were stimulated on day 9.

METHOD DETAILS

Macrophage stimulation conditions. BMDMs were stimulated with indicated concentrations of lipopolysaccharide (LPS, Sigma Aldrich), murine TNF (R&D), a TLR1/2 agonist, the synthetic triacylated lipoprotein Pam3CSK4 (P3C4), a TLR3 agonist, low molecular weight

polyinosine-polycytidylic acid (Poly(I:C) (p(I:C)), Invivogen), a TLR9 agonist, the synthetic CpG ODN 1668 (CpG) (Invivogen).

Live-cell imaging. Bone-marrow macrophages were replated on day 4 at 20,000 or 15,000/cm^2 in an 8-well ibidi SlideTek chamber, for imaging at an appropriate density (approx. 60,000/cm^2) on day 6 or day 7. 2 hours prior to stimulation, a solution of 2.5 ng/mL Hoechst 33342 was added to the BMDM culture media. After the start of imaging, additional culture media containing stimulus (TNF, LPS, poly(I:C), CpG, or P3C4) was injected into the chamber *in situ*. Cells were imaged at 5-minute intervals on a Zeiss Axio Observer platform with live-cell incubation, using epifluorescent excitation from a Sutter Lambda XL light source. Images were recorded on a Hamamatsu Orca Flash 2.0 CCD camera.

QUANTIFICATION AND STATISTICAL ANALYSIS

Image analysis and processing

Microscopy time-lapse images were exported for single-cell tracking and measurement in MATLAB R2016a. The tracking routines followed those used in earlier work (Selimkhanov et al., 2014). Briefly, cells were identified using DIC images, then segmented, guided by markers from the Hoechst image. Segmented cells were linked into trajectories across successive images, then nuclear and cytoplasmic boundaries were saved and used to define measurement regions in other fluorescent channels, including mVenus-NFκB. Nuclear NFκB levels were quantified on a per-cell basis, normalized to image background levels, then were baseline-subtracted. Mitotic cells, as well as cells that drifted out of the field of view, were excluded from analysis. The toolboxes used for this analysis are available at GitHub.

Machine Learning Classifier

Construction of classification models. I trained an ensemble of 100 decision trees using the fitcensemble function from the Statistics and Machine Learning Toolbox from MathWorks. Decision tree models are simple, highly interpretable, and can be displayed graphically (James et al., 2013). Consequently, the decision process of the classifier can be easily interrogated. However, decision tree models have two key disadvantages: (1) modest prediction performance (Caruana and Niculescu-Mizil, 2006) and (2) high variance due to overfitting (James et al., 2013). Both disadvantages can be mitigated by aggregating an ensemble of decision trees. Empirical comparison of classification models show that ensembles of decision trees outperform other classification algorithms across of a variety of problem sets (Caruana and Niculescu-Mizil, 2006).

We used a bootstrap aggregation (bag) method for constructing the ensembles. Each tree in the ensemble is trained on a bootstrapped replica of the data—each replica is a random selection of the data with replacement. The predictions from the ensemble model are determined by a majority vote from each individual tree prediction. We trained the ensemble to learn the stimulus labels (TNF, Pam3CSK4, CpG, LPS, and poly(I:C)) from a subset of features or transformed features generated from autoencoders (MathWorks, 2017).

Decision tree parameters. To construct each decision tree, the software considers all possible ways to split the data into two nodes based on the values of every predictor. Then, it chooses the best splitting decision based on constraints imposed by training parameters, such as the minimum number of observations that must be present in a child node (MinLeafSize) and a predictor selection criterion. The software recursively splits each child

node until a stopping criterion is reached. The stopping criteria include (1) obtaining a pure node that contains only observations from a single class, (2) reaching the minimum number of observations for a parent node (MinParentSize), (3) reaching a split that would produce a child node with fewer observations than MinLeafSize, and (4) reaching the maximum number of splits (MaxNumSplits). We used default values for MinLeafSize, MinParentSize, and MaxNumSplits: 1, 10, sample size – 1, respectively (MathWorks, 2017).

Since the standard prediction selection process at each node may be biased, we used a predictor selection technique, the interaction-curvature test, which minimizes predictor selection bias, enhances interpretation of the model, and facilitates inference of predictor importance. The interaction-curvature technique selects a predictor to split at each node based on the *p*-values of curvature and interaction tests. Whereas the curvature test examines the null hypothesis that the predictor and response variables are unassociated, the interaction test examines the null hypothesis that a pair of predictor variables and the response variable are unassociated. A node with no tests that yield *p*-values ≤ 0.05 is not split. At each node, the predictor or pair of predictors that yield the minimum significant *p*-value (0.05) is chosen for splitting. To split the node, the software chooses the splitting rule that maximizes the impurity gain—difference in the impurity of the node (calculated using Gini's diversity index) and the impurity of its children nodes (MathWorks, 2017).

Evaluation. We evaluated the performance of the classifiers using 5-fold cross validation, an independent testing data set, or out of bag cross validation. We used the following performance metrics: true positive rate (recall), positive predictive value (precision), area under the Receiver Operating Characteristic (ROC) curve, F1 score, Matthews correlation

coefficient, markedness, informedness and mean classification margin (Akosa, 2017; Powers, 2007; Vihinen, 2012).

Data and code availability

Software associated with the image processing and data analysis are available at:

https://github.com/Adewunmi91/MACKtrack,

https://github.com/Adewunmi91/nfkb_dynamics,

https://github.com/Adewunmi91/nfkb_classification

Acknowledgement

Results in this chapter were adapted from a manuscript in revision:

Taylor, B.*, **Adelaja, A*.,** Liu, Y., Luecke, S., Hoffmann, A. (2020). Identification and physiological significance of temporal NFκB signaling codewords deployed by macrophages to classify immune threats. bioRxiv. DOI: https://doi.org/10.1101/2020.05.23.112862

Bibliography

Akosa, J.S., 2017. Predictive Accuracy : A Misleading Performance Measure for Highly Imbalanced Data. SAS Glob. Forum 942, 1–12.

Alpaydin, E., 2014. Introduction to Machine Learning Ethem Alpaydin., Introduction to machine learning.

Barken, D., Wang, C.J., Kearns, J., Cheong, R., Hoffmann, A., Levchenko, A., 2005. Comment on "Oscillations in NF-κB Signaling Control the Dynamics of Gene Expression." Science 308, 52; author reply 52. https://doi.org/10.1126/science.1107904

Bauer, J., Bahmer, F.A., Wörl, J., Neuhuber, W., Schuler, G., Fartasch, M., 2001. A strikingly constant ratio exists between Langerhans cells and other epidermal cells in human skin. A stereologic study using the optical disector method and the confocal laser scanning microscope. J. Invest. Dermatol. 116, 313–8. https://doi.org/10.1046/j.1523-1747.2001.01247.x

Behar, M., Hoffmann, A., 2010. Understanding the temporal codes of intra-cellular signals. Curr. Opin. Genet. Dev. 20, 684–693. https://doi.org/10.1016/j.gde.2010.09.007

Benoit, M., Desnues, B., Mege, J.-L., 2008. Macrophage Polarization in Bacterial Infections. J. Immunol. 181, 3733–3739. https://doi.org/10.4049/jimmunol.181.6.3733

Caruana, R., Niculescu-Mizil, A., 2006. An empirical comparison of supervised learning algorithms. Proc. 23rd Int. Conf. Mach. Learn. C, 161–168. https://doi.org/10.1145/1143844.1143865

Cheng, C.S., Behar, M.S., Suryawanshi, G.W., Feldman, K.E., Spreafico, R., Hoffmann, A., 2017. Iterative Modeling Reveals Evidence of Sequential Transcriptional Control Mechanisms. Cell Syst. 4, 330-343.e5. https://doi.org/10.1016/j.cels.2017.01.012

Cheng, Q.J., Ohta, S., Sheu, K.M., Spreafico, R., Adelaja, A., Taylor, B., Hoffmann, A., 2020. NFκB dynamics determine the stimulus-specificity of epigenomic reprogramming in macrophages. bioRxiv. https://doi.org/10.1101/2020.02.18.954602

Cheng, Z., Taylor, B., Ourthiague, D.R., Hoffmann, A., 2015. Distinct single-cell signaling characteristics are conferred by the MyD88 and TRIF pathways during TLR4 activation. Sci. Signal. 8, ra69. https://doi.org/10.1126/scisignal.aaa5208

Chovatiya, R., Medzhitov, R., 2014. Stress, inflammation, and defense of homeostasis. Mol.

Cell. https://doi.org/10.1016/j.molcel.2014.03.030

Cleynen, I., Vermeire, S., 2012. Paradoxical inflammation induced by anti-TNF agents in patients with IBD. Nat. Rev. Gastroenterol. Hepatol. 9, 496–503. https://doi.org/10.1038/nrgastro.2012.125

Covert, M.W., Leung, T.H., Gaston, J.E., Baltimore, D., 2005. Achieving stability of lipopolysaccharide-induced NF-kappaB activation. Science 309, 1854–7. https://doi.org/10.1126/science.1112304

De Lorenzi, R., Gareus, R., Fengler, S., Pasparakis, M., 2009. GFP-p65 knock-in mice as a tool to study NF-kappaB dynamics in vivo. Genesis 47, 323–9. https://doi.org/10.1002/dvg.20468

Gottschalk, R.A., Martins, A.J., Angermann, B.R., Dutta, B., Ng, C.E., Uderhardt, S., Tsang, J.S., Fraser, I.D.C., Meier-Schellersheim, M., Germain, R.N., 2016. Distinct NF-κB and MAPK Activation Thresholds Uncouple Steady-State Microbe Sensing from Anti-pathogen Inflammatory Responses. Cell Syst. 2, 378–390. https://doi.org/10.1016/j.cels.2016.04.016

Harris, R.A., 2017. Macrophage Metabolism As Therapeutic Target for Cancer , Atherosclerosis , and Obesity 8. https://doi.org/10.3389/fimmu.2017.00289

Hoffmann, A., Baltimore, D., 2006. Circuitry of nuclear factor kappaB signaling. Immunol. Rev. 210, 171–186. https://doi.org/10.1111/j.0105-2896.2006.00375.x

Hoffmann, A., Levchenko, A., Scott, M.L., Baltimore, D., 2002. The IκB-NF-κB Signaling Module: Temporal Control and Selective Gene Activation. Science 298, 1241–5. https://doi.org/10.1126/science.1071914

James, G., Witten, D., Hastie, T., Tibshirani, R., 2013. An Introduction to Statistical Learning, Springer Texts in Statistics. Springer New York, New York, NY. https://doi.org/10.1007/978-1-4614-7138-7

Kalliolias, G.D., Ivashkiv, L.B., 2015. TNF biology, pathogenic mechanisms and emerging therapeutic strategies. Nat. Rev. Rheumatol. 12, 49–62. https://doi.org/10.1038/nrrheum.2015.169

Kearns, J.D., Basak, S., Werner, S.L., Huang, C.S., Hoffmann, A., 2006. IκBε provides negative feedback to control NF-κB oscillations, signaling dynamics, and inflammatory gene expression. J. Cell Biol. 173, 659–664. https://doi.org/10.1083/jcb.200510155

Koushik, S. V, Chen, H., Thaler, C., Puhl, H.L., Vogel, S.S., 2006. Cerulean, Venus, and VenusY67C FRET reference standards. Biophys. J. 91, L99–L101. https://doi.org/10.1529/biophysj.106.096206

Lane, K., Van Valen, D., DeFelice, M.M., Macklin, D.N., Kudo, T., Jaimovich, A., Carr, A., Meyer, T., Pe'er, D., Boutet, S.C., Covert, M.W., 2017. Measuring Signaling and RNA-Seq in the Same Cell Links Gene Expression to Dynamic Patterns of NF-κB Activation. Cell Syst. 4, 458-469.e5. https://doi.org/10.1016/j.cels.2017.03.010

Lee, R.E.C., Walker, S.R., Savery, K., Frank, D.A., Gaudet, S., 2014. Fold change of nuclear NF-κB determines TNF-induced transcription in single cells. Mol. Cell 53, 867–879. https://doi.org/10.1016/j.molcel.2014.01.026

Lee, T.K., Denny, E.M., Sanghvi, J.C., Gaston, J.E., Maynard, N.D., Hughey, J.J., Covert, M.W., 2009. A noisy paracrine signal determines the cellular NF-kappaB response to lipopolysaccharide. Sci. Signal. 2, ra65. https://doi.org/10.1126/scisignal.2000599

Lisi, S., Sisto, M., Lofrumento, D.D., D'Amore, M., 2012. Altered IκBα expression promotes NF-κB activation in monocytes from primary Sjo gren's syndrome patients. Pathology 44, 557–561. https://doi.org/10.1097/PAT.0b013e3283580388

Marshak-Rothstein, A., 2006. Toll-like receptors in systemic autoimmune disease. Nat. Rev. Immunol. 6, 823–835. https://doi.org/10.1038/nri1957

Martin, E.W., Pacholewska, A., Patel, H., Dashora, H., Sung, M.-H., 2020. Integrative analysis suggests cell type–specific decoding of NF-κB dynamics. Sci. Signal. 13, eaax7195. https://doi.org/10.1126/scisignal.aax7195

Martinez, F.O., Gordon, S., 2014. The M1 and M2 paradigm of macrophage activation: time for reassessment. F1000Prime Rep. 6, 13. https://doi.org/10.12703/P6-13

MathWorks, 2017. Statistics and Machine Learning Toolbox™ User's Guide. Natick, MA.

Medzhitov, R., Horng, T., 2009. Transcriptional control of the inflammatory response. Nat. Rev. Immunol. https://doi.org/10.1038/nri2634

Mosser, D.M., Edwards, J.P., 2008. Exploring the full spectrum of macrophage activation. Nat. Rev. Immunol. 8, 958–69. https://doi.org/10.1038/nri2448

Mothes, J., Busse, D., Kofahl, B., Wolf, J., 2015. Sources of dynamic variability in NF-κB signal transduction: a mechanistic model. Bioessays 37, 452–62. https://doi.org/10.1002/bies.201400113

Murray, P.J., Wynn, T.A., 2011. Protective and pathogenic functions of macrophage subsets. Nat. Rev. Immunol. 11, 723–37. https://doi.org/10.1038/nri3073

Murray, P.J.J., Allen, J.E.E., Biswas, S.K.K., Fisher, E.A.A., Gilroy, D.W.W., Goerdt, S.,

Gordon, S., Hamilton, J.A.A., Ivashkiv, L.B.B., Lawrence, T., Locati, M., Mantovani, A., Martinez, F.O.O., Mege, J.-L., Mosser, D.M.M., Natoli, G., Saeij, J.P.P., Schultze, J.L.L., Shirey, K.A.A., Sica, A., Suttles, J., Udalova, I., van Ginderachter, J.A., Vogel, S.N.N., Wynn, T.A.A., Goerdt, S., Ivashkiv, L.B.B., Sica, A., Mosser, D.M.M., Shirey, K.A.A., Natoli, G., Gilroy, D.W.W., Martinez, F.O.O., Gordon, S., Allen, J.E.E., Schultze, J.L.L., Mantovani, A., Murray, P.J.J., Wynn, T.A.A., Biswas, S.K.K., Suttles, J., Udalova, I., Hamilton, J.A.A., van Ginderachter, J.A., Mege, J.-L., Locati, M., Fisher, E.A.A., Lawrence, T., Allen, J.E.E., Biswas, S.K.K., Fisher, E.A.A., Gilroy, D.W.W., Goerdt, S., Gordon, S., Hamilton, J.A.A., Ivashkiv, L.B.B., Lawrence, T., Locati, M., Mantovani, A., Martinez, F.O.O., Mege, J.-L., Mosser, D.M.M., Natoli, G., Saeij, J.P.P., Schultze, J.L.L., Shirey, K.A.A., Sica, A., Suttles, J., Udalova, I., van Ginderachter, J.A., Vogel, S.N.N., Wynn, T.A.A., van Ginderachter, J.A., Vogel, S.N.N., Wynn, T.A.A., van Ginderachter, J.A., Vogel, S.N.N., Wynn, T.A.A., 2014. Macrophage Activation and Polarization: Nomenclature and Experimental Guidelines. Immunity 41, 14–20. https://doi.org/10.1016/j.immuni.2014.06.008

Nordmark, G., Wang, C., Vasaitis, L., Eriksson, P., Theander, E., Kvarnström, M., Forsblad-d'Elia, H., Jazebi, H., Sjöwall, C., Reksten, T.R., Brun, J.G., Jonsson, M. V., Johnsen, S.J., Wahren-Herlenius, M., Omdal, R., Jonsson, R., Bowman, S., Ng, W.F., Eloranta, M.L., Syvänen, A.C., 2013. Association of Genes in the NF-κB Pathway with Antibody-Positive Primary Sjögren's Syndrome. Scand. J. Immunol. 78, 447–454. https://doi.org/10.1111/sji.12101

O'Dea, E., Hoffmann, A., 2009. NF-κB signaling. Wiley Interdiscip. Rev. Syst. Biol. Med. 1, 107–15. https://doi.org/10.1002/wsbm.30

Ou, T.T., Lin, C.H., Lin, Y.C., Li, R.N., Tsai, W.C., Liu, H.W., Yen, J.H., 2008. IkBα promoter polymorphisms in patients with primary Sjögren's syndrome. J. Clin. Immunol. 28, 440–444. https://doi.org/10.1007/s10875-008-9212-5

Pękalski, J., Zuk, P.J., Kochańczyk, M., Junkin, M., Kellogg, R., Tay, S., Lipniacki, T., 2013. Spontaneous NF-κB activation by autocrine TNFα signaling: a computational analysis. PLoS One 8, e78887. https://doi.org/10.1371/journal.pone.0078887

Peng, B., Ling, J., Lee, A.J., Wang, Z., Chang, Z., Jin, W., Kang, Y., Zhang, R., Shim, D., Wang, H., Fleming, J.B., Zheng, H., Sun, S.-C., Chiao, P.J., 2010. Defective feedback regulation of NF-κB underlies Sjögren's syndrome in mice with mutated κB enhancers of the IκBα promoter. Proc. Natl. Acad. Sci. 107, 15193–15198. https://doi.org/10.1073/pnas.1005533107

Peng, Bailu, Ling, J., Lee, A.J., Wang, Z., Chang, Z., Jin, W., Kang, Y., Zhang, R., Shim, D., Wang, H., Fleming, J.B., Zheng, H., Sun, S.C., Chiao, P.J., 2010. Defective feedback regulation of NF-κB underlies Sjögren's syndrome in mice with mutated κB enhancers of the IκBα promoter. Proc. Natl. Acad. Sci. U. S. A. 107, 15193–15198. https://doi.org/10.1073/pnas.1005533107

Pollard, J.W., 2009. Trophic macrophages in development and disease. Nat. Rev. Immunol. 9, 259–70. https://doi.org/10.1038/nri2528

Powers, D.M.W., 2007. Evaluation: From Precision, Recall and F-Factor to ROC, Informedness, Markedness & Correlation.

Purvis, J.E., Lahav, G., 2013. Encoding and decoding cellular information through signaling dynamics. Cell 152, 945–56. https://doi.org/10.1016/j.cell.2013.02.005

Ruedl, C., Khameneh, H.J., Karjalainen, K., 2008. Manipulation of immune system via immortal bone marrow stem cells. Int. Immunol. 20, 1211–1218. https://doi.org/10.1093/intimm/dxn079

Selimkhanov, J., Taylor, B., Yao, J., Pilko, A., Albeck, J., Hoffmann, A., Tsimring, L., Wollman, R., 2014. Systems biology. Accurate information transmission through dynamic biochemical signaling networks. Science 346, 1370–3. https://doi.org/10.1126/science.1254933

Sen, S., Cheng, Z., Sheu, K.M., Chen, Y.H., Hoffmann, A., 2020. Gene Regulatory Strategies that Decode the Duration of NFκB Dynamics Contribute to LPS- versus TNF-Specific Gene Expression. Cell Syst. 10, 169-182.e5. https://doi.org/10.1016/j.cels.2019.12.004

Sisto, M., Lisi, S., Lofrumento, D.D., Ingravallo, G., De Lucro, R., D'Amore, M., 2013. Salivary gland expression level of IκBα regulatory protein in Sjögren's syndrome. J. Mol. Histol. 44, 447–454. https://doi.org/10.1007/s10735-013-9487-6

Sung, M.-H., Salvatore, L., De Lorenzi, R., Indrawan, A., Pasparakis, M., Hager, G.L., Bianchi, M.E., Agresti, A., 2009. Sustained oscillations of NF-kappaB produce distinct genome scanning and gene expression profiles. PLoS One 4, e7163. https://doi.org/10.1371/journal.pone.0007163

Takeshita, S., Kaji, K., Kudo, A., 2000. Identification and characterization of the new osteoclast progenitor with macrophage phenotypes being able to differentiate into mature osteoclasts. J. Bone Miner. Res. 15, 1477–88. https://doi.org/10.1359/jbmr.2000.15.8.1477

Takeuchi, Osamu Akira, S., 2010. Pattern Recognition Receptors and Inflammation. Cell

140, 805–820. https://doi.org/10.1016/j.cell.2010.01.022

Tay, S., Hughey, J.J., Lee, T.K., Lipniacki, T., Quake, S.R., Covert, M.W., 2010. Single-cell NF-kappaB dynamics reveal digital activation and analogue information processing. Nature 466, 267–71. https://doi.org/10.1038/nature09145

Taylor, B., Adelaja, A., Liu, Y., Luecke, S., Hoffmann, A., 2020. Identification and physiological significance of temporal NFκB signaling codewords deployed by macrophages to classify immune threats. bioRxiv 2020.05.23.112862. https://doi.org/10.1101/2020.05.23.112862

Vihinen, M., 2012. How to evaluate performance of prediction methods? Measures and their interpretation in variation effect analysis. BMC Genomics 13, S2. https://doi.org/10.1186/1471-2164-13-S4-S2

Vladimer, G.I., Marty-Roix, R., Ghosh, S., Weng, D., Lien, E., 2013. Inflammasomes and host defenses against bacterial infections. Curr. Opin. Microbiol. 16, 23–31. https://doi.org/10.1016/j.mib.2012.11.008

Werner, S.L., Barken, D., Hoffmann, A., 2005. Stimulus Specificity of Gene Expression Programs Determined by Temporal Control of IKK Activity. Science 309, 1857–61. https://doi.org/10.1126/science.1113319

Werner, S.L., Kearns, J.D., Zadorozhnaya, V., Lynch, C., O'Dea, E., Boldin, M.P., Ma, A., Baltimore, D., Hoffmann, A., 2008. Encoding NF- B temporal control in response to TNF: distinct roles for the negative regulators I B and A20. Genes Dev. 22, 2093–2101. https://doi.org/10.1101/gad.1680708

Wynn, T. a., Chawla, A., Pollard, J.W., 2013. Macrophage biology in development,

homeostasis and disease. Nature 496, 445–455. https://doi.org/10.1038/nature12034

Zambrano, S., De Toma, I., Piffer, A., Bianchi, M.E., Agresti, A., 2016. NF-κB oscillations translate into functionally related patterns of gene expression. Elife 5, e09100. https://doi.org/10.7554/eLife.09100

Chapter 3 : Characterizing the role of cytokine milieu on stimulus-specific NFκB signaling in macrophages.

Abstract

Macrophages are sentinels and guardians of tissue integrity. They coordinate stress and immune responses to host cytokines and pathogen-associated molecular patterns. As initiators of inflammation, macrophages must distinguish between different classes of stimuli to generate context-appropriate response. Failure to properly distinguish between different stimuli underlies the etiology of many inflammatory diseases. Due to the heterogeneity of macrophages, examining their responses with cell population-based assays is challenging. To fully dissect the responses of macrophages to different stimuli, single cell resolution of macrophage inflammatory responses is required. In this study, I tested the hypothesis that the cytokine milieu regulates the stimulus specificity of the macrophage inflammatory response via NFκB signaling dynamics (temporal pattern of NFκB activity).

Using time-lapse microscopy in primary macrophages, I examined the temporal pattern of NFκB nuclear translocations in response to host- and pathogen-associated ligands in different cytokine microenvironments. Analysis of NFκB signaling dynamics using supervised machine learning revealed that IFNγ conditioning of M_1 macrophages abrogates the identification of virus-associated ligands. Strikingly, this analysis shows that NFκB dynamics are insufficient to distinguish virus-associated and bacterium-associated ligands in M_1 macrophages; however, the classification performance of host-associated vs. pathogen-associated ligands using NFκB dynamics is improved in the context of IFNγ conditioning. M_{2a} conditioning of macrophages with IL-4 improves classification performance of virus-, bacterium- and host-associated ligands using NFκB dynamics. Further, TNF conditioning of macrophages improves dose classification of NFκB stimuli. These studies show that cytokine milieu of macrophages control the stimulus-specificity of NFκB signaling.

Introduction

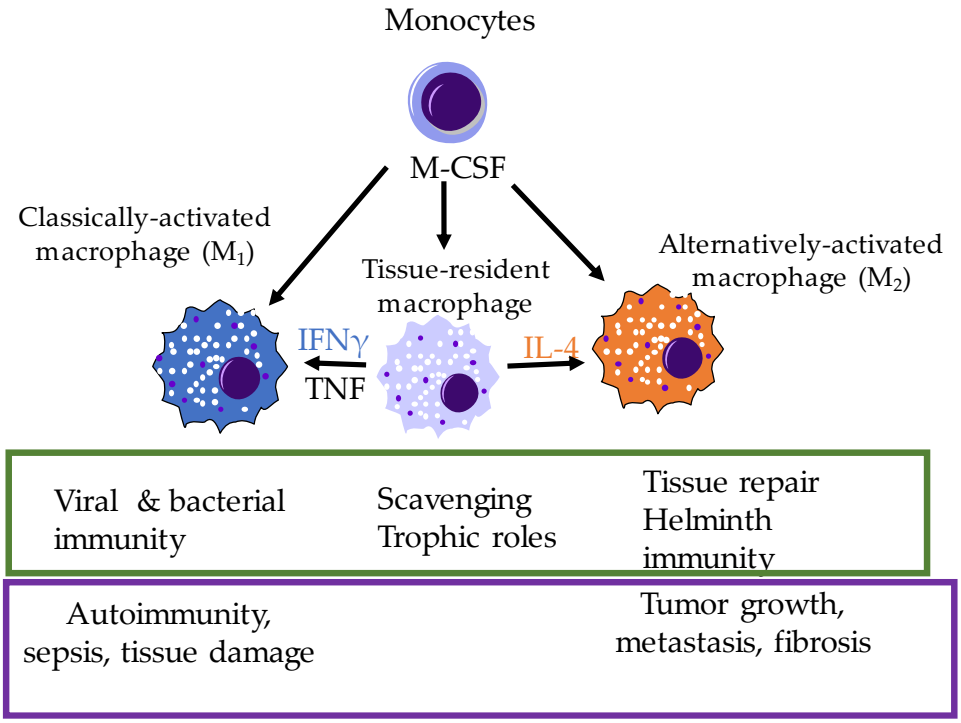

Figure 3.1. Cytokine contexts in tissue microenvironments alter macrophage functions in health and disease.

Macrophages are key regulators of inflammation, which controls diverse physiological and pathological processes (Mosser and Edwards, 2008). Inflammation is a transient response to noxious conditions such as infection or tissue injury (Chovatiya and Medzhitov, 2014). Its physiological role is to recruit leukocytes and plasma to the affected tissue to clear pathogens, remove debris, and restore homeostasis. Misregulation of macrophage-mediated

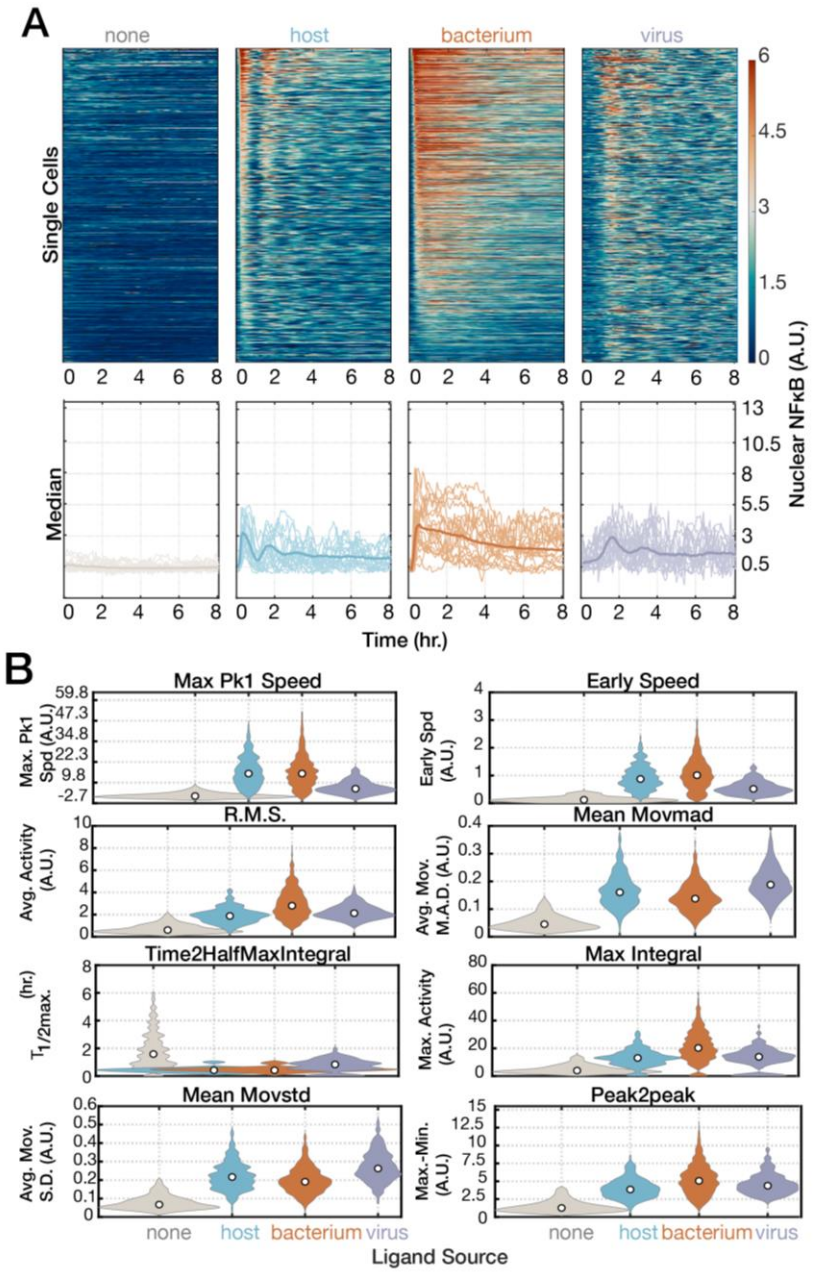

Figure 3.2. NFκB dynamics are specific to pathogen class in naïve (M_0) macrophages.

(A) Single-cell NFκB nuclear translocation dynamics in response to host-associated ligands (TNF), bacterium-associated ligands (Pam3CSK4, CpG, LPS), virus-associated ligands (p(I:C)) (top). Median NFκB trajectories and sample trajectories (bottom). Trajectories are sorted by maximum 1st peak speed. (B) Violin plots of the top 8 features that distinguish ligand types: average activity, difference between maximum and minimum NFκB values, maximum amplitude, early speed, maximum peak 1 speed, early speed, average moving mean absolute deviation, average moving variance, average peak amplitude.

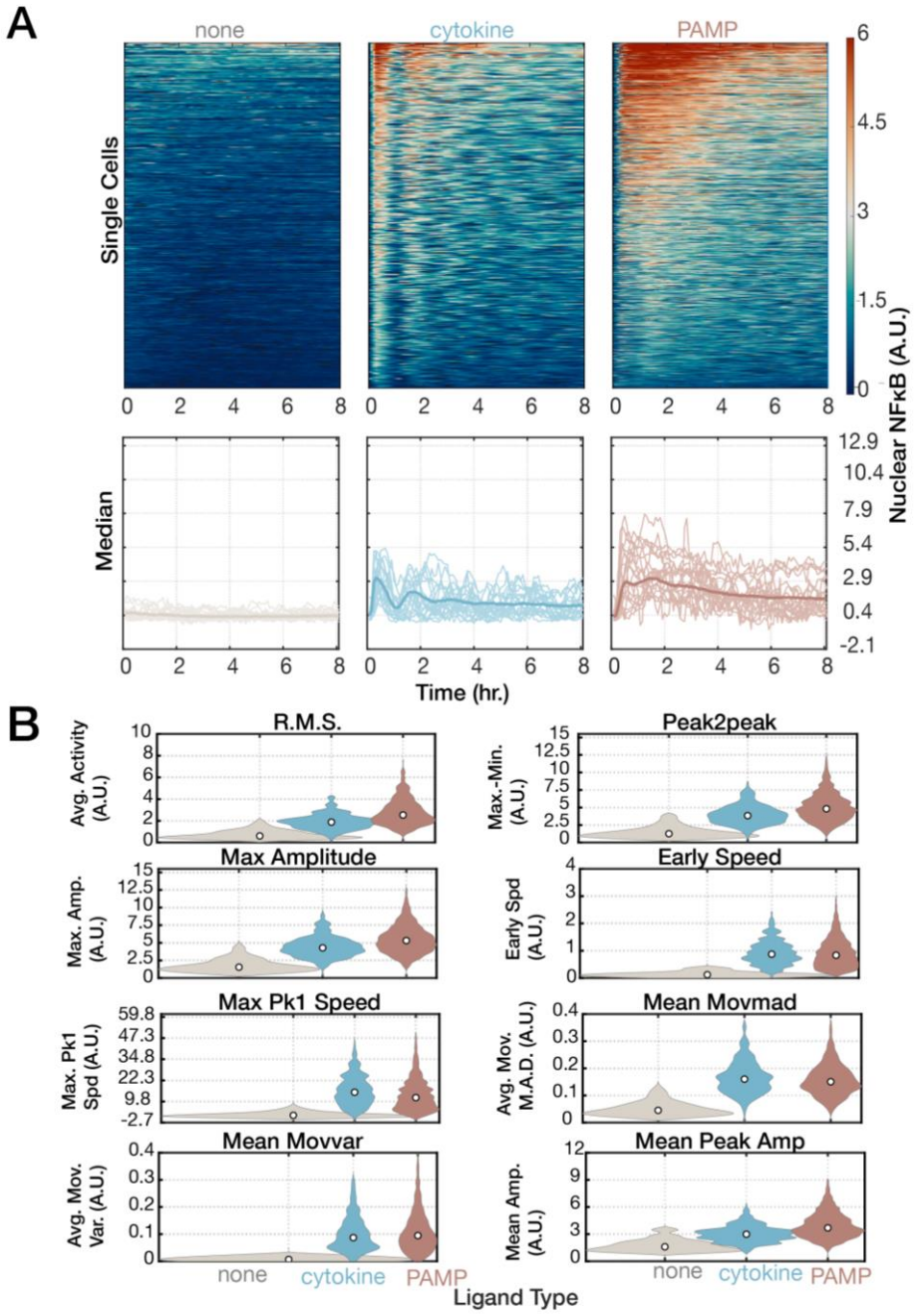

Figure 3.3. Host- vs. pathogen-specific NFκB dynamics in M_0 macrophages.

(A) Single-cell NFκB nuclear translocation trajectories grouped by stimulus-type (cytokine from host, pathogen-associated molecular patterns (PAMP) (top). Median NFκB trajectories and sample trajectories (bottom). Trajectories are sorted by average activity (root-mean-square). (B) Violin plots of the top 8 features that distinguish ligand sources in M_0 macrophages: maximum 1st peak speed (Max Pk1 speed), early speed, average activity (rms), average moving mean absolute deviation (Mean Movmad), Time to half-maximum activity (Time2HalfMaxIntegral), total activity (Max Integral), average moving standard deviation (Mean Movstd), and difference between maximum and minimum NFκB values (Peak2peak).

inflammatory responses is associated with many human pathologies (Murray and Wynn, 2011). In these conditions, inflammation does not restore homeostasis but contributes to the progression of the disease or tissue damage. Indeed, diseased tissue microenvironments lead to alterations in macrophage functions, such that these cells become key drivers of disease. For example, chronic inflammatory diseases such as pulmonary fibrosis and atherosclerosis are mediated by specialized, conditioned macrophages (Pollard, 2009) . Three important cytokines in tissue microenvironments that condition macrophages are IFNγ, IL-4, and TNF.

Macrophages adopt a wide spectrum of states that are associated with distinct physiological and pathological functions, which are dependent on the cytokine milieu (Fig. 3.1). Whereas classically activated macrophages (M_1) are induced by IFNγ +/- TLR ligands, alternatively activated macrophages (M_2) are induced by IL-4 (M_{2a}). M_1 and M_{2a} macrophages represent two extremes of spectrum. TNF is a pleiotropic cytokine with disparate and context-specific functions in homeostasis and pathology (Kalliolias and Ivashkiv, 2015). TNF is crucial to the macrophage function in health and disease. Given that macrophages produce TNF spontaneously (Pękalski et al., 2013) and in response to nucleic acids present during infection and tissue injury, tonic exposure to TNF is ubiquitous.

The NFκB transcription factor is the primary signal dependent transcription factor (SDTF) for inflammatory gene expression (O'Dea and Hoffmann, 2009). Cytokines, such as TNF, and nucleic acids, such as dsRNA and CpG DNA, and bacterial cell wall components, such as lipopolysaccharides and lipopeptides, induce the nuclear localization of NFκB by inducing the degradation of IκB (O'Dea and Hoffmann, 2009). Since IκBs form several negative feedback loops, NFκB signaling is highly dynamic, and may be oscillatory or non-

oscillatory (Hoffmann et al., 2002; Kearns et al., 2006). Although oscillatory signaling dynamics have been reported since 2002, precise understanding of their function remains elusive (Behar and Hoffmann, 2010). Lack of progress in the understanding the functions of NFκB oscillation is partly due to technological limitations. Population averages of NFκB signaling that is reported in bulk assays often yield misleading results. Whereas individual trajectories of NFκB nuclear translocation may show oscillatory NFκB, averages of those oscillatory trajectories may appear non-oscillatory. Recent studies show that the temporal pattern of NFκB nuclear translocation (signaling dynamics) is stimulus-specific (Taylor et al., 2020) and that the oscillatory character of NFκB dynamics regulate reprogramming of the macrophage epigenome in a stimulus-specific manner (Cheng et al., 2020).

The effect that cytokine milieu of macrophages has on the stimulus-specificity of NFκB signaling dynamics is unknown. Whether conditioning of macrophages by TNF, IL-4, and IFNγ control how well NFκB stimuli are distinguished using NFκB signaling dynamics has not been reported in literature. Detailed understanding of how cytokine milieu regulate stimulus-specificity of inflammatory responses mediated by NFκB may yield insights into the pathogenesis of inflammatory disorders and identify novel therapeutic strategies.

Results

"Polarizing" cytokine milieus regulate stimulus-specific NFκB signaling dynamics.

To examine whether the cytokine milieu of macrophages control the NFκB signaling dynamics, I used time-lapse, live cell microscopy to examine the localization of endogenously expressed, fluorescently-tagged NFκB RelA in primary macrophages. I stimulated bone marrow derived macrophages (BMDMs) from mVenus-RelA expressing mice with host-, virus- and bacterium-associated ligands (10 ng/mL TNF; 100 μg/mL p(I:C);

100 nM CpG, 100 ng/mL P3C4, 100 ng/mL LPS; respectively) and monitored the nuclear localization of NFκB in individual BMDMs for several hours. Using automated cell tracking and image analysis, I quantified the trajectories of NFκB nuclear translocation and computed features from the time series trajectories.

In naïve macrophages (M_0) with unperturbed, control cytokine milieu, NFκB signaling dynamics show stimulus specificity (Fig. 3.2). Heatmaps of NFκB responses in individual M_0 macrophages show that NFκB responses to host-associated ligands (TNF) and virus-associated molecular patterns (VAMPs) have robust oscillatory dynamics compared to the NFκB responses to bacterium-associated molecular patterns (BAMPs) (Fig. 3.2A). NFκB response to TNF and BAMPs (bacterium-associated molecular pattern (BAMPs) have earlier onsets and rapid kinetics (max pk1 speed, early speed, time to half-maximum, Fig.3.2A,B). When NFκB signaling dynamics are grouped by ligand type (host/cytokine vs. pathogen-associated molecular pattern (PAMP)), it is apparent that the oscillatory character may be a major distinguishing feature of host-associated ligands (Fig. 3.3A); however, features that describe average activity and peak heights appear to be distinguishing as well (Fig. 3.3B).

To examine whether stimulus-specific NFκB dynamics are altered in classically activated (M_1) macrophages, I pre-stimulated BMDMs with 10 ng/mL of IFNγ 24 hours before stimulating with host-associated ligands, BAMPs, and VAMPs (10 ng/mL TNF; 100 μg/mL p(I:C); 100 nM CpG, 100 ng/mL P3C4, 100 ng/mL LPS; respectively). Visual inspection of the single cell trajectories of NFκB activity in M_1 macrophages reveal that the oscillatory character that distinguishes TNF and VAMPs/p(I:C) from BAMPs is abrogated in response to VAMPs/p(I:C) but not in response to TNF (Fig. 3.4A); however, the activation delay the distinguishes VAMPs/p(I:C) in M_0 remains in M_1 macrophages (Fig.3.4A and B).

When NFκB signaling dynamics are grouped by ligand type (host/cytokine vs. PAMPs), the oscillatory character is not only a distinguishing feature, but a defining feature of NFκB response to host/cytokine ligands (Fig. 3.5A). Features that describe oscillatory potential such as the power in the frequency band of NFκB oscillations (oscpower), and the prominence frequency modes in the Fourier transform of NFκB signaling dynamics (oscfreq) are clearly specific for TNF/cytokine stimulation in M1 macrophages (Fig. 3.5B).

To examine whether stimulus-specific NFκB dynamics are altered in alternatively activated (M_{2a}) macrophages, I pre-stimulated BMDMs with 10 ng/mL of IL-4 24 hours before stimulating with host-associated ligands, BAMPs, and VAMPs (10 ng/mL TNF; 100 μg/mL p(I:C); 100 nM CpG, 100 ng/mL P3C4, 100 ng/mL LPS; respectively). Visual inspection of the single-cell trajectories and averages of NFκB activity in M_{2a} macrophages revealed that the NFκB response to VAMPs/p(I:C) is almost indistinguishable from no-treatment controls (Fig. 3.6A). Features that describe peak heights (Pk1 Amp), prominence (Pk1 prom), translocation speed (Max Pk1 Speed, Early Speed, Max Derivative) clearly distinguish TNF/cytokine and BAMPs from p(I:C)/VAMPs (Fig. 3.6B). When NFκB signaling dynamics are grouped by ligand type (host/cytokine vs. PAMPs), features that show stimulus specificity are ones that describe the quality of oscillations, rather than presence of oscillations: number of peaks, variability of trough to peak heights, frequency range (Fig. 3.7B).

To examine the extent to which stimulus-specific NFκB dynamics are altered by M_1 and M_{2a} conditioning, I compared the single cell trajectories of nuclear NFκB and descriptive features of NFκB signaling in response to TNF (Fig. 3.13A,B), P3C4 (Fig. 3.14A,B), CpG (Fig. 3.15A,B), LPS (Fig. 3.16A,B), and p(I:C) (Fig. 3.17A,B) in M_0, M_1 and M_{2a}. Using a simple decision tree algorithm, I quantified how distinguishable ligand-induced NFκB

dynamics in conditioned macrophages are (Fig. 3.13-18 C, D) and how similar ligand-induced NFκB dynamics are between pairs of conditioned macrophages. The off-diagonal values in the confusion matrices (Fig. 3.13-18 C) reflect how similar the pairs of conditions on the X and Y-axis are; whereas, the diagonal values reflect how distinct or identifiable the responses are. For example, TNF-induced NFκB dynamics in M_0 and M_1 are indistinguishable (Fig. 3.13C); in contrast, p(I:C)-induced NFκB dynamics in M_0 and M_{2a} are very distinguishable (Fig. 3.17C). The classification algorithm employed allows for visual inspection of the decision process for classifying M_0, M_1, and M_{2a} conditions using values of NFκB dynamical features (Fig. 3.13-17D).

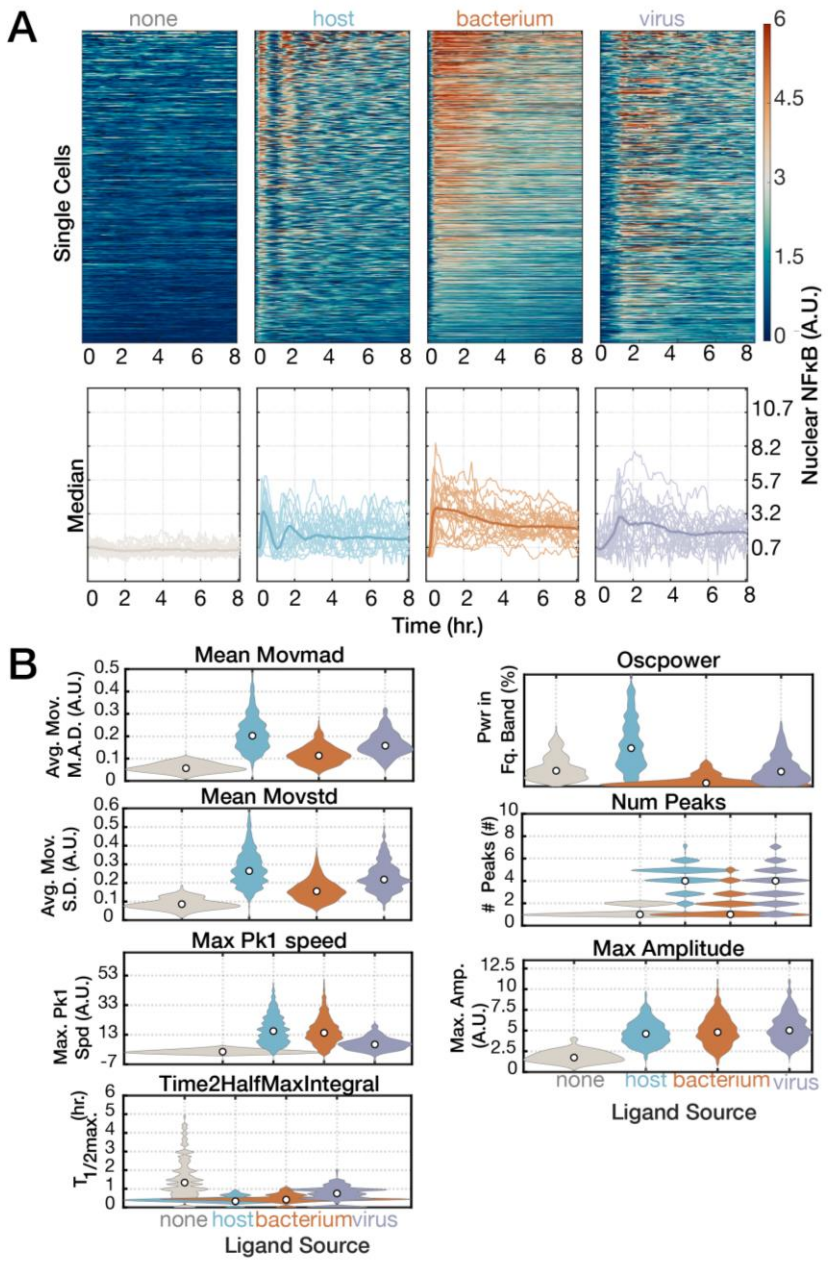

Figure 3.4. Pathogen class specificity of NFκB dynamics in M_1 macrophages.

(A) Single-cell NFκB nuclear translocation dynamics in IFNγ-prestimulated macrophages (M_1, classically activated) in response to host-associated ligands (TNF), bacterium-associated ligands (Pam3CSK4, CpG, LPS), virus-associated ligands (p(I:C)) (top). Median NFκB trajectories and sample trajectories (bottom). Trajectories are ordered by maximum 1st peak speed. (B) Violin plots of the top 7 features that distinguish ligand sources in M_1 macrophages: average moving mean absolute deviation (Mean Movmad), oscillatory power (Oscpower), average moving standard deviation (Mean Movstd), number of peaks, maximum 1st peak speed (Max Pk1 speed), maximum amplitude, and Time to half-maximum activity (Time2HalfMaxIntegral).

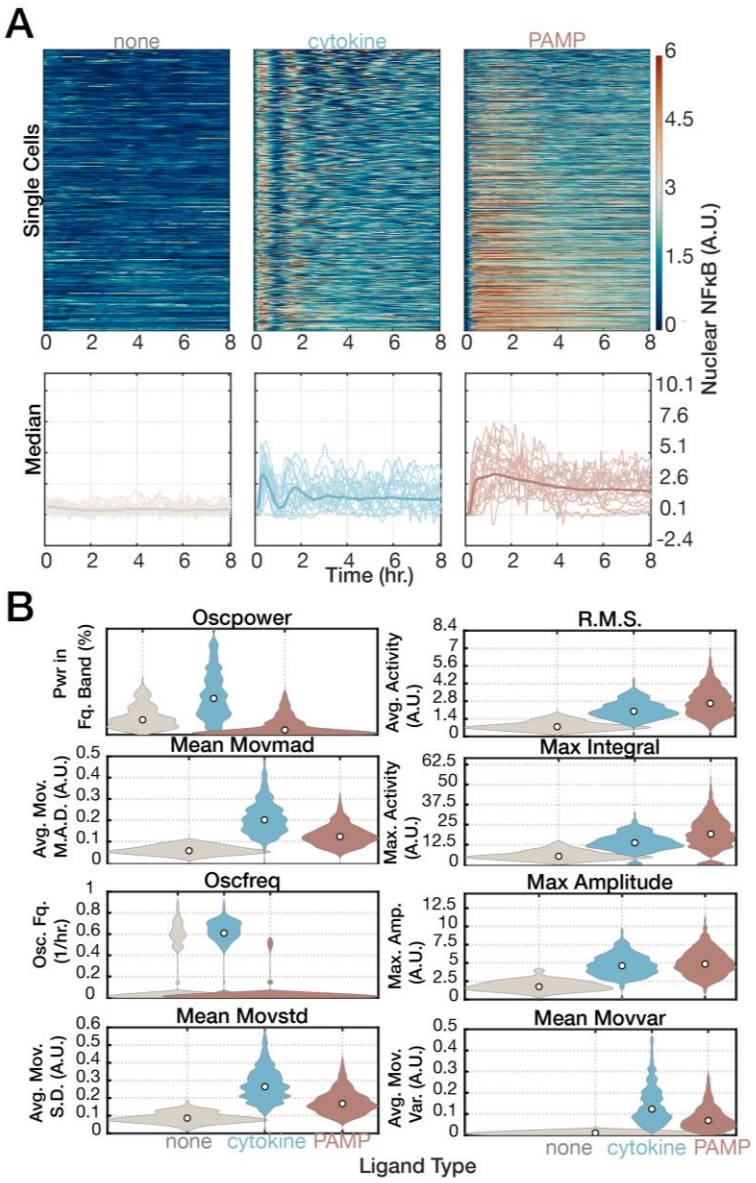

Figure 3.5. Host- vs. pathogen-specific NFκB dynamics M_1 macrophages.

(A) Single-cell NFκB nuclear translocation trajectories grouped by stimulus type (cytokine from host, pathogen-associated molecular patterns (top). Median NFκB trajectories and sample trajectories (bottom). Trajectories are ordered by average activity (root-mean-square). (B) Violin plots of the top 8 features that distinguish ligand types in M_1 macrophages: power in the frequency band corresponding to NFκB oscillations (0.3 – 1 hr^{-1}) (Oscpower), average activity, average moving mean absolute deviation, maximum activity, frequency of oscillations, maximum peak, average moving standard deviation, and average moving variance.

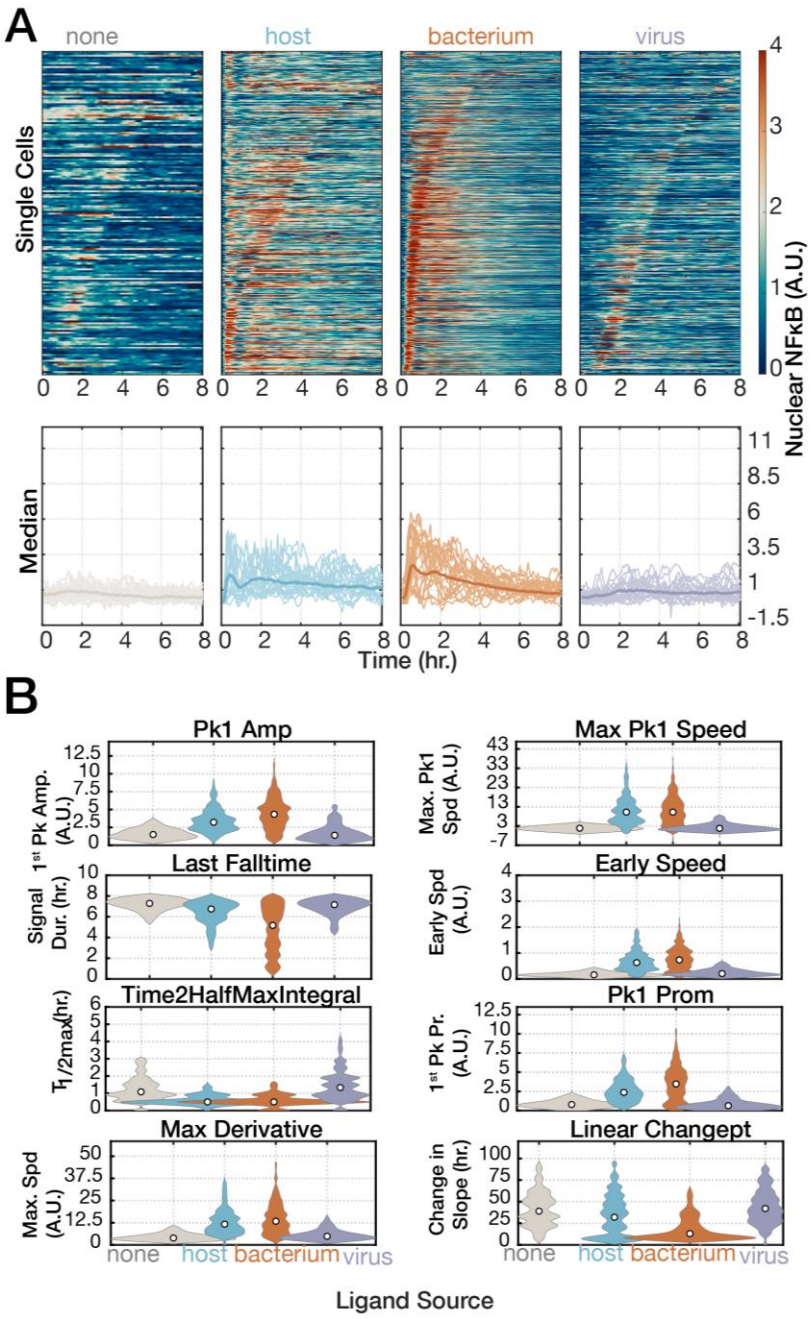

Figure 3.6. Stimulus-specific NFκB dynamics in alternatively activated (M_{2a}) macrophages.

(A) Single-cell NFκB nuclear translocation dynamics in IL-4-prestimulated macrophages (M_{2a}, alternatively-activated) in response to host-associated ligands (TNF), bacterium-associated ligands (Pam3CSK4, CpG, LPS), virus-associated ligands (poly(I:C)) (top). Median NFκB trajectories and sample trajectories (bottom). Trajectories sorted by the change point in the slope of NFκB trajectories. (B) Violin plots of the top 8 features that distinguish ligand sources in M_{2a} macrophages: 1st peak amplitude, maximum 1st peak speed, signal duration, early speed, Time to half-maximum activity, 1st peak prominence, maximum speed, change in the slope NFκB.

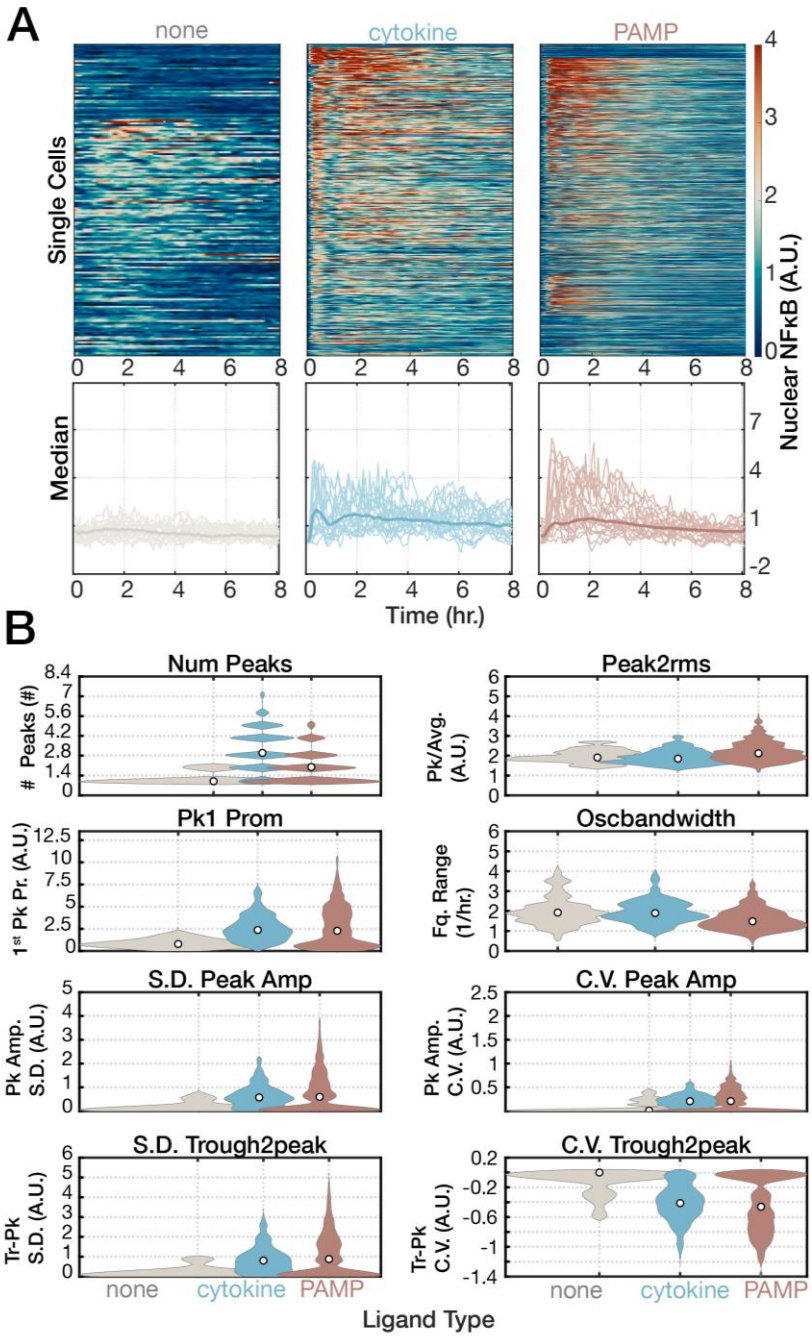

Figure 3.7. Features of NFκB dynamics that distinguish types of NFκB stimuli in M_{2a} macrophages.

(A) Single-cell NFκB nuclear translocation trajectories grouped by stimulus-type (cytokine from host, pathogen-associated molecular patterns) (top). Median NFκB trajectories and sample trajectories (bottom). Trajectories sorted by standard deviation of peak amplitudes. (B)Violin plots of the top 8 features that distinguish ligand types in M_{2a} macrophages: number of peaks, ratio of peak height to average (Peak2rms), 1st peak prominence, range of oscillatory frequencies, standard deviation of peak heights, coefficient of variation of peak heights, standard deviation of the difference from peak troughs to peak heights, coefficient of variation of the difference from peak troughs to peak heights.

Classification of ligand source using NFκB dynamics is abrogated in M_1 macrophages.

To quantitively characterize the extent to which conditioning of macrophages by polarizing cytokines, IFNγ and IL-4, affects the stimulus specificity of NFκB activity in macrophages, I employed supervised machine learning to classify the stimulus information using the temporal pattern of NFκB nuclear localization alone. Using the first 8 hours of NFκB signaling activity, I trained decision tree classifiers using either the time series traces (after dimensionality reduction using an autoencoder) or using descriptive features of NFκB dynamics. Further, I used an error correcting output code (ECOC) ensemble scheme to simplify the multi-class learning problem into a series of binary decision problems using a binary complete coding design which uses all binary combinations of classes. This approach allows for straightforward interrogation of the important features that distinguish all binary combination of classes. This approach trains $2^{(K-1)}$ -1 binary classifiers where K is the number of classes; for ligand source classification were K = 4 (none, host, virus, bacterium), 7 binary classifiers will be trained:

(1) none, host, bacterium vs. virus;

(2) none, host, virus vs. bacterium;

(3) none, host vs. bacterium, virus;

(4) none, bacterium, virus vs. host;

(5) none, bacterium vs. host, virus;

(6) none, virus vs. host, bacterium;

(7) none vs. host, bacterium, virus.

For example, the most important for each binary classification in the M_0 case is

(1) maximum 1st peak speed,

(2) total activity,

(3) average activity ,

(4) maximum 1st peak speed,

(5) number of peaks,

(6) time to half-maximum activity, and

(7) difference between the maximum and minimum of the trajectory (Table 3.1).

Comparison of the ligand source classifiers on M_1 data to M_0 revealed that classification performance of "virus" with NFκB dynamics is most affected by M_1 conditioning (Fig. 3.8). The primary source of confusion appears to be "bacterium". The precision of "virus" classification falls from 95.4 % in M_0 to 49.4 % , where 46.4 % of "virus" predictions are actually "bacterium" (Fig. 3.8A). Similarly, the sensitivity of "virus" classification diminishes from 74.8 % to 53.7 %, where 36.4 % of data from "virus" group misclassified as "bacterium" (Fig. 3.8A). Other performance metrics describe this observation as well: F1 score for "virus" falls from 0.85 to 0.5; markedness falls from 0.9 to 0.4, mean margin fell from 0.3 to 0.05; false discovery rate rose from 0.05 to 0.5 (Fig. 3.8B). Conversely, the classification of "host" improves in M_1 macrophages. The precision rises from 79.1 % to 88.1%; whereas, the sensitivity rises from 75.3 % to 92.4 % (Fig. 3.8C). When classifying ligand types ("cytokine" vs. "PAMP"), the improved classification of "cytokine"/" host" remains consistent with precision increasing from 81.6 % to 93.7% and sensitivity rising from 67.4 % to 85.5 % (Fig. 3.8C). Further, the mean margin increases from 28 % to 53 % (Fig. 3. 8D). Furthermore, F1 score and markedness are increased in M_1 condition.

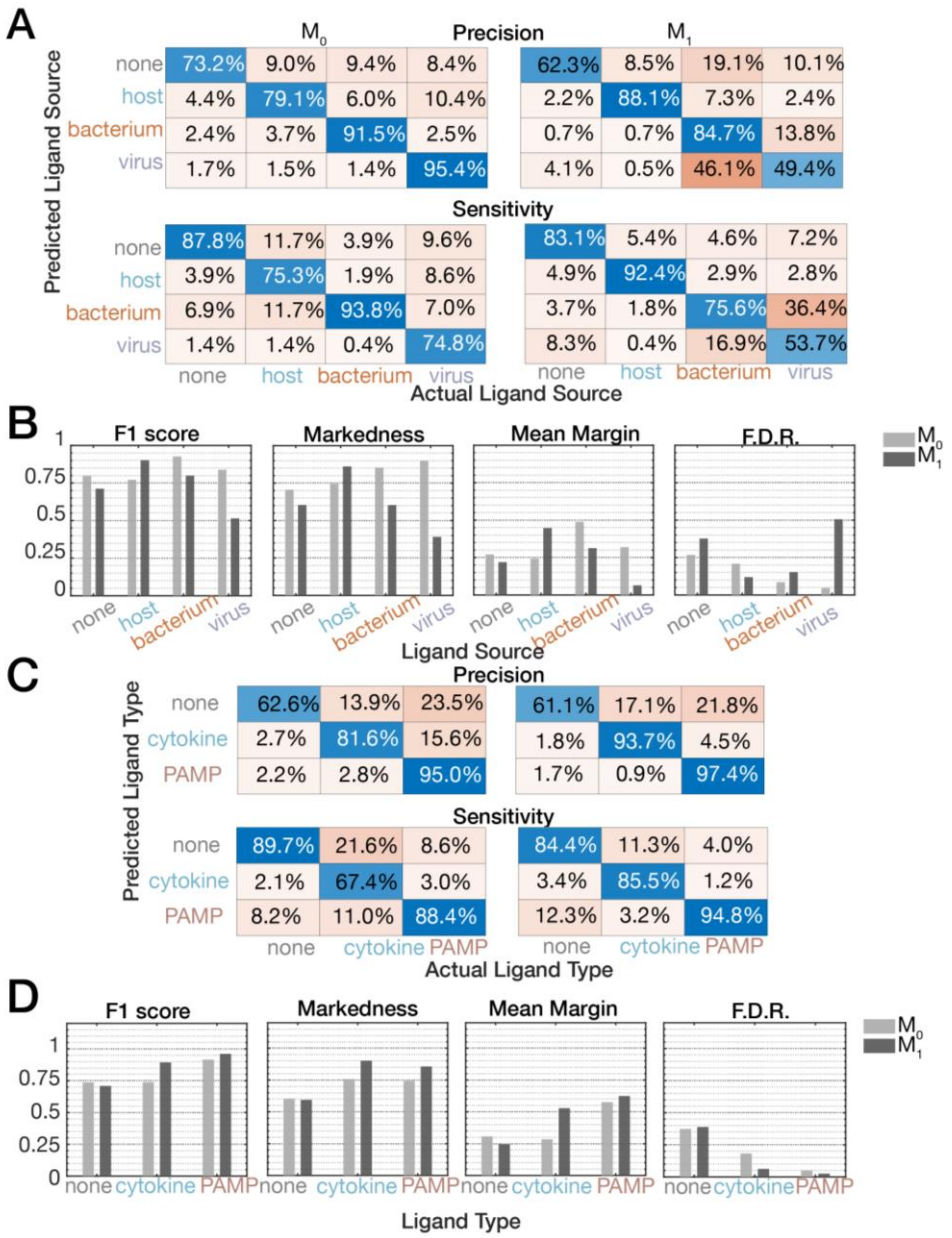

Figure 3.8. Classification performance of ligand source, but not ligand type, is diminished in M_1 macrophages.

(A) Top: confusion matrix of classification precision of ligand source (host, bacterium, virus) in naïve macrophages, M_0, (left) and M_1 macrophages (right). Bottom: confusion matrix of classification sensitivity in naïve macrophages (left) and M_1 macrophages (right). (B) Performance metrics of ligand source classification in M_0 vs. M_1: F1 score (harmonic mean of precision and sensitivity), markedness, mean margin (confidence in the classification; difference between the probability of the correct choice and highest probability of the incorrect choices), and false discovery rate (FDR). (C) Top: confusion matrix of classification precision of ligand type (cytokine and PAMP) in naïve macrophages, M_0, (left) and M_1 macrophages (right). Bottom: confusion matrix of classification sensitivity in naïve macrophages (left) and M_1 macrophages (right). (D) Performance metrics of ligand source classification in M_0 vs. M_1: F1 score, markedness, mean margin (confidence in the classification; difference between the probability of the correct choice and highest probability of the incorrect choices), and false discovery rate.

Classification of ligand source using NFκB dynamics is improved in M_{2a} macrophages.

In contrast with M_1 conditioning, the comparison of the ligand source classifiers on M_{2a} data to M_0 revealed that classification performance of "host" with NFκB dynamics is most affected by M_{2a} conditioning (Fig. 3.9A). The precision of "host" classification rises from 79.1% to 88.6 % with the increase coming from reduction in the misclassification of "virus" as "host" (Fig. 3.9A). Remarkable, the sensitivity of "host" classification rises from 75.3 % to 97.9 %. The F1 score, informedness (probability of an informed classification decision based on the data) and mean margin increase dramatically for "host" classification in M_{2a} conditioning (Fig. 3.9B). Interestingly, when data are grouped by ligand type, M_{2a} conditioning affects only the precision of "none" classification (Fig. 3.9C) with an increase from 62.6 % to 73.6 %, with all improvements deriving from the reduction of the misclassification of "cytokine" as "none". Interestingly, the sensitivity of "cytokine" classification increases from 67.4 % to 96.5% (Fig. 3.9 C). Furthermore, the informedness and mean margin are performance metrics significantly increased for "cytokine" classification in M_{2a} conditioning.

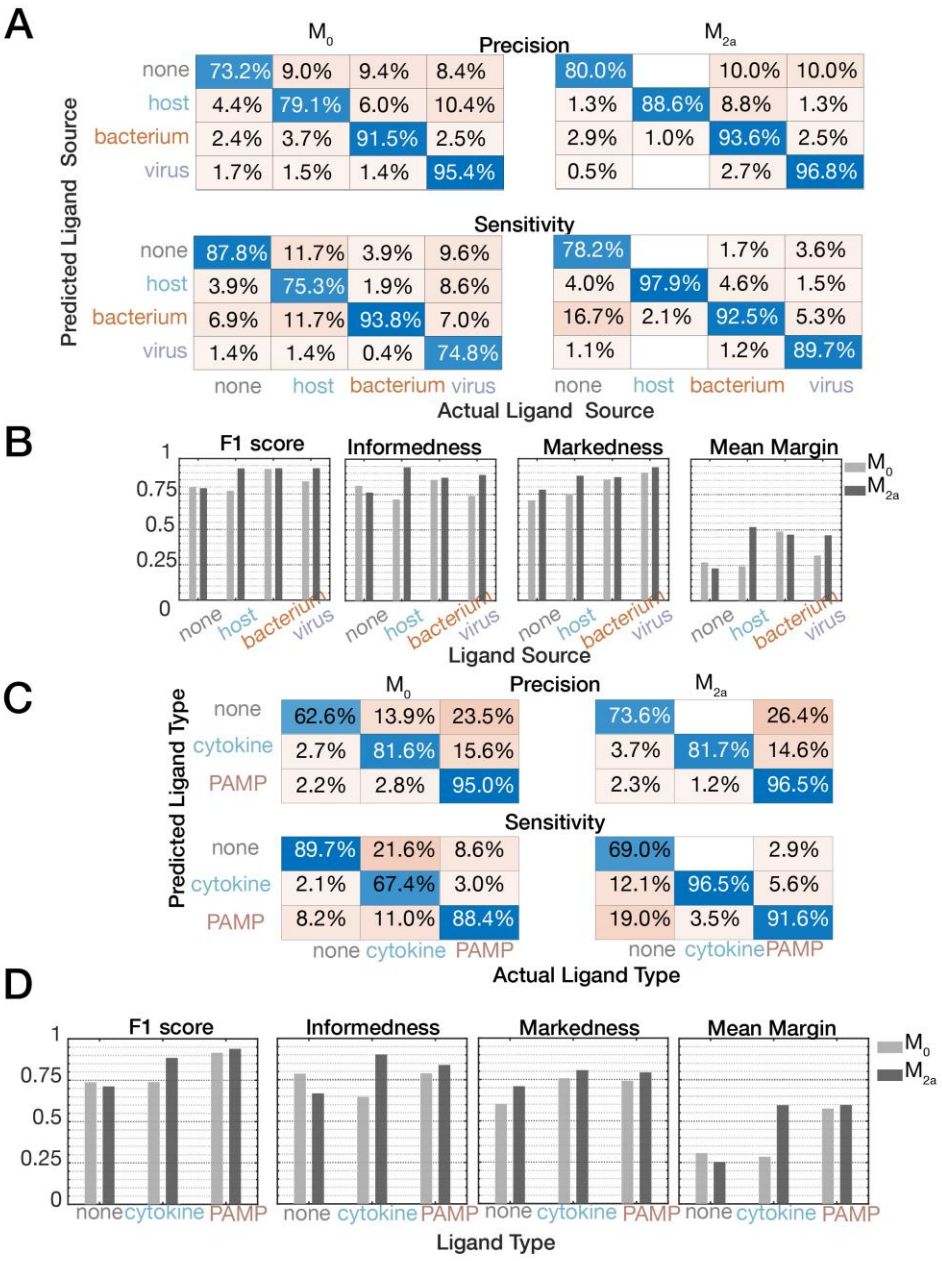

Figure 3.9. Sensitivity of ligand source and ligand type classification is enhanced in M_{2a} macrophages.

(A) Top: confusion matrix of classification precision of ligand source (host, bacterium, virus) in naïve macrophages, M_0, (left) and M_{2a} macrophages (right). Bottom: confusion matrix of classification sensitivity in naïve macrophages (left) and M_1 macrophages (right). (B) Performance metrics of ligand source classification in M_0 vs. M_{2a}: F1 score (harmonic mean of precision and sensitivity), informedness, markedness, mean margin (confidence in the classification; difference between the probability of the correct choice and highest probability of the incorrect choices). (C) Top: confusion matrix of classification precision of ligand type (cytokine and PAMP) in naïve macrophages, M_0, (left) and M_{2a} macrophages (right). Bottom: confusion matrix of classification sensitivity in naïve macrophages (left) and M_{2a} macrophages (right). (D) Performance metrics of ligand source classification in M_0 vs. M_{2a}: F1 score, informedness, markedness, and mean margin (confidence in the classification; difference between the probability of the correct choice and highest probability of the incorrect choices).

Paracrine TNF enhances dose classification of PAMPs.

TNF is ubiquitous in the cytokine milieu of macrophages (Kalliolias and Ivashkiv, 2015). The homeostatic and pathologic roles of TNF on stimulus discrimination in macrophages are not known. TNF levels in tissue microenvironments are controlled by constitutive, tonic release (as an emergent property of spontaneous release by many individual cells) and by paracrine release in feedforward response to PAMPs. To examine the effect that paracrine, feedforward TNF has on stimulus specificity, I examined the dose response of NFκB signaling dynamics to TLR9 stimulation by CpG in the presence and absence of paracrine, feedforward TNF. I stimulated BMDMs with co-treatments of CpG with a soluble decoy TNF receptor (sTNFR2), which abolishes the feedforward TNF response by competing with membrane bound TNFR on BMDMs for TNF binding (Lee et al., 2009). Time-lapse, live cell imaging results show that NFκB trajectories are mostly oscillatory in response to low doses of CpG (33 nM) in the presence of feedforward, paracrine TNF (Fig. 3.10A). A single cell heatmap of 33 nM CpG clearly shows a delay in the onset of NFκB nuclear translocation in these oscillatory trajectories (Fig. 3.10A). At 100 nM CpG, it is very apparent that the non-oscillatory trajectories (near the top) have a faster onset than the oscillatory trajectories (near the bottom). Further, the proportion of trajectories with oscillatory character is inversely correlated with the dose of CpG (Fig. 3.10E). When the feedforward TNF is abolished with sTNFR2 co-stimulation, oscillatory trajectories are significantly diminished, which is apparent in the 33 nM CpG stimulation (Fig. 3.10B). Comparing the median responses to 33 nM CpG in the presence (Fig. 3.10A) and absence of paracrine, feedforward TNF (Fig. 3.10B) reveals a significant reduction in the amount of nuclear NFκB. This reduction in average responses is due to loss of the subpopulation of trajectories that are oscillatory rather than a consistent reduction in the amplitudes of all trajectories.

Interestingly, at high doses of CpG (1000 nM), some trajectories with oscillatory character remain even in the presence of sTNFR2 competition. (Fig. 3.10E). Using the aforementioned supervised machine learning approach, I examined the effect that loss of feedforward paracrine TNF has on dose classification. The results reveal that loss of paracrine, feedforward TNF abrogates the precision and sensitivity of dose classification at intermediate (100 nM) and high doses (1000 nM) of CpG (Fig. 3.10C and D). Unsurprisingly, the primary causes of misclassification errors in the absence of feedforward TNF are the adjacent doses (Fig. 3.10C and D).

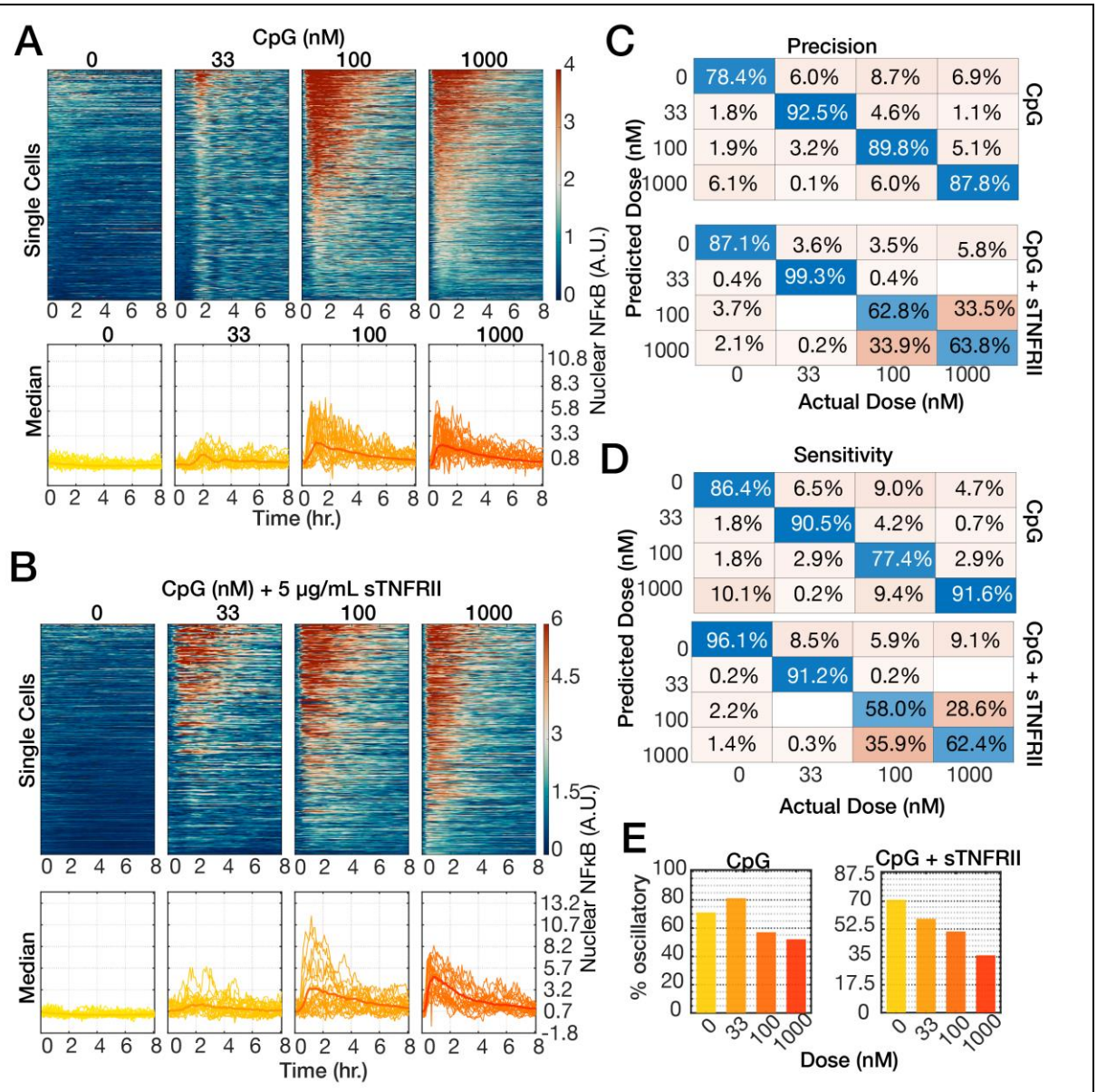

Figure 3.10. Paracrine TNF enhances dose classification of inflammatory ligands in macrophages.

(A) Top: Single-cell trajectories of NFκB nuclear translocation in response to 0, 33, 100, and 1000 nM CpG. Heatmaps ordered by 1st peak height. Bottom: median nuclear NFκB and sample trajectories. (B) Top: Single-cell trajectories of NFκB nuclear translocation in response 5 μg/mL soluble TNFR II + 0, 33, 100, and 1000 nM CpG. Heatmaps ordered by mean average moving mean absolute deviation. Bottom: median nuclear NFκB and sample trajectories. (C) Top: classification precision of CpG doses in the presence of paracrine TNF (without soluble TNFRII). Bottom: classification precision of CpG doses in the absence of paracrine TNF (with soluble TNFRII). (D) Top: classification sensitivity of CpG doses in the presence of paracrine TNF (without soluble TNFRII). Bottom: classification sensitivity of CpG doses in the absence of paracrine TNF (with soluble TNFRII). (E) Proportion of oscillatory trajectories and ratio of oscillatory trajectories to non-oscillatory trajectories as a function of CpG doses in the presence (left) or absence (right) of paracrine TNF.

Constitutive, tonic TNF enhances stimulus and dose classification.

To examine the effect that constitutive, tonic TNF has on stimulus discrimination in primary macrophages, I bred *tnf*$^{-/-}$ mice into the mVenus-RelA background and examined NFκB signaling dynamics in responses to various ligands and doses (Fig. 3.11 and Fig. 3.18). Single cell NFκB trajectories reveal loss of oscillatory trajectories in response to TNF/host and abolition of responsiveness to p(I:C)/VAMPs (Fig. 3.11A). The top features that confer ligand specificity describe speed (maximum 1st peak speed, early speed) and peak height (1st peak amplitude, maximum amplitude, difference of maximum and minimum activity) (Fig. 3.11C). Classification of ligand source using descriptive NFκB features reveals a significant reduction in the precision of "virus" classification from 70.8% to 49.8%, largely due to misclassification of "none" as virus (Fig. 3.11B). Similarly, the sensitivity of "virus" classification significantly decreases from 72.1% to 44.2% in TNF-deficient macrophages, largely due to misidentification of "virus" as either "none" or "bacterium" (Fig. 3.11D). Furthermore, the markedness of "none "and mean margin of "none" and "virus" are drastically reduced (Fig. 3.11E). To examine whether the loss of constitutive, tonic TNF controls the dose response of NFκB dynamics, I compared the response to 0.1, 1, and 10 ng/mL TNF in *tnf*$^{-/-}$ BMDMs to "wt" control BMDMs (Fig. 3.12). Single cell trajectories reveal loss of NFκB oscillations at all doses in the absence of constitutive, tonic TNF release (Fig. 3.12A and B). Examination of dose classification performance reveals a sharp decrease in the precision and sensitivity of dose classification at intermediate and high doses (Fig. 3.12C). Precision dropped from 94.8% and 91.1% to 76.9% and 66.5% for intermediate (1 ng/mL) and high doses (10 ng/mL), respectively, in the *tnf*$^{-/-}$ condition. Sensitivity dropped precipitously from 83.3% to 43.2% (Fig. 3.12C). Unsurprisingly, the adjacent doses were the sources of confusion. The F1 score,

markedness, and mean margin of the intermediate dose (1 ng/mL) are dramatically reduced in the *tnf*$^{-/-}$ condition (Fig. 3.12D). Features that describe duration (Off Times and Num Peaks) and variability of the trajectories (Mean Movmad, Mean Movvar) are less important for distinguishing doses in the *tnf*$^{-/-}$ condition (Fig. 3.12E vs. F).

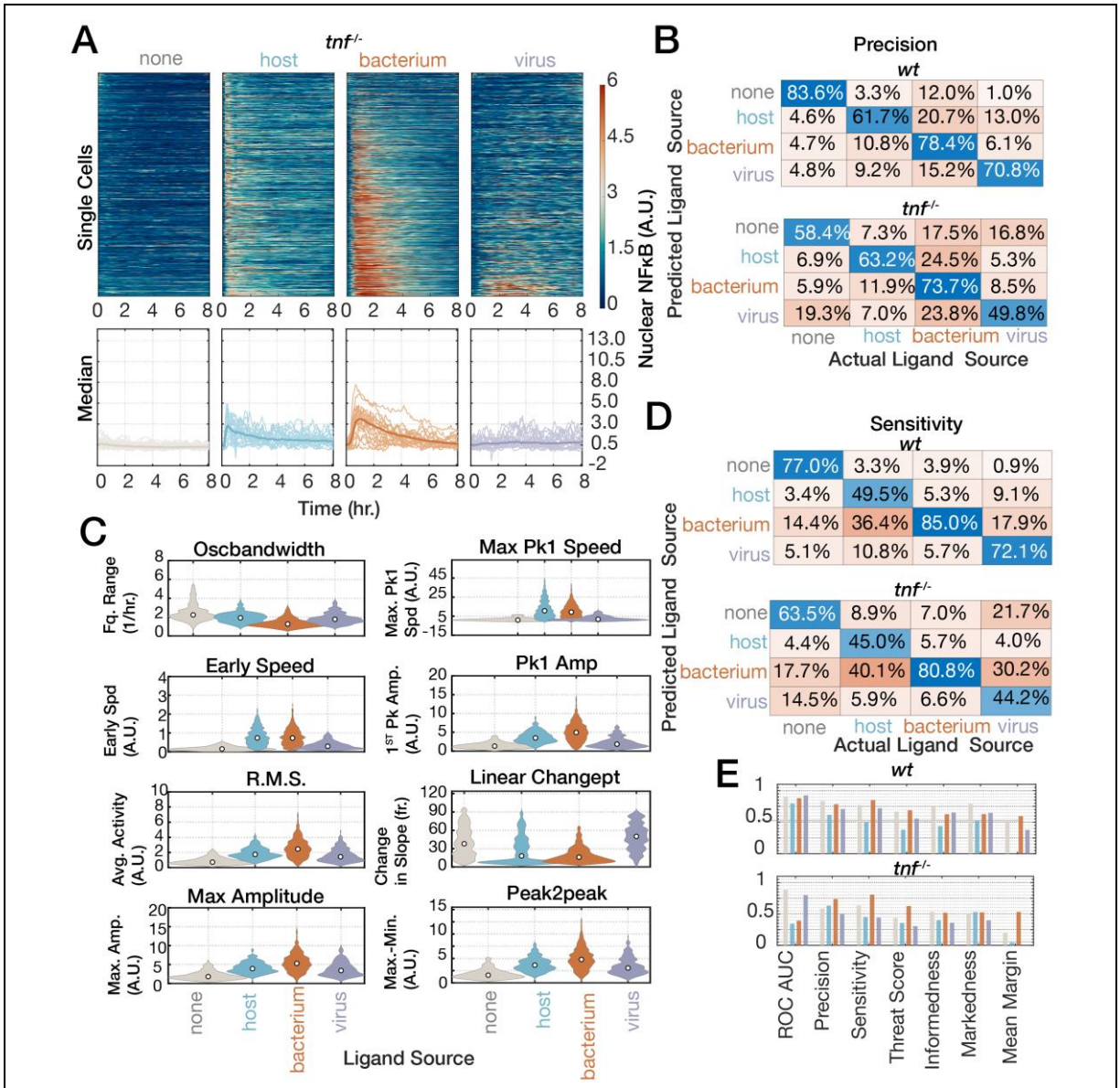

Figure 3.11. Loss of tonic TNF diminishes precision and sensitivity of ligand classification.

(A) Top: Single-cell NFκB nuclear translocation trajectories in *tnf*$^{-/-}$ BMDMs in response to host-associated ligands (10 ng/mL TNF), bacterium-associated ligands (10 ng/mL P3C4, 100 nM CpG, 100 ng/mL LPS), virus-associated ligands (100 μg/mL p(I:C)). Heatmaps ordered by frequency range of trajectories. Bottom: median NFκB nuclear translocation trajectory and sample trajectories. (B) Precision of ligand source classification using NFκB dynamical features in wt (top) and *tnf*$^{-/-}$ (bottom) BMDMs. (C) Top 8 features that distinguish ligand sources in *tnf*$^{-/-}$ BMDMs: frequency range, maximum 1st peak speed, early speed, 1st peak amplitude, average activity, change in slope, maximum peak height, range of peak amplitudes. (D) Sensitivity of ligand source classification using NFκB dynamical features in wt (top) and *tnf*$^{-/-}$ (bottom) BMDMs. (E) performance of ligand source classification using NFκB dynamical features in wt (top) and *tnf*$^{-/-}$ (bottom) BMDMs.

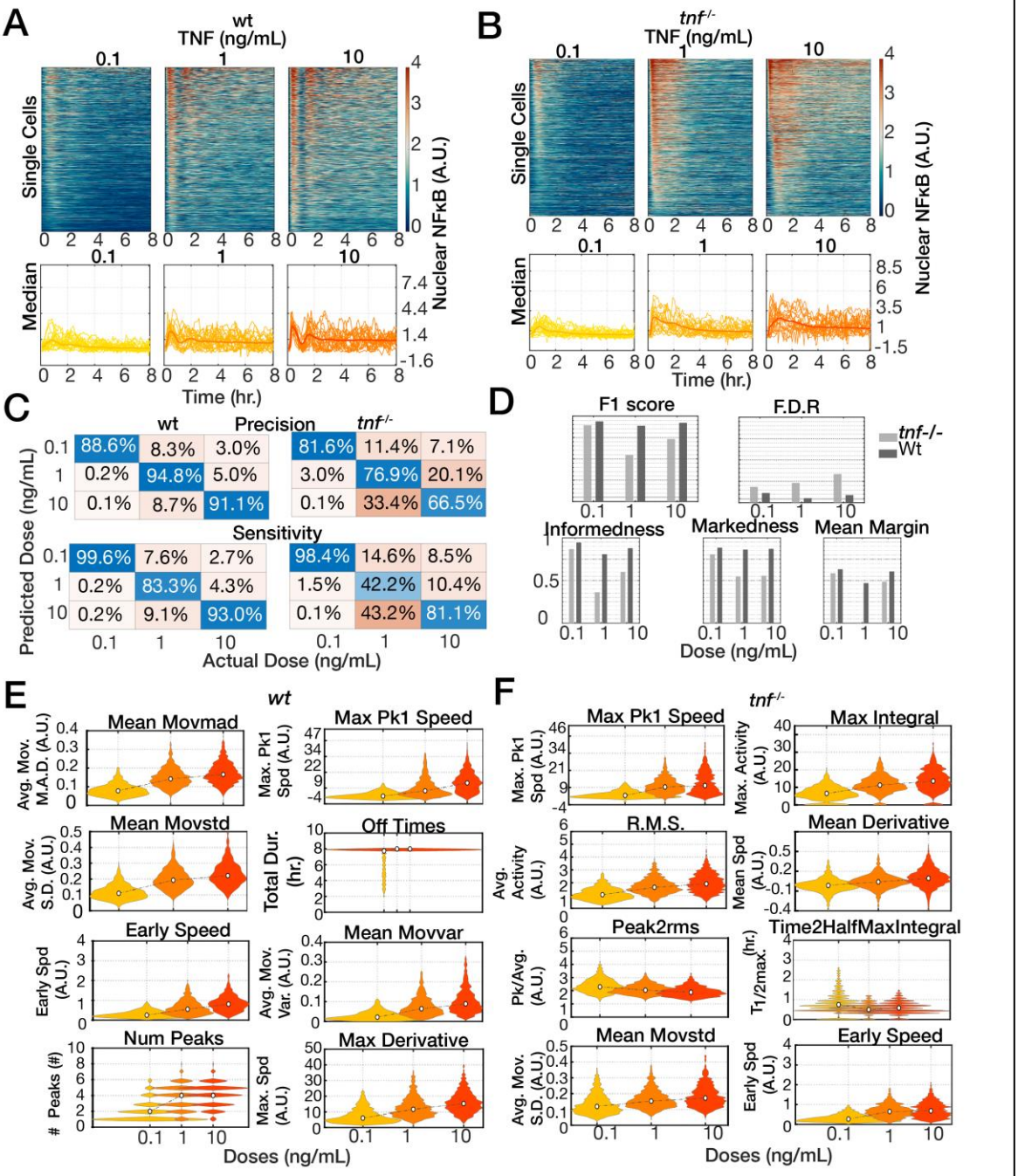

Figure 3.12. Loss of tonic TNF diminishes precision and sensitivity of dose classification.

(A) Top: Single-cell NFκB nuclear translocation trajectories in response to 0.1, 1, 10 ng/mL of TNF in wt BMDMs. Heatmaps ordered by maximum 1st peak speed. Bottom: median nuclear NFκB and sample trajectories. (B) Top: Single-cell NFκB nuclear translocation trajectories in response to 0.1, 1, 10 ng/mL of TNF in the absence of tonic TNF (*tnf*$^{-/-}$) BMDMs. Heatmaps ordered by average moving M.A.D. Bottom: median nuclear NFκB and sample trajectories. (C) Top: Precision of dose classification in wt (left) and *tnf*$^{-/-}$ BMDMs (right). Bottom: Sensitivity of dose classification in wt (left) and *tnf*$^{-/-}$ BMDMs (right).

Figure 3.12. Loss of tonic TNF diminishes precision and sensitivity of ligand classification.

(D) Performance metrics of dose classification in the presence and absence and tonic TNF: F1 score (harmonic mean of precision and sensitivity), informedness, markedness, and mean margin (confidence in the classification; difference between the probability of the correct choice and highest probability of the incorrect choices). (E) Top 8 dose responsive features of NFκB dynamics to 0.1, 1, 10 ng/mL of TNF in the presence of tonic TNF: average mean absolute deviation, maximum 1st peak speed, average moving standard deviation, total duration, early speed, average moving variance, number of peaks, maximum speed of NFκB nuclear translocation. (F) Top 8 dose responsive features of NFκB dynamics to 0.1, 1, 10 ng/mL of TNF in the absence of tonic TNF: maximum 1st peak speed, maximum activity, average activity, mean speed, ratio of tallest peak to average, time to half-maximum activity, average moving standard deviation, and early speed.

Discussion

In this work, I examined the role of the cytokine milieu in controlling the stimulus specificity of temporal pattern of NFκB nuclear translocation (signaling dynamics). Using time-lapse, live-cell imaging, I monitored and measured the signaling dynamics of fluorescently-tagged RelA subunit of NFκB in primary macrophages in response to various ligands and doses and in different cytokine contexts. The combination of high dimensional time series single-cell data and supervised machine learning approaches revealed the effect of the cytokine milieu on the signaling dynamics of NFκB in macrophages. Here I report three main findings: (1) My results show that IFNγ conditioning (M_1 polarization) enhances the classification of host-associated and pathogen-associated ligands via NFκB dynamics; however, the IFNγ conditioning diminishes the classification between virus-associated and bacterium-associated ligands using NFκB signaling dynamics; (2) IL-4 conditioning (M_2 polarization) enhances the ligand classification broadly. (3) TNF conditioning enhances ligand and dose classification.

Rigorous examination of NFκB signaling in macrophages in diverse cytokine contexts required: (1) high temporal resolution, (2) single cell resolution, and (3) cells with physiologic response to diverse ligands and cytokine contexts. Development of new

experimental and computational tools that meet these criteria enabled these discoveries by facilitating the generation of large quantities of high-quality experimental data.

High temporal resolution is essential since the NFκB activity is highly dynamic (Hoffmann et al., 2002). Single cell resolution is required since many characteristics of NFκB activity, such as unsynchronized oscillations, are not apparent using bulk assays (Tay et al., 2010). The heterogeneity of macrophage responses further necessitates the use of single-cell assays to distinguish changes in the spread of responses and location of responses. A new mVenus-RelA knock-in mouse strain expressing fluorescent NFκB at endogenous levels allows for interrogation of physiologically relevant NFκB responses in primary macrophages. The development of this experimental system is useful because many cell lines are unresponsive to ligands and cytokine milieus of interest (Cheng et al., 2015). Further, ectopic expression of reporters may lead to artefactual NFκB responses (Barken et al., 2005). Tracking NFκB activity in the same cells over time require the use of environmentally-controlled microscopy instruments, coupled with an automated image analysis pipeline (Cheng et al., 2015; Selimkhanov et al., 2014). An automated imaging analysis pipeline is essential to convert the thousands of images in an experiment to useful NFκB measurements in individual cells over many hours. Pattern recognition and machine learning approaches were essential to retrieve knowledge from the large quantities of data generated. Data preprocessing, feature engineering, and dimensionality reduction techniques are essential components of the analysis workflow.

With the necessary experimental and analysis workflows established, I sought to characterize the effect that the cytokine milieu has on NFκB signaling dynamics. "Polarizing" cytokines IFNγ and IL-4, the inflammatory cytokine, TNF, are well known regulators of macrophage function in health and disease conditions that span infectious

diseases (bacteria, viruses, parasites), autoimmune disorders (rheumatoid arthritis, inflammatory bowel disease, etc.) and cancers (Benoit et al., 2008; Martinez and Gordon, 2014; Mosser and Edwards, 2008; Murray et al., 2014). Given the technical requirements for examining NFκB signaling dynamics, it is not known whether the cytokine milieu regulates NFκB signaling dynamics in primary macrophages. The results of these studies are of great interest to the field since characteristics of NFκB signaling dynamics are correlated with gene expression (Hoffmann et al., 2002; Lane et al., 2017; Martin et al., 2020; Werner et al., 2005). Examination of stimulus specificity of NFκB signaling in different cytokine contexts may yield insights into novel approaches to target NFκB activity in a context-specific manner. The results of IFNγ conditioning (M_1 polarization) on stimulus-specific NFκB activity suggests a tradeoff between host-pathogen discrimination and bacterium-virus discrimination. NFκB dynamics from virus-associated ligands and bacterium-associated ligands are less distinguishable in M_1 macrophages (Fig. 3.8A, B); however, NFκB dynamics from host-associated ligands and pathogen-associated ligands are more distinguishable (Fig. 3.8C,D). This tradeoff is probably mediated by stimulus-specific perturbation of oscillations in M_1 macrophages. Host-associated ligands (TNF) and virus-associated ligands (p(I:C)) induce NFκB activity with oscillatory character in naïve, M_0, macrophages; however, M_1 macrophages induce NFκB activity with oscillatory character in response to TNF (Fig. 3.13A), but not p(I:C) (Fig. 3.17) (Harris, 2017).

The results of IL-4 conditioning (M_{2a} polarization) on stimulus-specific NFκB activity suggest that NFκB dynamics are more distinguishable (Fig. 3.9) across ligand labels: ligand source (Fig. 3.9.A,B) and ligand type (Fig. 3.9.C,D). The stimulus specificity in M2a macrophages may be due to the differential effects on MyD88-mediated signaling vs. TRIF-mediated signaling (Takeuchi, Osamu Akira, 2010). Examination of single cell NFκB

dynamics in M2a macrophages show that NFκB dynamics in response to bacterial PAMPs that signal through MyD88 exclusively (P3C4 and CpG) tend to have shorter duration (Last Falltime), lower total activity (Max Integral) and higher peak to average ratio (Peak2rms) compared to naïve macrophages (Fig. 3.14, 3.15). Further, NFκB dynamics in response to ligands that signal through TRIF (LPS, p(I:C)) have lower average activity (R.M.S), maximum peak heights (Max Amplitude) and lower maximum speed (Max Derivative).

The effects of TNF conditioning and feedforward TNF on stimulus-specific NFκB signaling suggest that constitutive, tonic TNF confers both ligand specificity and dose specificity and that feedforward TNF confers dose specificity. To study the effects of constitutive, tonic TNF on NFκB signaling dynamics and stimulus specificity, I bred *tnf*$^{\Delta/-}$ mice into the mVenus-RelA background and examine the response to TNF, P3C4, CpG, LPS, and p(I:C) (Fig. 3.18). Interrogation of the ligand classification performance in the absence of tonic TNF showed that NFκB signaling dynamics from both host- and virus-associated ligands are confused for NFκB signaling dynamics induced by bacterial PAMPs (Fig. 3.11B,C). Visual inspection of single cell NFκB signaling dynamics showed that a distinct lack of oscillatory character in the trajectories (Fig. 3.11A, 3.18A). The responses to bacterial PAMPs appear indistinguishable from each other (Fig. 3.18A, B). The features that distinguish TNF response from the bacterial PAMPs describe average activity (R.M.S.) and peak heights (1st peak height, maximum peak height, difference between maximum and minimum activity).

Interestingly, the NFκB activity upon p(I:C) stimulation shows a lack of response in the absence of tonic TNF (Fig. 3.18A), similar to the observation in M_{2a} macrophages (Fig. 3.9). In contrast to M_{2a} macrophages, TNF-induced NFκB dynamics in *tnf*$^{\Delta/-}$ are less distinguishable due to abolition of NFκB oscillations. This observation highlights a role for

oscillatory dynamics in stimulus-classification. The molecular mechanism behind the loss of NFκB oscillations in the absence of tonic TNF is not known. Immunoblot analysis of IKK activity upstream of NFκB suggest that the kinetics of IKK activation may be sensitized (Fig. 3.19A). Multi-stimulus math modeling shows that IKK activation kinetics alone are sufficient to reproduce both oscillatory and non-oscillatory dynamics and that higher IKK activity may yield non-oscillatory dynamics (Taylor et al., 2020). These results suggest elevated IKK in the absence of tonic TNF may yield non-oscillatory dynamics (Fig. 3.19C). Two hypotheses that may explain elevated IKK activity in the absence of tonic TNF are elevated surface expression of TNF receptors and lower abundance of negative feedback regulator such as A20 (Werner et al., 2008). An alternate explanation is the loss of tonic TNF diminishes the strength of negative feedback by IκBα (Fig. 3.19C). Understanding the mechanism by which constitutive, tonic TNF confers stimulus specificity will be of great interest, as many patients are on anti-TNF therapy and a subset of those patients develop paradoxical inflammation, which appears to have an autoimmune etiology (Cleynen and Vermeire, 2012). These anti-TNF therapies carry black box warnings for infectious diseases by *Legionella, Listeria,* and *Mycobacteria*, all of which are intracellular bacteria that infect macrophages (Vladimer et al., 2013). Interestingly, results from feedforward TNF blockade with sTNFR2 showed the abrogation of dose specificity of NFκB signaling in response to CpG, a bacterial PAMP that signals from the endosome (Fig. 3.10C,D). The abrogation of oscillatory NFκB dynamics in the context of feedforward TNF blockade again highlights a role for NFκB oscillations in stimulus specificity of NFκB activity.

Supplemental Figures

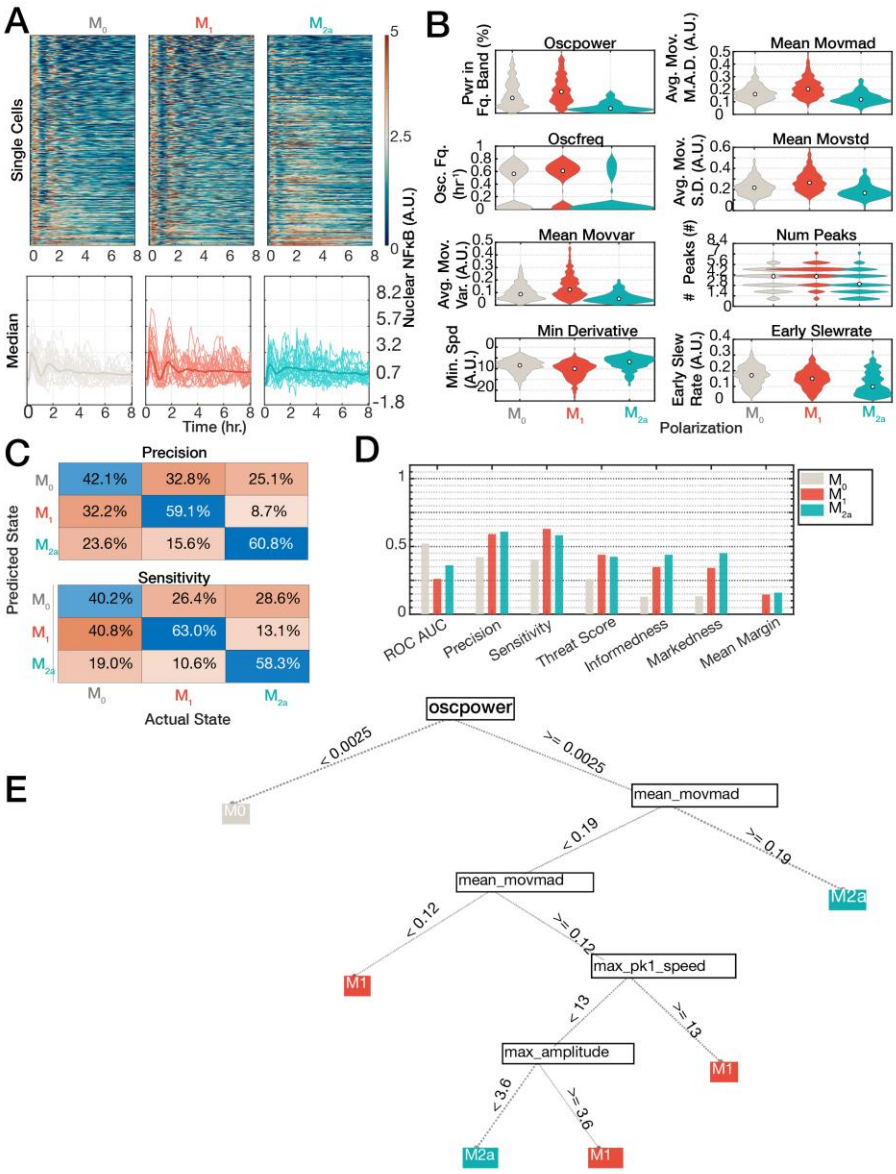

Figure 3.13. Effect of macrophage polarization on TNF-induced NFκB signaling.

(A) Top: Single-cell trajectories of NFκB nuclear translocation in response to 10 ng/mL TNF. Heatmaps ordered by power in the oscillation frequencies of NFκB activity. Bottom: median nuclear NFκB and sample trajectories. (B) Top 8 features of TNF-responsive NFκB dynamics that distinguish the polarization states: power in the oscillation frequencies of NFκB activity, average moving median absolute deviation, frequency of NFκB oscillations, average moving standard deviation, mean moving variance, number of peaks, minimum speed, early slew rate. (C) Top: Precision of polarization of classification. Bottom: Sensitivity of polarization classification. (D) Performance metrics of polarization classification: Area under the receiver operating characteristic curve, precision, recall (sensitivity), threat score, informedness, markedness, and mean margin. (E) Sample decision tree for classifying polarization state from TNF-responsive NFκB signaling dynamics.

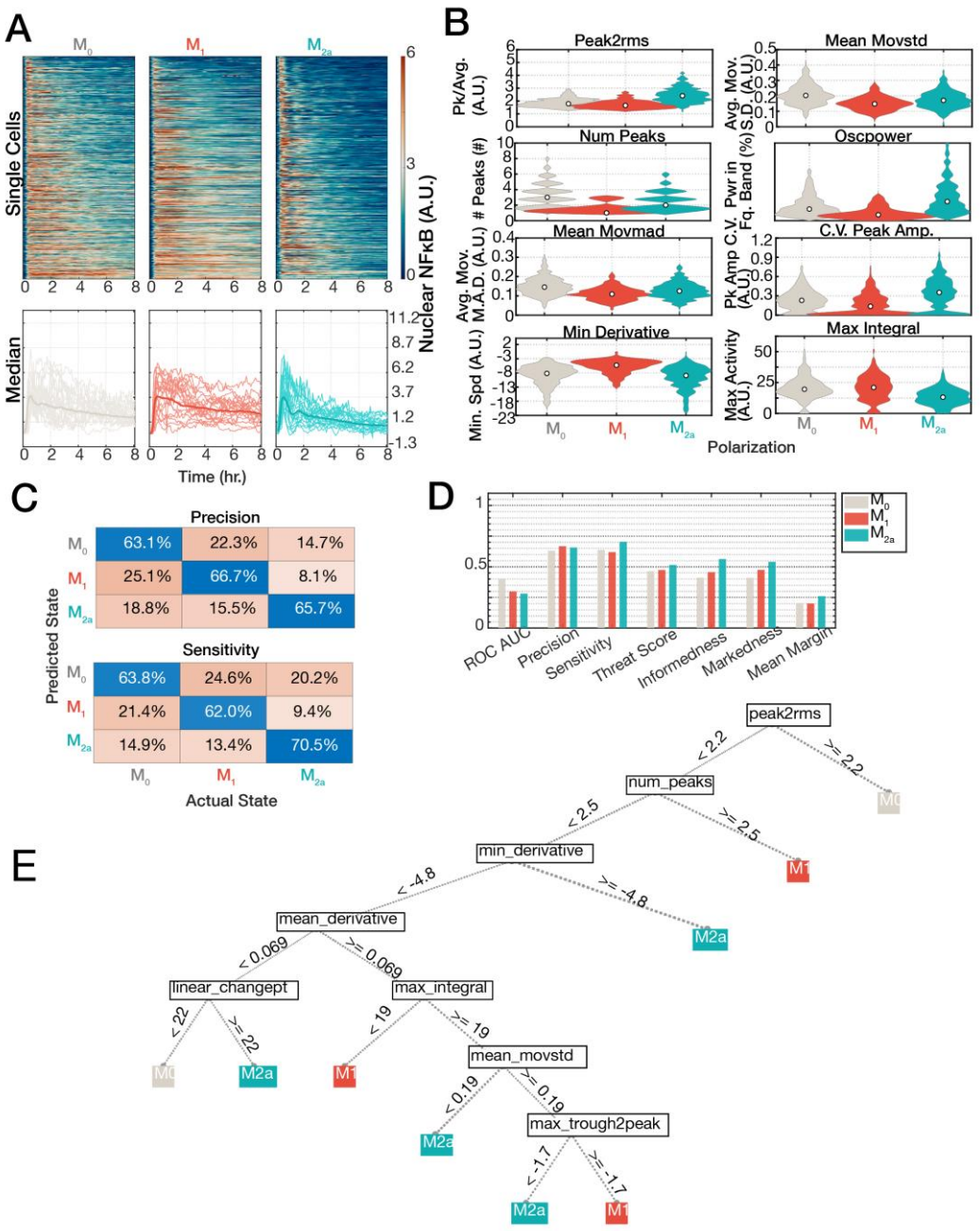

Figure 3.14. Effect of macrophage polarization on P3C4-induced NFκB signaling.
(A) Top: Single-cell trajectories of NFκB nuclear translocation in response to 100 ng/mL P3C4. Heatmaps ordered by ratio of tallest peak to average activity. (B) Top 8 features of P3C4-responsive NFκB dynamics that distinguish the polarization states: ratio of tallest peak to average activity, average moving standard deviation, number of peaks, power in the frequency band of NFκB oscillations, average moving median absolute deviation, coefficient of variation of peak heights, minimum speed, minimum speed and maximum activity. (C) Top: Precision of polarization of classification. Bottom: Sensitivity of polarization classification. (D) Performance metrics of polarization classification: Area under the receiver operating characteristic curve, precision, recall (sensitivity), threat score, informedness, markedness, and mean margin. (E) Sample decision tree for classifying polarization state from P3C4-responsive NFκB signaling dynamics.

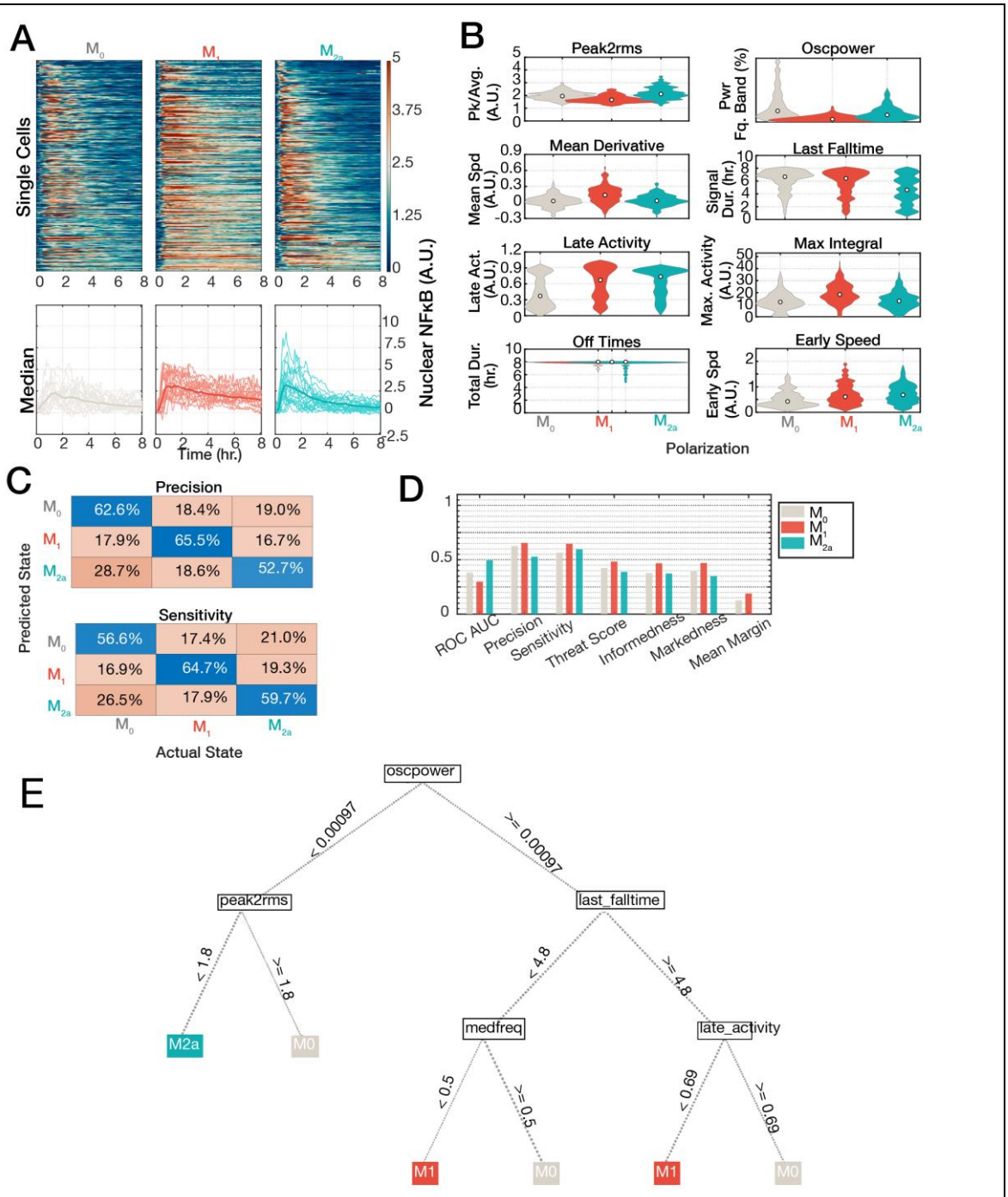

Figure 3.15. Effect of macrophage polarization on CpG-induced NFκB signaling.
(A) Top: Single-cell trajectories of NFκB nuclear translocation in response to 100 nM CpG. Heatmaps ordered by ratio of tallest peak to average activity. (B) Top 8 features of CpG-responsive NFκB dynamics that distinguish the polarization states: ratio of tallest peak to average activity, power in the frequency band of NFκB oscillations, average speed, signal duration, late activity, total activity, total duration, and early speed.(C) Top: Precision of polarization of classification. Bottom: Sensitivity of polarization classification. (D) Performance metrics of polarization classification: Area under the receiver operating characteristic curve, precision, recall (sensitivity), threat score, informedness, markedness, and mean margin. (E) Sample decision tree for classifying polarization state from CpG-responsive NFκB signaling dynamics.

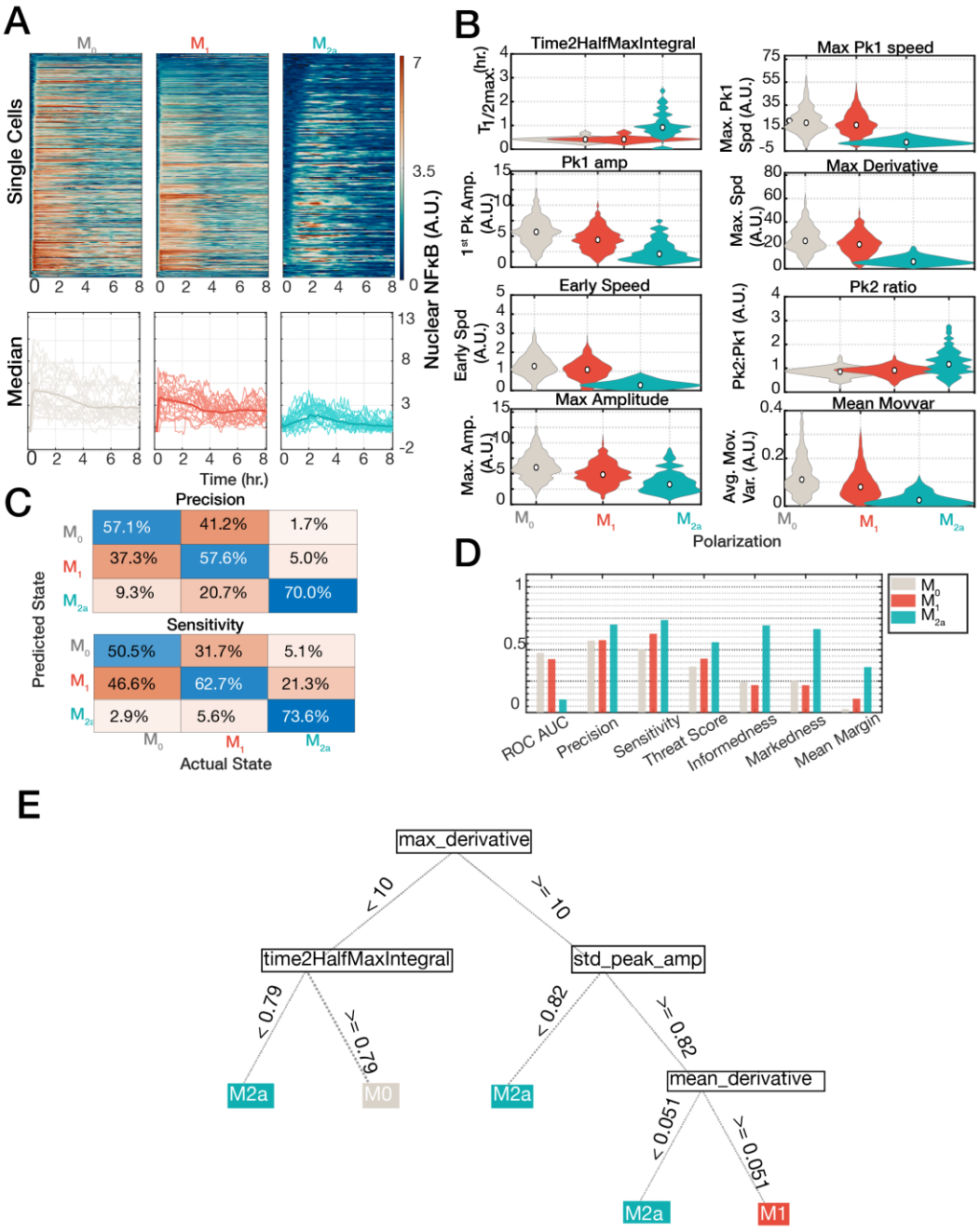

Figure 3.16. Effect of macrophage polarization on LPS-induced NFκB signaling.
(A) Top: Single-cell trajectories of NFκB nuclear translocation in response to 100 ng/mL CpG. Heatmaps ordered by time to half-maximum activity. Bottom: median nuclear NFκB and sample trajectories. (B) Top 8 features of LPS-responsive NFκB dynamics that distinguish the polarization states: time to half-maximum activity, maximum 1st peak speed, 1st peak height, maximum translocation speed, early speed, ratio of 2nd peak to the 1st peak, maximum peak height, average moving standard deviation. (C) Top: Precision of polarization of classification. Bottom: Sensitivity of polarization classification. (D) Performance metrics of polarization classification: Area under the receiver operating characteristic curve, precision, recall (sensitivity), threat score, informedness, markedness, and mean margin. (E) Sample decision tree for classifying polarization state from LPS-responsive NFκB signaling dynamics.

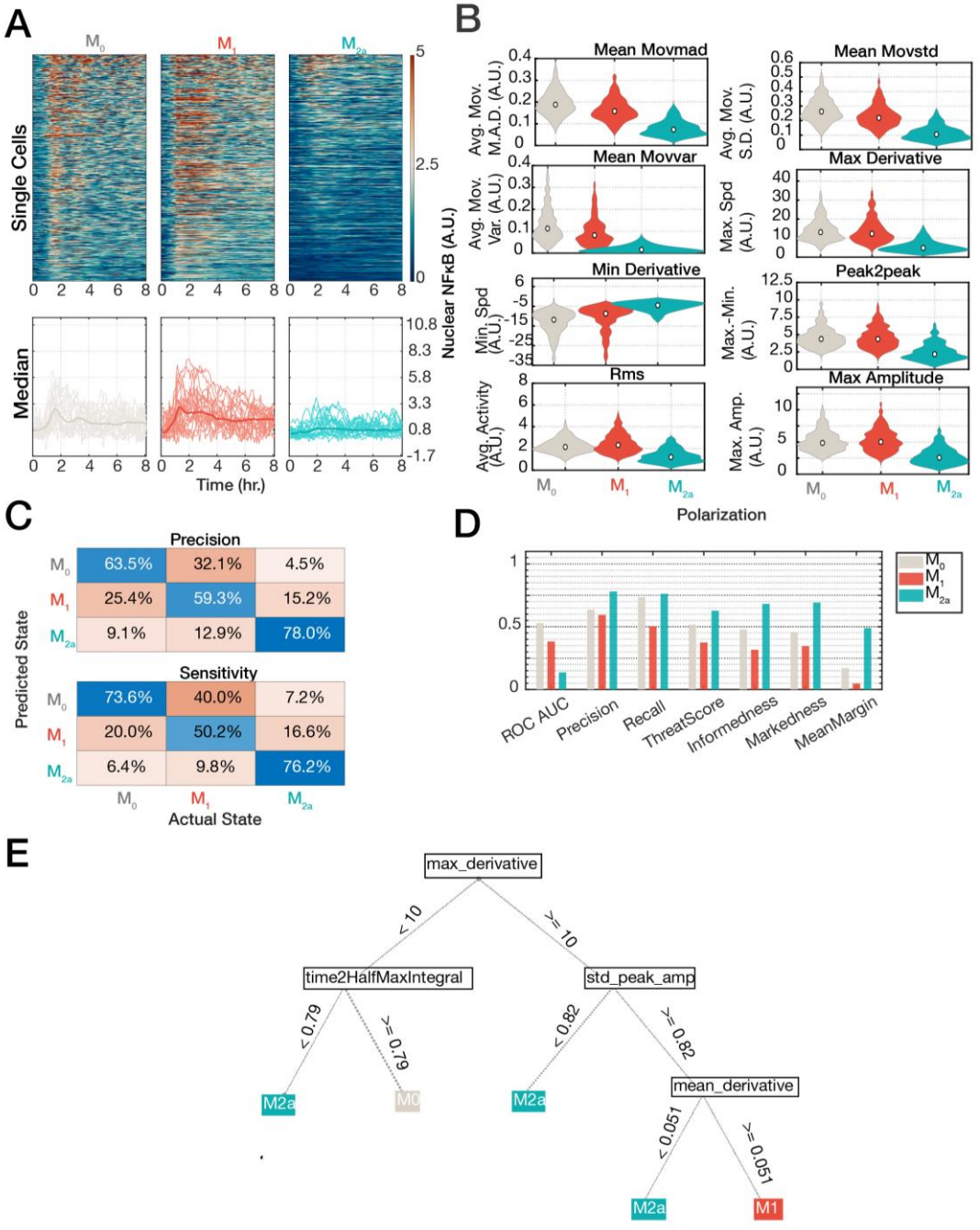

Figure 3.17. Effect of macrophage polarization on p(I:C)-induced NFκB signaling.
(A) Top: Single-cell trajectories of NFκB nuclear translocation in response to 100 μg/mL poly(I:C). Heatmaps ordered by average moving median absolute deviation. Bottom: median nuclear NFκB and sample trajectories. (B) Top 8 features of p(I:C)-responsive NFκB dynamics that distinguish the polarization states: average moving median absolute deviation, average moving standard deviation, average moving variance, maximum speed, minimum speed, difference between maximum and minimum values, average activity, and maximum peak height. (C) Top: Precision of polarization of classification. Bottom: Sensitivity of polarization classification. (D) Performance metrics of polarization classification: Area under the receiver operating characteristic curve, precision, recall (sensitivity), threat score, informedness, markedness, & mean margin. (E) Sample decision tree for classifying polarization state from p(I:C)-responsive NFκB signaling dynamics.

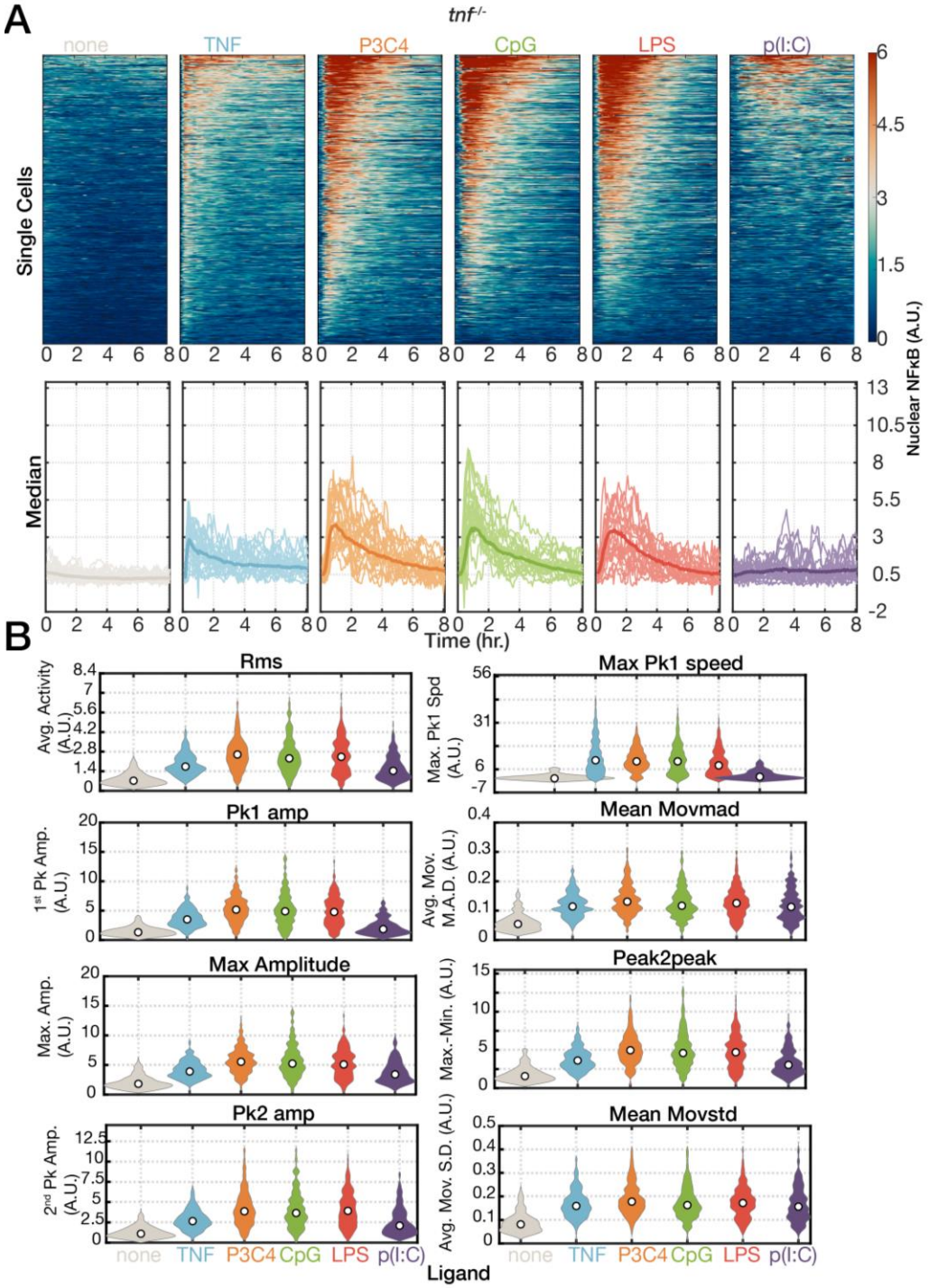

Figure 3.18. Ligand-specific NFκB dynamics in the absence of tonic TNF.

(A) Top: Single-cell trajectories of NFκB dynamics in response 10 ng/mL TNF, 10 ng/mL P3C4, 100 nM CpG, 100 ng/mL LPS, and 100 μg/mL p(I:C). Heatmaps ordered by average activity. Bottom: median nuclear NFκB and sample trajectories.(B) Top 8 features that distinguish ligands: average, maximum 1st peak speed, 1st peak height, average moving median absolute deviation, maximum peak height, difference of maximum and minimum amplitudes, 2nd peak height, and average moving standard deviation.

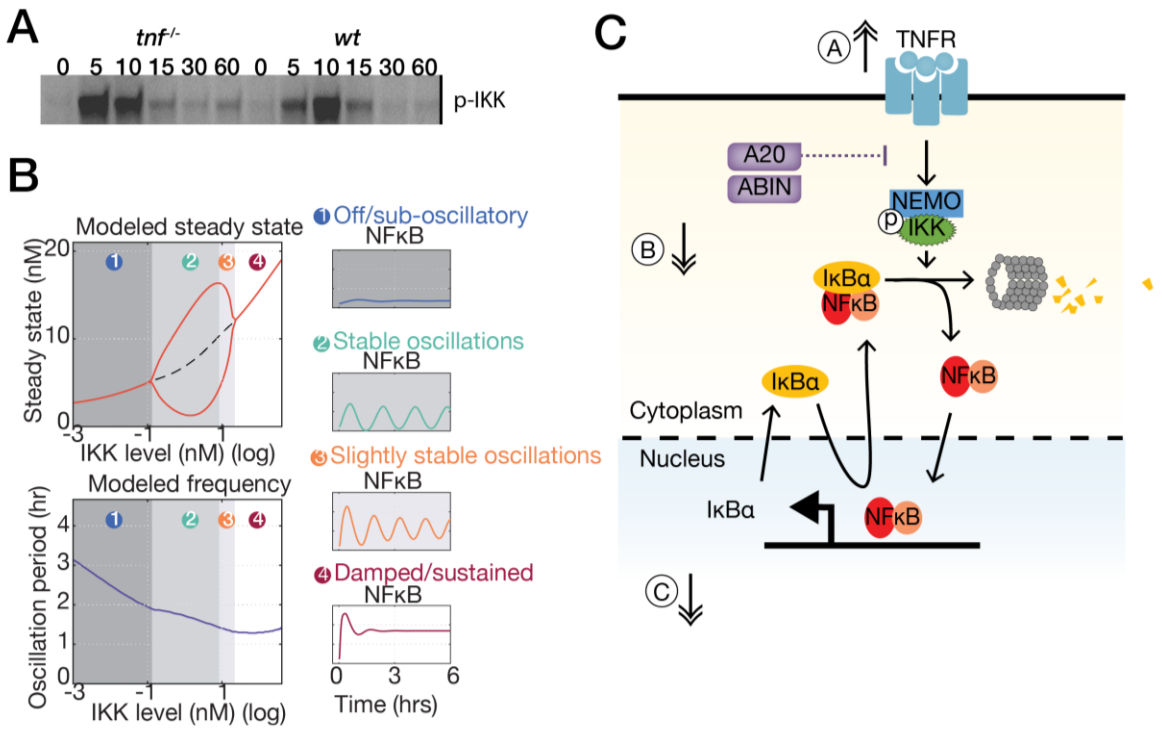

Figure 3.19. IKK activation kinetics may regulate loss of NFκB oscillations in the absence of tonic TNF.

(A)Phospho-IKK immunoblot show faster activation kinetics in *tnf-/-* BMDMs compared to wt controls. (B) Top left: Steady state values of nuclear NFκB and primary oscillation frequency are shown as a function of active IKK level. Bottom left: Simulated trajectories of IKK activation and nuclear NFκB at each of 4 regimes in the steady state diagram. Modeling and simulations by Brooks Taylor. (C) Candidate mechanisms for the loss of NFκB oscillations in the absence of tonic TNF: (C.A) Increase in TNF receptor abundance (C.B) Disinhibition of IKK due to the reduction of enzymatic negative feedback by A20. (C.C) Decrease in IκBα inducibility.

Tables

Table 3.1. Top features for classifying ligand source in M_0 macrophages

Learner	Positive	Negative	Features	Rank
1	none, host, bacterium	virus	max_pk1_speed	1
2	none, host, virus	bacterium	max_integral	1
3	none, host	bacterium, virus	rms	1
4	none, bacterium, virus	host	max_pk1_speed	1
5	none, bacterium	host, virus	num_peaks	1
6	none, virus	host, bacterium	time2HalfMaxIntegral	1
7	none	host, bacterium, virus	peak2peak	1
1	none, host, bacterium	virus	time2HalfMaxIntegral	2
2	none, host, virus	bacterium	rms	2
3	none, host	bacterium, virus	peak2peak	2

4	none, bacterium, virus	host	time2HalfMaxIntegral	2
5	none, bacterium	host, virus	pk2_prom	2
6	none, virus	host, bacterium	max_pk1_speed	2
7	none	host, bacterium, virus	rms	2
1	none, host, bacterium	virus	early_speed	3
2	none, host, virus	bacterium	max_pk1_speed	3
3	none, host	bacterium, virus	max_amplitude	3
4	none, bacterium, virus	host	early_slewrate	3
5	none, bacterium	host, virus	oscpower	3
6	none, virus	host, bacterium	early_speed	3
7	none	host, bacterium, virus	max_amplitude	3
1	none, host, bacterium	virus	mean_movstd	4
2	none, host, virus	bacterium	pk1_amp	4
3	none, host	bacterium, virus	max_integral	4
4	none, bacterium, virus	host	oscpower	4
5	none, bacterium	host, virus	mean_movmad	4
6	none, virus	host, bacterium	pk1_amp	4
7	none	host, bacterium, virus	mean_movmad	4
1	none, host, bacterium	virus	mean_movmad	5
2	none, host, virus	bacterium	oscpower	5
3	none, host	bacterium, virus	early_speed	5
4	none, bacterium, virus	host	linear_changept	5
5	none, bacterium	host, virus	mean_movstd	5
6	none, virus	host, bacterium	max_derivative	5
7	none	host, bacterium, virus	early_speed	5
1	none, host, bacterium	virus	min_derivative	6
2	none, host, virus	bacterium	early_speed	6
3	none, host	bacterium, virus	pk2_amp	6
4	none, bacterium, virus	host	num_peaks	6
5	none, bacterium	host, virus	oscfreq	6
6	none, virus	host, bacterium	mean_movmad	6
7	none	host, bacterium, virus	mean_peak_amp	6
1	none, host, bacterium	virus	oscpower	7
2	none, host, virus	bacterium	time2HalfMaxIntegral	7
3	none, host	bacterium, virus	time2HalfMaxIntegral	7
4	none, bacterium, virus	host	pk2_prom	7
5	none, bacterium	host, virus	min_derivative	7
6	none, virus	host, bacterium	mean_movstd	7
7	none	host, bacterium, virus	mean_movvar	7
1	none, host, bacterium	virus	num_peaks	8
2	none, host, virus	bacterium	peak2peak	8
3	none, host	bacterium, virus	mean_movmad	8

4	none, bacterium, virus	host	min_derivative	8
5	none, bacterium	host, virus	max_amplitude	8
6	none, virus	host, bacterium	max_integral	8
7	none	host, bacterium, virus	median_peak_amp	8
1	none, host, bacterium	virus	max_derivative	9
2	none, host, virus	bacterium	max_pentropy	9
3	none, host	bacterium, virus	mean_peak_amp	9
4	none, bacterium, virus	host	pk1_time	9
5	none, bacterium	host, virus	mean_movvar	9
6	none, virus	host, bacterium	mean_movvar	9
7	none	host, bacterium, virus	mean_movstd	9
1	none, host, bacterium	virus	max_integral	10
2	none, host, virus	bacterium	max_derivative	10
3	none, host	bacterium, virus	off_times	10
4	none, bacterium, virus	host	early_activity	10
5	none, bacterium	host, virus	rms	10
6	none, virus	host, bacterium	max_pentropy	10
7	none	host, bacterium, virus	mean_trough2peak	10
1	none, host, bacterium	virus	pk1_time	11
2	none, host, virus	bacterium	max_amplitude	11
3	none, host	bacterium, virus	mean_movvar	11
4	none, bacterium, virus	host	mean_movstd	11
5	none, bacterium	host, virus	max_derivative	11
6	none, virus	host, bacterium	pk1_prom	11
7	none	host, bacterium, virus	off_times	11
1	none, host, bacterium	virus	early_activity	12
2	none, host, virus	bacterium	mean_peak_amp	12
3	none, host	bacterium, virus	pk1_amp	12
4	none, bacterium, virus	host	early_speed	12
5	none, bacterium	host, virus	off_times	12
6	none, virus	host, bacterium	max_amplitude	12
7	none	host, bacterium, virus	max_derivative	12
1	none, host, bacterium	virus	early_slewrate	13
2	none, host, virus	bacterium	linear_changept	13
3	none, host	bacterium, virus	median_peak_amp	13
4	none, bacterium, virus	host	pk1_prom	13
5	none, bacterium	host, virus	pk2_amp	13
6	none, virus	host, bacterium	rms	13
7	none	host, bacterium, virus	pk1_amp	13
1	none, host, bacterium	virus	max_pentropy	14
2	none, host, virus	bacterium	median_peak_amp	14
3	none, host	bacterium, virus	max_pk1_speed	14

4	none, bacterium, virus	host	early_risetime	14
5	none, bacterium	host, virus	max_integral	14
6	none, virus	host, bacterium	early_slewrate	14
7	none	host, bacterium, virus	pk2_amp	14
1	none, host, bacterium	virus	mean_movvar	15
2	none, host, virus	bacterium	peak2rms	15
3	none, host	bacterium, virus	max_derivative	15
4	none, bacterium, virus	host	max_integral	15
5	none, bacterium	host, virus	peak2peak	15
6	none, virus	host, bacterium	early_activity	15
7	none	host, bacterium, virus	max_pk1_speed	15
1	none, host, bacterium	virus	early_risetime	16
2	none, host, virus	bacterium	oscfreq	16
3	none, host	bacterium, virus	mean_movstd	16
4	none, bacterium, virus	host	pk1_amp	16
5	none, bacterium	host, virus	peakfreq	16
6	none, virus	host, bacterium	peak2peak	16
7	none	host, bacterium, virus	max_integral	16
1	none, host, bacterium	virus	oscfreq	17
2	none, host, virus	bacterium	cv_trough2peak	17
3	none, host	bacterium, virus	late_speed	17
4	none, bacterium, virus	host	median_derivative	17
5	none, bacterium	host, virus	early_speed	17
6	none, virus	host, bacterium	linear_changept	17
7	none	host, bacterium, virus	time2HalfMaxIntegral	17
1	none, host, bacterium	virus	pk1_amp	18
2	none, host, virus	bacterium	pk2_amp	18
3	none, host	bacterium, virus	mean_trough2peak	18
4	none, bacterium, virus	host	min_ipt	18
5	none, bacterium	host, virus	cv_trough2peak	18
6	none, virus	host, bacterium	peakfreq	18
7	none	host, bacterium, virus	peakfreq	18
1	none, host, bacterium	virus	late_speed	19
2	none, host, virus	bacterium	mean_derivative	19
3	none, host	bacterium, virus	peakfreq	19
4	none, bacterium, virus	host	mean_movmad	19
5	none, bacterium	host, virus	peak2rms	19
6	none, virus	host, bacterium	late_slewrate	19
7	none	host, bacterium, virus	min_derivative	19
1	none, host, bacterium	virus	rms	20
2	none, host, virus	bacterium	pk1_prom	20
3	none, host	bacterium, virus	std_trough2peak	20

4	none, bacterium, virus	host	oscfreq	20
5	none, bacterium	host, virus	pk1_amp	20
6	none, virus	host, bacterium	off_times	20
7	none	host, bacterium, virus	late_speed	20
1	none, host, bacterium	virus	pk2_prom	21
2	none, host, virus	bacterium	mean_movvar	21
3	none, host	bacterium, virus	cv_trough2peak	21
4	none, bacterium, virus	host	mean_movvar	21
5	none, bacterium	host, virus	pk1_prom	21
6	none, virus	host, bacterium	pk2_amp	21
7	none	host, bacterium, virus	pk1_prom	21
1	none, host, bacterium	virus	late_slewrate	22
2	none, host, virus	bacterium	std_trough2peak	22
3	none, host	bacterium, virus	min_derivative	22
4	none, bacterium, virus	host	rms	22
5	none, bacterium	host, virus	linear_changept	22
6	none, virus	host, bacterium	oscpower	22
7	none	host, bacterium, virus	fold_change	22
1	none, host, bacterium	virus	peak2rms	23
2	none, host, virus	bacterium	early_activity	23
3	none, host	bacterium, virus	mean_derivative	23
4	none, bacterium, virus	host	mean_derivative	23
5	none, bacterium	host, virus	time2HalfMaxIntegral	23
6	none, virus	host, bacterium	min_derivative	23
7	none	host, bacterium, virus	cv_peak2trough	23
1	none, host, bacterium	virus	peak2peak	24
2	none, host, virus	bacterium	mean_movmad	24
3	none, host	bacterium, virus	std_peak_amp	24
4	none, bacterium, virus	host	late_speed	24
5	none, bacterium	host, virus	max_pk1_speed	24
6	none, virus	host, bacterium	cv_trough2peak	24
7	none	host, bacterium, virus	std_peak2trough	24
1	none, host, bacterium	virus	pk1_prom	25
2	none, host, virus	bacterium	mean_movstd	25
3	none, host	bacterium, virus	cv_peak_amp	25
4	none, bacterium, virus	host	peakfreq	25
5	none, bacterium	host, virus	max_pentropy	25
6	none, virus	host, bacterium	std_trough2peak	25
7	none	host, bacterium, virus	mean_peak2trough	25
1	none, host, bacterium	virus	pk2_ratio	26
2	none, host, virus	bacterium	late_slewrate	26
3	none, host	bacterium, virus	pk1_prom	26

4	none, bacterium, virus	host	max_derivative	26
5	none, bacterium	host, virus	std_trough2peak	26
6	none, virus	host, bacterium	pk1_time	26
7	none	host, bacterium, virus	peak2rms	26
1	none, host, bacterium	virus	mean_derivative	27
2	none, host, virus	bacterium	off_times	27
3	none, host	bacterium, virus	median_trough2peak	27
4	none, bacterium, virus	host	max_amplitude	27
5	none, bacterium	host, virus	std_peak2trough	27
6	none, virus	host, bacterium	late_speed	27
7	none	host, bacterium, virus	std_changept	27
1	none, host, bacterium	virus	median_peak_amp	28
2	none, host, virus	bacterium	min_derivative	28
3	none, host	bacterium, virus	num_peaks	28
4	none, bacterium, virus	host	peak2peak	28
5	none, bacterium	host, virus	cv_peak2trough	28
6	none, virus	host, bacterium	mean_derivative	28
7	none	host, bacterium, virus	pk2_width	28
1	none, host, bacterium	virus	max_amplitude	29
2	none, host, virus	bacterium	late_activity	29
3	none, host	bacterium, virus	linear_changept	29
4	none, bacterium, virus	host	pk2_width	29
5	none, bacterium	host, virus	late_activity	29
6	none, virus	host, bacterium	mean_trough2peak	29
7	none	host, bacterium, virus	oscbandwidth	29
1	none, host, bacterium	virus	pk2_amp	30
2	none, host, virus	bacterium	peakfreq	30
3	none, host	bacterium, virus	pk2_prom	30
4	none, bacterium, virus	host	peak2rms	30
5	none, bacterium	host, virus	max_peak2trough	30
6	none, virus	host, bacterium	mean_peak_amp	30
7	none	host, bacterium, virus	num_peaks	30
1	none, host, bacterium	virus	last_falltime	31
2	none, host, virus	bacterium	late_speed	31
3	none, host	bacterium, virus	fold_change	31
4	none, bacterium, virus	host	fold_change	31
5	none, bacterium	host, virus	mean_peak2trough	31
6	none, virus	host, bacterium	median_peak_amp	31
7	none	host, bacterium, virus	max_pentropy	31
1	none, host, bacterium	virus	pk2_width	32
2	none, host, virus	bacterium	mean_trough2peak	32
3	none, host	bacterium, virus	peak2rms	32

4	none, bacterium, virus	host	medfreq	32
5	none, bacterium	host, virus	std_peak_amp	32
6	none, virus	host, bacterium	std_peak_amp	32
7	none	host, bacterium, virus	mean_derivative	32
1	none, host, bacterium	virus	pk1_width	33
2	none, host, virus	bacterium	last_falltime	33
3	none, host	bacterium, virus	early_activity	33
4	none, bacterium, virus	host	pk1_width	33
5	none, bacterium	host, virus	median_trough2peak	33
6	none, virus	host, bacterium	cv_peak_amp	33
7	none	host, bacterium, virus	pk2_prom	33
1	none, host, bacterium	virus	pk2_time	34
2	none, host, virus	bacterium	oscbandwidth	34
3	none, host	bacterium, virus	early_slewrate	34
4	none, bacterium, virus	host	meanfreq	34
5	none, bacterium	host, virus	mean_trough2peak	34
6	none, virus	host, bacterium	median_trough2peak	34
7	none	host, bacterium, virus	pk1_width	34
1	none, host, bacterium	virus	mean_changept	35
2	none, host, virus	bacterium	pk2_prom	35
3	none, host	bacterium, virus	oscpower	35
4	none, bacterium, virus	host	pk2_ratio	35
5	none, bacterium	host, virus	median_peak_amp	35
6	none, virus	host, bacterium	pk2_ratio	35
7	none	host, bacterium, virus	max_peak2trough	35
1	none, host, bacterium	virus	median_derivative	36
2	none, host, virus	bacterium	pk1_time	36
3	none, host	bacterium, virus	early_risetime	36
4	none, bacterium, virus	host	last_falltime	36
5	none, bacterium	host, virus	cv_peak_amp	36
6	none, virus	host, bacterium	early_risetime	36
7	none	host, bacterium, virus	late_slewrate	36
1	none, host, bacterium	virus	cv_trough2peak	37
2	none, host, virus	bacterium	early_risetime	37
3	none, host	bacterium, virus	oscfreq	37
4	none, bacterium, virus	host	pk2_amp	37
5	none, bacterium	host, virus	late_speed	37
6	none, virus	host, bacterium	pk2_width	37
7	none	host, bacterium, virus	early_risetime	37
1	none, host, bacterium	virus	late_activity	38
2	none, host, virus	bacterium	pk2_width	38
3	none, host	bacterium, virus	oscbandwidth	38

4	none, bacterium, virus	host	pk2_time	38
5	none, bacterium	host, virus	median_peak2trough	38
6	none, virus	host, bacterium	peak2rms	38
7	none	host, bacterium, virus	oscfreq	38
1	none, host, bacterium	virus	std_trough2peak	39
2	none, host, virus	bacterium	num_peaks	39
3	none, host	bacterium, virus	max_pentropy	39
4	none, bacterium, virus	host	oscbandwidth	39
5	none, bacterium	host, virus	pk1_time	39
6	none, virus	host, bacterium	oscbandwidth	39
7	none	host, bacterium, virus	mean_changept	39
1	none, host, bacterium	virus	linear_changept	40
2	none, host, virus	bacterium	std_ipt	40
3	none, host	bacterium, virus	min_ipt	40
4	none, bacterium, virus	host	mean_trough2peak	40
5	none, bacterium	host, virus	mean_peak_amp	40
6	none, virus	host, bacterium	num_peaks	40
7	none	host, bacterium, virus	median_peak2trough	40
1	none, host, bacterium	virus	max_peak2trough	41
2	none, host, virus	bacterium	fold_change	41
3	none, host	bacterium, virus	pk1_time	41
4	none, bacterium, virus	host	mean_ipt	41
5	none, bacterium	host, virus	pk2_ratio	41
6	none, virus	host, bacterium	pk1_width	41
7	none	host, bacterium, virus	std_peak_amp	41
1	none, host, bacterium	virus	meanfreq	42
2	none, host, virus	bacterium	cv_ipt	42
3	none, host	bacterium, virus	late_activity	42
4	none, bacterium, virus	host	cv_ipt	42
5	none, bacterium	host, virus	late_slewrate	42
6	none, virus	host, bacterium	last_falltime	42
7	none	host, bacterium, virus	cv_trough2peak	42
1	none, host, bacterium	virus	oscbandwidth	43
2	none, host, virus	bacterium	early_slewrate	43
3	none, host	bacterium, virus	cv_peak2trough	43
4	none, bacterium, virus	host	late_activity	43
5	none, bacterium	host, virus	fold_change	43
6	none, virus	host, bacterium	median_derivative	43
7	none	host, bacterium, virus	oscpower	43
1	none, host, bacterium	virus	fold_change	44
2	none, host, virus	bacterium	pk2_time	44
3	none, host	bacterium, virus	pk2_width	44

4	none, bacterium, virus	host	median_ipt	44
5	none, bacterium	host, virus	early_activity	44
6	none, virus	host, bacterium	oscfreq	44
7	none	host, bacterium, virus	pk2_ratio	44
1	none, host, bacterium	virus	mean_peak2trough	45
2	none, host, virus	bacterium	pk1_width	45
3	none, host	bacterium, virus	pk1_width	45
4	none, bacterium, virus	host	std_peak_amp	45
5	none, bacterium	host, virus	cv_ipt	45
6	none, virus	host, bacterium	max_peak2trough	45
7	none	host, bacterium, virus	last_falltime	45
1	none, host, bacterium	virus	median_peak2trough	46
2	none, host, virus	bacterium	powerbw	46
3	none, host	bacterium, virus	medfreq	46
4	none, bacterium, virus	host	late_slewrate	46
5	none, bacterium	host, virus	oscbandwidth	46
6	none, virus	host, bacterium	fold_change	46
7	none	host, bacterium, virus	std_trough2peak	46
1	none, host, bacterium	virus	cv_peak_amp	47
2	none, host, virus	bacterium	pk2_ratio	47
3	none, host	bacterium, virus	pk2_time	47
4	none, bacterium, virus	host	median_trough2peak	47
5	none, bacterium	host, virus	std_ipt	47
6	none, virus	host, bacterium	late_activity	47
7	none	host, bacterium, virus	cv_peak_amp	47
1	none, host, bacterium	virus	std_peak2trough	48
2	none, host, virus	bacterium	medfreq	48
3	none, host	bacterium, virus	median_ipt	48
4	none, bacterium, virus	host	std_trough2peak	48
5	none, bacterium	host, virus	mean_derivative	48
6	none, virus	host, bacterium	std_peak2trough	48
7	none	host, bacterium, virus	pk1_time	48
1	none, host, bacterium	virus	max_trough2peak	49
2	none, host, virus	bacterium	late_falltime	49
3	none, host	bacterium, virus	median_derivative	49
4	none, bacterium, virus	host	std_peak2trough	49
5	none, bacterium	host, virus	early_risetime	49
6	none, virus	host, bacterium	mean_peak2trough	49
7	none	host, bacterium, virus	max_trough2peak	49
1	none, host, bacterium	virus	max_ipt	50
2	none, host, virus	bacterium	median_derivative	50
3	none, host	bacterium, virus	mean_ipt	50

4	none, bacterium, virus	host	max_trough2peak	50
5	none, bacterium	host, virus	mean_changept	50
6	none, virus	host, bacterium	pk2_time	50
7	none	host, bacterium, virus	pk2_time	50
1	none, host, bacterium	virus	medfreq	51
2	none, host, virus	bacterium	meanfreq	51
3	none, host	bacterium, virus	pk2_ratio	51
4	none, bacterium, virus	host	max_pentropy	51
5	none, bacterium	host, virus	powerbw	51
6	none, virus	host, bacterium	pk2_prom	51
7	none	host, bacterium, virus	linear_changept	51
1	none, host, bacterium	virus	std_changept	52
2	none, host, virus	bacterium	max_peak2trough	52
3	none, host	bacterium, virus	std_peak2trough	52
4	none, bacterium, virus	host	cv_trough2peak	52
5	none, bacterium	host, virus	pk2_width	52
6	none, virus	host, bacterium	meanfreq	52
7	none	host, bacterium, virus	early_activity	52
1	none, host, bacterium	virus	mean_ipt	53
2	none, host, virus	bacterium	std_changept	53
3	none, host	bacterium, virus	meanfreq	53
4	none, bacterium, virus	host	off_times	53
5	none, bacterium	host, virus	last_falltime	53
6	none, virus	host, bacterium	mean_changept	53
7	none	host, bacterium, virus	median_trough2peak	53
1	none, host, bacterium	virus	powerbw	54
2	none, host, virus	bacterium	max_trough2peak	54
3	none, host	bacterium, virus	max_trough2peak	54
4	none, bacterium, virus	host	late_falltime	54
5	none, bacterium	host, virus	early_slewrate	54
6	none, virus	host, bacterium	median_peak2trough	54
7	none	host, bacterium, virus	early_slewrate	54
1	none, host, bacterium	virus	peakfreq	55
2	none, host, virus	bacterium	median_peak2trough	55
3	none, host	bacterium, virus	late_slewrate	55
4	none, bacterium, virus	host	cv_peak2trough	55
5	none, bacterium	host, virus	pk1_width	55
6	none, virus	host, bacterium	medfreq	55
7	none	host, bacterium, virus	median_derivative	55
1	none, host, bacterium	virus	late_falltime	56
2	none, host, virus	bacterium	mean_peak2trough	56
3	none, host	bacterium, virus	late_falltime	56

4	none, bacterium, virus	host	median_peak2trough	56
5	none, bacterium	host, virus	median_derivative	56
6	none, virus	host, bacterium	std_changept	56
7	none	host, bacterium, virus	late_activity	56
1	none, host, bacterium	virus	std_ipt	57
2	none, host, virus	bacterium	min_ipt	57
3	none, host	bacterium, virus	last_falltime	57
4	none, bacterium, virus	host	max_peak2trough	57
5	none, bacterium	host, virus	min_ipt	57
6	none, virus	host, bacterium	cv_peak2trough	57
7	none	host, bacterium, virus	powerbw	57
1	none, host, bacterium	virus	cv_peak2trough	58
2	none, host, virus	bacterium	mean_ipt	58
3	none, host	bacterium, virus	mean_peak2trough	58
4	none, bacterium, virus	host	std_ipt	58
5	none, bacterium	host, virus	mean_ipt	58
6	none, virus	host, bacterium	min_ipt	58
7	none	host, bacterium, virus	late_falltime	58
1	none, host, bacterium	virus	off_times	59
2	none, host, virus	bacterium	median_ipt	59
3	none, host	bacterium, virus	powerbw	59
4	none, bacterium, virus	host	mean_changept	59
5	none, bacterium	host, virus	late_falltime	59
6	none, virus	host, bacterium	late_falltime	59
7	none	host, bacterium, virus	meanfreq	59
1	none, host, bacterium	virus	min_ipt	60
2	none, host, virus	bacterium	cv_peak2trough	60
3	none, host	bacterium, virus	median_peak2trough	60
4	none, bacterium, virus	host	max_ipt	60
5	none, bacterium	host, virus	median_ipt	60
6	none, virus	host, bacterium	mean_ipt	60
7	none	host, bacterium, virus	medfreq	60
1	none, host, bacterium	virus	median_ipt	61
2	none, host, virus	bacterium	mean_changept	61
3	none, host	bacterium, virus	max_peak2trough	61
4	none, bacterium, virus	host	mean_peak_amp	61
5	none, bacterium	host, virus	meanfreq	61
6	none, virus	host, bacterium	max_trough2peak	61
7	none	host, bacterium, virus	cv_ipt	61
1	none, host, bacterium	virus	cv_ipt	62
2	none, host, virus	bacterium	max_ipt	62
3	none, host	bacterium, virus	std_changept	62

4	none, bacterium, virus	host	std_changept	62
5	none, bacterium	host, virus	medfreq	62
6	none, virus	host, bacterium	std_ipt	62
7	none	host, bacterium, virus	max_ipt	62
1	none, host, bacterium	virus	mean_peak_amp	63
2	none, host, virus	bacterium	std_peak2trough	63
3	none, host	bacterium, virus	max_ipt	63
4	none, bacterium, virus	host	powerbw	63
5	none, bacterium	host, virus	std_changept	63
6	none, virus	host, bacterium	cv_ipt	63
7	none	host, bacterium, virus	min_ipt	63
1	none, host, bacterium	virus	median_trough2peak	64
2	none, host, virus	bacterium	cv_peak_amp	64
3	none, host	bacterium, virus	mean_changept	64
4	none, bacterium, virus	host	median_peak_amp	64
5	none, bacterium	host, virus	max_trough2peak	64
6	none, virus	host, bacterium	max_ipt	64
7	none	host, bacterium, virus	std_ipt	64
1	none, host, bacterium	virus	std_peak_amp	65
2	none, host, virus	bacterium	median_trough2peak	65
3	none, host	bacterium, virus	cv_ipt	65
4	none, bacterium, virus	host	cv_peak_amp	65
5	none, bacterium	host, virus	pk2_time	65
6	none, virus	host, bacterium	median_ipt	65
7	none	host, bacterium, virus	mean_ipt	65
1	none, host, bacterium	virus	mean_trough2peak	66
2	none, host, virus	bacterium	std_peak_amp	66
3	none, host	bacterium, virus	std_ipt	66
4	none, bacterium, virus	host	mean_peak2trough	66
5	none, bacterium	host, virus	max_ipt	66
6	none, virus	host, bacterium	powerbw	66
7	none	host, bacterium, virus	median_ipt	66

Table 3.2. Top features for classifying ligand types in M_0 macrophages.

Learner	Positive	Negative	Features	Rank
1	none, cytokine	PAMP	rms	1
2	none, PAMP	cytokine	max_pk1_speed	1
3	none	cytokine, PAMP	peak2peak	1
1	none, cytokine	PAMP	peak2peak	2
2	none, PAMP	cytokine	time2HalfMaxIntegral	2
3	none	cytokine, PAMP	rms	2
1	none, cytokine	PAMP	max_amplitude	3
2	none, PAMP	cytokine	early_slewrate	3
3	none	cytokine, PAMP	max_amplitude	3
1	none, cytokine	PAMP	max_integral	4
2	none, PAMP	cytokine	oscpower	4
3	none	cytokine, PAMP	mean_movmad	4
1	none, cytokine	PAMP	early_speed	5
2	none, PAMP	cytokine	linear_changept	5
3	none	cytokine, PAMP	early_speed	5
1	none, cytokine	PAMP	pk2_amp	6
2	none, PAMP	cytokine	num_peaks	6
3	none	cytokine, PAMP	mean_peak_amp	6
1	none, cytokine	PAMP	time2HalfMaxIntegral	7
2	none, PAMP	cytokine	pk2_prom	7
3	none	cytokine, PAMP	mean_movvar	7
1	none, cytokine	PAMP	mean_movmad	8
2	none, PAMP	cytokine	min_derivative	8
3	none	cytokine, PAMP	median_peak_amp	8
1	none, cytokine	PAMP	mean_peak_amp	9
2	none, PAMP	cytokine	pk1_time	9
3	none	cytokine, PAMP	mean_movstd	9
1	none, cytokine	PAMP	off_times	10
2	none, PAMP	cytokine	early_activity	10
3	none	cytokine, PAMP	mean_trough2peak	10
1	none, cytokine	PAMP	mean_movvar	11
2	none, PAMP	cytokine	mean_movstd	11
3	none	cytokine, PAMP	off_times	11
1	none, cytokine	PAMP	pk1_amp	12
2	none, PAMP	cytokine	early_speed	12
3	none	cytokine, PAMP	max_derivative	12
1	none, cytokine	PAMP	median_peak_amp	13
2	none, PAMP	cytokine	pk1_prom	13
3	none	cytokine, PAMP	pk1_amp	13

1	none, cytokine	PAMP	max_pk1_speed	14
2	none, PAMP	cytokine	early_risetime	14
3	none	cytokine, PAMP	pk2_amp	14
1	none, cytokine	PAMP	max_derivative	15
2	none, PAMP	cytokine	max_integral	15
3	none	cytokine, PAMP	max_pk1_speed	15
1	none, cytokine	PAMP	mean_movstd	16
2	none, PAMP	cytokine	pk1_amp	16
3	none	cytokine, PAMP	max_integral	16
1	none, cytokine	PAMP	late_speed	17
2	none, PAMP	cytokine	median_derivative	17
3	none	cytokine, PAMP	time2HalfMaxIntegral	17
1	none, cytokine	PAMP	mean_trough2peak	18
2	none, PAMP	cytokine	min_ipt	18
3	none	cytokine, PAMP	peakfreq	18
1	none, cytokine	PAMP	peakfreq	19
2	none, PAMP	cytokine	mean_movmad	19
3	none	cytokine, PAMP	min_derivative	19
1	none, cytokine	PAMP	std_trough2peak	20
2	none, PAMP	cytokine	oscfreq	20
3	none	cytokine, PAMP	late_speed	20
1	none, cytokine	PAMP	cv_trough2peak	21
2	none, PAMP	cytokine	mean_movvar	21
3	none	cytokine, PAMP	pk1_prom	21
1	none, cytokine	PAMP	min_derivative	22
2	none, PAMP	cytokine	rms	22
3	none	cytokine, PAMP	fold_change	22
1	none, cytokine	PAMP	mean_derivative	23
2	none, PAMP	cytokine	mean_derivative	23
3	none	cytokine, PAMP	cv_peak2trough	23
1	none, cytokine	PAMP	std_peak_amp	24
2	none, PAMP	cytokine	late_speed	24
3	none	cytokine, PAMP	std_peak2trough	24
1	none, cytokine	PAMP	cv_peak_amp	25
2	none, PAMP	cytokine	peakfreq	25
3	none	cytokine, PAMP	mean_peak2trough	25
1	none, cytokine	PAMP	pk1_prom	26
2	none, PAMP	cytokine	max_derivative	26
3	none	cytokine, PAMP	peak2rms	26
1	none, cytokine	PAMP	median_trough2peak	27
2	none, PAMP	cytokine	max_amplitude	27
3	none	cytokine, PAMP	std_changept	27

1	none, cytokine	PAMP	num_peaks	28
2	none, PAMP	cytokine	peak2peak	28
3	none	cytokine, PAMP	pk2_width	28
1	none, cytokine	PAMP	linear_changept	29
2	none, PAMP	cytokine	pk2_width	29
3	none	cytokine, PAMP	oscbandwidth	29
1	none, cytokine	PAMP	pk2_prom	30
2	none, PAMP	cytokine	peak2rms	30
3	none	cytokine, PAMP	num_peaks	30
1	none, cytokine	PAMP	fold_change	31
2	none, PAMP	cytokine	fold_change	31
3	none	cytokine, PAMP	max_pentropy	31
1	none, cytokine	PAMP	peak2rms	32
2	none, PAMP	cytokine	medfreq	32
3	none	cytokine, PAMP	mean_derivative	32
1	none, cytokine	PAMP	early_activity	33
2	none, PAMP	cytokine	pk1_width	33
3	none	cytokine, PAMP	pk2_prom	33
1	none, cytokine	PAMP	early_slewrate	34
2	none, PAMP	cytokine	meanfreq	34
3	none	cytokine, PAMP	pk1_width	34
1	none, cytokine	PAMP	oscpower	35
2	none, PAMP	cytokine	pk2_ratio	35
3	none	cytokine, PAMP	early_risetime	35
1	none, cytokine	PAMP	early_risetime	36
2	none, PAMP	cytokine	last_falltime	36
3	none	cytokine, PAMP	max_peak2trough	36
1	none, cytokine	PAMP	oscfreq	37
2	none, PAMP	cytokine	pk2_amp	37
3	none	cytokine, PAMP	late_slewrate	37
1	none, cytokine	PAMP	oscbandwidth	38
2	none, PAMP	cytokine	pk2_time	38
3	none	cytokine, PAMP	oscfreq	38
1	none, cytokine	PAMP	max_pentropy	39
2	none, PAMP	cytokine	oscbandwidth	39
3	none	cytokine, PAMP	mean_changept	39
1	none, cytokine	PAMP	min_ipt	40
2	none, PAMP	cytokine	mean_trough2peak	40
3	none	cytokine, PAMP	median_peak2trough	40
1	none, cytokine	PAMP	pk1_time	41
2	none, PAMP	cytokine	mean_ipt	41
3	none	cytokine, PAMP	cv_trough2peak	41

1	none, cytokine	PAMP	late_activity	42
2	none, PAMP	cytokine	cv_ipt	42
3	none	cytokine, PAMP	std_peak_amp	42
1	none, cytokine	PAMP	cv_peak2trough	43
2	none, PAMP	cytokine	late_activity	43
3	none	cytokine, PAMP	last_falltime	43
1	none, cytokine	PAMP	pk2_width	44
2	none, PAMP	cytokine	median_ipt	44
3	none	cytokine, PAMP	oscpower	44
1	none, cytokine	PAMP	pk1_width	45
2	none, PAMP	cytokine	std_peak_amp	45
3	none	cytokine, PAMP	pk2_ratio	45
1	none, cytokine	PAMP	medfreq	46
2	none, PAMP	cytokine	late_slewrate	46
3	none	cytokine, PAMP	cv_peak_amp	46
1	none, cytokine	PAMP	pk2_time	47
2	none, PAMP	cytokine	median_trough2peak	47
3	none	cytokine, PAMP	std_trough2peak	47
1	none, cytokine	PAMP	median_ipt	48
2	none, PAMP	cytokine	std_trough2peak	48
3	none	cytokine, PAMP	max_trough2peak	48
1	none, cytokine	PAMP	median_derivative	49
2	none, PAMP	cytokine	std_peak2trough	49
3	none	cytokine, PAMP	pk2_time	49
1	none, cytokine	PAMP	mean_ipt	50
2	none, PAMP	cytokine	max_trough2peak	50
3	none	cytokine, PAMP	early_slewrate	50
1	none, cytokine	PAMP	pk2_ratio	51
2	none, PAMP	cytokine	max_pentropy	51
3	none	cytokine, PAMP	linear_changept	51
1	none, cytokine	PAMP	std_peak2trough	52
2	none, PAMP	cytokine	cv_trough2peak	52
3	none	cytokine, PAMP	pk1_time	52
1	none, cytokine	PAMP	meanfreq	53
2	none, PAMP	cytokine	off_times	53
3	none	cytokine, PAMP	median_trough2peak	53
1	none, cytokine	PAMP	max_trough2peak	54
2	none, PAMP	cytokine	late_falltime	54
3	none	cytokine, PAMP	median_derivative	54
1	none, cytokine	PAMP	late_slewrate	55
2	none, PAMP	cytokine	cv_peak2trough	55
3	none	cytokine, PAMP	early_activity	55

1	none, cytokine	PAMP	late_falltime	56
2	none, PAMP	cytokine	median_peak2trough	56
3	none	cytokine, PAMP	late_activity	56
1	none, cytokine	PAMP	last_falltime	57
2	none, PAMP	cytokine	max_peak2trough	57
3	none	cytokine, PAMP	powerbw	57
1	none, cytokine	PAMP	mean_peak2trough	58
2	none, PAMP	cytokine	std_ipt	58
3	none	cytokine, PAMP	late_falltime	58
1	none, cytokine	PAMP	powerbw	59
2	none, PAMP	cytokine	mean_changept	59
3	none	cytokine, PAMP	medfreq	59
1	none, cytokine	PAMP	median_peak2trough	60
2	none, PAMP	cytokine	max_ipt	60
3	none	cytokine, PAMP	cv_ipt	60
1	none, cytokine	PAMP	max_peak2trough	61
2	none, PAMP	cytokine	mean_peak_amp	61
3	none	cytokine, PAMP	meanfreq	61
1	none, cytokine	PAMP	std_changept	62
2	none, PAMP	cytokine	std_changept	62
3	none	cytokine, PAMP	min_ipt	62
1	none, cytokine	PAMP	max_ipt	63
2	none, PAMP	cytokine	powerbw	63
3	none	cytokine, PAMP	median_ipt	63
1	none, cytokine	PAMP	mean_changept	64
2	none, PAMP	cytokine	median_peak_amp	64
3	none	cytokine, PAMP	std_ipt	64
1	none, cytokine	PAMP	cv_ipt	65
2	none, PAMP	cytokine	cv_peak_amp	65
3	none	cytokine, PAMP	mean_ipt	65
1	none, cytokine	PAMP	std_ipt	66
2	none, PAMP	cytokine	mean_peak2trough	66
3	none	cytokine, PAMP	max_ipt	66

Learner	Positive	Negative	Features	Rank
1	none, host, bacterium	virus	mean_movmad	1
2	none, host, virus	bacterium	max_pentropy	1
3	none, host	bacterium, virus	oscpower	1
4	none, bacterium, virus	host	num_peaks	1
5	none, bacterium	host, virus	oscpower	1

6	none, virus	host, bacterium	max_pk1_speed	1
7	none	host, bacterium, virus	rms	1
1	none, host, bacterium	virus	mean_movstd	2
2	none, host, virus	bacterium	oscpower	2
3	none, host	bacterium, virus	mean_peak_amp	2
4	none, bacterium, virus	host	mean_movmad	2
5	none, bacterium	host, virus	mean_movmad	2
6	none, virus	host, bacterium	time2HalfMaxIntegral	2
7	none	host, bacterium, virus	max_amplitude	2
1	none, host, bacterium	virus	mean_movvar	3
2	none, host, virus	bacterium	oscfreq	3
3	none, host	bacterium, virus	median_peak_amp	3
4	none, bacterium, virus	host	oscpower	3
5	none, bacterium	host, virus	num_peaks	3
6	none, virus	host, bacterium	early_speed	3
7	none	host, bacterium, virus	early_speed	3
1	none, host, bacterium	virus	max_amplitude	4
2	none, host, virus	bacterium	peak2rms	4
3	none, host	bacterium, virus	oscfreq	4
4	none, bacterium, virus	host	mean_movstd	4
5	none, bacterium	host, virus	oscfreq	4
6	none, virus	host, bacterium	pk1_amp	4
7	none	host, bacterium, virus	mean_peak_amp	4
1	none, host, bacterium	virus	time2HalfMaxIntegral	5
2	none, host, virus	bacterium	max_pk1_speed	5
3	none, host	bacterium, virus	peak2rms	5
4	none, bacterium, virus	host	oscfreq	5
5	none, bacterium	host, virus	mean_movstd	5
6	none, virus	host, bacterium	max_integral	5
7	none	host, bacterium, virus	median_peak_amp	5
1	none, host, bacterium	virus	max_pk1_speed	6
2	none, host, virus	bacterium	time2HalfMaxIntegral	6

3	none, host	bacterium, virus	max_pentropy	6
4	none, bacterium, virus	host	mean_movvar	6
5	none, bacterium	host, virus	max_pentropy	6
6	none, virus	host, bacterium	max_derivative	6
7	none	host, bacterium, virus	peak2peak	6
1	none, host, bacterium	virus	min_derivative	7
2	none, host, virus	bacterium	max_integral	7
3	none, host	bacterium, virus	rms	7
4	none, bacterium, virus	host	min_derivative	7
5	none, bacterium	host, virus	peak2rms	7
6	none, virus	host, bacterium	rms	7
7	none	host, bacterium, virus	mean_trough2peak	7
1	none, host, bacterium	virus	peak2peak	8
2	none, host, virus	bacterium	num_peaks	8
3	none, host	bacterium, virus	max_integral	8
4	none, bacterium, virus	host	pk2_prom	8
5	none, bacterium	host, virus	pk2_prom	8
6	none, virus	host, bacterium	mean_peak_amp	8
7	none	host, bacterium, virus	mean_movvar	8
1	none, host, bacterium	virus	early_speed	9
2	none, host, virus	bacterium	early_speed	9
3	none, host	bacterium, virus	max_amplitude	9
4	none, bacterium, virus	host	max_pk1_speed	9
5	none, bacterium	host, virus	min_derivative	9
6	none, virus	host, bacterium	median_peak_amp	9
7	none	host, bacterium, virus	max_derivative	9
1	none, host, bacterium	virus	late_speed	10
2	none, host, virus	bacterium	mean_movmad	10
3	none, host	bacterium, virus	mean_movmad	10
4	none, bacterium, virus	host	peak2rms	10
5	none, bacterium	host, virus	cv_peak_amp	10
6	none, virus	host, bacterium	max_amplitude	10

7	none	host, bacterium, virus	pk1_amp	10
1	none, host, bacterium	virus	pk1_time	11
2	none, host, virus	bacterium	mean_movstd	11
3	none, host	bacterium, virus	mean_derivative	11
4	none, bacterium, virus	host	time2HalfMaxIntegral	11
5	none, bacterium	host, virus	mean_movvar	11
6	none, virus	host, bacterium	mean_movvar	11
7	none	host, bacterium, virus	max_integral	11
1	none, host, bacterium	virus	std_peak_amp	12
2	none, host, virus	bacterium	rms	12
3	none, host	bacterium, virus	peak2peak	12
4	none, bacterium, virus	host	max_pentropy	12
5	none, bacterium	host, virus	std_peak2trough	12
6	none, virus	host, bacterium	peak2peak	12
7	none	host, bacterium, virus	max_pk1_speed	12
1	none, host, bacterium	virus	num_peaks	13
2	none, host, virus	bacterium	pk2_prom	13
3	none, host	bacterium, virus	mean_movstd	13
4	none, bacterium, virus	host	early_speed	13
5	none, bacterium	host, virus	late_activity	13
6	none, virus	host, bacterium	mean_movstd	13
7	none	host, bacterium, virus	time2HalfMaxIntegral	13
1	none, host, bacterium	virus	pk2_amp	14
2	none, host, virus	bacterium	linear_changept	14
3	none, host	bacterium, virus	pk1_amp	14
4	none, bacterium, virus	host	median_derivative	14
5	none, bacterium	host, virus	cv_peak2trough	14
6	none, virus	host, bacterium	mean_trough2peak	14
7	none	host, bacterium, virus	pk2_amp	14
1	none, host, bacterium	virus	rms	15
2	none, host, virus	bacterium	last_falltime	15
3	none, host	bacterium, virus	num_peaks	15

4	none, bacterium, virus	host	rms	15
5	none, bacterium	host, virus	std_peak_amp	15
6	none, virus	host, bacterium	mean_movmad	15
7	none	host, bacterium, virus	mean_movmad	15
1	none, host, bacterium	virus	cv_peak_amp	16
2	none, host, virus	bacterium	late_slewrate	16
3	none, host	bacterium, virus	max_pk1_speed	16
4	none, bacterium, virus	host	max_amplitude	16
5	none, bacterium	host, virus	max_integral	16
6	none, virus	host, bacterium	pk2_amp	16
7	none	host, bacterium, virus	off_times	16
1	none, host, bacterium	virus	max_pentropy	17
2	none, host, virus	bacterium	mean_derivative	17
3	none, host	bacterium, virus	time2HalfMaxIntegral	17
4	none, bacterium, virus	host	max_derivative	17
5	none, bacterium	host, virus	cv_trough2peak	17
6	none, virus	host, bacterium	pk2_ratio	17
7	none	host, bacterium, virus	mean_movstd	17
1	none, host, bacterium	virus	max_derivative	18
2	none, host, virus	bacterium	late_activity	18
3	none, host	bacterium, virus	pk2_amp	18
4	none, bacterium, virus	host	pk1_amp	18
5	none, bacterium	host, virus	peakfreq	18
6	none, virus	host, bacterium	oscpower	18
7	none	host, bacterium, virus	peakfreq	18
1	none, host, bacterium	virus	oscpower	19
2	none, host, virus	bacterium	max_derivative	19
3	none, host	bacterium, virus	mean_movvar	19
4	none, bacterium, virus	host	early_activity	19
5	none, bacterium	host, virus	std_trough2peak	19
6	none, virus	host, bacterium	pk1_prom	19
7	none	host, bacterium, virus	late_speed	19

1	none, host, bacterium	virus	std_trough2peak	20
2	none, host, virus	bacterium	std_peak2trough	20
3	none, host	bacterium, virus	late_slewrate	20
4	none, bacterium, virus	host	pk1_prom	20
5	none, bacterium	host, virus	late_speed	20
6	none, virus	host, bacterium	off_times	20
7	none	host, bacterium, virus	min_derivative	20
1	none, host, bacterium	virus	pk2_prom	21
2	none, host, virus	bacterium	cv_peak2trough	21
3	none, host	bacterium, virus	max_derivative	21
4	none, bacterium, virus	host	early_slewrate	21
5	none, bacterium	host, virus	rms	21
6	none, virus	host, bacterium	pk2_width	21
7	none	host, bacterium, virus	oscpower	21
1	none, host, bacterium	virus	max_integral	22
2	none, host, virus	bacterium	min_derivative	22
3	none, host	bacterium, virus	early_speed	22
4	none, bacterium, virus	host	max_integral	22
5	none, bacterium	host, virus	std_ipt	22
6	none, virus	host, bacterium	peakfreq	22
7	none	host, bacterium, virus	pk1_prom	22
1	none, host, bacterium	virus	early_activity	23
2	none, host, virus	bacterium	median_peak_amp	23
3	none, host	bacterium, virus	pk2_prom	23
4	none, bacterium, virus	host	peak2peak	23
5	none, bacterium	host, virus	late_slewrate	23
6	none, virus	host, bacterium	late_speed	23
7	none	host, bacterium, virus	mean_peak2trough	23
1	none, host, bacterium	virus	max_peak2trough	24
2	none, host, virus	bacterium	mean_peak_amp	24
3	none, host	bacterium, virus	min_derivative	24
4	none, bacterium, virus	host	pk1_time	24

5	none, bacterium	host, virus	cv_ipt	24
6	none, virus	host, bacterium	std_peak_amp	24
7	none	host, bacterium, virus	max_peak2trough	24
1	none, host, bacterium	virus	pk2_width	25
2	none, host, virus	bacterium	pk1_amp	25
3	none, host	bacterium, virus	peakfreq	25
4	none, bacterium, virus	host	cv_ipt	25
5	none, bacterium	host, virus	last_falltime	25
6	none, virus	host, bacterium	cv_peak_amp	25
7	none	host, bacterium, virus	std_peak2trough	25
1	none, host, bacterium	virus	pk1_amp	26
2	none, host, virus	bacterium	cv_trough2peak	26
3	none, host	bacterium, virus	off_times	26
4	none, bacterium, virus	host	cv_peak2trough	26
5	none, bacterium	host, virus	mean_derivative	26
6	none, virus	host, bacterium	min_derivative	26
7	none	host, bacterium, virus	oscbandwidth	26
1	none, host, bacterium	virus	fold_change	27
2	none, host, virus	bacterium	early_activity	27
3	none, host	bacterium, virus	std_trough2peak	27
4	none, bacterium, virus	host	std_peak2trough	27
5	none, bacterium	host, virus	pk1_time	27
6	none, virus	host, bacterium	pk1_width	27
7	none	host, bacterium, virus	median_peak2trough	27
1	none, host, bacterium	virus	pk2_ratio	28
2	none, host, virus	bacterium	cv_peak_amp	28
3	none, host	bacterium, virus	late_activity	28
4	none, bacterium, virus	host	min_ipt	28
5	none, bacterium	host, virus	medfreq	28
6	none, virus	host, bacterium	std_trough2peak	28
7	none	host, bacterium, virus	cv_peak2trough	28
1	none, host, bacterium	virus	early_risetime	29

2	none, host, virus	bacterium	peakfreq	29
3	none, host	bacterium, virus	cv_trough2peak	29
4	none, bacterium, virus	host	std_ipt	29
5	none, bacterium	host, virus	pk2_ratio	29
6	none, virus	host, bacterium	early_activity	29
7	none	host, bacterium, virus	num_peaks	29
1	none, host, bacterium	virus	mean_derivative	30
2	none, host, virus	bacterium	std_trough2peak	30
3	none, host	bacterium, virus	std_peak_amp	30
4	none, bacterium, virus	host	median_trough2peak	30
5	none, bacterium	host, virus	peak2peak	30
6	none, virus	host, bacterium	peak2rms	30
7	none	host, bacterium, virus	pk2_prom	30
1	none, host, bacterium	virus	early_slewrate	31
2	none, host, virus	bacterium	peak2peak	31
3	none, host	bacterium, virus	cv_peak_amp	31
4	none, bacterium, virus	host	cv_trough2peak	31
5	none, bacterium	host, virus	max_amplitude	31
6	none, virus	host, bacterium	max_pentropy	31
7	none	host, bacterium, virus	max_trough2peak	31
1	none, host, bacterium	virus	cv_trough2peak	32
2	none, host, virus	bacterium	mean_movvar	32
3	none, host	bacterium, virus	median_derivative	32
4	none, bacterium, virus	host	mean_trough2peak	32
5	none, bacterium	host, virus	max_derivative	32
6	none, virus	host, bacterium	mean_derivative	32
7	none	host, bacterium, virus	peak2rms	32
1	none, host, bacterium	virus	off_times	33
2	none, host, virus	bacterium	std_peak_amp	33
3	none, host	bacterium, virus	max_trough2peak	33
4	none, bacterium, virus	host	std_trough2peak	33
5	none, bacterium	host, virus	time2HalfMaxIntegral	33
6	none, virus	host, bacterium	medfreq	33

7	none	host, bacterium, virus	std_peak_amp	33
1	none, host, bacterium	virus	linear_changept	34
2	none, host, virus	bacterium	cv_ipt	34
3	none, host	bacterium, virus	early_slewrate	34
4	none, bacterium, virus	host	pk2_amp	34
5	none, bacterium	host, virus	max_pk1_speed	34
6	none, virus	host, bacterium	cv_trough2peak	34
7	none	host, bacterium, virus	fold_change	34
1	none, host, bacterium	virus	oscbandwidth	35
2	none, host, virus	bacterium	pk2_width	35
3	none, host	bacterium, virus	mean_trough2peak	35
4	none, bacterium, virus	host	pk2_width	35
5	none, bacterium	host, virus	pk2_width	35
6	none, virus	host, bacterium	oscbandwidth	35
7	none	host, bacterium, virus	cv_peak_amp	35
1	none, host, bacterium	virus	peak2rms	36
2	none, host, virus	bacterium	pk1_time	36
3	none, host	bacterium, virus	pk1_prom	36
4	none, bacterium, virus	host	mean_peak_amp	36
5	none, bacterium	host, virus	max_peak2trough	36
6	none, virus	host, bacterium	pk2_prom	36
7	none	host, bacterium, virus	max_pentropy	36
1	none, host, bacterium	virus	mean_trough2peak	37
2	none, host, virus	bacterium	max_amplitude	37
3	none, host	bacterium, virus	late_speed	37
4	none, bacterium, virus	host	median_peak_amp	37
5	none, bacterium	host, virus	meanfreq	37
6	none, virus	host, bacterium	median_trough2peak	37
7	none	host, bacterium, virus	median_trough2peak	37
1	none, host, bacterium	virus	mean_peak_amp	38
2	none, host, virus	bacterium	mean_trough2peak	38
3	none, host	bacterium, virus	oscbandwidth	38

4	none, bacterium, virus	host	cv_peak_amp	38
5	none, bacterium	host, virus	pk2_amp	38
6	none, virus	host, bacterium	pk2_time	38
7	none	host, bacterium, virus	medfreq	38
1	none, host, bacterium	virus	peakfreq	39
2	none, host, virus	bacterium	pk2_amp	39
3	none, host	bacterium, virus	fold_change	39
4	none, bacterium, virus	host	median_peak2trough	39
5	none, bacterium	host, virus	median_derivative	39
6	none, virus	host, bacterium	meanfreq	39
7	none	host, bacterium, virus	pk2_width	39
1	none, host, bacterium	virus	last_falltime	40
2	none, host, virus	bacterium	early_slewrate	40
3	none, host	bacterium, virus	pk2_width	40
4	none, bacterium, virus	host	late_speed	40
5	none, bacterium	host, virus	oscbandwidth	40
6	none, virus	host, bacterium	num_peaks	40
7	none	host, bacterium, virus	late_slewrate	40
1	none, host, bacterium	virus	late_slewrate	41
2	none, host, virus	bacterium	medfreq	41
3	none, host	bacterium, virus	median_trough2peak	41
4	none, bacterium, virus	host	std_peak_amp	41
5	none, bacterium	host, virus	median_peak2trough	41
6	none, virus	host, bacterium	fold_change	41
7	none	host, bacterium, virus	mean_derivative	41
1	none, host, bacterium	virus	pk1_width	42
2	none, host, virus	bacterium	late_speed	42
3	none, host	bacterium, virus	pk1_time	42
4	none, bacterium, virus	host	fold_change	42
5	none, bacterium	host, virus	mean_peak_amp	42
6	none, virus	host, bacterium	std_changept	42
7	none	host, bacterium, virus	meanfreq	42

1	none, host, bacterium	virus	pk1_prom	43
2	none, host, virus	bacterium	max_trough2peak	43
3	none, host	bacterium, virus	early_risetime	43
4	none, bacterium, virus	host	peakfreq	43
5	none, bacterium	host, virus	mean_peak2trough	43
6	none, virus	host, bacterium	late_activity	43
7	none	host, bacterium, virus	pk2_ratio	43
1	none, host, bacterium	virus	std_changept	44
2	none, host, virus	bacterium	oscbandwidth	44
3	none, host	bacterium, virus	linear_changept	44
4	none, bacterium, virus	host	mean_ipt	44
5	none, bacterium	host, virus	pk1_amp	44
6	none, virus	host, bacterium	min_ipt	44
7	none	host, bacterium, virus	pk2_time	44
1	none, host, bacterium	virus	median_derivative	45
2	none, host, virus	bacterium	pk2_ratio	45
3	none, host	bacterium, virus	pk2_time	45
4	none, bacterium, virus	host	median_ipt	45
5	none, bacterium	host, virus	median_peak_amp	45
6	none, virus	host, bacterium	median_peak2trough	45
7	none	host, bacterium, virus	late_activity	45
1	none, host, bacterium	virus	median_peak_amp	46
2	none, host, virus	bacterium	pk2_time	46
3	none, host	bacterium, virus	cv_peak2trough	46
4	none, bacterium, virus	host	medfreq	46
5	none, bacterium	host, virus	powerbw	46
6	none, virus	host, bacterium	last_falltime	46
7	none	host, bacterium, virus	mean_changept	46
1	none, host, bacterium	virus	pk2_time	47
2	none, host, virus	bacterium	pk1_prom	47
3	none, host	bacterium, virus	early_activity	47
4	none, bacterium, virus	host	off_times	47

5	none, bacterium	host, virus	early_speed	47
6	none, virus	host, bacterium	late_slewrate	47
7	none	host, bacterium, virus	late_falltime	47
1	none, host, bacterium	virus	oscfreq	48
2	none, host, virus	bacterium	median_trough2peak	48
3	none, host	bacterium, virus	medfreq	48
4	none, bacterium, virus	host	early_risetime	48
5	none, bacterium	host, virus	early_activity	48
6	none, virus	host, bacterium	late_falltime	48
7	none	host, bacterium, virus	oscfreq	48
1	none, host, bacterium	virus	late_activity	49
2	none, host, virus	bacterium	powerbw	49
3	none, host	bacterium, virus	std_peak2trough	49
4	none, bacterium, virus	host	max_trough2peak	49
5	none, bacterium	host, virus	early_slewrate	49
6	none, virus	host, bacterium	max_trough2peak	49
7	none	host, bacterium, virus	std_trough2peak	49
1	none, host, bacterium	virus	max_trough2peak	50
2	none, host, virus	bacterium	late_falltime	50
3	none, host	bacterium, virus	max_peak2trough	50
4	none, bacterium, virus	host	meanfreq	50
5	none, bacterium	host, virus	linear_changept	50
6	none, virus	host, bacterium	early_slewrate	50
7	none	host, bacterium, virus	std_changept	50
1	none, host, bacterium	virus	mean_peak2trough	51
2	none, host, virus	bacterium	early_risetime	51
3	none, host	bacterium, virus	powerbw	51
4	none, bacterium, virus	host	max_peak2trough	51
5	none, bacterium	host, virus	fold_change	51
6	none, virus	host, bacterium	median_derivative	51
7	none	host, bacterium, virus	cv_trough2peak	51
1	none, host, bacterium	virus	meanfreq	52

2	none, host, virus	bacterium	fold_change	52
3	none, host	bacterium, virus	pk1_width	52
4	none, bacterium, virus	host	mean_peak2trough	52
5	none, bacterium	host, virus	pk1_width	52
6	none, virus	host, bacterium	powerbw	52
7	none	host, bacterium, virus	pk1_width	52
1	none, host, bacterium	virus	late_falltime	53
2	none, host, virus	bacterium	mean_peak2trough	53
3	none, host	bacterium, virus	meanfreq	53
4	none, bacterium, virus	host	pk2_time	53
5	none, bacterium	host, virus	early_risetime	53
6	none, virus	host, bacterium	mean_ipt	53
7	none	host, bacterium, virus	pk1_time	53
1	none, host, bacterium	virus	median_trough2peak	54
2	none, host, virus	bacterium	pk1_width	54
3	none, host	bacterium, virus	mean_peak2trough	54
4	none, bacterium, virus	host	pk1_width	54
5	none, bacterium	host, virus	min_ipt	54
6	none, virus	host, bacterium	max_peak2trough	54
7	none	host, bacterium, virus	linear_changept	54
1	none, host, bacterium	virus	medfreq	55
2	none, host, virus	bacterium	meanfreq	55
3	none, host	bacterium, virus	pk2_ratio	55
4	none, bacterium, virus	host	late_slewrate	55
5	none, bacterium	host, virus	pk1_prom	55
6	none, virus	host, bacterium	std_ipt	55
7	none	host, bacterium, virus	last_falltime	55
1	none, host, bacterium	virus	mean_changept	56
2	none, host, virus	bacterium	off_times	56
3	none, host	bacterium, virus	median_peak2trough	56
4	none, bacterium, virus	host	late_activity	56
5	none, bacterium	host, virus	median_trough2peak	56
6	none, virus	host, bacterium	median_ipt	56

7	none	host, bacterium, virus	early_risetime	56
1	none, host, bacterium	virus	std_peak2trough	57
2	none, host, virus	bacterium	median_peak2trough	57
3	none, host	bacterium, virus	last_falltime	57
4	none, bacterium, virus	host	mean_derivative	57
5	none, bacterium	host, virus	mean_ipt	57
6	none, virus	host, bacterium	early_risetime	57
7	none	host, bacterium, virus	median_derivative	57
1	none, host, bacterium	virus	median_ipt	58
2	none, host, virus	bacterium	max_peak2trough	58
3	none, host	bacterium, virus	late_falltime	58
4	none, bacterium, virus	host	powerbw	58
5	none, bacterium	host, virus	median_ipt	58
6	none, virus	host, bacterium	pk1_time	58
7	none	host, bacterium, virus	early_activity	58
1	none, host, bacterium	virus	max_ipt	59
2	none, host, virus	bacterium	mean_changept	59
3	none, host	bacterium, virus	max_ipt	59
4	none, bacterium, virus	host	pk2_ratio	59
5	none, bacterium	host, virus	pk2_time	59
6	none, virus	host, bacterium	mean_peak2trough	59
7	none	host, bacterium, virus	early_slewrate	59
1	none, host, bacterium	virus	median_peak2trough	60
2	none, host, virus	bacterium	median_ipt	60
3	none, host	bacterium, virus	mean_ipt	60
4	none, bacterium, virus	host	late_falltime	60
5	none, bacterium	host, virus	max_ipt	60
6	none, virus	host, bacterium	linear_changept	60
7	none	host, bacterium, virus	min_ipt	60
1	none, host, bacterium	virus	cv_peak2trough	61
2	none, host, virus	bacterium	median_derivative	61
3	none, host	bacterium, virus	median_ipt	61

4	none, bacterium, virus	host	oscbandwidth	61
5	none, bacterium	host, virus	late_falltime	61
6	none, virus	host, bacterium	cv_ipt	61
7	none	host, bacterium, virus	cv_ipt	61
1	none, host, bacterium	virus	cv_ipt	62
2	none, host, virus	bacterium	mean_ipt	62
3	none, host	bacterium, virus	min_ipt	62
4	none, bacterium, virus	host	linear_changept	62
5	none, bacterium	host, virus	mean_changept	62
6	none, virus	host, bacterium	oscfreq	62
7	none	host, bacterium, virus	max_ipt	62
1	none, host, bacterium	virus	mean_ipt	63
2	none, host, virus	bacterium	max_ipt	63
3	none, host	bacterium, virus	cv_ipt	63
4	none, bacterium, virus	host	max_ipt	63
5	none, bacterium	host, virus	std_changept	63
6	none, virus	host, bacterium	cv_peak2trough	63
7	none	host, bacterium, virus	mean_ipt	63
1	none, host, bacterium	virus	powerbw	64
2	none, host, virus	bacterium	min_ipt	64
3	none, host	bacterium, virus	std_ipt	64
4	none, bacterium, virus	host	mean_changept	64
5	none, bacterium	host, virus	max_trough2peak	64
6	none, virus	host, bacterium	max_ipt	64
7	none	host, bacterium, virus	median_ipt	64
1	none, host, bacterium	virus	std_ipt	65
2	none, host, virus	bacterium	std_ipt	65
3	none, host	bacterium, virus	std_changept	65
4	none, bacterium, virus	host	last_falltime	65
5	none, bacterium	host, virus	mean_trough2peak	65
6	none, virus	host, bacterium	mean_changept	65

7	none	host, bacterium, virus	powerbw	65
1	none, host, bacterium	virus	min_ipt	66
2	none, host, virus	bacterium	std_changept	66
3	none, host	bacterium, virus	mean_changept	66
4	none, bacterium, virus	host	std_changept	66
5	none, bacterium	host, virus	off_times	66
6	none, virus	host, bacterium	std_peak2trough	66
7	none	host, bacterium, virus	std_ipt	66

Table 3.3. Top features for classifying ligand sources in M_1 macrophages.

Learner	Positive	Negative	Features	Rank
1	none, host, bacterium	virus	mean_movmad	1
2	none, host, virus	bacterium	max_pentropy	1
3	none, host	bacterium, virus	oscpower	1
4	none, bacterium, virus	host	num_peaks	1
5	none, bacterium	host, virus	oscpower	1
6	none, virus	host, bacterium	max_pk1_speed	1
7	none	host, bacterium, virus	rms	1
1	none, host, bacterium	virus	mean_movstd	2
2	none, host, virus	bacterium	oscpower	2
3	none, host	bacterium, virus	mean_peak_amp	2
4	none, bacterium, virus	host	mean_movmad	2
5	none, bacterium	host, virus	mean_movmad	2
6	none, virus	host, bacterium	time2HalfMaxIntegral	2
7	none	host, bacterium, virus	max_amplitude	2
1	none, host, bacterium	virus	mean_movvar	3
2	none, host, virus	bacterium	oscfreq	3
3	none, host	bacterium, virus	median_peak_amp	3
4	none, bacterium, virus	host	oscpower	3
5	none, bacterium	host, virus	num_peaks	3
6	none, virus	host, bacterium	early_speed	3
7	none	host, bacterium, virus	early_speed	3

1	none, host, bacterium	virus	max_amplitude	4
2	none, host, virus	bacterium	peak2rms	4
3	none, host	bacterium, virus	oscfreq	4
4	none, bacterium, virus	host	mean_movstd	4
5	none, bacterium	host, virus	oscfreq	4
6	none, virus	host, bacterium	pk1_amp	4
7	none	host, bacterium, virus	mean_peak_amp	4
1	none, host, bacterium	virus	time2HalfMaxIntegral	5
2	none, host, virus	bacterium	max_pk1_speed	5
3	none, host	bacterium, virus	peak2rms	5
4	none, bacterium, virus	host	oscfreq	5
5	none, bacterium	host, virus	mean_movstd	5
6	none, virus	host, bacterium	max_integral	5
7	none	host, bacterium, virus	median_peak_amp	5
1	none, host, bacterium	virus	max_pk1_speed	6
2	none, host, virus	bacterium	time2HalfMaxIntegral	6
3	none, host	bacterium, virus	max_pentropy	6
4	none, bacterium, virus	host	mean_movvar	6
5	none, bacterium	host, virus	max_pentropy	6
6	none, virus	host, bacterium	max_derivative	6
7	none	host, bacterium, virus	peak2peak	6
1	none, host, bacterium	virus	min_derivative	7
2	none, host, virus	bacterium	max_integral	7
3	none, host	bacterium, virus	rms	7
4	none, bacterium, virus	host	min_derivative	7
5	none, bacterium	host, virus	peak2rms	7
6	none, virus	host, bacterium	rms	7
7	none	host, bacterium, virus	mean_trough2peak	7
1	none, host, bacterium	virus	peak2peak	8
2	none, host, virus	bacterium	num_peaks	8
3	none, host	bacterium, virus	max_integral	8
4	none, bacterium, virus	host	pk2_prom	8

5	none, bacterium	host, virus	pk2_prom	8
6	none, virus	host, bacterium	mean_peak_amp	8
7	none	host, bacterium, virus	mean_movvar	8
1	none, host, bacterium	virus	early_speed	9
2	none, host, virus	bacterium	early_speed	9
3	none, host	bacterium, virus	max_amplitude	9
4	none, bacterium, virus	host	max_pk1_speed	9
5	none, bacterium	host, virus	min_derivative	9
6	none, virus	host, bacterium	median_peak_amp	9
7	none	host, bacterium, virus	max_derivative	9
1	none, host, bacterium	virus	late_speed	10
2	none, host, virus	bacterium	mean_movmad	10
3	none, host	bacterium, virus	mean_movmad	10
4	none, bacterium, virus	host	peak2rms	10
5	none, bacterium	host, virus	cv_peak_amp	10
6	none, virus	host, bacterium	max_amplitude	10
7	none	host, bacterium, virus	pk1_amp	10
1	none, host, bacterium	virus	pk1_time	11
2	none, host, virus	bacterium	mean_movstd	11
3	none, host	bacterium, virus	mean_derivative	11
4	none, bacterium, virus	host	time2HalfMaxIntegral	11
5	none, bacterium	host, virus	mean_movvar	11
6	none, virus	host, bacterium	mean_movvar	11
7	none	host, bacterium, virus	max_integral	11
1	none, host, bacterium	virus	std_peak_amp	12
2	none, host, virus	bacterium	rms	12
3	none, host	bacterium, virus	peak2peak	12
4	none, bacterium, virus	host	max_pentropy	12
5	none, bacterium	host, virus	std_peak2trough	12
6	none, virus	host, bacterium	peak2peak	12
7	none	host, bacterium, virus	max_pk1_speed	12
1	none, host, bacterium	virus	num_peaks	13

2	none, host, virus	bacterium	pk2_prom	13
3	none, host	bacterium, virus	mean_movstd	13
4	none, bacterium, virus	host	early_speed	13
5	none, bacterium	host, virus	late_activity	13
6	none, virus	host, bacterium	mean_movstd	13
7	none	host, bacterium, virus	time2HalfMaxIntegral	13
1	none, host, bacterium	virus	pk2_amp	14
2	none, host, virus	bacterium	linear_changept	14
3	none, host	bacterium, virus	pk1_amp	14
4	none, bacterium, virus	host	median_derivative	14
5	none, bacterium	host, virus	cv_peak2trough	14
6	none, virus	host, bacterium	mean_trough2peak	14
7	none	host, bacterium, virus	pk2_amp	14
1	none, host, bacterium	virus	rms	15
2	none, host, virus	bacterium	last_falltime	15
3	none, host	bacterium, virus	num_peaks	15
4	none, bacterium, virus	host	rms	15
5	none, bacterium	host, virus	std_peak_amp	15
6	none, virus	host, bacterium	mean_movmad	15
7	none	host, bacterium, virus	mean_movmad	15
1	none, host, bacterium	virus	cv_peak_amp	16
2	none, host, virus	bacterium	late_slewrate	16
3	none, host	bacterium, virus	max_pk1_speed	16
4	none, bacterium, virus	host	max_amplitude	16
5	none, bacterium	host, virus	max_integral	16
6	none, virus	host, bacterium	pk2_amp	16
7	none	host, bacterium, virus	off_times	16
1	none, host, bacterium	virus	max_pentropy	17
2	none, host, virus	bacterium	mean_derivative	17
3	none, host	bacterium, virus	time2HalfMaxIntegral	17
4	none, bacterium, virus	host	max_derivative	17
5	none, bacterium	host, virus	cv_trough2peak	17
6	none, virus	host, bacterium	pk2_ratio	17

7	none	host, bacterium, virus	mean_movstd	17
1	none, host, bacterium	virus	max_derivative	18
2	none, host, virus	bacterium	late_activity	18
3	none, host	bacterium, virus	pk2_amp	18
4	none, bacterium, virus	host	pk1_amp	18
5	none, bacterium	host, virus	peakfreq	18
6	none, virus	host, bacterium	oscpower	18
7	none	host, bacterium, virus	peakfreq	18
1	none, host, bacterium	virus	oscpower	19
2	none, host, virus	bacterium	max_derivative	19
3	none, host	bacterium, virus	mean_movvar	19
4	none, bacterium, virus	host	early_activity	19
5	none, bacterium	host, virus	std_trough2peak	19
6	none, virus	host, bacterium	pk1_prom	19
7	none	host, bacterium, virus	late_speed	19
1	none, host, bacterium	virus	std_trough2peak	20
2	none, host, virus	bacterium	std_peak2trough	20
3	none, host	bacterium, virus	late_slewrate	20
4	none, bacterium, virus	host	pk1_prom	20
5	none, bacterium	host, virus	late_speed	20
6	none, virus	host, bacterium	off_times	20
7	none	host, bacterium, virus	min_derivative	20
1	none, host, bacterium	virus	pk2_prom	21
2	none, host, virus	bacterium	cv_peak2trough	21
3	none, host	bacterium, virus	max_derivative	21
4	none, bacterium, virus	host	early_slewrate	21
5	none, bacterium	host, virus	rms	21
6	none, virus	host, bacterium	pk2_width	21
7	none	host, bacterium, virus	oscpower	21
1	none, host, bacterium	virus	max_integral	22
2	none, host, virus	bacterium	min_derivative	22
3	none, host	bacterium, virus	early_speed	22

4	none, bacterium, virus	host	max_integral	22
5	none, bacterium	host, virus	std_ipt	22
6	none, virus	host, bacterium	peakfreq	22
7	none	host, bacterium, virus	pk1_prom	22
1	none, host, bacterium	virus	early_activity	23
2	none, host, virus	bacterium	median_peak_amp	23
3	none, host	bacterium, virus	pk2_prom	23
4	none, bacterium, virus	host	peak2peak	23
5	none, bacterium	host, virus	late_slewrate	23
6	none, virus	host, bacterium	late_speed	23
7	none	host, bacterium, virus	mean_peak2trough	23
1	none, host, bacterium	virus	max_peak2trough	24
2	none, host, virus	bacterium	mean_peak_amp	24
3	none, host	bacterium, virus	min_derivative	24
4	none, bacterium, virus	host	pk1_time	24
5	none, bacterium	host, virus	cv_ipt	24
6	none, virus	host, bacterium	std_peak_amp	24
7	none	host, bacterium, virus	max_peak2trough	24
1	none, host, bacterium	virus	pk2_width	25
2	none, host, virus	bacterium	pk1_amp	25
3	none, host	bacterium, virus	peakfreq	25
4	none, bacterium, virus	host	cv_ipt	25
5	none, bacterium	host, virus	last_falltime	25
6	none, virus	host, bacterium	cv_peak_amp	25
7	none	host, bacterium, virus	std_peak2trough	25
1	none, host, bacterium	virus	pk1_amp	26
2	none, host, virus	bacterium	cv_trough2peak	26
3	none, host	bacterium, virus	off_times	26
4	none, bacterium, virus	host	cv_peak2trough	26
5	none, bacterium	host, virus	mean_derivative	26
6	none, virus	host, bacterium	min_derivative	26
7	none	host, bacterium, virus	oscbandwidth	26

1	none, host, bacterium	virus	fold_change	27
2	none, host, virus	bacterium	early_activity	27
3	none, host	bacterium, virus	std_trough2peak	27
4	none, bacterium, virus	host	std_peak2trough	27
5	none, bacterium	host, virus	pk1_time	27
6	none, virus	host, bacterium	pk1_width	27
7	none	host, bacterium, virus	median_peak2trough	27
1	none, host, bacterium	virus	pk2_ratio	28
2	none, host, virus	bacterium	cv_peak_amp	28
3	none, host	bacterium, virus	late_activity	28
4	none, bacterium, virus	host	min_ipt	28
5	none, bacterium	host, virus	medfreq	28
6	none, virus	host, bacterium	std_trough2peak	28
7	none	host, bacterium, virus	cv_peak2trough	28
1	none, host, bacterium	virus	early_risetime	29
2	none, host, virus	bacterium	peakfreq	29
3	none, host	bacterium, virus	cv_trough2peak	29
4	none, bacterium, virus	host	std_ipt	29
5	none, bacterium	host, virus	pk2_ratio	29
6	none, virus	host, bacterium	early_activity	29
7	none	host, bacterium, virus	num_peaks	29
1	none, host, bacterium	virus	mean_derivative	30
2	none, host, virus	bacterium	std_trough2peak	30
3	none, host	bacterium, virus	std_peak_amp	30
4	none, bacterium, virus	host	median_trough2peak	30
5	none, bacterium	host, virus	peak2peak	30
6	none, virus	host, bacterium	peak2rms	30
7	none	host, bacterium, virus	pk2_prom	30
1	none, host, bacterium	virus	early_slewrate	31
2	none, host, virus	bacterium	peak2peak	31
3	none, host	bacterium, virus	cv_peak_amp	31
4	none, bacterium, virus	host	cv_trough2peak	31

5	none, bacterium	host, virus	max_amplitude	31
6	none, virus	host, bacterium	max_pentropy	31
7	none	host, bacterium, virus	max_trough2peak	31
1	none, host, bacterium	virus	cv_trough2peak	32
2	none, host, virus	bacterium	mean_movvar	32
3	none, host	bacterium, virus	median_derivative	32
4	none, bacterium, virus	host	mean_trough2peak	32
5	none, bacterium	host, virus	max_derivative	32
6	none, virus	host, bacterium	mean_derivative	32
7	none	host, bacterium, virus	peak2rms	32
1	none, host, bacterium	virus	off_times	33
2	none, host, virus	bacterium	std_peak_amp	33
3	none, host	bacterium, virus	max_trough2peak	33
4	none, bacterium, virus	host	std_trough2peak	33
5	none, bacterium	host, virus	time2HalfMaxIntegral	33
6	none, virus	host, bacterium	medfreq	33
7	none	host, bacterium, virus	std_peak_amp	33
1	none, host, bacterium	virus	linear_changept	34
2	none, host, virus	bacterium	cv_ipt	34
3	none, host	bacterium, virus	early_slewrate	34
4	none, bacterium, virus	host	pk2_amp	34
5	none, bacterium	host, virus	max_pk1_speed	34
6	none, virus	host, bacterium	cv_trough2peak	34
7	none	host, bacterium, virus	fold_change	34
1	none, host, bacterium	virus	oscbandwidth	35
2	none, host, virus	bacterium	pk2_width	35
3	none, host	bacterium, virus	mean_trough2peak	35
4	none, bacterium, virus	host	pk2_width	35
5	none, bacterium	host, virus	pk2_width	35
6	none, virus	host, bacterium	oscbandwidth	35
7	none	host, bacterium, virus	cv_peak_amp	35
1	none, host, bacterium	virus	peak2rms	36

2	none, host, virus	bacterium	pk1_time	36
3	none, host	bacterium, virus	pk1_prom	36
4	none, bacterium, virus	host	mean_peak_amp	36
5	none, bacterium	host, virus	max_peak2trough	36
6	none, virus	host, bacterium	pk2_prom	36
7	none	host, bacterium, virus	max_pentropy	36
1	none, host, bacterium	virus	mean_trough2peak	37
2	none, host, virus	bacterium	max_amplitude	37
3	none, host	bacterium, virus	late_speed	37
4	none, bacterium, virus	host	median_peak_amp	37
5	none, bacterium	host, virus	meanfreq	37
6	none, virus	host, bacterium	median_trough2peak	37
7	none	host, bacterium, virus	median_trough2peak	37
1	none, host, bacterium	virus	mean_peak_amp	38
2	none, host, virus	bacterium	mean_trough2peak	38
3	none, host	bacterium, virus	oscbandwidth	38
4	none, bacterium, virus	host	cv_peak_amp	38
5	none, bacterium	host, virus	pk2_amp	38
6	none, virus	host, bacterium	pk2_time	38
7	none	host, bacterium, virus	medfreq	38
1	none, host, bacterium	virus	peakfreq	39
2	none, host, virus	bacterium	pk2_amp	39
3	none, host	bacterium, virus	fold_change	39
4	none, bacterium, virus	host	median_peak2trough	39
5	none, bacterium	host, virus	median_derivative	39
6	none, virus	host, bacterium	meanfreq	39
7	none	host, bacterium, virus	pk2_width	39
1	none, host, bacterium	virus	last_falltime	40
2	none, host, virus	bacterium	early_slewrate	40
3	none, host	bacterium, virus	pk2_width	40
4	none, bacterium, virus	host	late_speed	40
5	none, bacterium	host, virus	oscbandwidth	40
6	none, virus	host, bacterium	num_peaks	40

7	none	host, bacterium, virus	late_slewrate	40
1	none, host, bacterium	virus	late_slewrate	41
2	none, host, virus	bacterium	medfreq	41
3	none, host	bacterium, virus	median_trough2peak	41
4	none, bacterium, virus	host	std_peak_amp	41
5	none, bacterium	host, virus	median_peak2trough	41
6	none, virus	host, bacterium	fold_change	41
7	none	host, bacterium, virus	mean_derivative	41
1	none, host, bacterium	virus	pk1_width	42
2	none, host, virus	bacterium	late_speed	42
3	none, host	bacterium, virus	pk1_time	42
4	none, bacterium, virus	host	fold_change	42
5	none, bacterium	host, virus	mean_peak_amp	42
6	none, virus	host, bacterium	std_changept	42
7	none	host, bacterium, virus	meanfreq	42
1	none, host, bacterium	virus	pk1_prom	43
2	none, host, virus	bacterium	max_trough2peak	43
3	none, host	bacterium, virus	early_risetime	43
4	none, bacterium, virus	host	peakfreq	43
5	none, bacterium	host, virus	mean_peak2trough	43
6	none, virus	host, bacterium	late_activity	43
7	none	host, bacterium, virus	pk2_ratio	43
1	none, host, bacterium	virus	std_changept	44
2	none, host, virus	bacterium	oscbandwidth	44
3	none, host	bacterium, virus	linear_changept	44
4	none, bacterium, virus	host	mean_ipt	44
5	none, bacterium	host, virus	pk1_amp	44
6	none, virus	host, bacterium	min_ipt	44
7	none	host, bacterium, virus	pk2_time	44
1	none, host, bacterium	virus	median_derivative	45
2	none, host, virus	bacterium	pk2_ratio	45
3	none, host	bacterium, virus	pk2_time	45

4	none, bacterium, virus	host	median_ipt	45
5	none, bacterium	host, virus	median_peak_amp	45
6	none, virus	host, bacterium	median_peak2trough	45
7	none	host, bacterium, virus	late_activity	45
1	none, host, bacterium	virus	median_peak_amp	46
2	none, host, virus	bacterium	pk2_time	46
3	none, host	bacterium, virus	cv_peak2trough	46
4	none, bacterium, virus	host	medfreq	46
5	none, bacterium	host, virus	powerbw	46
6	none, virus	host, bacterium	last_falltime	46
7	none	host, bacterium, virus	mean_changept	46
1	none, host, bacterium	virus	pk2_time	47
2	none, host, virus	bacterium	pk1_prom	47
3	none, host	bacterium, virus	early_activity	47
4	none, bacterium, virus	host	off_times	47
5	none, bacterium	host, virus	early_speed	47
6	none, virus	host, bacterium	late_slewrate	47
7	none	host, bacterium, virus	late_falltime	47
1	none, host, bacterium	virus	oscfreq	48
2	none, host, virus	bacterium	median_trough2peak	48
3	none, host	bacterium, virus	medfreq	48
4	none, bacterium, virus	host	early_risetime	48
5	none, bacterium	host, virus	early_activity	48
6	none, virus	host, bacterium	late_falltime	48
7	none	host, bacterium, virus	oscfreq	48
1	none, host, bacterium	virus	late_activity	49
2	none, host, virus	bacterium	powerbw	49
3	none, host	bacterium, virus	std_peak2trough	49
4	none, bacterium, virus	host	max_trough2peak	49
5	none, bacterium	host, virus	early_slewrate	49
6	none, virus	host, bacterium	max_trough2peak	49
7	none	host, bacterium, virus	std_trough2peak	49

1	none, host, bacterium	virus	max_trough2peak	50
2	none, host, virus	bacterium	late_falltime	50
3	none, host	bacterium, virus	max_peak2trough	50
4	none, bacterium, virus	host	meanfreq	50
5	none, bacterium	host, virus	linear_changept	50
6	none, virus	host, bacterium	early_slewrate	50
7	none	host, bacterium, virus	std_changept	50
1	none, host, bacterium	virus	mean_peak2trough	51
2	none, host, virus	bacterium	early_risetime	51
3	none, host	bacterium, virus	powerbw	51
4	none, bacterium, virus	host	max_peak2trough	51
5	none, bacterium	host, virus	fold_change	51
6	none, virus	host, bacterium	median_derivative	51
7	none	host, bacterium, virus	cv_trough2peak	51
1	none, host, bacterium	virus	meanfreq	52
2	none, host, virus	bacterium	fold_change	52
3	none, host	bacterium, virus	pk1_width	52
4	none, bacterium, virus	host	mean_peak2trough	52
5	none, bacterium	host, virus	pk1_width	52
6	none, virus	host, bacterium	powerbw	52
7	none	host, bacterium, virus	pk1_width	52
1	none, host, bacterium	virus	late_falltime	53
2	none, host, virus	bacterium	mean_peak2trough	53
3	none, host	bacterium, virus	meanfreq	53
4	none, bacterium, virus	host	pk2_time	53
5	none, bacterium	host, virus	early_risetime	53
6	none, virus	host, bacterium	mean_ipt	53
7	none	host, bacterium, virus	pk1_time	53
1	none, host, bacterium	virus	median_trough2peak	54
2	none, host, virus	bacterium	pk1_width	54
3	none, host	bacterium, virus	mean_peak2trough	54
4	none, bacterium, virus	host	pk1_width	54

5	none, bacterium	host, virus	min_ipt	54
6	none, virus	host, bacterium	max_peak2trough	54
7	none	host, bacterium, virus	linear_changept	54
1	none, host, bacterium	virus	medfreq	55
2	none, host, virus	bacterium	meanfreq	55
3	none, host	bacterium, virus	pk2_ratio	55
4	none, bacterium, virus	host	late_slewrate	55
5	none, bacterium	host, virus	pk1_prom	55
6	none, virus	host, bacterium	std_ipt	55
7	none	host, bacterium, virus	last_falltime	55
1	none, host, bacterium	virus	mean_changept	56
2	none, host, virus	bacterium	off_times	56
3	none, host	bacterium, virus	median_peak2trough	56
4	none, bacterium, virus	host	late_activity	56
5	none, bacterium	host, virus	median_trough2peak	56
6	none, virus	host, bacterium	median_ipt	56
7	none	host, bacterium, virus	early_risetime	56
1	none, host, bacterium	virus	std_peak2trough	57
2	none, host, virus	bacterium	median_peak2trough	57
3	none, host	bacterium, virus	last_falltime	57
4	none, bacterium, virus	host	mean_derivative	57
5	none, bacterium	host, virus	mean_ipt	57
6	none, virus	host, bacterium	early_risetime	57
7	none	host, bacterium, virus	median_derivative	57
1	none, host, bacterium	virus	median_ipt	58
2	none, host, virus	bacterium	max_peak2trough	58
3	none, host	bacterium, virus	late_falltime	58
4	none, bacterium, virus	host	powerbw	58
5	none, bacterium	host, virus	median_ipt	58
6	none, virus	host, bacterium	pk1_time	58
7	none	host, bacterium, virus	early_activity	58
1	none, host, bacterium	virus	max_ipt	59

2	none, host, virus	bacterium	mean_changept	59
3	none, host	bacterium, virus	max_ipt	59
4	none, bacterium, virus	host	pk2_ratio	59
5	none, bacterium	host, virus	pk2_time	59
6	none, virus	host, bacterium	mean_peak2trough	59
7	none	host, bacterium, virus	early_slewrate	59
1	none, host, bacterium	virus	median_peak2trough	60
2	none, host, virus	bacterium	median_ipt	60
3	none, host	bacterium, virus	mean_ipt	60
4	none, bacterium, virus	host	late_falltime	60
5	none, bacterium	host, virus	max_ipt	60
6	none, virus	host, bacterium	linear_changept	60
7	none	host, bacterium, virus	min_ipt	60
1	none, host, bacterium	virus	cv_peak2trough	61
2	none, host, virus	bacterium	median_derivative	61
3	none, host	bacterium, virus	median_ipt	61
4	none, bacterium, virus	host	oscbandwidth	61
5	none, bacterium	host, virus	late_falltime	61
6	none, virus	host, bacterium	cv_ipt	61
7	none	host, bacterium, virus	cv_ipt	61
1	none, host, bacterium	virus	cv_ipt	62
2	none, host, virus	bacterium	mean_ipt	62
3	none, host	bacterium, virus	min_ipt	62
4	none, bacterium, virus	host	linear_changept	62
5	none, bacterium	host, virus	mean_changept	62
6	none, virus	host, bacterium	oscfreq	62
7	none	host, bacterium, virus	max_ipt	62
1	none, host, bacterium	virus	mean_ipt	63
2	none, host, virus	bacterium	max_ipt	63
3	none, host	bacterium, virus	cv_ipt	63
4	none, bacterium, virus	host	max_ipt	63
5	none, bacterium	host, virus	std_changept	63
6	none, virus	host, bacterium	cv_peak2trough	63

7	none	host, bacterium, virus	mean_ipt	63
1	none, host, bacterium	virus	powerbw	64
2	none, host, virus	bacterium	min_ipt	64
3	none, host	bacterium, virus	std_ipt	64
4	none, bacterium, virus	host	mean_changept	64
5	none, bacterium	host, virus	max_trough2peak	64
6	none, virus	host, bacterium	max_ipt	64
7	none	host, bacterium, virus	median_ipt	64
1	none, host, bacterium	virus	std_ipt	65
2	none, host, virus	bacterium	std_ipt	65
3	none, host	bacterium, virus	std_changept	65
4	none, bacterium, virus	host	last_falltime	65
5	none, bacterium	host, virus	mean_trough2peak	65
6	none, virus	host, bacterium	mean_changept	65
7	none	host, bacterium, virus	powerbw	65
1	none, host, bacterium	virus	min_ipt	66
2	none, host, virus	bacterium	std_changept	66
3	none, host	bacterium, virus	mean_changept	66
4	none, bacterium, virus	host	std_changept	66
5	none, bacterium	host, virus	off_times	66
6	none, virus	host, bacterium	std_peak2trough	66
7	none	host, bacterium, virus	std_ipt	66

Table 3.4. Top features for classifying ligand types in M_1 macrophages.

Learner	Positive	Negative	Features	Rank
1	none, cytokine	PAMP	oscpower	1
2	none, PAMP	cytokine	num_peaks	1
3	none	cytokine, PAMP	rms	1
1	none, cytokine	PAMP	mean_peak_amp	2
2	none, PAMP	cytokine	mean_movmad	2
3	none	cytokine, PAMP	max_amplitude	2
1	none, cytokine	PAMP	median_peak_amp	3
2	none, PAMP	cytokine	oscpower	3
3	none	cytokine, PAMP	early_speed	3

1	none, cytokine	PAMP	oscfreq	4
2	none, PAMP	cytokine	mean_movstd	4
3	none	cytokine, PAMP	mean_peak_amp	4
1	none, cytokine	PAMP	peak2rms	5
2	none, PAMP	cytokine	oscfreq	5
3	none	cytokine, PAMP	median_peak_amp	5
1	none, cytokine	PAMP	max_pentropy	6
2	none, PAMP	cytokine	mean_movvar	6
3	none	cytokine, PAMP	peak2peak	6
1	none, cytokine	PAMP	rms	7
2	none, PAMP	cytokine	min_derivative	7
3	none	cytokine, PAMP	mean_trough2peak	7
1	none, cytokine	PAMP	max_integral	8
2	none, PAMP	cytokine	pk2_prom	8
3	none	cytokine, PAMP	mean_movvar	8
1	none, cytokine	PAMP	max_amplitude	9
2	none, PAMP	cytokine	max_pk1_speed	9
3	none	cytokine, PAMP	max_derivative	9
1	none, cytokine	PAMP	mean_movmad	10
2	none, PAMP	cytokine	peak2rms	10
3	none	cytokine, PAMP	pk1_amp	10
1	none, cytokine	PAMP	mean_derivative	11
2	none, PAMP	cytokine	time2HalfMaxIntegral	11
3	none	cytokine, PAMP	max_integral	11
1	none, cytokine	PAMP	peak2peak	12
2	none, PAMP	cytokine	max_pentropy	12
3	none	cytokine, PAMP	max_pk1_speed	12
1	none, cytokine	PAMP	mean_movstd	13
2	none, PAMP	cytokine	early_speed	13
3	none	cytokine, PAMP	time2HalfMaxIntegral	13
1	none, cytokine	PAMP	pk1_amp	14
2	none, PAMP	cytokine	median_derivative	14
3	none	cytokine, PAMP	pk2_amp	14
1	none, cytokine	PAMP	num_peaks	15
2	none, PAMP	cytokine	rms	15
3	none	cytokine, PAMP	mean_movmad	15
1	none, cytokine	PAMP	max_pk1_speed	16
2	none, PAMP	cytokine	max_amplitude	16
3	none	cytokine, PAMP	off_times	16
1	none, cytokine	PAMP	time2HalfMaxIntegral	17
2	none, PAMP	cytokine	max_derivative	17
3	none	cytokine, PAMP	mean_movstd	17

1	none, cytokine	PAMP	pk2_amp	18
2	none, PAMP	cytokine	pk1_amp	18
3	none	cytokine, PAMP	peakfreq	18
1	none, cytokine	PAMP	mean_movvar	19
2	none, PAMP	cytokine	early_activity	19
3	none	cytokine, PAMP	late_speed	19
1	none, cytokine	PAMP	late_slewrate	20
2	none, PAMP	cytokine	pk1_prom	20
3	none	cytokine, PAMP	min_derivative	20
1	none, cytokine	PAMP	max_derivative	21
2	none, PAMP	cytokine	early_slewrate	21
3	none	cytokine, PAMP	oscpower	21
1	none, cytokine	PAMP	early_speed	22
2	none, PAMP	cytokine	max_integral	22
3	none	cytokine, PAMP	pk1_prom	22
1	none, cytokine	PAMP	pk2_prom	23
2	none, PAMP	cytokine	peak2peak	23
3	none	cytokine, PAMP	mean_peak2trough	23
1	none, cytokine	PAMP	min_derivative	24
2	none, PAMP	cytokine	pk1_time	24
3	none	cytokine, PAMP	max_peak2trough	24
1	none, cytokine	PAMP	peakfreq	25
2	none, PAMP	cytokine	cv_ipt	25
3	none	cytokine, PAMP	std_peak2trough	25
1	none, cytokine	PAMP	off_times	26
2	none, PAMP	cytokine	cv_peak2trough	26
3	none	cytokine, PAMP	oscbandwidth	26
1	none, cytokine	PAMP	std_trough2peak	27
2	none, PAMP	cytokine	std_peak2trough	27
3	none	cytokine, PAMP	median_peak2trough	27
1	none, cytokine	PAMP	late_activity	28
2	none, PAMP	cytokine	min_ipt	28
3	none	cytokine, PAMP	cv_peak2trough	28
1	none, cytokine	PAMP	cv_trough2peak	29
2	none, PAMP	cytokine	std_ipt	29
3	none	cytokine, PAMP	num_peaks	29
1	none, cytokine	PAMP	std_peak_amp	30
2	none, PAMP	cytokine	median_trough2peak	30
3	none	cytokine, PAMP	pk2_prom	30
1	none, cytokine	PAMP	cv_peak_amp	31
2	none, PAMP	cytokine	cv_trough2peak	31
3	none	cytokine, PAMP	max_trough2peak	31

1	none, cytokine	PAMP	median_derivative	32
2	none, PAMP	cytokine	mean_trough2peak	32
3	none	cytokine, PAMP	peak2rms	32
1	none, cytokine	PAMP	max_trough2peak	33
2	none, PAMP	cytokine	std_trough2peak	33
3	none	cytokine, PAMP	std_peak_amp	33
1	none, cytokine	PAMP	early_slewrate	34
2	none, PAMP	cytokine	pk2_amp	34
3	none	cytokine, PAMP	fold_change	34
1	none, cytokine	PAMP	mean_trough2peak	35
2	none, PAMP	cytokine	pk2_width	35
3	none	cytokine, PAMP	cv_peak_amp	35
1	none, cytokine	PAMP	pk1_prom	36
2	none, PAMP	cytokine	mean_peak_amp	36
3	none	cytokine, PAMP	max_pentropy	36
1	none, cytokine	PAMP	late_speed	37
2	none, PAMP	cytokine	median_peak_amp	37
3	none	cytokine, PAMP	median_trough2peak	37
1	none, cytokine	PAMP	oscbandwidth	38
2	none, PAMP	cytokine	cv_peak_amp	38
3	none	cytokine, PAMP	medfreq	38
1	none, cytokine	PAMP	fold_change	39
2	none, PAMP	cytokine	median_peak2trough	39
3	none	cytokine, PAMP	pk2_width	39
1	none, cytokine	PAMP	pk2_width	40
2	none, PAMP	cytokine	late_speed	40
3	none	cytokine, PAMP	late_slewrate	40
1	none, cytokine	PAMP	median_trough2peak	41
2	none, PAMP	cytokine	std_peak_amp	41
3	none	cytokine, PAMP	mean_derivative	41
1	none, cytokine	PAMP	pk1_time	42
2	none, PAMP	cytokine	fold_change	42
3	none	cytokine, PAMP	meanfreq	42
1	none, cytokine	PAMP	early_risetime	43
2	none, PAMP	cytokine	peakfreq	43
3	none	cytokine, PAMP	pk2_ratio	43
1	none, cytokine	PAMP	linear_changept	44
2	none, PAMP	cytokine	mean_ipt	44
3	none	cytokine, PAMP	pk2_time	44
1	none, cytokine	PAMP	pk2_time	45
2	none, PAMP	cytokine	median_ipt	45
3	none	cytokine, PAMP	late_activity	45

1	none, cytokine	PAMP	cv_peak2trough	46
2	none, PAMP	cytokine	medfreq	46
3	none	cytokine, PAMP	mean_changept	46
1	none, cytokine	PAMP	early_activity	47
2	none, PAMP	cytokine	off_times	47
3	none	cytokine, PAMP	late_falltime	47
1	none, cytokine	PAMP	medfreq	48
2	none, PAMP	cytokine	early_risetime	48
3	none	cytokine, PAMP	oscfreq	48
1	none, cytokine	PAMP	std_peak2trough	49
2	none, PAMP	cytokine	max_trough2peak	49
3	none	cytokine, PAMP	std_trough2peak	49
1	none, cytokine	PAMP	max_peak2trough	50
2	none, PAMP	cytokine	meanfreq	50
3	none	cytokine, PAMP	std_changept	50
1	none, cytokine	PAMP	powerbw	51
2	none, PAMP	cytokine	max_peak2trough	51
3	none	cytokine, PAMP	cv_trough2peak	51
1	none, cytokine	PAMP	pk1_width	52
2	none, PAMP	cytokine	mean_peak2trough	52
3	none	cytokine, PAMP	pk1_width	52
1	none, cytokine	PAMP	meanfreq	53
2	none, PAMP	cytokine	pk2_time	53
3	none	cytokine, PAMP	pk1_time	53
1	none, cytokine	PAMP	mean_peak2trough	54
2	none, PAMP	cytokine	pk1_width	54
3	none	cytokine, PAMP	linear_changept	54
1	none, cytokine	PAMP	pk2_ratio	55
2	none, PAMP	cytokine	late_slewrate	55
3	none	cytokine, PAMP	last_falltime	55
1	none, cytokine	PAMP	median_peak2trough	56
2	none, PAMP	cytokine	late_activity	56
3	none	cytokine, PAMP	early_risetime	56
1	none, cytokine	PAMP	last_falltime	57
2	none, PAMP	cytokine	mean_derivative	57
3	none	cytokine, PAMP	median_derivative	57
1	none, cytokine	PAMP	late_falltime	58
2	none, PAMP	cytokine	powerbw	58
3	none	cytokine, PAMP	early_activity	58
1	none, cytokine	PAMP	max_ipt	59
2	none, PAMP	cytokine	pk2_ratio	59
3	none	cytokine, PAMP	early_slewrate	59

1	none, cytokine	PAMP	mean_ipt	60
2	none, PAMP	cytokine	late_falltime	60
3	none	cytokine, PAMP	min_ipt	60
1	none, cytokine	PAMP	median_ipt	61
2	none, PAMP	cytokine	oscbandwidth	61
3	none	cytokine, PAMP	cv_ipt	61
1	none, cytokine	PAMP	min_ipt	62
2	none, PAMP	cytokine	linear_changept	62
3	none	cytokine, PAMP	max_ipt	62
1	none, cytokine	PAMP	cv_ipt	63
2	none, PAMP	cytokine	max_ipt	63
3	none	cytokine, PAMP	mean_ipt	63
1	none, cytokine	PAMP	std_ipt	64
2	none, PAMP	cytokine	mean_changept	64
3	none	cytokine, PAMP	median_ipt	64
1	none, cytokine	PAMP	std_changept	65
2	none, PAMP	cytokine	last_falltime	65
3	none	cytokine, PAMP	powerbw	65
1	none, cytokine	PAMP	mean_changept	66
2	none, PAMP	cytokine	std_changept	66
3	none	cytokine, PAMP	std_ipt	66

Table 3.5. Top features for classifying ligand sources in M_{2a} macrophages.

Learner	Positive	Negative	Features	Rank
1	host, none, bacterium	virus	max_pk1_speed	1
2	host, none, virus	bacterium	linear_changept	1
3	host, none	bacterium, virus	peak2rms	1
4	host, bacterium, virus	none	median_peak_amp	1
5	host, bacterium	none, virus	max_pk1_speed	1
6	host, virus	none, bacterium	linear_changept	1
7	host	none, bacterium, virus	peak2rms	1
1	host, none, bacterium	virus	time2HalfMaxIntegral	2
2	host, none, virus	bacterium	pk1_amp	2
3	host, none	bacterium, virus	late_activity	2
4	host, bacterium, virus	none	mean_trough2peak	2
5	host, bacterium	none, virus	early_speed	2
6	host, virus	none, bacterium	late_activity	2

7	host	none, bacterium, virus	pk2_ratio	2
1	host, none, bacterium	virus	pk1_amp	3
2	host, none, virus	bacterium	last_falltime	3
3	host, none	bacterium, virus	oscbandwidth	3
4	host, bacterium, virus	none	mean_peak_amp	3
5	host, bacterium	none, virus	time2HalfMaxIntegral	3
6	host, virus	none, bacterium	last_falltime	3
7	host	none, bacterium, virus	num_peaks	3
1	host, none, bacterium	virus	early_speed	4
2	host, none, virus	bacterium	late_activity	4
3	host, none	bacterium, virus	cv_trough2peak	4
4	host, bacterium, virus	none	early_speed	4
5	host, bacterium	none, virus	pk1_amp	4
6	host, virus	none, bacterium	cv_trough2peak	4
7	host	none, bacterium, virus	pk1_amp	4
1	host, none, bacterium	virus	pk1_prom	5
2	host, none, virus	bacterium	pk1_prom	5
3	host, none	bacterium, virus	pk1_prom	5
4	host, bacterium, virus	none	peak2peak	5
5	host, bacterium	none, virus	pk1_prom	5
6	host, virus	none, bacterium	pk1_amp	5
7	host	none, bacterium, virus	linear_changept	5
1	host, none, bacterium	virus	max_derivative	6
2	host, none, virus	bacterium	peak2peak	6
3	host, none	bacterium, virus	std_trough2peak	6
4	host, bacterium, virus	none	mean_movmad	6
5	host, bacterium	none, virus	max_derivative	6
6	host, virus	none, bacterium	pk2_ratio	6
7	host	none, bacterium, virus	pk1_prom	6
1	host, none, bacterium	virus	linear_changept	7
2	host, none, virus	bacterium	cv_trough2peak	7
3	host, none	bacterium, virus	pk2_ratio	7

4	host, bacterium, virus	none	max_pk1_speed	7
5	host, bacterium	none, virus	mean_movvar	7
6	host, virus	none, bacterium	peak2rms	7
7	host	none, bacterium, virus	pk2_prom	7
1	host, none, bacterium	virus	mean_peak_amp	8
2	host, none, virus	bacterium	pk2_ratio	8
3	host, none	bacterium, virus	pk1_amp	8
4	host, bacterium, virus	none	mean_movvar	8
5	host, bacterium	none, virus	peak2peak	8
6	host, virus	none, bacterium	std_trough2peak	8
7	host	none, bacterium, virus	late_activity	8
1	host, none, bacterium	virus	mean_movvar	9
2	host, none, virus	bacterium	max_amplitude	9
3	host, none	bacterium, virus	mean_trough2peak	9
4	host, bacterium, virus	none	max_derivative	9
5	host, bacterium	none, virus	max_amplitude	9
6	host, virus	none, bacterium	pk1_prom	9
7	host	none, bacterium, virus	last_falltime	9
1	host, none, bacterium	virus	peak2peak	10
2	host, none, virus	bacterium	early_speed	10
3	host, none	bacterium, virus	max_pk1_speed	10
4	host, bacterium, virus	none	max_amplitude	10
5	host, bacterium	none, virus	mean_movmad	10
6	host, virus	none, bacterium	peak2peak	10
7	host	none, bacterium, virus	max_pk1_speed	10
1	host, none, bacterium	virus	max_amplitude	11
2	host, none, virus	bacterium	std_trough2peak	11
3	host, none	bacterium, virus	last_falltime	11
4	host, bacterium, virus	none	mean_movstd	11
5	host, bacterium	none, virus	mean_movstd	11
6	host, virus	none, bacterium	max_amplitude	11
7	host	none, bacterium, virus	cv_peak_amp	11

1	host, none, bacterium	virus	median_peak_amp	12
2	host, none, virus	bacterium	peak2rms	12
3	host, none	bacterium, virus	early_speed	12
4	host, bacterium, virus	none	late_speed	12
5	host, bacterium	none, virus	pk2_amp	12
6	host, virus	none, bacterium	early_speed	12
7	host	none, bacterium, virus	oscbandwidth	12
1	host, none, bacterium	virus	mean_movmad	13
2	host, none, virus	bacterium	time2HalfMaxIntegral	13
3	host, none	bacterium, virus	median_trough2peak	13
4	host, bacterium, virus	none	max_integral	13
5	host, bacterium	none, virus	mean_peak_amp	13
6	host, virus	none, bacterium	mean_derivative	13
7	host	none, bacterium, virus	mean_movstd	13
1	host, none, bacterium	virus	mean_trough2peak	14
2	host, none, virus	bacterium	max_pk1_speed	14
3	host, none	bacterium, virus	time2HalfMaxIntegral	14
4	host, bacterium, virus	none	rms	14
5	host, bacterium	none, virus	rms	14
6	host, virus	none, bacterium	oscbandwidth	14
7	host	none, bacterium, virus	max_derivative	14
1	host, none, bacterium	virus	min_derivative	15
2	host, none, virus	bacterium	max_derivative	15
3	host, none	bacterium, virus	mean_peak_amp	15
4	host, bacterium, virus	none	pk1_prom	15
5	host, bacterium	none, virus	linear_changept	15
6	host, virus	none, bacterium	early_activity	15
7	host	none, bacterium, virus	mean_movmad	15
1	host, none, bacterium	virus	mean_movstd	16
2	host, none, virus	bacterium	median_derivative	16
3	host, none	bacterium, virus	peak2peak	16
4	host, bacterium, virus	none	pk1_amp	16

5	host, bacterium	none, virus	median_peak_amp	16
6	host, virus	none, bacterium	time2HalfMaxIntegral	16
7	host	none, bacterium, virus	early_speed	16
1	host, none, bacterium	virus	cv_trough2peak	17
2	host, none, virus	bacterium	early_slewrate	17
3	host, none	bacterium, virus	max_derivative	17
4	host, bacterium, virus	none	time2HalfMaxIntegral	17
5	host, bacterium	none, virus	min_derivative	17
6	host, virus	none, bacterium	median_derivative	17
7	host	none, bacterium, virus	std_peak_amp	17
1	host, none, bacterium	virus	pk2_ratio	18
2	host, none, virus	bacterium	mean_movvar	18
3	host, none	bacterium, virus	median_peak_amp	18
4	host, bacterium, virus	none	fold_change	18
5	host, bacterium	none, virus	max_integral	18
6	host, virus	none, bacterium	early_slewrate	18
7	host	none, bacterium, virus	cv_trough2peak	18
1	host, none, bacterium	virus	std_trough2peak	19
2	host, none, virus	bacterium	oscbandwidth	19
3	host, none	bacterium, virus	mean_movmad	19
4	host, bacterium, virus	none	off_times	19
5	host, bacterium	none, virus	mean_trough2peak	19
6	host, virus	none, bacterium	mean_trough2peak	19
7	host	none, bacterium, virus	std_trough2peak	19
1	host, none, bacterium	virus	pk2_amp	20
2	host, none, virus	bacterium	early_activity	20
3	host, none	bacterium, virus	std_peak_amp	20
4	host, bacterium, virus	none	oscbandwidth	20
5	host, bacterium	none, virus	cv_trough2peak	20
6	host, virus	none, bacterium	num_peaks	20
7	host	none, bacterium, virus	mean_trough2peak	20
1	host, none, bacterium	virus	last_falltime	21

2	host, none, virus	bacterium	min_derivative	21
3	host, none	bacterium, virus	mean_movstd	21
4	host, bacterium, virus	none	pk2_amp	21
5	host, bacterium	none, virus	std_trough2peak	21
6	host, virus	none, bacterium	max_derivative	21
7	host	none, bacterium, virus	max_integral	21
1	host, none, bacterium	virus	std_peak_amp	22
2	host, none, virus	bacterium	mean_trough2peak	22
3	host, none	bacterium, virus	linear_changept	22
4	host, bacterium, virus	none	min_derivative	22
5	host, bacterium	none, virus	peakfreq	22
6	host, virus	none, bacterium	median_peak_amp	22
7	host	none, bacterium, virus	peak2peak	22
1	host, none, bacterium	virus	rms	23
2	host, none, virus	bacterium	late_speed	23
3	host, none	bacterium, virus	cv_peak_amp	23
4	host, bacterium, virus	none	mean_derivative	23
5	host, bacterium	none, virus	last_falltime	23
6	host, virus	none, bacterium	max_pk1_speed	23
7	host	none, bacterium, virus	pk2_amp	23
1	host, none, bacterium	virus	pk1_time	24
2	host, none, virus	bacterium	std_peak_amp	24
3	host, none	bacterium, virus	meanfreq	24
4	host, bacterium, virus	none	peakfreq	24
5	host, bacterium	none, virus	std_peak_amp	24
6	host, virus	none, bacterium	mean_peak_amp	24
7	host	none, bacterium, virus	mean_movvar	24
1	host, none, bacterium	virus	early_slewrate	25
2	host, none, virus	bacterium	num_peaks	25
3	host, none	bacterium, virus	max_integral	25
4	host, bacterium, virus	none	late_falltime	25
5	host, bacterium	none, virus	cv_peak_amp	25
6	host, virus	none, bacterium	mean_changept	25

7	host	none, bacterium, virus	meanfreq	25
1	host, none, bacterium	virus	mean_derivative	26
2	host, none, virus	bacterium	median_trough2peak	26
3	host, none	bacterium, virus	mean_movvar	26
4	host, bacterium, virus	none	early_activity	26
5	host, bacterium	none, virus	early_slewrate	26
6	host, virus	none, bacterium	early_risetime	26
7	host	none, bacterium, virus	medfreq	26
1	host, none, bacterium	virus	cv_peak_amp	27
2	host, none, virus	bacterium	pk2_width	27
3	host, none	bacterium, virus	mean_derivative	27
4	host, bacterium, virus	none	late_activity	27
5	host, bacterium	none, virus	late_speed	27
6	host, virus	none, bacterium	mean_movvar	27
7	host	none, bacterium, virus	time2HalfMaxIntegral	27
1	host, none, bacterium	virus	peakfreq	28
2	host, none, virus	bacterium	cv_peak_amp	28
3	host, none	bacterium, virus	pk2_amp	28
4	host, bacterium, virus	none	pk1_width	28
5	host, bacterium	none, virus	pk1_time	28
6	host, virus	none, bacterium	std_peak_amp	28
7	host	none, bacterium, virus	rms	28
1	host, none, bacterium	virus	median_trough2peak	29
2	host, none, virus	bacterium	mean_peak_amp	29
3	host, none	bacterium, virus	late_speed	29
4	host, bacterium, virus	none	median_trough2peak	29
5	host, bacterium	none, virus	pk2_ratio	29
6	host, virus	none, bacterium	mean_movstd	29
7	host	none, bacterium, virus	off_times	29
1	host, none, bacterium	virus	max_integral	30
2	host, none, virus	bacterium	max_trough2peak	30
3	host, none	bacterium, virus	max_amplitude	30

4	host, bacterium, virus	none	early_risetime	30
5	host, bacterium	none, virus	median_trough2peak	30
6	host, virus	none, bacterium	max_integral	30
7	host	none, bacterium, virus	early_activity	30
1	host, none, bacterium	virus	pk2_prom	31
2	host, none, virus	bacterium	std_changept	31
3	host, none	bacterium, virus	rms	31
4	host, bacterium, virus	none	pk2_ratio	31
5	host, bacterium	none, virus	pk2_time	31
6	host, virus	none, bacterium	fold_change	31
7	host	none, bacterium, virus	max_amplitude	31
1	host, none, bacterium	virus	early_activity	32
2	host, none, virus	bacterium	oscpower	32
3	host, none	bacterium, virus	early_risetime	32
4	host, bacterium, virus	none	std_changept	32
5	host, bacterium	none, virus	off_times	32
6	host, virus	none, bacterium	cv_peak_amp	32
7	host	none, bacterium, virus	max_trough2peak	32
1	host, none, bacterium	virus	pk2_time	33
2	host, none, virus	bacterium	pk2_amp	33
3	host, none	bacterium, virus	medfreq	33
4	host, bacterium, virus	none	meanfreq	33
5	host, bacterium	none, virus	num_peaks	33
6	host, virus	none, bacterium	median_trough2peak	33
7	host	none, bacterium, virus	min_derivative	33
1	host, none, bacterium	virus	median_derivative	34
2	host, none, virus	bacterium	rms	34
3	host, none	bacterium, virus	pk2_prom	34
4	host, bacterium, virus	none	max_pentropy	34
5	host, bacterium	none, virus	early_risetime	34
6	host, virus	none, bacterium	pk2_width	34
7	host	none, bacterium, virus	mean_derivative	34

1	host, none, bacterium	virus	early_risetime	35
2	host, none, virus	bacterium	median_peak2trough	35
3	host, none	bacterium, virus	pk1_time	35
4	host, bacterium, virus	none	median_derivative	35
5	host, bacterium	none, virus	pk2_prom	35
6	host, virus	none, bacterium	late_speed	35
7	host	none, bacterium, virus	pk1_time	35
1	host, none, bacterium	virus	late_speed	36
2	host, none, virus	bacterium	mean_derivative	36
3	host, none	bacterium, virus	early_activity	36
4	host, bacterium, virus	none	peak2rms	36
5	host, bacterium	none, virus	max_pentropy	36
6	host, virus	none, bacterium	rms	36
7	host	none, bacterium, virus	pk2_time	36
1	host, none, bacterium	virus	late_slewrate	37
2	host, none, virus	bacterium	mean_movstd	37
3	host, none	bacterium, virus	min_derivative	37
4	host, bacterium, virus	none	pk2_time	37
5	host, bacterium	none, virus	oscpower	37
6	host, virus	none, bacterium	mean_movmad	37
7	host	none, bacterium, virus	median_trough2peak	37
1	host, none, bacterium	virus	num_peaks	38
2	host, none, virus	bacterium	mean_movmad	38
3	host, none	bacterium, virus	num_peaks	38
4	host, bacterium, virus	none	pk2_width	38
5	host, bacterium	none, virus	medfreq	38
6	host, virus	none, bacterium	min_derivative	38
7	host	none, bacterium, virus	mean_peak2trough	38
1	host, none, bacterium	virus	oscpower	39
2	host, none, virus	bacterium	pk2_prom	39
3	host, none	bacterium, virus	oscpower	39
4	host, bacterium, virus	none	pk1_time	39

5	host, bacterium	none, virus	early_activity	39
6	host, virus	none, bacterium	oscpower	39
7	host	none, bacterium, virus	max_pentropy	39
1	host, none, bacterium	virus	peak2rms	40
2	host, none, virus	bacterium	max_integral	40
3	host, none	bacterium, virus	median_derivative	40
4	host, bacterium, virus	none	early_slewrate	40
5	host, bacterium	none, virus	meanfreq	40
6	host, virus	none, bacterium	pk2_amp	40
7	host	none, bacterium, virus	oscpower	40
1	host, none, bacterium	virus	fold_change	41
2	host, none, virus	bacterium	mean_peak2trough	41
3	host, none	bacterium, virus	early_slewrate	41
4	host, bacterium, virus	none	medfreq	41
5	host, bacterium	none, virus	median_derivative	41
6	host, virus	none, bacterium	medfreq	41
7	host	none, bacterium, virus	median_derivative	41
1	host, none, bacterium	virus	meanfreq	42
2	host, none, virus	bacterium	median_peak_amp	42
3	host, none	bacterium, virus	peakfreq	42
4	host, bacterium, virus	none	late_slewrate	42
5	host, bacterium	none, virus	late_slewrate	42
6	host, virus	none, bacterium	max_trough2peak	42
7	host	none, bacterium, virus	cv_peak2trough	42
1	host, none, bacterium	virus	max_pentropy	43
2	host, none, virus	bacterium	late_slewrate	43
3	host, none	bacterium, virus	fold_change	43
4	host, bacterium, virus	none	max_trough2peak	43
5	host, bacterium	none, virus	pk2_width	43
6	host, virus	none, bacterium	pk2_prom	43
7	host	none, bacterium, virus	early_risetime	43
1	host, none, bacterium	virus	pk1_width	44

2	host, none, virus	bacterium	peakfreq	44
3	host, none	bacterium, virus	pk2_width	44
4	host, bacterium, virus	none	oscpower	44
5	host, bacterium	none, virus	pk1_width	44
6	host, virus	none, bacterium	off_times	44
7	host	none, bacterium, virus	std_peak2trough	44
1	host, none, bacterium	virus	off_times	45
2	host, none, virus	bacterium	late_falltime	45
3	host, none	bacterium, virus	max_pentropy	45
4	host, bacterium, virus	none	last_falltime	45
5	host, bacterium	none, virus	oscbandwidth	45
6	host, virus	none, bacterium	peakfreq	45
7	host	none, bacterium, virus	median_peak2trough	45
1	host, none, bacterium	virus	mean_changept	46
2	host, none, virus	bacterium	std_peak2trough	46
3	host, none	bacterium, virus	late_falltime	46
4	host, bacterium, virus	none	powerbw	46
5	host, bacterium	none, virus	std_changept	46
6	host, virus	none, bacterium	meanfreq	46
7	host	none, bacterium, virus	fold_change	46
1	host, none, bacterium	virus	late_activity	47
2	host, none, virus	bacterium	meanfreq	47
3	host, none	bacterium, virus	pk1_width	47
4	host, bacterium, virus	none	std_peak_amp	47
5	host, bacterium	none, virus	fold_change	47
6	host, virus	none, bacterium	std_changept	47
7	host	none, bacterium, virus	mean_peak_amp	47
1	host, none, bacterium	virus	max_peak2trough	48
2	host, none, virus	bacterium	early_risetime	48
3	host, none	bacterium, virus	pk2_time	48
4	host, bacterium, virus	none	linear_changept	48
5	host, bacterium	none, virus	peak2rms	48
6	host, virus	none, bacterium	max_pentropy	48

7	host	none, bacterium, virus	pk2_width	48
1	host, none, bacterium	virus	std_changept	49
2	host, none, virus	bacterium	pk1_time	49
3	host, none	bacterium, virus	max_trough2peak	49
4	host, bacterium, virus	none	pk2_prom	49
5	host, bacterium	none, virus	max_trough2peak	49
6	host, virus	none, bacterium	pk1_time	49
7	host	none, bacterium, virus	late_speed	49
1	host, none, bacterium	virus	pk2_width	50
2	host, none, virus	bacterium	max_pentropy	50
3	host, none	bacterium, virus	mean_peak2trough	50
4	host, bacterium, virus	none	cv_trough2peak	50
5	host, bacterium	none, virus	mean_derivative	50
6	host, virus	none, bacterium	late_falltime	50
7	host	none, bacterium, virus	peakfreq	50
1	host, none, bacterium	virus	powerbw	51
2	host, none, virus	bacterium	pk2_time	51
3	host, none	bacterium, virus	max_peak2trough	51
4	host, bacterium, virus	none	mean_changept	51
5	host, bacterium	none, virus	oscfreq	51
6	host, virus	none, bacterium	pk1_width	51
7	host	none, bacterium, virus	max_peak2trough	51
1	host, none, bacterium	virus	oscbandwidth	52
2	host, none, virus	bacterium	fold_change	52
3	host, none	bacterium, virus	off_times	52
4	host, bacterium, virus	none	std_trough2peak	52
5	host, bacterium	none, virus	late_activity	52
6	host, virus	none, bacterium	mean_peak2trough	52
7	host	none, bacterium, virus	early_slewrate	52
1	host, none, bacterium	virus	oscfreq	53
2	host, none, virus	bacterium	medfreq	53
3	host, none	bacterium, virus	late_slewrate	53

4	host, bacterium, virus	none	num_peaks	53
5	host, bacterium	none, virus	late_falltime	53
6	host, virus	none, bacterium	late_slewrate	53
7	host	none, bacterium, virus	median_peak_amp	53
1	host, none, bacterium	virus	medfreq	54
2	host, none, virus	bacterium	mean_changept	54
3	host, none	bacterium, virus	median_ipt	54
4	host, bacterium, virus	none	cv_peak_amp	54
5	host, bacterium	none, virus	cv_ipt	54
6	host, virus	none, bacterium	cv_ipt	54
7	host	none, bacterium, virus	pk1_width	54
1	host, none, bacterium	virus	late_falltime	55
2	host, none, virus	bacterium	off_times	55
3	host, none	bacterium, virus	median_peak2trough	55
4	host, bacterium, virus	none	oscfreq	55
5	host, bacterium	none, virus	mean_peak2trough	55
6	host, virus	none, bacterium	std_ipt	55
7	host	none, bacterium, virus	mean_changept	55
1	host, none, bacterium	virus	mean_peak2trough	56
2	host, none, virus	bacterium	max_peak2trough	56
3	host, none	bacterium, virus	mean_changept	56
4	host, bacterium, virus	none	cv_ipt	56
5	host, bacterium	none, virus	mean_changept	56
6	host, virus	none, bacterium	pk2_time	56
7	host	none, bacterium, virus	late_falltime	56
1	host, none, bacterium	virus	max_trough2peak	57
2	host, none, virus	bacterium	powerbw	57
3	host, none	bacterium, virus	std_changept	57
4	host, bacterium, virus	none	cv_peak2trough	57
5	host, bacterium	none, virus	median_peak2trough	57
6	host, virus	none, bacterium	std_peak2trough	57
7	host	none, bacterium, virus	oscfreq	57

1	host, none, bacterium	virus	min_ipt	58
2	host, none, virus	bacterium	pk1_width	58
3	host, none	bacterium, virus	oscfreq	58
4	host, bacterium, virus	none	max_ipt	58
5	host, bacterium	none, virus	cv_peak2trough	58
6	host, virus	none, bacterium	max_peak2trough	58
7	host	none, bacterium, virus	late_slewrate	58
1	host, none, bacterium	virus	median_peak2trough	59
2	host, none, virus	bacterium	cv_peak2trough	59
3	host, none	bacterium, virus	powerbw	59
4	host, bacterium, virus	none	max_peak2trough	59
5	host, bacterium	none, virus	std_peak2trough	59
6	host, virus	none, bacterium	cv_peak2trough	59
7	host	none, bacterium, virus	mean_ipt	59
1	host, none, bacterium	virus	cv_ipt	60
2	host, none, virus	bacterium	std_ipt	60
3	host, none	bacterium, virus	mean_ipt	60
4	host, bacterium, virus	none	mean_ipt	60
5	host, bacterium	none, virus	max_ipt	60
6	host, virus	none, bacterium	oscfreq	60
7	host	none, bacterium, virus	std_changept	60
1	host, none, bacterium	virus	max_ipt	61
2	host, none, virus	bacterium	cv_ipt	61
3	host, none	bacterium, virus	cv_peak2trough	61
4	host, bacterium, virus	none	mean_peak2trough	61
5	host, bacterium	none, virus	max_peak2trough	61
6	host, virus	none, bacterium	median_peak2trough	61
7	host	none, bacterium, virus	std_ipt	61
1	host, none, bacterium	virus	mean_ipt	62
2	host, none, virus	bacterium	oscfreq	62
3	host, none	bacterium, virus	std_peak2trough	62
4	host, bacterium, virus	none	median_ipt	62

5	host, bacterium	none, virus	powerbw	62
6	host, virus	none, bacterium	mean_ipt	62
7	host	none, bacterium, virus	median_ipt	62
1	host, none, bacterium	virus	median_ipt	63
2	host, none, virus	bacterium	mean_ipt	63
3	host, none	bacterium, virus	max_ipt	63
4	host, bacterium, virus	none	median_peak2trough	63
5	host, bacterium	none, virus	median_ipt	63
6	host, virus	none, bacterium	median_ipt	63
7	host	none, bacterium, virus	min_ipt	63
1	host, none, bacterium	virus	std_ipt	64
2	host, none, virus	bacterium	median_ipt	64
3	host, none	bacterium, virus	min_ipt	64
4	host, bacterium, virus	none	min_ipt	64
5	host, bacterium	none, virus	min_ipt	64
6	host, virus	none, bacterium	min_ipt	64
7	host	none, bacterium, virus	cv_ipt	64
1	host, none, bacterium	virus	cv_peak2trough	65
2	host, none, virus	bacterium	max_ipt	65
3	host, none	bacterium, virus	std_ipt	65
4	host, bacterium, virus	none	std_ipt	65
5	host, bacterium	none, virus	mean_ipt	65
6	host, virus	none, bacterium	powerbw	65
7	host	none, bacterium, virus	max_ipt	65
1	host, none, bacterium	virus	std_peak2trough	66
2	host, none, virus	bacterium	min_ipt	66
3	host, none	bacterium, virus	cv_ipt	66
4	host, bacterium, virus	none	std_peak2trough	66
5	host, bacterium	none, virus	std_ipt	66
6	host, virus	none, bacterium	max_ipt	66
7	host	none, bacterium, virus	powerbw	66

Table 3.6. Top features for classifying ligand types in M_{2a} macrophages.

Learner	Positive	Negative	Features	Rank
1	cytokine, none	PAMP	peak2rms	1
2	cytokine, PAMP	none	median_peak_amp	1
3	cytokine	none, PAMP	peak2rms	1
1	cytokine, none	PAMP	late_activity	2
2	cytokine, PAMP	none	mean_trough2peak	2
3	cytokine	none, PAMP	pk2_ratio	2
1	cytokine, none	PAMP	oscbandwidth	3
2	cytokine, PAMP	none	mean_peak_amp	3
3	cytokine	none, PAMP	num_peaks	3
1	cytokine, none	PAMP	cv_trough2peak	4
2	cytokine, PAMP	none	early_speed	4
3	cytokine	none, PAMP	pk1_amp	4
1	cytokine, none	PAMP	pk1_prom	5
2	cytokine, PAMP	none	peak2peak	5
3	cytokine	none, PAMP	linear_changept	5
1	cytokine, none	PAMP	std_trough2peak	6
2	cytokine, PAMP	none	mean_movmad	6
3	cytokine	none, PAMP	pk1_prom	6
1	cytokine, none	PAMP	pk2_ratio	7
2	cytokine, PAMP	none	max_pk1_speed	7
3	cytokine	none, PAMP	pk2_prom	7
1	cytokine, none	PAMP	pk1_amp	8
2	cytokine, PAMP	none	mean_movvar	8
3	cytokine	none, PAMP	late_activity	8
1	cytokine, none	PAMP	mean_trough2peak	9
2	cytokine, PAMP	none	max_derivative	9
3	cytokine	none, PAMP	last_falltime	9
1	cytokine, none	PAMP	max_pk1_speed	10
2	cytokine, PAMP	none	late_speed	10
3	cytokine	none, PAMP	max_pk1_speed	10
1	cytokine, none	PAMP	last_falltime	11
2	cytokine, PAMP	none	mean_movstd	11
3	cytokine	none, PAMP	cv_peak_amp	11
1	cytokine, none	PAMP	early_speed	12
2	cytokine, PAMP	none	max_amplitude	12
3	cytokine	none, PAMP	oscbandwidth	12
1	cytokine, none	PAMP	median_trough2peak	13
2	cytokine, PAMP	none	max_integral	13
3	cytokine	none, PAMP	mean_movstd	13

1	cytokine, none	PAMP	time2HalfMaxIntegral	14
2	cytokine, PAMP	none	rms	14
3	cytokine	none, PAMP	max_derivative	14
1	cytokine, none	PAMP	mean_peak_amp	15
2	cytokine, PAMP	none	pk1_prom	15
3	cytokine	none, PAMP	mean_movmad	15
1	cytokine, none	PAMP	peak2peak	16
2	cytokine, PAMP	none	pk1_amp	16
3	cytokine	none, PAMP	early_speed	16
1	cytokine, none	PAMP	max_derivative	17
2	cytokine, PAMP	none	time2HalfMaxIntegral	17
3	cytokine	none, PAMP	std_peak_amp	17
1	cytokine, none	PAMP	mean_movmad	18
2	cytokine, PAMP	none	off_times	18
3	cytokine	none, PAMP	cv_trough2peak	18
1	cytokine, none	PAMP	median_peak_amp	19
2	cytokine, PAMP	none	oscbandwidth	19
3	cytokine	none, PAMP	std_trough2peak	19
1	cytokine, none	PAMP	std_peak_amp	20
2	cytokine, PAMP	none	fold_change	20
3	cytokine	none, PAMP	mean_trough2peak	20
1	cytokine, none	PAMP	mean_movstd	21
2	cytokine, PAMP	none	min_derivative	21
3	cytokine	none, PAMP	max_integral	21
1	cytokine, none	PAMP	linear_changept	22
2	cytokine, PAMP	none	pk2_amp	22
3	cytokine	none, PAMP	peak2peak	22
1	cytokine, none	PAMP	cv_peak_amp	23
2	cytokine, PAMP	none	mean_derivative	23
3	cytokine	none, PAMP	pk2_amp	23
1	cytokine, none	PAMP	meanfreq	24
2	cytokine, PAMP	none	late_falltime	24
3	cytokine	none, PAMP	mean_movvar	24
1	cytokine, none	PAMP	max_integral	25
2	cytokine, PAMP	none	peakfreq	25
3	cytokine	none, PAMP	meanfreq	25
1	cytokine, none	PAMP	mean_movvar	26
2	cytokine, PAMP	none	late_activity	26
3	cytokine	none, PAMP	medfreq	26
1	cytokine, none	PAMP	mean_derivative	27
2	cytokine, PAMP	none	early_activity	27
3	cytokine	none, PAMP	time2HalfMaxIntegral	27

1	cytokine, none	PAMP	pk2_amp	28
2	cytokine, PAMP	none	pk1_width	28
3	cytokine	none, PAMP	rms	28
1	cytokine, none	PAMP	late_speed	29
2	cytokine, PAMP	none	median_trough2peak	29
3	cytokine	none, PAMP	off_times	29
1	cytokine, none	PAMP	max_amplitude	30
2	cytokine, PAMP	none	early_risetime	30
3	cytokine	none, PAMP	early_activity	30
1	cytokine, none	PAMP	rms	31
2	cytokine, PAMP	none	peak2rms	31
3	cytokine	none, PAMP	max_amplitude	31
1	cytokine, none	PAMP	medfreq	32
2	cytokine, PAMP	none	pk2_ratio	32
3	cytokine	none, PAMP	max_trough2peak	32
1	cytokine, none	PAMP	early_risetime	33
2	cytokine, PAMP	none	std_changept	33
3	cytokine	none, PAMP	min_derivative	33
1	cytokine, none	PAMP	pk2_prom	34
2	cytokine, PAMP	none	early_slewrate	34
3	cytokine	none, PAMP	mean_derivative	34
1	cytokine, none	PAMP	pk1_time	35
2	cytokine, PAMP	none	median_derivative	35
3	cytokine	none, PAMP	pk1_time	35
1	cytokine, none	PAMP	early_activity	36
2	cytokine, PAMP	none	pk1_time	36
3	cytokine	none, PAMP	pk2_time	36
1	cytokine, none	PAMP	min_derivative	37
2	cytokine, PAMP	none	meanfreq	37
3	cytokine	none, PAMP	median_trough2peak	37
1	cytokine, none	PAMP	num_peaks	38
2	cytokine, PAMP	none	max_pentropy	38
3	cytokine	none, PAMP	mean_peak2trough	38
1	cytokine, none	PAMP	oscpower	39
2	cytokine, PAMP	none	medfreq	39
3	cytokine	none, PAMP	max_pentropy	39
1	cytokine, none	PAMP	median_derivative	40
2	cytokine, PAMP	none	pk2_time	40
3	cytokine	none, PAMP	oscpower	40
1	cytokine, none	PAMP	early_slewrate	41
2	cytokine, PAMP	none	pk2_width	41
3	cytokine	none, PAMP	median_derivative	41

1	cytokine, none	PAMP	peakfreq	42
2	cytokine, PAMP	none	oscpower	42
3	cytokine	none, PAMP	cv_peak2trough	42
1	cytokine, none	PAMP	fold_change	43
2	cytokine, PAMP	none	last_falltime	43
3	cytokine	none, PAMP	early_risetime	43
1	cytokine, none	PAMP	pk2_width	44
2	cytokine, PAMP	none	max_trough2peak	44
3	cytokine	none, PAMP	std_peak2trough	44
1	cytokine, none	PAMP	max_pentropy	45
2	cytokine, PAMP	none	late_slewrate	45
3	cytokine	none, PAMP	median_peak2trough	45
1	cytokine, none	PAMP	late_falltime	46
2	cytokine, PAMP	none	std_peak_amp	46
3	cytokine	none, PAMP	fold_change	46
1	cytokine, none	PAMP	pk1_width	47
2	cytokine, PAMP	none	powerbw	47
3	cytokine	none, PAMP	mean_peak_amp	47
1	cytokine, none	PAMP	pk2_time	48
2	cytokine, PAMP	none	linear_changept	48
3	cytokine	none, PAMP	pk2_width	48
1	cytokine, none	PAMP	max_trough2peak	49
2	cytokine, PAMP	none	pk2_prom	49
3	cytokine	none, PAMP	late_speed	49
1	cytokine, none	PAMP	mean_peak2trough	50
2	cytokine, PAMP	none	cv_trough2peak	50
3	cytokine	none, PAMP	peakfreq	50
1	cytokine, none	PAMP	max_peak2trough	51
2	cytokine, PAMP	none	std_trough2peak	51
3	cytokine	none, PAMP	max_peak2trough	51
1	cytokine, none	PAMP	off_times	52
2	cytokine, PAMP	none	mean_changept	52
3	cytokine	none, PAMP	early_slewrate	52
1	cytokine, none	PAMP	late_slewrate	53
2	cytokine, PAMP	none	num_peaks	53
3	cytokine	none, PAMP	median_peak_amp	53
1	cytokine, none	PAMP	median_ipt	54
2	cytokine, PAMP	none	cv_peak_amp	54
3	cytokine	none, PAMP	pk1_width	54
1	cytokine, none	PAMP	cv_peak2trough	55
2	cytokine, PAMP	none	oscfreq	55
3	cytokine	none, PAMP	mean_changept	55

1	cytokine, none	PAMP	mean_changept	56
2	cytokine, PAMP	none	cv_ipt	56
3	cytokine	none, PAMP	late_falltime	56
1	cytokine, none	PAMP	std_changept	57
2	cytokine, PAMP	none	cv_peak2trough	57
3	cytokine	none, PAMP	oscfreq	57
1	cytokine, none	PAMP	oscfreq	58
2	cytokine, PAMP	none	max_ipt	58
3	cytokine	none, PAMP	late_slewrate	58
1	cytokine, none	PAMP	powerbw	59
2	cytokine, PAMP	none	max_peak2trough	59
3	cytokine	none, PAMP	mean_ipt	59
1	cytokine, none	PAMP	mean_ipt	60
2	cytokine, PAMP	none	mean_ipt	60
3	cytokine	none, PAMP	std_changept	60
1	cytokine, none	PAMP	median_peak2trough	61
2	cytokine, PAMP	none	mean_peak2trough	61
3	cytokine	none, PAMP	std_ipt	61
1	cytokine, none	PAMP	std_peak2trough	62
2	cytokine, PAMP	none	median_ipt	62
3	cytokine	none, PAMP	median_ipt	62
1	cytokine, none	PAMP	max_ipt	63
2	cytokine, PAMP	none	median_peak2trough	63
3	cytokine	none, PAMP	min_ipt	63
1	cytokine, none	PAMP	min_ipt	64
2	cytokine, PAMP	none	min_ipt	64
3	cytokine	none, PAMP	cv_ipt	64
1	cytokine, none	PAMP	std_ipt	65
2	cytokine, PAMP	none	std_ipt	65
3	cytokine	none, PAMP	max_ipt	65
1	cytokine, none	PAMP	cv_ipt	66
2	cytokine, PAMP	none	std_peak2trough	66
3	cytokine	none, PAMP	powerbw	66

Material and methods

Mouse Models. The mVenus-RelA endogenously-tagged mouse line was generated by Ingenious Targeting Laboratory. A donor sequence encoding the monomeric variant of the Venus fluorescent protein (Koushik et al., 2006) joined by a short flexible linker sequence

directly upstream of the start codon of the murine *Rela* locus was used to generate, via homologous recombination, a tagged embryonic stem cell line, that was implanted to yield heterozygous mice. These mice were then bred with a mouse line constitutively expressing the *Flp* recombinase to remove the *Neo* resistance marker included in the homologous donor sequence. We then back-crossed the resultant mice with wild-type C57BL/6J mice to remove the *Flp* background and generate homozygously tagged mice. $tnf^{g/-}$ were bred (Jax: B6.129S-Tnf^{tm1Gkl}/J) into mVenus line to generate double homozygous, RelA $^{v/v}$, $tnf^{g/-}$.

Macrophage Cell Culture. BMDMs were prepared by culturing bone marrow monocytes from femurs of 8-12 week old in L929 -conditioned medium using standard methods (Cheng et al., 2015; Takeshita et al., 2000). BMDMs were re-plated in imaging dishes on day 4, then were stimulated on day 7 or day 8.

METHOD DETAILS

Macrophage stimulation conditions. BMDMs were stimulated with indicated concentrations of lipopolysaccharide (LPS, Sigma Aldrich), murine TNF (R&D), a TLR1/2 agonist, the synthetic triacylated lipoprotein Pam3CSK4 (P3C4), a TLR3 agonist, low molecular weight polyinosine-polycytidylic acid (p(I:C)), a TLR9 agonist, the synthetic CpG ODN 1668 (CpG). 5 µg/mL Soluble TNF receptor II was used to block paracrine, feedforward TNF (R& D). 24 hours before stimulation, the M_1 condition received fresh media with 10 ng/mL IFNγ (R&D), the M_{2a} condition received 10 ng/mL of IL-4 (R&D).

Live-cell imaging. Bone-marrow macrophages were replated on day 4 at 24,000 or 20,000/cm^2 in an 8-well ibidi SlideTek chamber, for imaging at an appropriate density (approx. 60,000/cm^2) on day 7 or day 8. 2 hours prior to stimulation, a solution of 2.5 ng/mL Hoechst 33342 was added to the BMDM culture media. After the start of imaging, additional culture media containing stimulus (TNF, LPS, poly (I:C), CpG, or P3C4) was

injected into the chamber *in situ*. Cells were imaged at 5-minute intervals on a Zeiss Axio Observer platform with live-cell incubation, using epifluorescent excitation from a Sutter Lambda XL light source. Images were recorded on a Hamamatsu Orca Flash 2.0 CCD camera.

QUANTIFICATION AND STATISTICAL ANALYSIS

Image analysis and processing

Microscopy time-lapse images were exported for single-cell tracking and measurement in MATLAB R2016a. The tracking routines followed those used in earlier work (Selimkhanov et al., 2014). Briefly, cells were identified using DIC images, then segmented, guided by markers from the Hoechst image. Segmented cells were linked into trajectories across successive images, then nuclear and cytoplasmic boundaries were saved and used to define measurement regions in other fluorescent channels, including mVenus-NFκB. Nuclear NFκB levels were quantified on a per-cell basis, normalized to image background levels, then were baseline-subtracted. Mitotic cells, as well as cells that drifted out of the field of view, were excluded from analysis. The toolboxes used for this analysis are available at GitHub.

Machine Learning Classifier

Construction of classification models I trained an ensemble of binary decision trees using the fitcecoc function from the Statistics and Machine Learning Toolbox from MathWorks. Decision tree models are simple, highly interpretable, and can be displayed graphically (James et al., 2013). Consequently, the decision process of the classifier can be easily interrogated. However, decision tree models have two key disadvantages: (1) modest prediction performance (Caruana and Niculescu-Mizil, 2006) and (2) high variance due to overfitting (James et al., 2013). Both disadvantages can be mitigated by aggregating an

ensemble of decision trees. Empirical comparison of classification models show that ensembles of decision trees outperform other classification algorithms across of a variety of problem sets (Caruana and Niculescu-Mizil, 2006).

I used an error correcting output code (ECOC) scheme to construct an ensemble. This approach allows for straightforward interrogation of the important features that distinguish all binary combination of classes. This approach trains $2^{(K-1)}$ -1 binary classifiers where K is the number of classes. Each tree in the ensemble is trained on data partitioned into a positive class, negative class or omitted class. In a binary complete scheme, data are partitioned into all combinations such that each class is partitioned at least once in a positive class and at least once in anegative class. The predictions from the ensemble model are determined by a majority vote from each individual tree prediction. We trained the ensemble to learn the ligand identity labels (TNF, P3C4, CpG, LPS, and p(I:C)), ligand source labels (host, bacterium, virus), and ligand type labels (cytokine, pathogen-associated molecular (PAMP)) using descriptive features or time series trajectories transformed with an autoencoder.

Decision tree parameters. To construct each decision tree, the software considers all possible ways to split the data into two nodes based on the values of every predictor. Then, it chooses the best splitting decision based on constraints imposed by training parameters, such as the minimum number of observations that must be present in a child node (MinLeafSize) and a predictor selection criterion. The software recursively splits each child node until a stopping criterion is reached. The stopping criteria include (1) obtaining a pure node that contains only observations from a single class, (2) reaching the minimum number of observations for a parent node (MinParentSize), (3) reaching a split that would produce a

child node with fewer observations than MinLeafSize, and (4) reaching the maximum number of splits (MaxNumSplits).

I used the default value of 10 for MinParentSize (MathWorks, 2020). The values from MinLeafSize and MaxNumSplits were obtained explicitly through hyperparameter optimization. Since the standard prediction selection process at each node may be biased, we used a predictor selection technique, interaction-curvature test, which minimizes predictor selection bias, enhances interpretation of the model, and facilitates inference of predictor importance. The interaction-curvature technique selects a predictor to split at each node based on the *p*-values of curvature and interaction tests. Whereas the curvature test examines the null hypothesis that the predictor and response variables are unassociated, the interaction test examines the null hypothesis that a pair of predictor variables and the response variable are unassociated. A node with no tests that yield *p*-values ≤ 0.05 is not split. At each node, the predictor or pair of predictors that yield the minimum significant *p*-value (0.05) is chosen for splitting. To split the node, the software chooses the splitting rule that maximizes the impurity gain—difference in the impurity of the node (calculated using Gini's diversity index) and the impurity of its children nodes (MathWorks, 2017).

Evaluation. I evaluated the performance of the classifiers using 5-fold cross validation, an independent testing data set, or out of bag cross validation. I used the following performance metrics: true positive rate (recall), positive predictive value (precision), area under the Receiver Operating Characteristic (ROC) curve, F1 score, Matthews correlation coefficient, markedness, threat score, informedness and mean classification margin (Akosa, 2017; Powers, 2007; Vihinen, 2012).

Data and code availability

Software associated with the image processing and are available at

https://github.com/Adewunmi91/MACKtrack,

https://github.com/Adewunmi91/nfkb_dynamics,

https://github.com/Adewunmi91/nfkb_classification

Bibliography

Akosa, J.S., 2017. Predictive Accuracy : A Misleading Performance Measure for Highly Imbalanced Data. SAS Glob. Forum 942, 1–12.

Barken, D., Wang, C.J., Kearns, J., Cheong, R., Hoffmann, A., Levchenko, A., 2005. Comment on "Oscillations in NF-κB Signaling Control the Dynamics of Gene Expression." Science 308, 52; author reply 52. https://doi.org/10.1126/science.1107904

Behar, M., Hoffmann, A., 2010. Understanding the temporal codes of intra-cellular signals. Curr. Opin. Genet. Dev. 20, 684–693. https://doi.org/10.1016/j.gde.2010.09.007

Benoit, M., Desnues, B., Mege, J.-L., 2008. Macrophage Polarization in Bacterial Infections. J. Immunol. 181, 3733–3739. https://doi.org/10.4049/jimmunol.181.6.3733

Caruana, R., Niculescu-Mizil, A., 2006. An empirical comparison of supervised learning algorithms. Proc. 23rd Int. Conf. Mach. Learn. C, 161–168. https://doi.org/10.1145/1143844.1143865

Cheng, Q.J., Ohta, S., Sheu, K.M., Spreafico, R., Adelaja, A., Taylor, B., Hoffmann, A., 2020. NFκB dynamics determine the stimulus-specificity of epigenomic reprogramming in macrophages. bioRxiv. https://doi.org/10.1101/2020.02.18.954602

Cheng, Z., Taylor, B., Ourthiague, D.R., Hoffmann, A., 2015. Distinct single-cell signaling

characteristics are conferred by the MyD88 and TRIF pathways during TLR4 activation. Sci. Signal. 8, ra69. https://doi.org/10.1126/scisignal.aaa5208

Chovatiya, R., Medzhitov, R., 2014. Stress, inflammation, and defense of homeostasis. Mol. Cell. https://doi.org/10.1016/j.molcel.2014.03.030

Cleynen, I., Vermeire, S., 2012. Paradoxical inflammation induced by anti-TNF agents in patients with IBD. Nat. Rev. Gastroenterol. Hepatol. 9, 496–503. https://doi.org/10.1038/nrgastro.2012.125

Harris, R.A., 2017. Macrophage Metabolism As Therapeutic Target for Cancer , Atherosclerosis , and Obesity 8. https://doi.org/10.3389/fimmu.2017.00289

Hoffmann, A., Levchenko, A., Scott, M.L., Baltimore, D., 2002. The IκB-NF-κB Signaling Module: Temporal Control and Selective Gene Activation. Science 298, 1241–5. https://doi.org/10.1126/science.1071914

James, G., Witten, D., Hastie, T., Tibshirani, R., 2013. An Introduction to Statistical Learning, Springer Texts in Statistics. Springer New York, New York, NY. https://doi.org/10.1007/978-1-4614-7138-7

Kalliolias, G.D., Ivashkiv, L.B., 2015. TNF biology, pathogenic mechanisms and emerging therapeutic strategies. Nat. Rev. Rheumatol. 12, 49–62. https://doi.org/10.1038/nrrheum.2015.169

Kearns, J.D., Basak, S., Werner, S.L., Huang, C.S., Hoffmann, A., 2006. IκBε provides negative feedback to control NF-κB oscillations, signaling dynamics, and inflammatory gene expression. J. Cell Biol. 173, 659–664. https://doi.org/10.1083/jcb.200510155

Koushik, S. V, Chen, H., Thaler, C., Puhl, H.L., Vogel, S.S., 2006. Cerulean, Venus, and

VenusY67C FRET reference standards. Biophys. J. 91, L99–L101. https://doi.org/10.1529/biophysj.106.096206

Lane, K., Van Valen, D., DeFelice, M.M., Macklin, D.N., Kudo, T., Jaimovich, A., Carr, A., Meyer, T., Pe'er, D., Boutet, S.C., Covert, M.W., 2017. Measuring Signaling and RNA-Seq in the Same Cell Links Gene Expression to Dynamic Patterns of NF-κB Activation. Cell Syst. 4, 458-469.e5. https://doi.org/10.1016/j.cels.2017.03.010

Lee, T.K., Denny, E.M., Sanghvi, J.C., Gaston, J.E., Maynard, N.D., Hughey, J.J., Covert, M.W., 2009. A noisy paracrine signal determines the cellular NF-kappaB response to lipopolysaccharide. Sci. Signal. 2, ra65. https://doi.org/10.1126/scisignal.2000599

Martin, E.W., Pacholewska, A., Patel, H., Dashora, H., Sung, M.-H., 2020. Integrative analysis suggests cell type–specific decoding of NF-κB dynamics. Sci. Signal. 13, eaax7195. https://doi.org/10.1126/scisignal.aax7195

Martinez, F.O., Gordon, S., 2014. The M1 and M2 paradigm of macrophage activation: time for reassessment. F1000Prime Rep. 6, 13. https://doi.org/10.12703/P6-13

MathWorks, 2017. Statistics and Machine Learning ToolboxTM User's Guide. Natick, MA.

Mosser, D.M., Edwards, J.P., 2008. Exploring the full spectrum of macrophage activation. Nat. Rev. Immunol. 8, 958–69. https://doi.org/10.1038/nri2448

Murray, P.J., Wynn, T.A., 2011. Protective and pathogenic functions of macrophage subsets. Nat. Rev. Immunol. 11, 723–37. https://doi.org/10.1038/nri3073

Murray, P.J.J., Allen, J.E.E., Biswas, S.K.K., Fisher, E.A.A., Gilroy, D.W.W., Goerdt, S., Gordon, S., Hamilton, J.A.A., Ivashkiv, L.B.B., Lawrence, T., Locati, M., Mantovani, A., Martinez, F.O.O., Mege, J.-L., Mosser, D.M.M., Natoli, G., Saeij, J.P.P., Schultze,

J.L.L., Shirey, K.A.A., Sica, A., Suttles, J., Udalova, I., van Ginderachter, J.A., Vogel, S.N.N., Wynn, T.A.A., Goerdt, S., Ivashkiv, L.B.B., Sica, A., Mosser, D.M.M., Shirey, K.A.A., Natoli, G., Gilroy, D.W.W., Martinez, F.O.O., Gordon, S., Allen, J.E.E., Schultze, J.L.L., Mantovani, A., Murray, P.J.J., Wynn, T.A.A., Biswas, S.K.K., Suttles, J., Udalova, I., Hamilton, J.A.A., van Ginderachter, J.A., Mege, J.-L., Locati, M., Fisher, E.A.A., Lawrence, T., Allen, J.E.E., Biswas, S.K.K., Fisher, E.A.A., Gilroy, D.W.W., Goerdt, S., Gordon, S., Hamilton, J.A.A., Ivashkiv, L.B.B., Lawrence, T., Locati, M., Mantovani, A., Martinez, F.O.O., Mege, J.-L., Mosser, D.M.M., Natoli, G., Saeij, J.P.P., Schultze, J.L.L., Shirey, K.A.A., Sica, A., Suttles, J., Udalova, I., van Ginderachter, J.A., Vogel, S.N.N., Wynn, T.A.A., van Ginderachter, J.A., Vogel, S.N.N., Wynn, T.A.A., van Ginderachter, J.A., Vogel, S.N.N., Wynn, T.A.A., 2014. Macrophage Activation and Polarization: Nomenclature and Experimental Guidelines. Immunity 41, 14–20. https://doi.org/10.1016/j.immuni.2014.06.008

O'Dea, E., Hoffmann, A., 2009. NF-κB signaling. Wiley Interdiscip. Rev. Syst. Biol. Med. 1, 107–15. https://doi.org/10.1002/wsbm.30

Pękalski, J., Zuk, P.J., Kochańczyk, M., Junkin, M., Kellogg, R., Tay, S., Lipniacki, T., 2013. Spontaneous NF-κB activation by autocrine TNFα signaling: a computational analysis. PLoS One 8, e78887. https://doi.org/10.1371/journal.pone.0078887

Pollard, J.W., 2009. Trophic macrophages in development and disease. Nat. Rev. Immunol. 9, 259–70. https://doi.org/10.1038/nri2528

Powers, D.M.W., 2007. Evaluation: From Precision, Recall and F-Factor to ROC, Informedness, Markedness & Correlation.

Selimkhanov, J., Taylor, B., Yao, J., Pilko, A., Albeck, J., Hoffmann, A., Tsimring, L.,

Wollman, R., 2014. Systems biology. Accurate information transmission through dynamic biochemical signaling networks. Science 346, 1370–3. https://doi.org/10.1126/science.1254933

Takeshita, S., Kaji, K., Kudo, A., 2000. Identification and characterization of the new osteoclast progenitor with macrophage phenotypes being able to differentiate into mature osteoclasts. J. Bone Miner. Res. 15, 1477–88. https://doi.org/10.1359/jbmr.2000.15.8.1477

Takeuchi, Osamu Akira, S., 2010. Pattern Recognition Receptors and Inflammation. Cell 140, 805–820. https://doi.org/10.1016/j.cell.2010.01.022

Tay, S., Hughey, J.J., Lee, T.K., Lipniacki, T., Quake, S.R., Covert, M.W., 2010. Single-cell NF-kappaB dynamics reveal digital activation and analogue information processing. Nature 466, 267–71. https://doi.org/10.1038/nature09145

Taylor, B., Adelaja, A., Liu, Y., Luecke, S., Hoffmann, A., 2020. Identification and physiological significance of temporal NFκB signaling codewords deployed by macrophages to classify immune threats. bioRxiv 2020.05.23.112862. https://doi.org/10.1101/2020.05.23.112862

Vihinen, M., 2012. How to evaluate performance of prediction methods? Measures and their interpretation in variation effect analysis. BMC Genomics 13, S2. https://doi.org/10.1186/1471-2164-13-S4-S2

Vladimer, G.I., Marty-Roix, R., Ghosh, S., Weng, D., Lien, E., 2013. Inflammasomes and host defenses against bacterial infections. Curr. Opin. Microbiol. 16, 23–31. https://doi.org/10.1016/j.mib.2012.11.008

Werner, S.L., Barken, D., Hoffmann, A., 2005. Stimulus Specificity of Gene Expression Programs Determined by Temporal Control of IKK Activity. Science 309, 1857–61. https://doi.org/10.1126/science.1113319

Werner, S.L., Kearns, J.D., Zadorozhnaya, V., Lynch, C., O'Dea, E., Boldin, M.P., Ma, A., Baltimore, D., Hoffmann, A., 2008. Encoding NF- B temporal control in response to TNF: distinct roles for the negative regulators I B and A20. Genes Dev. 22, 2093–2101. https://doi.org/10.1101/gad.1680708

Chapter 4 : Conclusions

The studies included in this dissertation have indicated a broad role for the temporal coding of NFκB activity in regulating the inflammatory functions of macrophages in health and disease. Broadly, I have shown that despite substantial heterogeneity in the responses of macrophages, the temporal pattern of NFκB activity conveys sufficient amount of information to distinguish stimuli from disparate sources. Using quantitative approaches such as supervised machine learning, I have quantified the extent to which the temporal pattern of NFκB activity alone can specify ligand identity, ligand source (host, virus, bacterium), and ligand type (cytokine/host, PAMP/pathogen) and even classify the quantity of ligands. Further, the results here show that stimulus specificity of NFκB activity in macrophages are perturbed in the context of a systemic autoimmune disease, Sjögren's syndrome, whose etiology is largely driven by the adaptive immune system. Furthermore, I have shown that cytokine milieus that largely dictate the immune functions of macrophages control the stimulus specificity of NFκB temporal activity. These studies lend credence to the notion that perturbation of NFκB temporal activity in specific contexts may provide novel therapeutic targets for autoimmune diseases, infectious diseases and malignancy.

In Chapter 2, I examined the stimulus specificity of temporal pattern of NFκB in the context of autoimmune disease-associated macrophages. The results show that the temporal patterns of NFκB activity are disrupted in an autoimmune disease model (SS) and that stimulus specificity of NFκB signaling in macrophages is greatly diminished as a consequence. The supervised machine learning approached revealed significant confusion of ligand identity; particularly, the sensitivity and precision of classifying the host cytokine, TNF, is greatly diminished: the temporal pattern of NFκB cannot distinguish between a ubiquitous host-associated ligand and pathogen-associated ligands. Furthermore, the

results revealed that the dose response of bacterium-associated ligands are altered in SS-associated macrophages. The sensitivity and precision of dose classification was greatly diminished due to the truncation of the dose response dynamic range: dose-specific NFκB dynamics are abolished in SS-associated macrophages.

In Chapter 3, I examined ligand and dose specificity of the temporal pattern of NFκB activity in the context of physiologically relevant cytokine milieus. The results revealed that in the context of M_1 polarization (conditioning by the Th_1 cytokine IFNγ), the ligand specificity of NFκB signaling is abrogated. In particular, the specificity of NFκB response to viral PAMP poly(I:C) is greatly diminished. Closer examination of the results show that the sensitivity and precision of classifying poly(I:C)-induced NFκB responses are greatly reduced in M_1 polarized macrophages due to the confusion of poly(I:C)-induced NFκB responses with those elicited by bacterium-associated ligands such as LPS, CpG and Pam3CSK4. In fact, the misclassification of host-associated ligands in the context of M_1 polarization was reduced. Furthermore, classifications of NFκB responses based on ligand type (cytokine vs. PAMP; host vs. pathogen) are more accurate in the context of M_1 polarization. These results suggest that NFκB dynamics rather convey information about ligand type, not ligand source, in M_1 polarized macrophages. M_1 polarization trades classification performance between bacterium-associated and virus-associated macrophages for better classification between host-associated and pathogen-associated ligands.

In contrast to M_1 polarization, M_{2a} polarization (conditioned by the Th2 cytokine IL-4) enhances the sensitivity and precision of ligand classification across the board. Closer inspection suggests the improved classification may be due to the stimulus-specific attenuation of NFκB responses: poly(I:C)-induced NFκB activity is attenuated in the context of M_{2a} polarization. Interestingly, despite attenuated NFκB responses to virus-

associated in M2a polarized macrophages, poly(I:C)-induced NFκB activity remains distinguishable from no treatment controls. Since high doses of ligand are used in the examination of ligand classification in the context of macrophage polarization, it is possible that the effect of macrophage polarization of ligand classification may differ at lower doses. For example, the misclassification of p(I:C)-induced NFκB responses may be elevated in ligand classification at lower doses.

Whereas I examined the effect of macrophage polarization on ligand classification, I examined the effect of paracrine TNF and tonic TNF on dose classification. The results showed that when paracrine TNF is blocked with a decoy, soluble TNF receptor, dose responsive NFκB dynamics and dose classification are diminished. The results showed an abrogation of the oscillatory NFκB dynamics that are apparent at low and intermediate doses of TLR ligands. The elevated misclassification in the absence of paracrine TNF appears to be due to confusion of intermediate and high doses of TLR ligands. My examination of the TNF dose response in the absence of the constitutive, tonic TNF revealed the abolition of NFκB oscillations. The results indicated that the performance of dose classification is greatly diminished in the absence of tonic TNF: the precision of high dose classification and sensitivity of intermediate dose classification are lower.

The results presented in this dissertation inform new lines of inquiry and future directions. Broadly, these lines of inquiry fall into three categories: decoding, combinatorial coding, and mechanism. Based on the conclusions from Chapters 2 and 3, an interesting line of inquiry would be to examine the functional consequences of loss of stimulus specificity of NFκB dynamics in macrophages in the context of Sjögren's syndrome associated macrophages and in conditioned macrophages (by IFNγ, IL-4 and TNF). Due to the heterogenous nature of macrophage responses, functional assays with single cell

resolution may be required to fully explore the functional and biological consequences for the loss of NFκB stimulus specificity. Consequently, single-cell RNA-seq and single-cell ATAC-seq may yield fruitful results. To derive stronger conclusions, coupling NFκB signaling dynamics to single-cell transcriptomics may allow sequential examination of NFκB signaling and NFκB-induced gene expression in the same cell. This approach is experimentally difficult to implement as it requires either the use of microfluidics or a sequential live cell imaging to fixed cell imaging pipeline that couples time-lapse microscopy of NFκB nuclear translocation to single molecule fluorescence *in situ* hybridization.

The second line of inquiry involves combinatorial coding. The results in this dissertation are focused only on the stimulus specificity of NFκB signaling. The ligands discussed in this dissertation activate other signaling pathways that are involved in innate immunity, such as IRF (e.g. IRF1, IRF3, IRF5) and MAPK signaling pathways (p38, Erk, JNK). A reductionist approach allows for clear and focused examination of hypotheses with a relatively simple and well controlled experimental design and analysis scheme; however, this approach will fail to capture the emergent phenomena that result from the interactions and complex crosstalk that exists among the different signaling pathways. This reductionist approach provides a launching pad to examine more exuberant and elaborate hypotheses that explore the emergent properties of combinatorial coding. Due to the technical complexity of such an undertaking, very few studies in literature have tackled the subject of combinatorial coding with rigor. The experimental and analytical tools presented in this manuscript will significantly reduce the barrier to undertaking future studies into combinatorial coding. The IMPDM experimental model system presented in Chapter 2 enablse the examination of physiological responses of NFκB activity. This model system

allows for relatively straight-forward genetic perturbations, unlike in BMDMs where silencing of transgenes is problematic. Since IMPDMs can be generated from existing transgenic mouse lines, the amount of *in vitro* genetic perturbation is also greatly reduced. For example, developing a reporter system to concurrently monitor NFκB, IRF and MAPK activation requires *in vitro* genetic perturbation of IRF and MAPK effector proteins, since IMPDMs with mVenus-RelA are available. The analysis pipeline can be readily extended to measure fluorescent reporters of MAPK and IRF signaling and generate dynamical features of signaling activity. These features can be fed into the supervised machine learning pipeline with no additional modifications.

Finally, the third line of inquiry would be to develop a mechanistic understanding of the results presented in Chapter 3. Multi-stimulus mathematical modeling of stimulus-specific NFκB activity showed that IKK-dependent degradation of IκBα suffices to recapitulate the diverse dynamics observed in response to TNF and TLR ligands in primary macrophages. Since the perturbations of NFκB signaling dynamics observed in the context of macrophage polarization are stimulus specific, modulation of NFκB signaling probably occurs upstream of IKK activation. Biochemical analysis of signaling proteins upstream of IKK is warranted to dissect the mechanisms by which IFNγ and IL-4 polarization regulate NFκB signaling dynamics. Genetic perturbation—knockin, knockout or knockdowns—of the proteins of interest will be necessary to confirm the results. Similarly, mechanistic understanding of how loss of tonic TNF abolishes NFκB will prove particularly useful to basic, translational, and clinical scientists. Anti-TNF therapy has proven indispensable for the treatments of many autoimmune pathologies, such as inflammatory bowel disease and rheumatoid arthritis. Interestingly, many patients on anti-TNF therapy develop paradoxical inflammatory conditions, whose pathogeneses are unknown. Furthermore,

anti-TNF drugs carry a black box warning for lethal infections from bacteria such as *Legionella pneumophila, Mycobacteria tuberculosis,* and *Listeria monocytogenes*, all of which replicate inside macrophages. It's clear that tonic TNF and paracrine TNF are essential for controlling lethal bacterial infections and autoimmunity. Since loss of tonic TNF abolishes NFκB oscillations and there is evidence that IKK activation kinetics are sufficient to produce oscillatory and non-oscillatory NFκB dynamics, examining of signaling proteins upstream of IKK may yield useful mechanistic insights. Furthermore, examination of NFκB signaling in a co-culture of $tnf^{\delta/-}$ macrophages with wildtype controls will be essential to prove that loss of NFκB oscillations is due to the loss of tonic TNF. Restoration of oscillatory dynamics in the co-culture should provide sufficient evidence that loss of tonic TNF is indeed causal for the abolition of NFκB oscillations.